

COO-4570-4
MITNE-215
MIT-EL-78-017

Archive

DESIGN AND FUEL MANAGEMENT OF PWR CORES TO
OPTIMIZE THE ONCE-THROUGH FUEL CYCLE
by

Edward K. Fujita
Michael J. Driscoll
David D. Lanning

DOE Contract No. EN-77-S-02-4570, Nuclear Engineering Department Report No. MITNE-215, Energy Laboratory Report. MIT-EL 78-017. August, 1978



DESIGN AND FUEL MANAGEMENT OF PWR CORES TO
OPTIMIZE THE ONCE-THROUGH FUEL CYCLE

by

Edward K. Fujita
Michael J. Driscoll
David D. Lanning

Department of Nuclear Engineering
and
Energy Laboratory
MASSACHUSETTS INSTITUTE OF TECHNOLOGY
Cambridge, Massachusetts 02139

Sponsored by

U.S. Department of Energy

NOTICE

This report was prepared as an account of work sponsored by the United States Government. Neither the United States nor the United States Department of Energy, nor any of their employees, nor any of their contractors, subcontractors, or their employees, makes any warranty, express or implied, or assumes any legal liability or responsibility for the accuracy, completeness or usefulness of any information, apparatus, product or process disclosed, or represents that its use would not infringe privately owned rights.

Printed in the United States of America

Available from

National Technical Information Service
U.S. Department of Commerce
5285 Port Royal Road
Springfield, VA 22161

Price: Printed Copy \$9.50; Microfiche \$3.00

DISTRIBUTION

NASAP Control Office
U.S. Department of Energy
Room F-409, Mail Stop B-107
Germantown, MD 20767

N.L. Shapiro
Mgr. Advanced Design Projects
Combustion Engineering Inc.
1000 Prospect Hill Rd.
Windsor, Conn. 06095

J.F. Jessick
Project Mgr.
Combustion Engineering Inc.
1000 Prospect Hill Rd.
Windsor, Conn. 06095

R.A. Matzie
Project Mgr.
Combustion Engineering Inc.
1000 Prospect Hill Rd.
Windsor, Conn. 06095

K.D. Kirby
Project Mgr.
Southern Science Applications, Inc.
P.O. Box 10
Dunedin, FL 33528

J.R. Engel
Project Mgr.
Oak Ridge National Lab.
P.O. Box Y
Oak Ridge TN 37830

M. Steinberg
Associated Universities, Inc.
Brookhaven National Lab.
Upton, NY 11973

F.L. Ribe
Principal Investigator
University of Washington
College of Engineering
Department of Nucl. Eng.
Seattle, WA 98195

S. Zwickler
Project Engineer
Burns and Roe
P.O. Box 663
Route 17, South
Paramus, N.J. 07652

C.E. Till
Director, Applied Physics
Argonne National Lab.
9700 South Cass Ave.
Argonne, IL 60439

M.C.J. Carlson
Mgr., Alternate Fuel Development
Hanford Engineering Devlpmnt. Lab
P.O. Box 1970
Richland, Washington 99352

A. Gietzen
Mgr., TRIGA Reactor Devlpmnt.
General Atomic Co.
P.O. Box 81608
San Diego, CA 92138

L.L. Lowrey
University of California
Los Alamos Scientific Lab.
P.O. Box 1663
Los Alamos, New Mexico 87545

D.E. Bartine
Project Mgr.
Oak Ridge National Lab.
P.O. Box X
Oak Ridge, TN 37830

R. Crowther
Project Mgr.
General Electric Co.
175 Curtner Ave.
San Jose, CA 95125

E. Straker
Project Mgr.
Science Applications, Inc.
8400 Westpark Drive
McLean, VA 22101

R.P. Omberg
Mgr., Advanced Concepts
Hanford Engineering Dev. Lab.
P.O. Box 1970
Richland WA 99352

S.M. Stoller
President
S.M. Stoller Corp.
1250 Broadway
New York, NY 10001

W.C. Lipinski
Project Mgr.
Argonne National Lab.
9700 South Cass Ave.
Argonne, IL 60439

W.R. Harris
Project Mgr.
RAND Corporation
1700 Main Street
Santa Monica, CA 90406

T.H. Row
Oak Ridge National Lab.
P.O. Box X
Oak Ridge, TN 37830

B.A. Pasternak
Research Director
Booz-Allen and Hamilton
4330 East-West Highway
Bethesda, MD 20014

A. Weitzberg
Principal Investigator
Science Applications, Inc.
8400 Westpark Dr.
McLean, VA 22101

M. Higgins
Vice President for Energy
and Environment
Science Applications, Inc.
8400 Westpark Dr.
McLean, VA 22101

I. Spiewak
Proj. Mgr, Nuclear Energy Assmts.
Oak Ridge National Lab.
P.O. Box Y, Bldg 9201-3
Oak Ridge, TN 37830

V. Uotinen
Project Mgr.
The Babcock and Wilcox Co.
P.O. Box 1260
Lynchburg, VA 24505

C. Sege
U.S. Department of Energy
Room F-403, Mail Stop B-107
Germantown, MD 20767

Peter M. Lang, Asst. Dir.
LWR Development Branch
Mail Stop G-434
U.S. Department of Energy
Washington, DC 20545

S. Strauch
Acting Deputy Director
Fuel Cycle Evaluation
U.S. Department of Energy
Room F-416, Mail Stop B-107
Germantown, MD 20767

B. Feldman
Chief, Reactor and Safegaurds
Branch
Office of Classification
U.S. Department of Energy
Room A-23204, Mail Stop A-23220
Germantown, MD 20545

Mr. John F. Foran
Resource Planning Assoc. Inc.
44 Brattle Street
Cambridge MA 02138

Dr. Bal Raj Sehgal
Nuclear Safety & Analysis Dept.
Electric Power Research
Institute
3412 Hillview Ave.
P.O. Box 10412
Palo Alto, CA 94304

Dr. A. Radkowsky
Tel-Aviv University
School of Engineering
Ramat-Aviv, Tel Aviv 69970
ISRAEL

Mr. C.M. Newstead
Brookhaven National Laboratory
Technical Support Organization
Bldg. 197
Upton, NY 11973

ABSTRACT

The once-through fuel cycle has been analyzed to see if there are substantial prospects for improved uranium ore utilization in current light water reactors, with a specific focus on pressurized water reactors. The types of changes which have been examined are: (1) re-optimization of fuel pin diameter and lattice pitch, (2) Axial power shaping by enrichment gradation in fresh fuel, (3) Use of 6-batch cores with semi-annual refueling, (4) Use of 6-batch cores with annual refueling, hence greater extended (~doubled) burnup, (5) Use of radial reflector assemblies, (6) Use of internally heterogeneous cores (simple seed/blanket configurations), (7) Use of power/temperature coastdown at the end of life to extend burnup, (8) Use of metal or diluted oxide fuel, (9) Use of thorium, and (10) Use of isotopically separated low σ_a cladding material.

State-of-the-art LWR computational methods, LEOPARD/PDQ-7/FLARE-G, were used to investigate these modifications. The most effective way found to improve uranium ore utilization is to increase the discharge burnup. Ore savings on the order of 20% can be realized if greatly extended burnup (~double that of current practice) is combined with an increase in the number of batches in the core from 3 to 6. The major conclusion of this study is that cumulative reductions in ore usage of on the order of 30% are foreseeable relative to a current PWR operating on the once-through fuel cycle, which is comparable to that expected for the same cores operated in the recycle mode.

R. Braitsch
Prog. Anal. for ETP
US Department of Energy
Room 7117
Casimir Pulaski Bldg.
20 Mass. Ave. NW
Washington, DC 20545

T. Abernathy
Chief, Documents Management Branch
Technical Information Center
U.S. Department of Energy
P.O. Box 62
Oak Ridge, TN 37830

(2 copies)

P. Afansenko
Int. Adv. to Asst. Secy. for ET
U.S. Department of Energy
Room A-220, Mail Stop A-229
Casimir Pulaski Bldg.
20 Mass. Ave. NW
Washington, DC, 20545

ACKNOWLEDGEMENTS

The work presented in this report has been performed primarily by the principal author, Edward Fujita, who has submitted substantially the same report in partial fulfillment of the requirements for the Sc.D. degree in Nuclear Engineering at M.I.T.

The present work was supported by a Department of Energy (DOE) contract administered through the M.I.T. Energy Laboratory. Computer calculations were carried out at the M.I.T. Information Processing Center and the Laboratory for Nuclear Science.

The authors would especially like to thank Mr. George Solan of the Yankee Atomic Electric Company for providing substantial information on the Maine Yankee Reactor. The principal author would also like to thank Dr. Andrew Cook and Francisco Correa for the information gained from many technical discussions.

Typing of this manuscript was ably handled by Ms. Cindi Mitaras and Mr. James Williams.

TABLE OF CONTENTS

	Page
Abstract	1
Acknowledgements	2
Table of Contents	3
List of Figures	6
List of Tables	8
CHAPTER I. INTRODUCTION	11
1.1. Foreword	11
1.2. Background and Previous Work	12
1.3. Research Objectives	13
1.4. Outline of Present Work	17
CHAPTER 2. ANALYTICAL AND NUMERICAL METHODS	19
2.1. Introduction	19
2.2. Computer Methods	20
2.2.1. The LEOPARD Code	20
2.2.2. The CHIMP Code	23
2.2.3. The PDQ-7 Code	25
2.2.4. The FLARE-G Code	26
2.2.5. The BAHAR Code	27
2.2.6. The MITCOST-II Code	28
2.2.7. The ECON Code	28
2.3. Ore Usage Model	29
2.3.1. Ore Usage as a Function of Reactor Characteristics	30
2.3.4. Identification of Key Characteristics	32
CHAPTER 3. HETEROGENEOUS CORES	46
3.1. Introduction	46
3.2. Previous Work	51
3.3. Depletion Model	53
3.3.1. Cross-Section Generation	53
3.3.2. Power Distributions	56
3.3.3. Depletion Chains	56
3.3.4. Calculational Procedures for Depletion Studies	59
3.4. Reactors Investigated	61
3.4.1. Zone Loaded Core	61
3.4.2. Seed-Blanket Cores	65
3.4.3. Movable Fuel Reactivity Control	67
3.4.4. Enhanced Reflector Design	67
3.5. Results	72
3.5.1. Zone Loading	72
3.5.1.1. Ore Usage Model	72
3.5.1.2. One Group Model	76

	<u>Page</u>
3.5.1.3 Representative Zone Loaded Cores	77
3.5.1.4 The Fuel Cycle Cost of Zone Loaded Cores	81
3.5.1.5 Xenon Oscillations	92
3.5.2 Seed/Blanket Cores	94
3.5.3 Movable Fuel Reactivity Control.	98
3.5.4 Enhanced Reflector Designs	100
3.6 Conclusions.	105
CHAPTER 4. SIX-BATCH HIGH BURNUP CORE	109
4.1 Introduction	109
4.2 Motivation.	110
4.2.1 Ore Usage Model	110
4.2.2 DOE Extended Burnup Studies.	111
4.2.3 Use of Isotopically Separated Improved Clad	114
4.3 Depletion Model.	116
4.3.1 Cross-Section Generation and BOC Power Distribution	116
4.3.2 Nodal Depletion	117
4.3.3 Reload Analysis	117
4.4 Reactor Investigated	118
4.5 Results.	121
4.5.1 Ore Savings.	121
4.5.2 Fuel Cycle Cost.	142
4.6 Conclusions	145
CHAPTER 5. COASTDOWN.	148
5.1 Introduction	148
5.2 Previous Work	149
5.3 Coastdown Model Development	151
5.3.1 Xenon Model.	153
5.3.2 Protactinium Model.	154
5.3.3 Temperature/Power Coefficient Model	156
5.3.4 Additional Burnup Gain Due to Coastdown	158
5.3.5 Coastdown Economics Model.	159
5.4 Reactor Investigated.	160
5.5 Results	162
5.5.1 Reactor Efficiency.	162
5.5.2 Reactivity Models.	164
5.5.3 Ore Savings and Fuel Cycle Cost.	175
5.5.4 Reactivity Addition From Reduced Pa ²³³ Burnout.	178
5.6 Conclusions.	183

	<u>Page</u>
CHAPTER 6. SUMMARY, CONCLUSIONS, AND RECOMMENDATIONS.	186
6.1 Introduction	186
6.2 Background and Research Objectives	187
6.3 Ore Usage Model.	188
6.4 Reference Reactor Design Basis.	190
6.5 Results	191
6.5.1 Use of Alternative Fuel Types.	191
6.5.2 Re-optimize Fuel Pin Diameter and Lattice Pitch.	193
6.5.3 Zone Loaded Cores	195
6.5.4 6-Batch High Burnup Core.	197
6.5.5 Enhanced Reflector Design	199
6.5.6 Internally Heterogeneous Core (Simple Seed/Blanket).	200
6.5.7 Coastdown.	201
6.5.8 Use of Isotopically Separated Low σ_a clad	202
6.5.9 Thorium in Uniform Lattices.	203
6.6 Conclusions	203
APPENDIX A. ORE USAGE MODEL	206
APPENDIX B. MASS PENALTY DUE TO POWER FLATTENING.	210
APPENDIX C. XENON AND PROTACTINIUM REACTIVITY MODELS	216
C.1 XENON MODEL.	216
C.2 PROTACTINIUM MODEL.	218
APPENDIX D. ADDITIONAL BURNUP GAIN DUE TO COASTDOWN.	222
APPENDIX E. THE EFFECT OF CORE POWER DENSITY ON FUEL CYCLE ECONOMICS.	229
APPENDIX F. ALTERNATIVE ECONOMICS MODEL FOR COASTDOWN	233
APPENDIX G. REFERENCES.	238

LIST OF FIGURES

	Page
Figure 2.1. LEOPARD Unit Cell Geometry.....	21
Figure 2.2. Annual Ore Consumption.....	44
Figure 3.1. Reactor Fuel Loading Scheme for a PWR.....	47
Figure 3.2. LEOPARD Geometrical Representations.....	54
Figure 3.3. Depletion and Fission Product Chains Used in the Present Study.....	57
Figure 3.4. Diffusion-Depletion Model.....	60
Figure 3.5. Reactor Core Cross-Section.....	62
Figure 3.6. Axial Seed-Blanket Geometry.....	66
Figure 3.7. Movable Fuel Reactivity Control, Design #1.....	68
Figure 3.8. Movable Fuel Reactivity Control, Design #2.....	69
Figure 3.9. Enhanced Reflector Study, PDQ-7 Geometrical Representation (Cylindrical).....	70
Figure 3.10. Zone Loaded Core Layout.....	79
Figure 3.11. Definition of Capacity Factor.....	82
Figure 3.12. Cosine Flux Distribution Vs. Power-Flattened Flux Distribution.....	95
Figure 3.13. Reactivity vs. Burnup for Seed/Blanket Cores.....	96
Figure 3.14. Enhanced Reflector Studies: K_{eff} vs. Time.....	101
Figure 4.1. Relative Ore Usage as a Function of Burnup and Batch Number.....	113
Figure 4.2. LWR Fuel Utilization Benefits (Proposed by DOE Based on Deferral of Reprocessing).....	115
Figure 4.3. Reactor Core Cross Section.....	119
Figure 5.1. Reactor Coolant Temperatures vs. Reactor Power for a Constant T_{Ave} Unit.....	163

	Page
Figure 5.2. Nuclear Steam Supply System Layout.....	165
Figure 5.3. Representative Plant Efficiency vs. Load for a Typical PWR.....	168
Figure 5.4. Fractional Change in Xe^{135} Worth vs. Load.....	171
Figure 5.5. Additional Burnup from Fuel Temperature Effects as A Function of Load.....	173
Figure 5.6. Additional Burnup From Moderator Temperature Effects as a Function of Average Moderator Temperature Reduction...	174
Figure 5.7. Relative Fuel Cycle Cost vs. Coastdown Duration.....	180
Figure 6.1. Relative Ore Usage as a Function of the Number of Core Batches and Burnup.....	198
Figure E.1. Cash Flow Diagrams: For Representative Example.....	230
Figure F.1. Definition of Capacity Factor Including Coastdown Operation.....	236
Figure F.2. Relative Cost of Electricity vs. Coastdown Duration.....	237

LIST OF TABLES

	Page
Table 2.1. Ore and Separative Work Requirements as a Function of Fuel-to-Coolant Volume Ratio, V_f/V_m	34
Table 2.2. Nuclear Fuel Cycle Cost Data.....	35
Table 2.3. Ore and Separative Work Requirements as a Function of Unit Cell Volume.....	36
Table 2.4. Equivalent Metal and Oxide Cores.....	38
Table 2.5. Effect of Power Level on Discharge Composition.....	41
Table 2.6. Equivalent U-235/U-238 Oxide Fuel Lattices: With and Without Diluent.....	43
Table 3.1. Fission Yields and Decay Constants.....	58
Table 3.2. Mechanical Design Features.....	63
Table 3.3. Enhanced Reflector Studies: Design Parameters.....	71
Table 3.4. Ore Savings Due to Power Shape Improvement (Thermal Power Upgrading).....	75
Table 3.5. Mass Penalty Due to Power Flattening.....	78
Table 3.6. Zone Loaded Core Characteristics.....	80
Table 3.7. Mass Flows for Zone Loaded Cores.....	85
Table 3.8. Levelized Fuel Cycle Cost at a Constant Capacity Factor of 75%.....	87
Table 3.9. Levelized Fuel Cycle Cost at a Constant Availability Based Capacity Factor of 90%.....	88
Table 3.10. Levelized Fuel Cycle Cost at a Constant Availability Based Capacity Factor of 80%.....	89
Table 3.11. Ore Usage ($STU_3O_8/GW(e)\text{-yr}$) for Zone Loaded Cores: Scenario (4).....	90
Table 3.12. Relative Ore Usage and Fuel Cycle Cost.....	91
Table 3.13. Average ϕ 's for Undamped Xenon Oscillation (Zero Temperature Coefficient).....	93

	Page
Table 3.14. Seed-Blanket Cores Examined in the Present Work	97
Table 3.15. Reactivity Calculation for Movable Fuel-Reactivity Control.....	99
Table 3.16. Thermal Absorption Properties of BeO, H ₂ O, and Boron.....	102
Table 3.17. Ore Savings: Enhanced Reflector Studies.....	104
Table 4.1. Relative Ore Usage for Six-Batch Cores.....	112
Table 4.2. Zion Reactor Core Design Data.....	120
Table 4.3. Initial Fuel Loading for 3-Batch and 6-Batch Cores.....	123
Table 4.4. Burnup and Electric Energy Generation History: 3-Batch Core Annual Refueling.....	124
Table 4.5. Burnup and Electric Energy Generation History: 6-Batch Core Semi-Annual Refueling.....	127
Table 4.6. Burnup and Electric Energy Generation History: 6-Batch Core, Annual Refueling.....	136
Table 4.7. Relative Ore Savings for 3-Batch and 6-Batch PWR Cores.....	141
Table 4.8. Levelized Nuclear Fuel Cost per Period, 3-Batch and 6-Batch Cores Annual Refueling.....	143
Table 4.9. Levelized Nuclear Fuel Cost per Period, 6-Batch Core Semi-Annual Refueling.....	144
Table 4.10. Levelized Nuclear Fuel Cycle Cost of 3-Batch and 6-Batch Cores.....	146
Table 5.1. Comparative Coastdown Capability for HTGR's and PWR's.....	152
Table 5.2. Charged and Discharged Masses for a ²³³ UO ₂ /ThO ₂ -Fueled PWR Reactor.....	161
Table 5.3. Nomenclature for Nuclear Steam Supply System: Figure 5.2..	166
Table 5.4. Steam Supply System Data.....	167
Table 5.5. Nuclear Parameters for Xenon Model.....	170
Table 5.6. Comparison of LEOPARD and More Exact Temperature Coefficient Values.....	172
Table 5.7. Ore Savings From Coastdown Operation.....	177
Table 5.8. Parameters for the Coastdown Scenario.....	179
Table 5.9. Spectrum Averaged Cross Sections for a Typical UO ₂ /ThO ₂ -Fueled PWR System.....	182

Table 6.1. Ore Savings for the Once-Through PWR Fuel Cycle.....	192
Table 6.2. Equivalent U-235/U-238 Oxide and Metal Fueled Lattices.....	194
Table D.1. Net Burnup Gain Due to Coastdown.....	226

CHAPTER 1

INTRODUCTION

1.1 FOREWORD

Until recently, it was envisioned that LWR reactors would serve an interim role, as precursors to Fast Breeder Reactors (FBR). The LWRs would remain the mainstay of commercial nuclear power development only until the breeder concept was shown to be commercially feasible and sufficient plutonium reserves were bred to permit their widespread deployment. This transition has not taken place, and it is not in prospect, particularly in the United States, for several decades; hence the role of LWRs in less transitory scenarios merits reassessment.

The present commercial attractiveness and useful lifetime of the LWR will depend upon the amount and price of available uranium resources; a breakeven yellowcake price of approximately \$150/lb U_3O_8 (compared to today's price of less than \$50/lb U_3O_8) is currently estimated for current LWRs competing with LMFBR or coal-fired units. The current restriction to a once through fuel cycle in the United States imposes an added burden. Therefore, a prime, long range, concern of the industry today must be on better utilization of uranium by optimizing both reactor core design and fuel management strategy. Evaluation of these prospects is the central objective of the present investigation.

Generally speaking, there are two divergent approaches being pursued today to optimize LWR ore utilization: (1) development of fundamentally altered LWR concepts (e.g. the LWBR [E- 1] and spectral shift reactors [E- 2]) (2) use of conventional LWR designs, with a minimum of reactor

and fuel cycle changes. The present work is of the latter genre; and, more importantly, only non-recycle concepts will be considered. These ground rules were established from the outset on quite pragmatic grounds: the United States nuclear industry is currently in a non-recycle mode of indefinite duration; and the less severe the changes proposed, the more rapidly they can be implemented and their benefits realized. However, it should be noted that some of the avenues to improvement would also benefit LWR cores operated in the recycle mode. Similarly we will limit our analysis to PWRs, which represent approximately two-thirds of the current United States and World LWR market; but, BWRs could profit equally well from many of the same changes.

1.2 BACKGROUND AND PREVIOUS WORK

In this section, a selective review of prior work pertinent to the present research will be presented. It is assumed that the reactor physics of current PWR designs is familiar to the reader so that only a brief summary of the once-through fuel cycle is given below.

The large PWRs in commercial service today have a three-batch-core and use a modified out-in-scatter fuel management program. In this scheme, one-third of the fuel assemblies are replaced by fresh fuel assemblies each year; the fresh fuel is loaded at the periphery of the core while the once-burned and twice-burned fuel is scattered in the interior of the core.

In the initial core, the enrichments for each lot of fuel are chosen such that the composition of the three initial fuel lots simulates twice-burned, once-burned, and fresh fuel in the steady state (e.g. following fission product build-up, U^{235} depletion, etc.). For example,

the initial core may contain enrichments of 2.25 w/o, 2.8 w/o, and 3.3 w/o, with the reload enrichment being 3.2 w/o. In addition, the enrichments are graded (arranged spatially) such that an undesirable power distribution (high power peaking, which is associated with uniformly loaded cores) does not result. Burnable poisons are also incorporated into the fuel assemblies to reduce power peaking.

The steady state cycle burnup and discharge burnup are approximately 11,000 MWD/MTU and 33,000 MWD/MTU, respectively; but the burnups in the initial transient cycles deviate significantly from the steady state values. For example, the average burnup for the first cycle is typically 17,000 MWD/MTU. This first cycle is usually followed by two short cycles (average cycle burnups \sim 9,000 MWD/MTU). This transient behavior then dies out since in subsequent cycles the reactor is fueled in an identical fashion such that its performance in each cycle attains a repetitive, steady-state behavior.

The steady state uranium ore requirement for PWRs operating on the once-through fuel cycle is approximately 200 ST U_3O_8 /GWe (rated)-yr [S-1] (based on a 75% capacity factor and 0.2 w/o enrichment plant tails). In addition, a one time initial ore investment (initial startup requirements) is required, which is approximately two times the steady state annual batch requirement. On the other hand, end-of-reactor life batches can be tailored to match the lower burnups asked of these batches, with resulting lower ore usage. Therefore, the 30-year uranium requirement for the reference PWR (once-through) is on the order of thirty annual batch reloads or 6,000 ST U_3O_8 /GWe.

In one sense the entire history of reactor development in general, and LWR systems in particular, is germane to the present work. As several

authors have noted, many improvements in LWR performance characteristics have been realized over the past twenty years, many of which contribute to better ore utilization [D- 1], [P-1] and [R- 1]. Furthermore, some of the suggestions made to improve ore utilization have rekindled the interest in previously examined (and by-passed) concepts, such as spectral shift control [E- 2]. However in another sense, very little has been done, or at least published, of specific use for present purposes, since, as has already been noted, the LWR era was viewed as a prelude to the age of the breeder, and efforts to prolong the former did not have a high priority. Illustrative of this frame of mind is the fact that few, if any, long range studies of the nuclear electric economy featured "advanced" LWR designs as one of the competitors.

Priorities have shifted rapidly in the past two years. At present there are many pertinent studies being conducted in parallel with the work discussed here. It is not the purpose of the present work, nor does the schedule permit us, to prepare a running summary of work in progress elsewhere. However, it will be quite useful to cite a few selected recent references to help establish the motivation and the framework of the present study.

Previous work of interest in this regard can be summarized by referring to two major studies, the first of which was recently completed by Argonne National Laboratory [T- 1]. The primary effort in the ANL study was to evaluate the fuel utilization characteristics of once-through fuel cycles, in particular the LWR once-through fuel cycle.

ANL identified five avenues for improvement, they are: (1) increase the discharge burnup of spent fuel, (2) reduce the metal/water ratio in

current lattices, (3) replace reactivity control using poisons by spectral-shift control, (4) reduce the irradiation period, and (5) employ thermal coastdown. They have found that increased burnup is the most straightforward and promising option for once-through fuel cycle improvement; the other options resulted in modest ore savings (5% to 10%).

The Atomic Industrial Forum [AIF] has recently completed a study [A-1] which debated the pros and cons of closing the back end of the fuel cycle via reprocessing and recycling of plutonium and uranium. Although the primary effort in the AIF study was to clarify the subject of reprocessing-recycle economics, considerable emphasis was also placed on the throwaway alternative. The AIF study is of interest here because of the benchmark economics data it has compiled, which can serve as the basis upon which the economic analyses performed in the present research can be founded. AIF selected nine studies on the economics of reprocessing-recycle; each study was sufficiently detailed and comprehensive to allow comparison with other studies. An arithmetic average of product or service unit costs for each fuel cycle transaction was calculated and reported by AIF for the data reported in the nine studies they examined.

The cost basis developed by AIF will be used as a data base when the economics of the once-through fuel cycle is analyzed. However, it should be recognized that many of the back end costs (e.g. interim storage, whole-assembly disposal, etc.) are not well defined. Front-end costs are also subject to considerable uncertainty. The resource grade/size/cost picture for U_3O_8 is widely debated, and the impact of technological breakthroughs in the area of isotope separation may well be profound. For that reason we have centered on ore utilization as the primary criterion,

and recommend the economic analyses only as qualitative and relative indicators.

1.3 RESEARCH OBJECTIVES

The main objective of this present work is to determine whether there are substantial prospects for improving the ore utilization performance of light water reactors by optimizing the reactor core and fuel cycle. As previously mentioned, the approach that will be taken to optimize LWR ore utilization will be use of conventional PWR designs, with a minimum of reactor core and fuel cycle changes; more importantly, only non-recycle concepts will be considered.

Generally speaking, there are three distinct approaches being pursued today to optimize LWR ore utilization: (1) increase the discharge burnup of the spent fuel, (2) reduce control poison requirements, and (3) reduce critical mass requirements at BOC. These general approaches can be embodied, singly or in combination in various specific design and/or operating procedures. Although some attention is given to establishing ultimate theoretical limits, the present work concentrated primarily on specifics. For example the following methods were investigated to increase the discharge burnup: (1) axial power flattening, (2) operating the reactor in coastdown scenarios at EOC, (3) increasing the number of batches in the core, and (4) increasing the refueling interval. Each of the above will be discussed in greater detail in the body of this report.

Ore utilization can be improved by reducing the control poison requirements since control poisons degrade the neutron economy by wasting neutrons on parasitic captures. There are two divergent approaches to reduce control poison requirements: (1) use of control materials that

will benefit from parasitic captures (e.g. fertile materials) and (2) reduce the amount of BOC reactivity needed to be held down by the control poisons. One obvious way to reduce the BOC reactivity is to reduce the reload enrichment, but a shorter irradiation period results. One possible way to avoid shorter cycle lengths would be to increase the conversion ratio of the reactor. This would reduce equilibrium enrichments and annual ore requirement by increased fissile production during the cycle.

Unfortunately the improved conversion ratio is coupled to a penalty in the initial startup requirements, as will be shown later. In view of the above, the following compromise scenarios will be investigated: (1) axial seed/blanket-cores, (2) movable-fertile-fuel reactivity control, and (3) enhanced reflector designs.

The initial objective will be to assemble the analytic and numerical models needed to analyze the reactor core and fuel cycle design changes. Once this is done, a cursory review of lattice design will be performed to put the significance of key independent design variables such as fuel pin diameter and pin-to-pin spacing into perspective. Finally, a neutronic and economic analysis will be performed of each of the options outlined above to see if there is improvement in ore usage.

1.4 OUTLINE OF PRESENT WORK

The work reported here is organized as follows. Chapter 2 will be concerned with developing the calculational methodology for analyzing the proposed design changes in the once-through fuel cycle; a discussion of the computer codes and analytical models used in this work will be given. Chapter 2 will also serve a preliminary screening function,

eliminating certain design changes as avenues for improving ore requirements in PWRs operating on the once-through fuel cycle.

In Chapter 3, various heterogeneous core configurations will be examined to see if the annual ore requirement is substantially reduced. A brief economic study (fuel cycle cost) is also given for each of the heterogeneous core configurations.

In Chapter 4, the six-batch high burnup core will be analyzed. The results of neutronic (power distribution, reload enrichment, etc.), economic (fuel cycle cost) and ore utilization studies will be presented and discussed.

In Chapter 5, various coastdown scenarios for PWRs will be examined with regard to the potential ore savings and reduced fuel cycle cost when reactors are operated in this manner. The application of simple models to analyze coastdown will be strongly emphasized.

Finally, in Chapter 6, the results and conclusions of the study will be summarized, together with recommendations for future work. Several appendices are included containing subsidiary analyses and data supporting the work reported in the main text.

CHAPTER 2

ANALYTICAL AND NUMERICAL METHODS

2.1 INTRODUCTION

A primary objective of reactor physics analysis is to provide the reactor designer or operator with information needed to make appropriate management decisions concerning the design, operation, safety and economics of the reactor plant. The starting point of any analysis is a well defined problem and a postulated set of reactor design characteristics, such as material compositions, dimensions, temperatures and thermal-hydraulic parameters. One is then prepared to devise a scheme to obtain the solution to the problem.

Over the past two decades, large investments in terms of research dollars and manpower have been made to establish computational algorithms to carry out such analyses. The state-of-the-art computer programs used in this present research have been tested and used by national laboratories, vendors, and utilities for fuel management analyses [A-1]. A brief description of these codes will be given in this chapter; the rationale for using these codes will be developed in subsequent chapters.

Computer codes are useful, but computational time and cost constraints may set practical limits on the number of solutions which can be investigated. Thus, the need for "simple" analytical methods for scoping calculations is evident; such methods can be used to scope out problems so that the analyst can concentrate on the most promising range of solutions. In this spirit the last section of this chapter will describe a simple model for evaluating uranium ore usage as a function of various governing parameters.

2.2 COMPUTER METHODS

In the sections which follow, a brief description of each computer code used in the present work will be given. The reader is directed to reference [A- 2] for a general discussion of computer methods for reactor analysis. This reference describes each of these codes in more detail, and it also describes other codes which perform the same functions. Detailed manuals for each code are also referenced, in which step-by-step instructions for implementation of the programs can be found. In what follows, only information relevant to current applications will be presented since the codes in question were neither modified nor used in a unique manner in the present research.

2.2.1 The LEOPARD Code [B- 1]

LEOPARD is a computer code which determines fast and thermal cross sections for square and hexagonal lattices. A neutron spectrum calculation (which is based on a modified MUFT [B- 2] - SOFOCATE [A- 3] model) is done for an "equivalent" unit cell. The unit cell (see Figure 2.1) consists of a cylindrical fuel rod, a metallic clad around the fuel rod, a moderator region surrounding the clad, and an extra region. The code can be used to calculate depletion effects for an infinite reactor; and the spectrum before each depletion time step is recomputed.

The LEOPARD code was written to perform spectrum calculations on fuel pin cells and supercells typical of PWR fuel assemblies presently in commercial use. The fuel pin geometry consists of the fuel and moderator regions as shown in Figure 2.1. When a supercell calculation is performed, a region (denoted the "extra" region) is introduced to account for water holes, water gaps between assemblies, control rod sheaths,

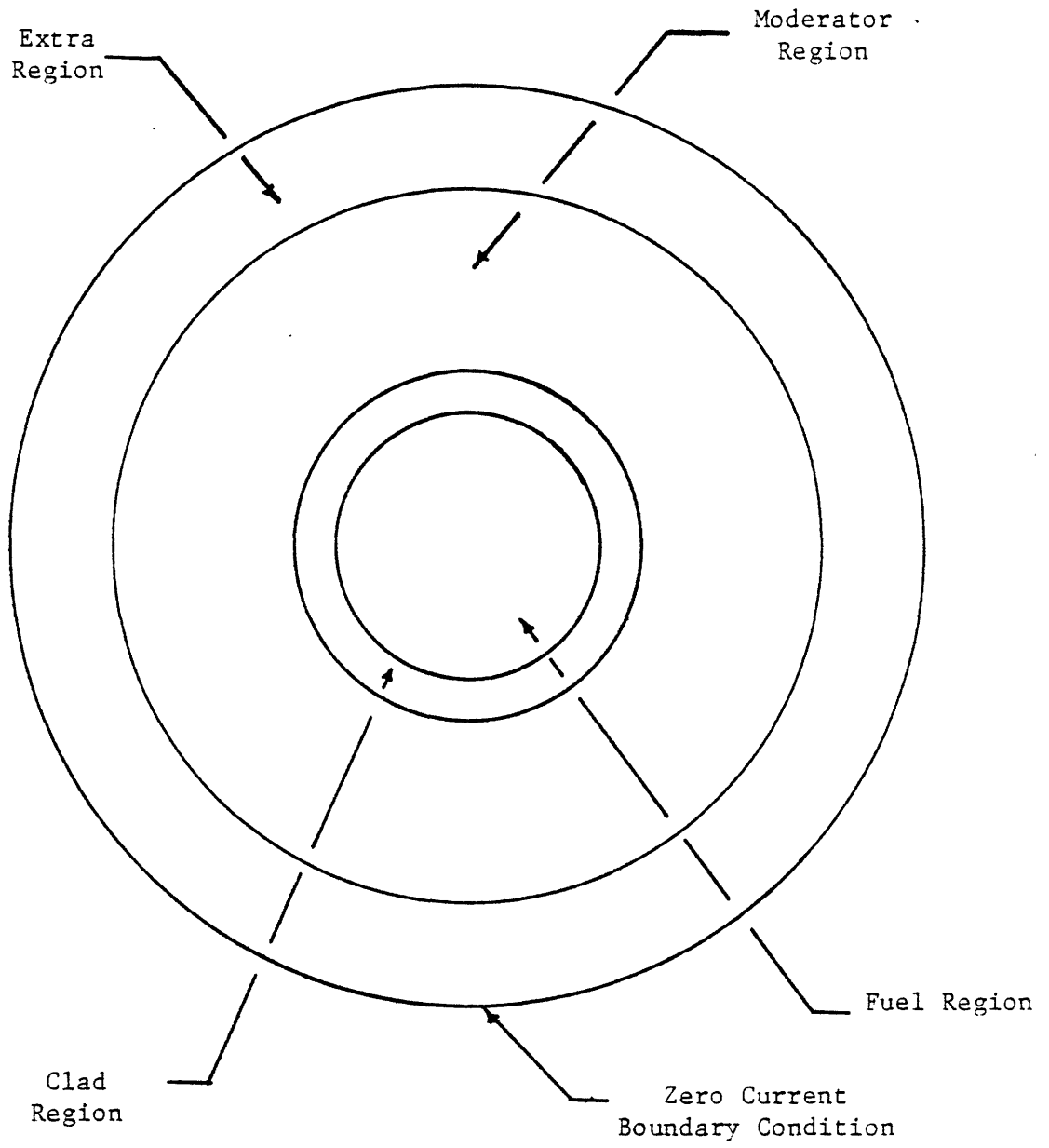


Figure 2.1 LEOPARD UNIT CELL GEOMETRY

spacer grids and structural material.

An EPRI version of LEOPARD [B-1] was used in the present work together with its microscopic cross section library derived from ENDF/B-IV (using a code called SPOTS [B-1]). Thus, the user need only supply region dimensions, material compositions, region temperatures and burnup time-steps.

As previously mentioned, the LEOPARD spectrum calculations are based on a modified MUFT-SOFOCATE model. The MUFT subprogram solves the Fourier transformed (with respect to space) Boltzmann equation using the B_1 approximation, to obtain the first two components of the flux and the slowing down densities. The spectrum is first calculated for 54 energy groups (.625 eV - 10 MeV) and then used to collapse the microscopic cross sections to 1 or 3 energy groups. The Grueling-Goertzel approximation is used to calculate the slowing down densities. The $L(U^{238})$ factor used in LEOPARD corrects for fertile resonance self-shielding, (incorporating the Dancoff effect and Doppler broadening) by normalizing to an experimental resonance integral correlation [S-2].

The SOFOCATE subprogram calculates the thermal spectrum (for 172 energy groups) by using the Wigner-Wilkins treatment. Both MUFT and SOFOCATE perform homogeneous unit cell calculations. This approximation is valid for epithermal calculations since the mean free path of a fast neutron is much greater than the dimensions of the unit cell. For thermal calculations the heterogeneity of the lattice must be taken into account. The SOFOCATE code includes the calculation of an energy dependent disadvantage factor using an approach similar to the ABH [A-4] method. The microscopic cross sections are then modified by the disadvantage factors, a conventional spectrum calculation is performed for a homogeneous

medium, and spectrum-averaged one-group thermal cross sections are computed. LEOPARD also corrects first group cross sections using a flux advantage factor.

One option of the LEOPARD code utilizes the Mixed Number Density (MND) thermal activation model [B- 3]. This model uses a boundary condition of neutron activation continuity rather than flux continuity over an energy interval. The MND boundary condition corrects for the discontinuity of thermal reaction rates due to a discontinuity in microscopic cross sections at material interfaces (fuel cell next to a water gap). The values of Σ_a and $\nu\Sigma_f$ are averaged over a Wigner Wilkins spectrum, but the values of D are averaged over a Maxwellian spectrum

LEOPARD also performs zero dimensional depletion calculations. Spatial effects are neglected, but the user may input a buckling value to account for leakage. The spectrum is calculated at the beginning of each depletion time-step; the spectrum averaged cross sections and the group fluxes are then used to solve the depletion equations (which determines the new isotopic concentration). This process is repeated for all depletion time steps.

2.2.2 CHIMP

The CHIMP code [C-1] was written by YAEC to handle the numerous data manipulation and input preparations associated with fuel management studies. CHIMP is composed of six sections, and performs the following operations:

1. Prepares two group macroscopic cross sections for the fueled region in the PDQ-7 program. The user must input macroscopic cross sections for all possible

combinations of boron concentration and burnup. CHIMP fits a spline curve through the data, allowing the user to obtain macroscopic cross sections at the desired burnups and boron concentrations.

2. Prepares two group macroscopic cross sections for unfueled regions of PDQ-7. The user must input macroscopic cross sections as a function of boron concentration. CHIMP fits a spline curve through the data, allowing the user to obtain macroscopic cross sections at different boron concentrations.
3. Prepares complete sets of input, including two-group macroscopic cross sections, for the FOG [F-1] code (not available at MIT and not used in the present work). The user must input macroscopic cross sections for all combinations of boron concentration and moderator temperature. CHIMP fits a spline curve through the data, allowing the user to obtain macroscopic cross sections at the desired moderator temperature and boron concentration.
4. Prepares complete sets of input for LEOPARD (fueled and unfueled cases). This program requires number densities as punched by LEOPARD for all possible combinations of burnups, boron concentrations, resonance temperatures, moderator temperatures, and moderator pressures. CHIMP fits a spline curve

through the data, allowing the user to obtain LEOPARD input decks at the desired burnup, boron concentration, resonance temperature, moderator temperature, and moderator pressure.

5. Prepares microscopic and macroscopic cross section table sets for HARMONY [B-4]. The code accepts microscopic cross section as punched by LEOPARD for each isotope contained in the LEOPARD cross section library. CHIMP then punches, for each isotope, microscopic and macroscopic table sets. These table sets can be either Master table sets (independent of burnup) or Interpolating table sets (function of burnup).

6. Prepares the polynomial fit constants for the two-group macroscopic cross sections used in the SIMULATE [V- 1] program. This part of the code performs two different types of calculations. First, the code calculates a polynomial fit for an arbitrary array of x and y data points. Second, the code calculates the "B" constants needed in SIMULATE for each fuel type. The inputs required for B constant calculations are the macroscopic cross sections at selected burnups.

2.2.3 The PDQ-7 Code

The PDQ-7 code [C- 2] solves the diffusion depletion equations in one, two, or three dimensions for rectangular, cylindrical, spherical, and hexagonal geometries. This code allows up to 5 energy groups, with

the thermal group represented by a single group or a pair of overlapping thermal groups [B- 5]. In addition to the standard eigenvalue solution to the diffusion equations, adjoint, boundary value, and fixed source calculations may be performed.

The depletion calculations and data management of the cross section data are handled by the HARMONY [B-4] system. This system provides a flexible representation of the time dependent depletion equation for any nuclide chain; the user inputs into the code the depletion equations that he wants the code to solve. HARMONY also provides a flexible representation of time-dependent macroscopic and microscopic cross sections. The user may input up to a fifth order polynomial cross section fit as a function of number density.

The code solves the diffusion equation by discretizing the energy variable and finite differencing (central) the equation in space. The one dimensional equations are solved by Gauss elimination and the two dimensional equations are solved using a single-line cyclic semi-iterative technique [V- 2]. For three dimensional problems, a block Gauss-Seidel procedure is used (each block represents a single plane). The equations for each plane are then solved by the same technique as used in two dimensions. A more detailed description of the solution scheme can be found in Reference [H- 1].

2.2.4 The FLARE-G Code

The FLARE-G [D-2] Code can be used to calculate a power distribution for a three-dimensional rectangular (XYZ) reactor. This nodal code is based on a modified one-group diffusion theory model in which the infinite medium multiplication factor k_{∞} and the migration area M^2 are

employed. The core reflector interface is treated by a modified albedo boundary condition. (This modified albedo boundary condition is not similar to the more familiar definition of albedo as the ratio of the partial "in" current divided the partial "out" current.)

The power density or neutron source at each node is a function of k_{∞} at that node, the source at the six neighboring nodes, and the transport kernel. The approximate transport kernel used in FLARE is a simple function of the migration area M^2 and the mesh spacing. FLARE-G calculates the k_{∞} for each node, accounting for the effects of neighboring control rods, local moderator density, power dependent equilibrium Xe and Sm, and local fuel exposure. The reactivity loss due to burnup is included by a simple fit of k_{∞} vs. exposure, exposure-weighted voids, and exposure-weighted local control. The reactivity effect due to changes in soluble poison concentration is accounted for by the partial fuel factors. (This is a multiplier on k_{∞} , only X-Y dependent.)

2.2.5 The BAHAR Code

The BAHAR Code [N-1] analyzes the thermodynamic characteristics of a PWR power plant. The user must input the component layout of the secondary cycle and the thermodynamic and mechanical data for each component. This program calculates the efficiency of the power plant, flowrates, pressure drops, and temperature drops for each component. The components of the primary cycle are: the reactor, steam generator (boiler) and the circulation pump. The components of the secondary cycle are: steam generator, high and low pressure turbine, feedwater heaters, coolers, condenser, pumps, and degasifier. The number of steam bleeds from the low pressure turbine is variable and there is an option to allow for

superheating of the steam.

2.2.6 MITCOST-II

The MITCOST-II Code [C- 3] is a nuclear fuel cycle economics code which can be used to analyze a series of nuclear fuel histories, each history spanning the entire life of a reactor. The user must specify the energy generation (burnup, electricity or heat), masses of individual isotopes charged and discharged, unit costs for individual materials and services, and the lag or lead time at which each fuel cycle transaction occurs. In addition, the user must specify the tax schedule and the depreciation method used for the analysis. The primary result calculated is the levelized unit nuclear fuel cost per batch. In addition, the code calculates additional indices of the economic performance of the nuclear fuel. They are: the revenue requirement per batch, the levelized unit fuel cost and the revenue requirement per period, and the revenue requirement and levelized nuclear fuel cost for those batches of nuclear fuel which are not being discharged at the end of the present irradiation period.

2.2.7 ECON Code [A- 5]

The ECON Code is a simple fuel cycle economics code. Basically, the model used in this code represents a simplification of the more exact treatment used in MITCOST. This model assumes a single cash flow at the mid-point of the irradiation interval instead of continuous cash flows over an interval and the model assumes steady state conditions (reload, enrichment and burnup are the same for each cycle) for the life of the reactor. The user must specify the energy generated by a batch of fuel,

the unit cost of each transaction (e.g. cost of ore, enrichment, etc.) the mass flow for each transaction, the economic parameters defining the discount factor, and the lead and lag times for each transaction. The primary result calculated is the levelized unit nuclear fuel cycle cost.

2.3 ORE USAGE MODEL

A prime, long range concern of the reactor industry today is better utilization of uranium resources. Many design and operating changes have been proposed to better utilize uranium ore in current Pressurized Water Reactors. Such changes must be evaluated in a consistent manner, considering both the ore investment needed to place a reactor system into operation and the ore needed to operate it for a certain period of years.

Different reactor systems should be compared after some years of post-startup operation. After this transient period, the annual demand for ore has settled down since the reactor has reached equilibrium conditions. When equilibrium occurs, the annual system uranium ore demand per GWe-yr, F'_s , can be represented by a simple linear combination of average annual ore usage and startup requirements:

$$F'_s = \dot{F} + rF \quad (2.1)$$

where

\dot{F} = annual makeup ore usage requirement, U_3O_8 /GWe-yr

F = initial startup requirement, U_3O_8 /GWe

r = growth rate of the nuclear electric system, r% per year/100

This function could be used to evaluate fuel utilization in different cycles and systems.

It should be noted that separately optimizing the annual ore usage component or the initial ore requirement will not necessarily optimize the F'_s function. It is generally true that changes in LWR core design which reduce one of the components, generally increase the other. For example, increasing the conversion ratio, C , will reduce the annual makeup requirements since $\dot{F} \propto (1 - C)$. On the other hand, the initial enrichment needed to start the core up is increased, hence the initial ore requirement is increased; thus a trade-off is involved in minimizing the overall system function.

2.3.1 Ore Usage as a Function of Reactor Characteristics

If we are to evaluate different reactor strategies the parameters F and \dot{F} should be related to the appropriate characteristics (lattice pitch, batch size, reload enrichment, etc.) of each system. The functional dependence of \dot{F} and F on these reactor characteristics will be examined in this section and in Appendix A.

For neutronically similar large PWR cores, the ratio of the annual ore usage by a system of reactors of a given design $[F'_{S_2}]$ to the annual ore usage of a reference case $[F'_{S_1}]$ can be shown to be (see Appendix A for derivation):

$$\frac{F'_{S_2}}{F'_{S_1}} = \frac{\left[1 + \frac{r}{100} N_2 T_2\right]}{\left[1 + \frac{r}{100} N_1 T_1\right]} \left[\left[\frac{X_1 - X_0}{X_1 - X_w} \right] \left(\frac{n_1}{n_2} \right) \left(\frac{n_{2+1}}{n_{1+1}} \right) + \left[\frac{X_0 - X_w}{X_1 - X_w} \right] \left(\frac{n_1}{n_2} \right) \left(\frac{T_1 E_1}{T_2 E_2} \right) \right] \quad (2.2)$$

where

- T = refueling interval, years
- N = equivalent number of reload batches in the initial startup core in terms of ore usage
- X = BOL enrichment of a reload batch at steady state
- X₀ = BOL enrichment at which k=1 with saturated Xe and Sm
- X_w = enrichment plant tails composition
- n = number of fuel batches in the core

This equation provides the capability of computing ore savings as a function of changes in core design and fuel management strategy. The effects of changing the average burnup of a discharged batch, B, the refueling interval, T, or batch heavy metal loading, P, can be studied using Equation 2.2 since:

$$\frac{B_2}{B_1} = \frac{T_2 n_2}{T_1 n_1} = \frac{T_2 P_1}{T_1 P_2} \quad (2.3)$$

Equation (2.2) can also be used to study the effect of changing the linear power rating or the power density of the fuel since:

$$P = \frac{\pi d^2}{4} \frac{A_c}{2} \frac{\rho}{n} L, \text{ MTHM} \quad (2.4)$$

$$B = 0.365 \left[\frac{4 \bar{q}' n T}{\pi d^2 \rho} \right] = 0.365 \left[\frac{\bar{q}''' T}{\rho} \right] \frac{\text{MWD}}{\text{MTHM}} \quad (2.5)$$

$$E = n \frac{A_c}{2} \frac{\bar{q}' L}{1000} = \frac{B n p}{365 T} = \frac{\bar{q}''' n p}{1000 \rho} \quad (2.6)$$

where

\bar{q}' = average linear power, kw/ft

\bar{q}''' = average power density, kw/ft³

ρ = fuel density, MTHM/ft³

d = fuel pin diameter, ft

p = lattice pitch, ft

L = active length of fuel pins, ft

A_c = cross-sectional area of core, ft²

Equation (2.2) is simple to evaluate, but still quite versatile. This function will be used to evaluate ore savings as a function of changes in core design and fuel management strategy.

2.3.2 Identification of Key Characteristics

The reactor designer at the start of any analysis must postulate a set of reactor characteristics; this set includes the reactor characteristics that are to be kept constant and the characteristics the designer wishes to change. This work from the outset eliminated two possible design changes, namely variation of lattice design and use of a different fuel type (e.g. oxide vs. metal fuel). As discussed below, it has been found that current PWR lattices (for a once-through fuel cycle) were already very nearly optimum for ore and separative work requirements and that use of metal fuel in current design LWRs offers no neutronic advantages over oxide fuels (as will be discussed in more detail shortly).

A study of the effect of unit cell size on ore and SWU utilization for the once-through fuel cycle (and also for different recycle scenarios) was performed by Garel [G- 1]. In his investigation, the fuel-to-coolant volume ratio, V_f/V_m , was kept constant, but the cell dimensions were changed.

He has calculated, using LEOPARD, the ore requirements, $\text{STU}_3\text{O}_8/\text{GW}(\text{e})\text{-yr}$, and the separative work requirements, $\text{MTSWU}/\text{GW}(\text{e})\text{-yr}$, as a function of unit cell volume for current design PWR's. His results for the once through fuel cycle are shown in Table 2.1. Also shown in Table 2.1 is the levelized nuclear fuel cycle cost for each cell volume. The fuel cycle cost was calculated using the ECON code and the economic data shown in Table 2.2 and Reference [A- 1]. The results show that varying the unit cell size (fuel pin diameter at a constant V_f/V_m ratio) has a negligible effect on ore and SWU requirements and nuclear fuel cycle costs. Thus, in effect, the fuel pin diameter in use today has already been optimized with regard to ore and SWU requirements.

Garel also studied the effect of fuel to coolant volume ratio on the ore and separative work requirements of PWR systems. In this investigation, the fuel-to-coolant volume ratio (lattice pitch) was varied, but the fuel pin diameter was kept constant. His results are summarized in Table 2.3. One of the pertinent observations is that the optimum V_f/V_m occurs near $V_f/V_m = 0.482$, which is representative of fuel-to-coolant volume ratios used in current PWR lattices. Thus, the current PWR lattice pitch is also optimum with respect to ore and SWU requirements.

We did not restrict ourselves to oxide fuels in our design studies. Advantages have often been claimed regarding the use of metal fuels, thorium in particular, in LWRs [Z- 1]. This contention has been examined, with an emphasis on core neutronics and it was concluded that the use of metal fuel in current design LWRs offers no evident fuel cycle advantages over continued reliance upon oxide fuels.

Metal-fueled lattices are not neutronically superior to oxide fueled lattices for the following reasons:

TABLE 2.1

ORE AND SEPARATIVE WORK REQUIREMENTS AS A
FUNCTION OF FUEL TO COOLANT VOLUME RATIO V_F/V_M

V_f/V_m	0.338	0.4816**	0.9161	1.497
Annual Makeup Requirements* STU ₃₀₈ /Gw(e)-yr	191.0	182.0	256.5	403.6
Separative Work Requirements* MTSWU/GW(e)-yr	117.4	109.4	175.0	310.2
Levelized Fuel Cycle Cost mills/kw-hr(e)	8.934	8.490	12.155	19.501

* basis of per GW(e)-yr (rated) at a 75% capacity factor and 0.2% tails

** representative of current PWR lattices

A polynomial fit to the data gives the following optima:

	$(V_f/V_m)_{opt.}$	Minimum Requirements
Annual makeup requirements	0.4684	181.88
Separative Work requirements	0.4694	109.34
Fuel cycle cost	0.4687	8.486

TABLE 2.2

NUCLEAR FUEL CYCLE COST DATA

Income Tax fraction	= 0.50
Bond fraction	= 0.50
Stock fraction	= 0.50
Rate of return to Bondholders	= 0.08 yr ⁻¹
Rate of return to Stockholders	= 0.16 yr ⁻¹
Thermal power	= 2440. MW
Efficiency	= 0.325
Capacity factor	= 0.75
Discharge Burnup	= 33,000 MWD/MTU

	Unit Cost [A-1]	Escalation Rate (yr ⁻¹)
Uranium value \$/lb U ₃ O ₈	38.92	0.10
UF ₆ Conversion Value \$/lb. U	1.95	0.06
Enrichment Value \$/SWU	94.00	0.06
UO ₂ Fuel Fabrication \$/kg HM	99.00	0.06
Throwaway Expenses* \$/kg HM	103.00	0.06

*includes spent fuel storage, transportation, and disposal for throwaway alternative

TABLE 2.3

ORE AND SEPARATIVE WORK REQUIREMENTS

AS A FUNCTION OF UNIT CELL VOLUME

	$V_o/2$	V_o	$1.5 V_o$
Annual Makeup Requirements* STU ₃ O ₈ /GW(e)yr	184.6	182.0	181.4
Separative Work Requirements* MTSWU/GW(e)yr	111.7	109.4	108.8
Levelized Fuel Cycle Cost mills/kw-hr(e)	8.617	8.490	8.461

*basis of per GW(e)yr (rated) at a 75% capacity factor and 0.2% tails

a. Oxygen in UO_2 (or ThO_2) absorbs only about 0.15% of the neutrons in a PWR core. Hence, use of even pure U or Th metal would result in a negligible improvement in the neutron economy. Alloying constituents which would almost certainly be required, would cause the metal fuel to waste considerably more neutrons in parasitic captures.

b. One can always vary fuel pin diameter and lattice pitch to find an oxide fueled lattice which is neutronicly equivalent to a metal-fueled lattice. That is, the two lattices would have essentially identical isotopic compositions over a given burnup history. A simple thought experiment supports the above contention; first change the fuel pin diameter to match resonance integrals; then vary the pitch-to-diameter ratio (fuel to moderator ratio) to match the ratio of epithermal to thermal reaction rates. We have verified this assertion using the LEOPARD code for both uranium and thorium fuels, as summarized in Table 2.4; note that the key parameters of U-233 and U-235 consumption differ by less than 0.3%.

Given neutronic equivalence, the charge and discharge fuel composition is the same for the same burnup. If one fuel can sustain a higher power density, then it will log the burnup in a shorter calendar interval; conversely more core reloads will be required over the same calendar interval; and to first order the fissile mass required per year will be the same. For example, if metal fuel could be run at twice the power density of oxide fuel, the metal core will contain half as much heavy metal as the oxide core; if the oxide assemblies reach design burnup in three years the metal assemblies will do so in 1.5 years, and twice as many metal assemblies must be purchased each year. This equivalence is exact for once-through fuel cycles: for full recycle, faster turnover provides

TABLE 2.4

EQUIVALENT METAL AND OXIDE CORES*

A. THORIUM FUELED (U-233/Th-232)

	<u>Metal</u>	<u>Oxide</u>
BOL U-233 enrichment	2.9 w%	2.9 w%
Fuel pellet diameter	0.26 in	0.37 in
Power density	75 kw/ℓ	75 kw/ℓ
Moderator to fuel ratio	2.084	1.722
Fuel density	11.71 g/cc	10.03 g/cc
BOL k_{∞}	1.25578	1.24829
EOL k_{∞} (@ 35,000 MWD/MT)	0.86774	0.86274
BOL resonance integral, Th	18.4026	18.4032
BOL fast/thermal flux ratio	5.64131	5.59926
Net U-233 consumption (KG/TONNE)	12.3625	12.3456

B. URANIUM FUELED (U-235/U-238)

	<u>Metal</u>	<u>Oxide</u>
BOL U-235 enrichment	3.0 w%	3.0 w%
Fuel pellet diameter	0.14 in	0.37 in
Power density	80.9 kw/ℓ	80.9 kw/ℓ
Moderator to fuel ratio	3.85	1.66
Fuel density	19.1 g/cc	10.04 g/cc
BOL k_{∞}	1.27567	1.27328
EOL k_{∞} (@ 35,000 MWD/MT)	0.88166	0.88354
BOL resonance integral, U-238	22.1439	22.1906
Fast/thermal flux ratio	4.99947	5.00125
Net U-235 consumption (KG/TONNE)	24.4476	24.3818
Net Pu-239 production (KG/TONNE)	4.7665	4.8689

*All calculations using EPRI-LEOPARD with its ENDF-IV σ -Set

a small second order benefit - similar to the effect of increasing the frequency of compounding interest in financial calculations.

If the mass flow is the same over a given time interval, the fissile mass flow in particular, then the fuel cycle cost will be very nearly the same for the oxide and metal fueled cores. Under these circumstances metal fuel would have an advantage over oxide fuel only if:

- a. fabrication costs were substantially lower, but even here, since fabrication costs account for only 10 to 15% of the total fuel cycle cost, the advantage could only be a small one;
- b. the use of metal fuel would somehow permit operation in a superior neutronic regime denied to oxide fuel; ultra tight pitch lattices for example. Since oxide fuel is already used in the very tight lattices of LMFBR's, there appears to be little room for excluding oxide in comparable LWR uses. Moreover in the once-through cores of this present study, current lattice pitches are near optimum;
- c. metal fuels can be used in high burnup regimes. Uranium metals in particular have had swelling problems [G-2], which has limited uranium metal fuels to low discharge burnups (8000 MWD/MTU); on the other hand thorium metal has exhibited better stability under irradiation than uranium metal;

- d. if metal fuel would allow a smaller capital cost, that is, if metal fuels could operate at a higher power density and a lower heavy metal inventory, then the capital cost of the plant would be smaller.

In the absence of convincing arguments to the contrary, metal fuel does not appear attractive for conventional LWRs. Use in other reactors, such as LMFBRs or LWRs with ultra-tight pitch lattices, where beneficial spectral hardening can be achieved, is still an open question [C- 4].

The calculations were extended to examine the effect of power level on isotopic composition at the same burnup (using current LWR lattice design as the basis). Table 2.4 compares key parameters for lattices described in Table 2.5 at 35,000 MWD/MT.

As can be seen, for fuel cycle ore usage calculations it may be assumed to first order that isotopic composition is a function of burnup only. This is an excellent assumption in uranium fueled lattices; in the thorium fueled lattices the agreement is not as good because Pa captures are reduced at lower power levels.

These calculations were extended to examine the use of diluents in oxide fuel pins. As used in the present context diluents are chemically stable materials having low neutron cross sections (such as ZrO_2 , BeO , CeO) mixed into the UO_2 fuel pellet, thus making the fuel less dense. The reduction in density effectively reduces the cross section of the fertile U-238 which in turn, results in lower fissile loadings to support criticality. For this reason advantages have sometimes been claimed regarding the use of diluents in LWRs [S- 3].

TABLE 2.5

EFFECT OF POWER LEVEL ON DISCHARGE COMPOSITION*

A. THORIUM FUELED (U-233/Th-232)

<u>Net U-233 Consumption (kg/T)</u>	<u>Metal Fuel</u>	<u>Oxide Fuel</u>
@ 50% Power	12.0250	11.9805
@ 100% Power	12.3625	12.3456

B. URANIUM FUELED (U-235/U-238)

<u>U-235 Consumption (kg/T)</u>	<u>Metal Fuel</u>	<u>Oxide Fuel</u>
@ 50% Power	24.4907	24.4236
@ 100% Power	24.4476	24.3818

<u>Net Pu-239 Production (kg/T)</u>	<u>Metal Fuel</u>	<u>Oxide Fuel</u>
@ 50% Power	4.7400	4.8425
@ 100% Power	4.7665	4.8689

*all cases have equal discharge burnup, 35,000 MWD/MTU

The same thought experiment which tested the neutronic advantages of using metal fuels in LWRs was used to test the above contention; namely the fuel pin diameter and the lattice pitch were varied to find an oxide-fueled lattice which is neutronicly equivalent to a diluent-containing-oxide-fueled lattice. Two diluent-plus-oxide fueled lattices were compared to a current design oxide fueled lattice, as shown in Table 2.6. One lattice contained 20% voids in the UO_2 pellets (i.e. 80% T.D.), which simulated ideal limiting conditions for a diluent material (no parasitic captures) while the other lattice contained ZrO_2 (20% by volume) in the UO_2 pellets, a more realistic situation. As shown, the key parameters of U-235 consumption and Pu-239 production differ by less than a few percent. Further iterative adjustments could undoubtedly improve the agreement. Hence, in the absence of convincing arguments to the contrary diluent-containing-fuels do not appear attractive for conventional LWRs unless the use of diluent-containing fuel would somehow permit operation in a superior neutronic regime denied to current oxide fuel designs.

Recently a study has been completed at MIT which studied the effect of the Th-232/U-238 ratio on the Conversion Ratio of PWRs [C-5]. Although the main emphasis was on various recycle modes, a brief investigation of non-recycle fuel cycles was carried out. Figure 2.2 shows the annual ore consumption ($STU_3O_8/GWe-yr$) versus the initial atom fraction of Th-232 in the fertile fuel for a 3-zone PWR in which the fuel is discharged at 33,000 MWD/MTU. As shown the ore consumption rises as the Th-232 fraction increases (for the non-recycle case). For recycle cases the annual ore consumption decreases as the atom fraction of Th-232 increases. Also shown in Figure 2.2 is a sharp discontinuity at 50% atom fraction

TABLE 2.6

EQUIVALENT U-235/U-238 OXIDE FUEL LATTICES;
WITH AND WITHOUT DILUENT

	<u>Ref. Oxide Lattice</u>	<u>Oxide Lattice Fuel 80% T.D.</u>	<u>Oxide Lattice Diluent in Fuel</u>
BOL U-235 enrichment, w/o	3.0	3.0	3.0
Fuel pellet diameter, in.	0.370	0.424	0.460
Power density, kw/liter	80.9	80.9	80.9
Moderator to fuel ratio	1.66	1.40	1.41
Fuel density, g/cc	10.04	8.76	8.76
BOL k_{∞}	1.27328	1.27146	1.26195
EOL k_{∞} (35,000 MWD/MT)	0.88354	0.88576	0.87935
BOL resonance integral, U-238	22.1906	22.2035	22.2875
Fast/thermal flux ratio	5.00125	5.12399	5.03070
Diluent			ZrO ₂ *
Net U-235 consumption (KG/TONNE)	24.3818	24.3076	24.3119
Net Pu-239 production (KG/TONNE)	4.8689	4.96160	4.97812

*20% by volume of the fuel region

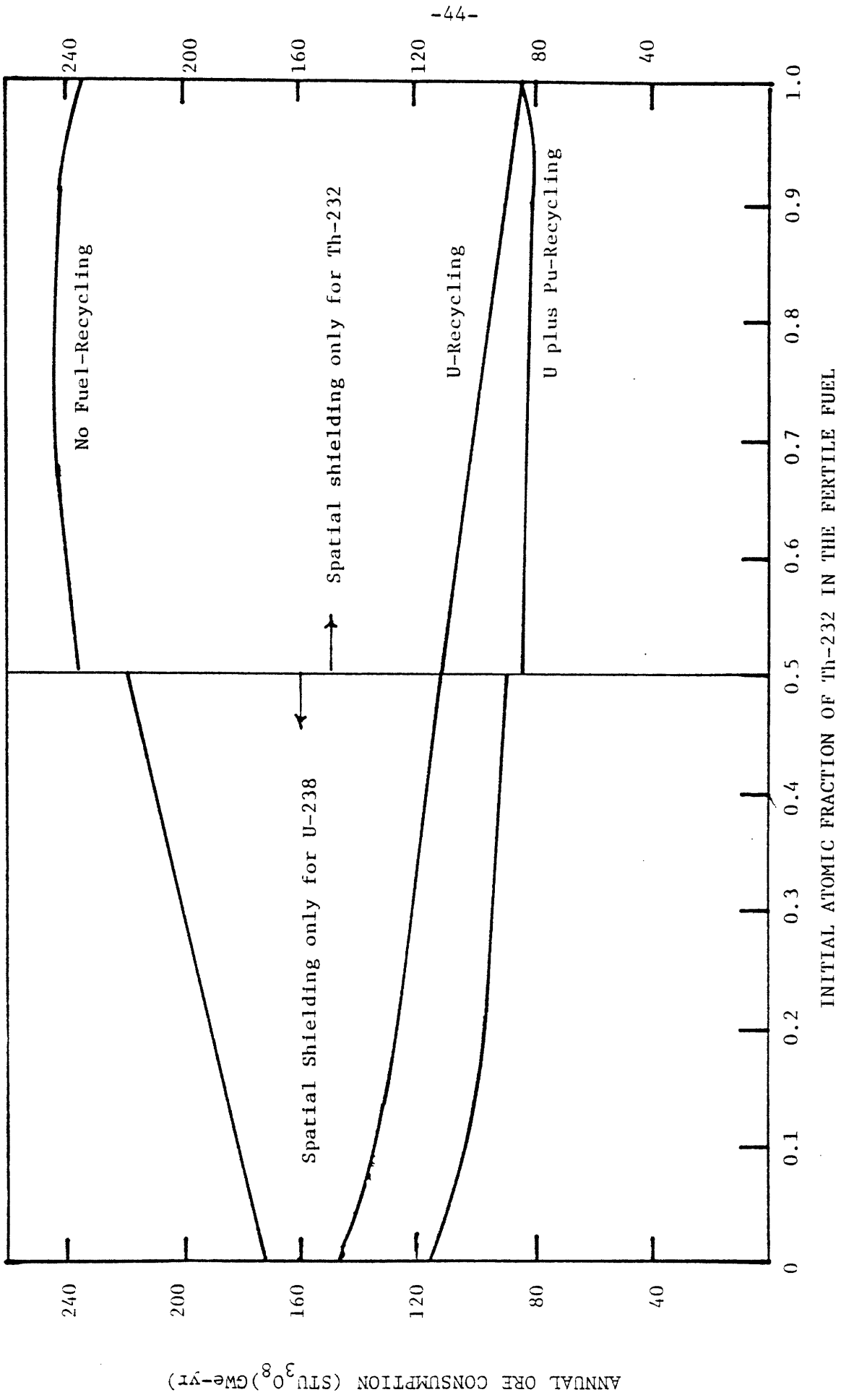


Figure 2.2 ANNUAL ORE CONSUMPTION IN MIXED THORIUM-URANIUM CORES [C-5]

of Th-232. This is due to LEOPARD's treatment of the spatial self-shielding for the heavy nuclides. LEOPARD only self-shields the most abundant fertile isotope (Th-232 or U-238) and assumes there is no self-shielding for the other heavy nuclides. Therefore a discontinuity exists when the self-shielding factors for the fertile isotope changes.

From these results it was concluded that ThO₂ should not be used in PWRs operating on the once-through fuel cycle. Consequently, this study will not pursue this area (mixed oxide fuels) any further.

For the reasons given above, we have eliminated lattice (pitch, diameter) optimization studies and fuel optimization studies (metal, diluent-containing fueled lattices, and mixed oxide fuels) as avenues for improving ore and separative work requirements in PWRs operating on the once-through fuel cycle. In the subsequent chapters we will discuss the more promising categories of design changes.

CHAPTER 3

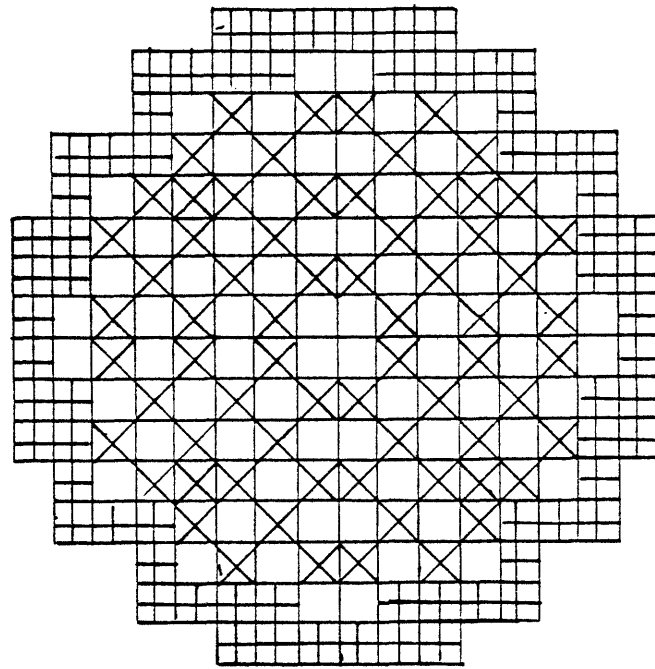
HETEROGENEOUS CORES

3.1 INTRODUCTION

The large PWRs in commercial operation today operate on a three batch cycle and use a modified out-in scatter fuel management program (see Figure 3.1). In this scheme, the fresh-fuel assemblies are generally located at the periphery of the core, and the once and twice burned fuel is placed in the interior of the core. The most reactive of the once or twice burned fuel assemblies are placed in areas which would otherwise tend to exhibit a depression in the power density, and the more highly depleted assemblies are placed in areas of high power density. In this way, coupling is improved among the once and twice burned fuel assemblies. This fuel cycling program gives favorable peak-to-average radial power distributions, both at beginning-of-cycle (generally the limiting state) and over the burnup cycle.

The modified out-in scatter fuel management program takes advantage of the heterogeneous composition of individual assemblies to flatten the power distribution. This suggests that other heterogeneous core configurations may exist which will further improve the power shape, and of greater current interest, reduce uranium ore consumption. We have briefly investigated four such heterogeneous core designs: (1) enrichment gradation in the axial direction, (2) a seed-blanket core, (3) movable fuel-reactivity control, and (4) enhanced reflector designs.

A substantial reduction of the peak-to-average power ratio can be attained by charging fuel of different enrichments to different zones in the reactor, or by using a different concentration of poison in



- Twice Burned Fuel
- Once Burned Fuel
- Fresh Fuel

Figure 3.1 REACTOR FUEL LOADING SCHEME FOR A PWR

different parts of the reactor. This is generally associated with radial power shaping. However the same techniques can be used to change the axial power distribution from the usual chopped cosine distribution (associated with uniform loading) to a power distribution in which more of the reactor operates at the maximum permissible power density. The rearrangement of materials to improve the axial power shape will be called "zone loading" here.

One type of zone loaded arrangement, which is close to optimum for a reactor in which the fuel linear power limits thermal output, is a reactor designed to have uniform power density over a substantial portion of the core. The uniform power density may be achieved by providing fuel in a central region of lower enrichment than in the peripheral regions of the reactor. In addition to providing a more uniform power density, zone loading provides a more uniform burnup (i.e. time-integrated power density).

Another method of reducing the annual reload requirements of PWRs is to increase the conversion ratio, C , since the reload requirements are proportional to $(1-C)$. One attractive possibility is the seed (fissile material) blanket (fertile material) reactor concept which achieves improved breeding by reducing reactivity control poison requirements and by increasing the uranium to structure ratio $(R-1)$. One way to achieve the seed/blanket geometry in a PWR would be to segregate the seed and blanket material in a PWR fuel pin (i.e. an extreme version of graded axial enrichment zone loading. Alternate layers of enriched fuel and blankets pellets would be stacked in a fuel pin. During the life of the core, the enriched fuel would be depleted, but fissile material will be produced in the blanket zones, which would compensate for some of the reactivity loss

due to burnup and fission product poisoning. In addition, the control poison requirement is reduced since the reactivity swing from BOL to EOL is reduced; therefore fewer parasitic absorptions occur and the reload enrichment decreases.

Approximately 5% of cycle-average fission neutrons are lost to the control poison in a typical PWR; hence if the control poison could be eliminated a modest, but not insignificant, ore savings could be achieved. The use of fertile material as control elements may replace the need for control poison. Various "movable" configurations of fertile and fissile material were investigated to see if control poisons could be replaced by movable fertile control rods. The results for the chosen configurations were not promising, but worth reporting.

It is usual to surround the core of a thermal reactor with a reflector region. In this way, many neutrons that would otherwise leak from the core, instead have elastic collisions with the reflector and are returned to the core. This leads to a reduction in critical mass requirements.

Presently, PWR cores are reflected by light water (containing soluble control poison) closely backed by a core shroud and barrel (materials with high absorption cross sections). The motivation for investigating enhanced reflector designs can be explained by the concept of reflector savings. (Reflector savings is defined as the decrease in the critical

dimensions of a reactor when the core is surrounded by a reflector). For an effectively infinitely thick reflector (thickness of reflector is greater than one or two diffusion lengths), the reflector savings, δ , is shown to be [L-1]:

$$\delta \approx \frac{\bar{D}_c}{\bar{D}_r} L_{T_r} \quad (3.1)$$

where

\bar{D}_c = average core diffusion coefficient, cm

\bar{D}_r = average reflector diffusion coefficient, cm

L_{T_r} = thermal diffusion length (reflector), cm
= $(D_r/\Sigma_{ar})^{1/2}$

If one notes that the diffusion length varies inversely with the square root of the absorption cross section, it follows from Equation (3.1) that the reflector savings increases as the absorption cross section of the reflector decreases. Thus the critical dimensions of the core tend to be smaller when the material used for the reflector has a low absorption cross section.

Beryllium oxide has an absorption cross section which is one order of magnitude lower than the absorption cross section of light water. Hence, by using beryllium oxide reflectors in PWRs modest ore savings should be achievable. Depleted UO_2 (0.2 w/o U^{235}) can also be considered for use as the reflector material. In this arrangement neutrons leaking from the core would be absorbed by fertile ^{238}U atoms and transformed into fissile plutonium. The buildup of plutonium atoms in the reflector should offset some of the reactivity loss due to the burnup process; hence the fissile loading required at BOL will be lower.

The reader will recognize that many of the above ideas have received extensive prior (and continuing) examination in the LWBR program [E-1]. The reason this limited re-evaluation is worthwhile lies in the concern of the present work with the once-through fuel cycle, as opposed to the LWBR, for which recycle is a necessity.

3.2 PREVIOUS WORK

A literature search has revealed that little work has been done in the area of axial zone loading to achieve power shape improvements and ore utilization in PWRs. But axial zoning has been used to some degree in other reactor types. Ducat [D-3] has found that internal blanket regions (parfait cores) in LMFBRs could be used to flatten the flux and power distribution in the plutonium-loaded zones of the core, particularly in the axial direction. The core designs of HTGR and CANDU reactors involve partial length fuel assemblies, which makes it possible to apply axial fuel management principles to flatten the power distribution. Hoppes [H- 2] has found for HTGRs that an axial push-through fuel scheme, with the proper choice of fuel composition, will result in an improved power shape. CANDU reactors employ bidirectional refueling [P- 2]; the bundles are pushed through the core in opposite directions in adjacent channels in order to smoothen and symmetrize the axial power shape. Until recently, LWR fuel rods were loaded with uniform enrichment in the axial direction; however it is understood that GE [P- 3] has recently proposed an axial zone loaded assembly for the BWR-6 which has four different axial enrichments and a non-uniform distribution of burnable poison.

While the neutronics of zone loaded PWR cores has not been studied, the thermal-hydraulic effects of changes in the axial power distribution has been examined. Boyd [B-6], for example, has investigated a variety of power shapes; our interest here is in his results for the flat power distribution and cosine power distribution; namely, that if the power distribution is changed from the cosine distribution to the flat distribution, the linear heat generation rating may be increased in such a way as to

preserve current thermal margins set for PWRs. For example, in a zone loaded core the peak-to-average power ratio is lower than for a uniformly loaded core; thus the peak linear heat generation rate is lower in a zone loaded core. The average linear heat generation rate can be increased in the zone loaded core such that the peak linear heat generation in the zone loaded and uniformly loaded core are identical; hence the zone loaded core may operate closer to the current thermal margins set for PWRs. In addition, Boyd used a single-channel thermal hydraulic code, which tends to give inherently conservative answers. From the above observations, we can postulate that zone loading to achieve a flatter axial power distribution and a higher power density core can be done in such a way as to preserve current thermal-hydraulic margins set for PWRs.

Previous work has shown that the cost incentive for increasing specific power is small; Gallagher [G- 3], for example has shown this for a PWR with a 10% higher specific power. This lack of sensitivity is due to the fact that isotopic compositions to first order are a function of burnup only and not the power level that the nuclear fuel was operated at (Section 2.3.2). For example, if a reactor can sustain a higher power density, then it will log the burnup in a shorter calendar interval; conversely more reloads will be required over the same interval; and to first order the fissile mass required per year will be the same; hence fuel cycle cost incentives are small.

The movable radial seed/blanket core has been developed at Bettis for the LWBR [E- 1]. A typical module contains a central seed which is movable and a stationary annular axial blanket. The position of the movable seed fuel assembly is changed relative to the stationary blanket

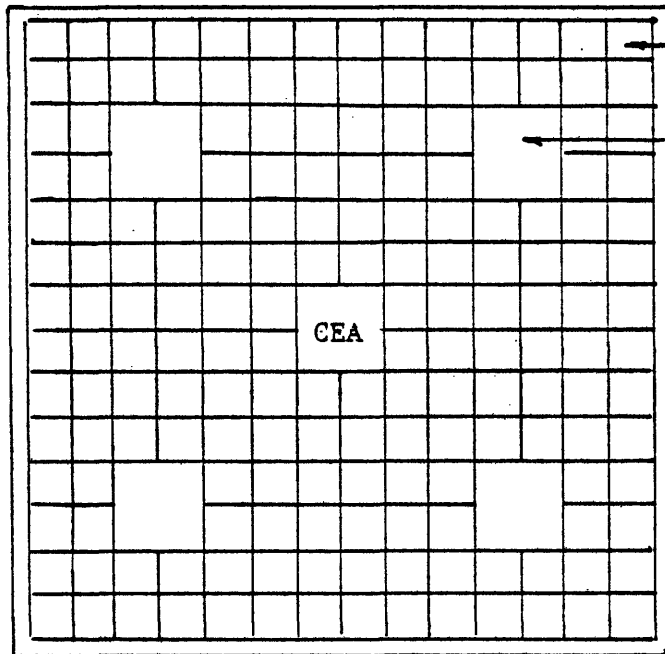
assembly to achieve criticality throughout the life of the core. Since the reactivity is controlled by varying the leakage of neutrons from high importance regions (seed) into low importance regions (blanket), control poisons (e.g. boron or gadolinium) can be eliminated; and this improves the neutron economy. We have briefly examined incorporation of a rudimentary movable axial seed/blanket concept into current PWRs. These design changes will be discussed in subsequent sections.

3.3 DEPLETION MODEL

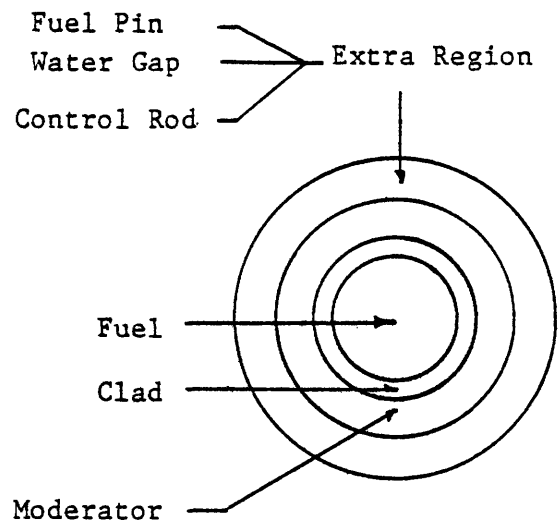
The use of the LEOPARD point depletion model is adequate for estimating fissile loading requirements, cycle lengths, and isotopic mass balances, but the determination of power distributions and core operating characteristics require that spatial calculations be performed. The few group PDQ-7 spatial diffusion depletion model used for this purpose will be described below.

3.3.1 Cross-Section Generation

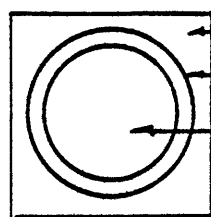
The LEOPARD Code was used to calculate diffusion theory parameters for "pincells" and "supercells". The "pincell" consists of a cylindrical fuel region which is surrounded by annular regions of clad and moderator. This geometric model is equivalent to one fuel pin in a water gap pin in a typical PWR assembly (Figure 3.2). The "supercell" has the same geometry as the pincell, but an additional annular region surrounds the clad. This region is called the "extra" region. The "extra" region accounts for that portion of a reactor core containing water gaps, control rod sheaths, and structural material. Hence, the supercell is LEOPARD's geometrical model of a typical PWR fuel assembly.



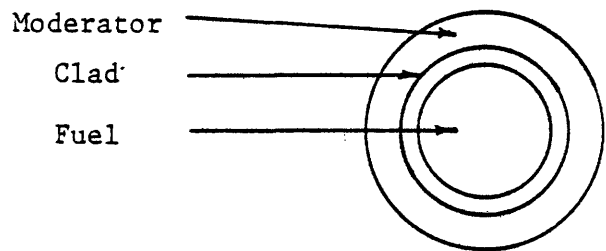
FUEL ASSEMBLY



LEOPARD SUPERCELL



Fuel Cell



Leopard Pin Cell

Figure 3.2 LEOPARD GEOMETRICAL REPRESENTATIONS

The calculations of diffusion theory parameters for pincells requires minimal input (region dimensions, material compositions and region temperatures), but the assembly-averaged diffusion theory parameters can not be calculated (at least not accurately) by the LEOPARD supercell model unless a diffusion theory spatial calculation for the fuel assembly is performed in parallel. A PDQ-7 spatial solution for one fuel assembly is performed first so that the fast-to-thermal flux ratio, ϕ_1/ϕ_2 , and the k_∞ of the assembly may be found. The supercell calculations are then performed iteratively, that is, the non-lattice peaking factor required by LEOPARD for each supercell run is varied until the ϕ_1/ϕ_2 ratio and the k_∞ of the LEOPARD supercell calculation match the results of the PDQ spatial calculation. When the ϕ_1/ϕ_2 ratios and the k 's match, the group constants calculated by the PDQ flux weighting procedure and the LEOPARD supercell calculations are equivalent.

Depletion studies require group constants as a function of burnup since the energy spectrum of a reactor core changes significantly when the fuel materials are depleted. The group constants needed for the depletion studies are obtained using the LEOPARD supercell depletion model.

As previously mentioned, this study used the EPRI-version of LEOPARD and its companion ENDF/B-IV cross section library. Garel [G-1] tested this code against 63 slightly enriched uranium (U-235/U-238) light water lattices (as well as 42 plutonium-enriched uranium oxide light water lattices and 5 ^{233}U enriched thorium oxide light water lattices). He found that the EPRI-LEOPARD code is suitable for cross section generation for conventional slightly enriched ($\text{U}^{235}\text{-U}^{238}$) light water lattices: the average k for the 63 cases was 1.00257.

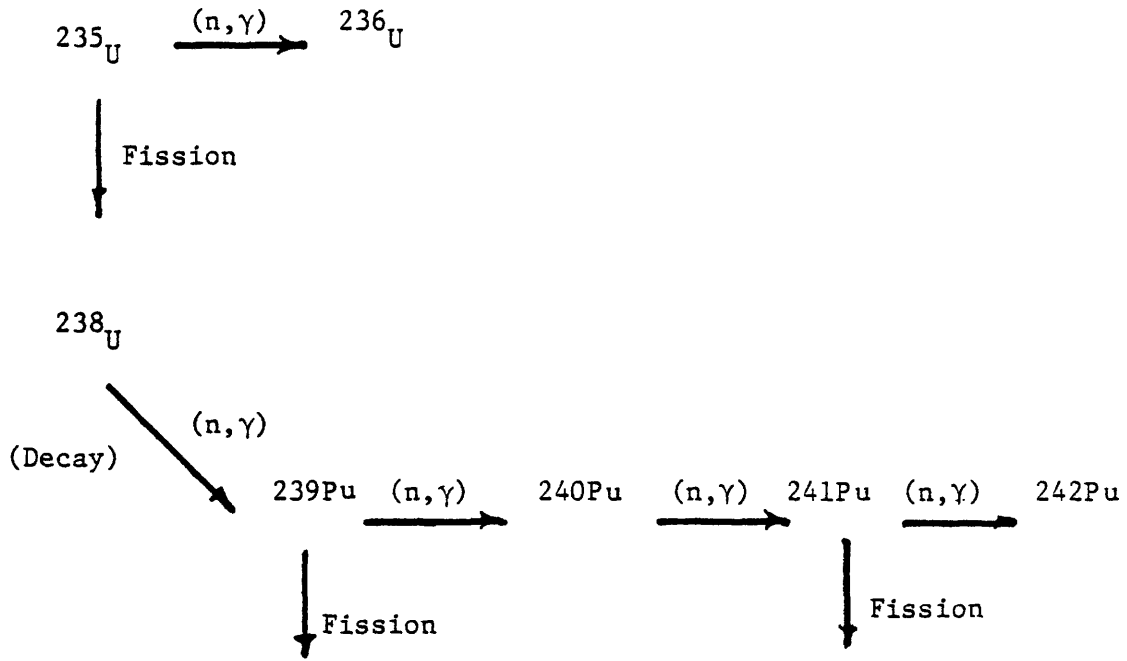
3.3.2 Power Distributions

The PDQ-7 code, described in Section 2.2.3 was used to calculate a power distribution for the reactor core. The power distribution was calculated at the beginning-of-cycle (BOC) and at various times during the life of the core. The calculation of the power distribution at various times during the life of the core requires a two step process. First, for an initial description of the reactor (geometry and composition known), the neutron flux distribution is found by PDQ for two energy groups and for all spatial mesh point locations. The spatial flux is combined with the nuclear cross sections ($\kappa \Sigma_f$) to obtain the power distribution. Next, using the power distribution from the spatial calculation, the differential equations describing the buildup and loss of nuclide concentrations are solved for that time interval. The solution of the depletion equations yields new nuclide concentrations which are used in the generation of two-group sections for the next spatial calculation.

3.3.3 Depletion Chains

The LEOPARD code uses a "simplified" fuel depletion and fission product chain structure to account for fission product poisoning and the buildup and burnout of isotopes. This same fuel depletion and fission product chain structure was implemented in the PDQ-7 depletion model (see Figure 3.3 and Table 3.1). A more elaborate chain structure was not used in the depletion model since the conclusions to be drawn

DEPLETION CHAINS



FISSION PRODUCT CHAINS

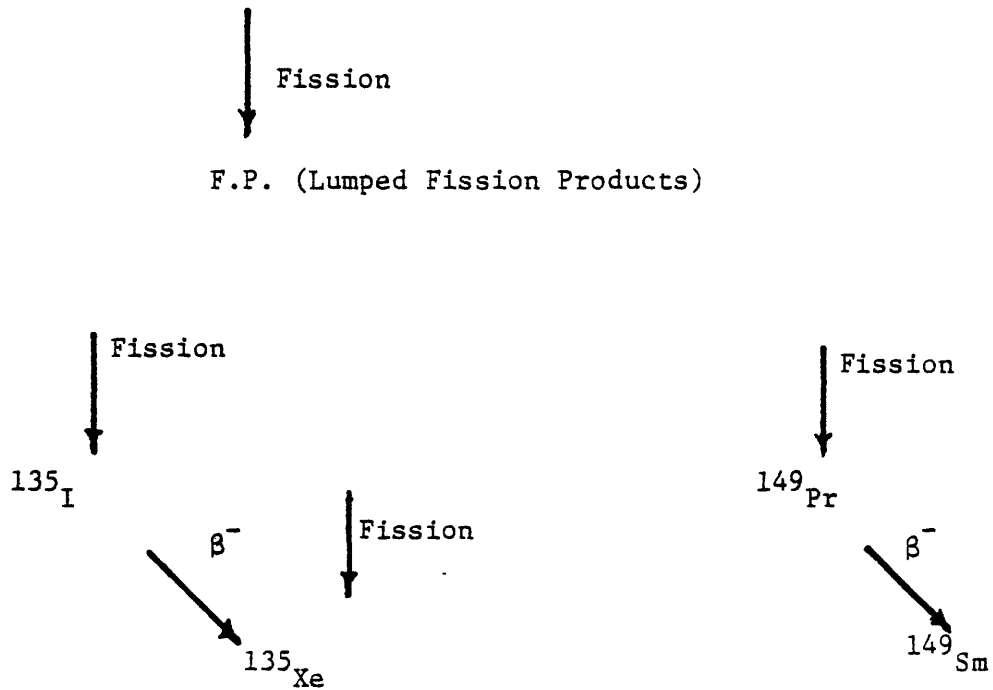


FIGURE 3.3 DEPLETION AND FISSION PRODUCT CHAINS USED IN THE PRESENT STUDY

TABLE 3.1

FISSION YIELDS AND DECAY CONSTANTS

<u>Element</u>	<u>I-135</u>	<u>Xe-135</u>	<u>Pr-149</u>	<u>Sm-149</u>	<u>λ, sec^{-1}</u>
U-235	0.062	0.002	0.0113	0	0
U-236	0.062	0.002	0.0113	0	0
U-238	0.062	0.002	0.02	0	0
Pu-239	0.070	0.002	0.0189	0	0
Pu-240	0.070	0.002	0.0189	0	0
Pu-241	0.063	0.002	0.02	0	0.17×10^{-8}
Pu-242	0.063	0.002	0.02	0	0
I-135					0.288×10^{-4}
Xe-135					0.211×10^{-4}
Pr-149					0.385×10^{-5}
Sm-149					0

from the present work do not depend upon an extremely accurate description of the nuclear properties of a PWR. In addition, the use of a detailed chain structure in PDQ-7 would significantly increase computer running time and memory requirements.

3.3.4 Calculational Procedures for Depletion Studies

The PDQ-7 diffusion-depletion model is summarized below and in Figure 3.4.

1. The LEOPARD code is used to calculate diffusion theory constants for all types of pincells: different enrichments and water cells.
2. The PDQ-7 code is then used to calculate a spatial solution for each type of assembly. The pincell cross-sections are flux weighted so that a homogenized set of cross sections is found for each type of assembly. The ϕ_1/ϕ_2 ratio and k_∞ for each assembly is also determined.

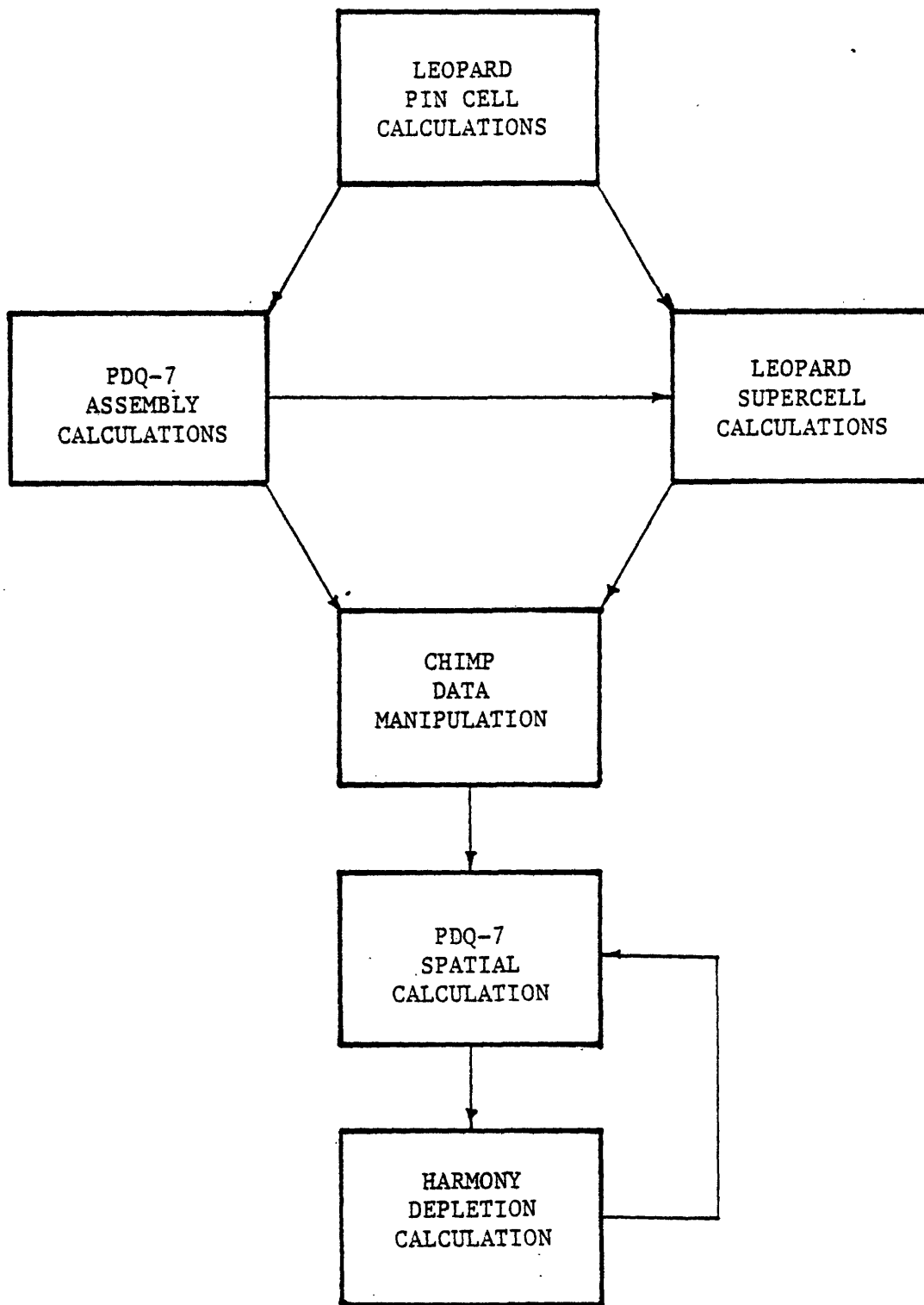


Figure 3.4 DIFFUSION-DEPLETION MODEL

3. LEOPARD supercell calculations are then performed until the PDQ ϕ_1/ϕ_2 and k_∞ , found in step 2, match the supercell results.
4. LEOPARD supercell depletion calculations are performed to obtain diffusion theory constants as a function of burnup.
5. The CHIMP code is used to manipulate the output from step 4 so that the data is suitable for PDQ-7 input.
6. PDQ-7 is used to calculate the power distribution for the entire core.
7. HARMONY uses the power distribution calculated in step 6 in the depletion equations to find the buildup or loss of each isotope.
8. Steps 6 and 7 are repeated until reactivity limited burnup is reached.

3.4 REACTORS INVESTIGATED

3.4.1 Zone Loaded Core

The C-E PWR system shown in Figure (3.5) was used as the design basis for this study. The assembly consists of a 14 x 14 array of fuel cells and five large control rod channels. The design characteristics for the assembly and reactor are shown in Table 3.2. This system was chosen to be the design basis since it is typical of a large PWR in

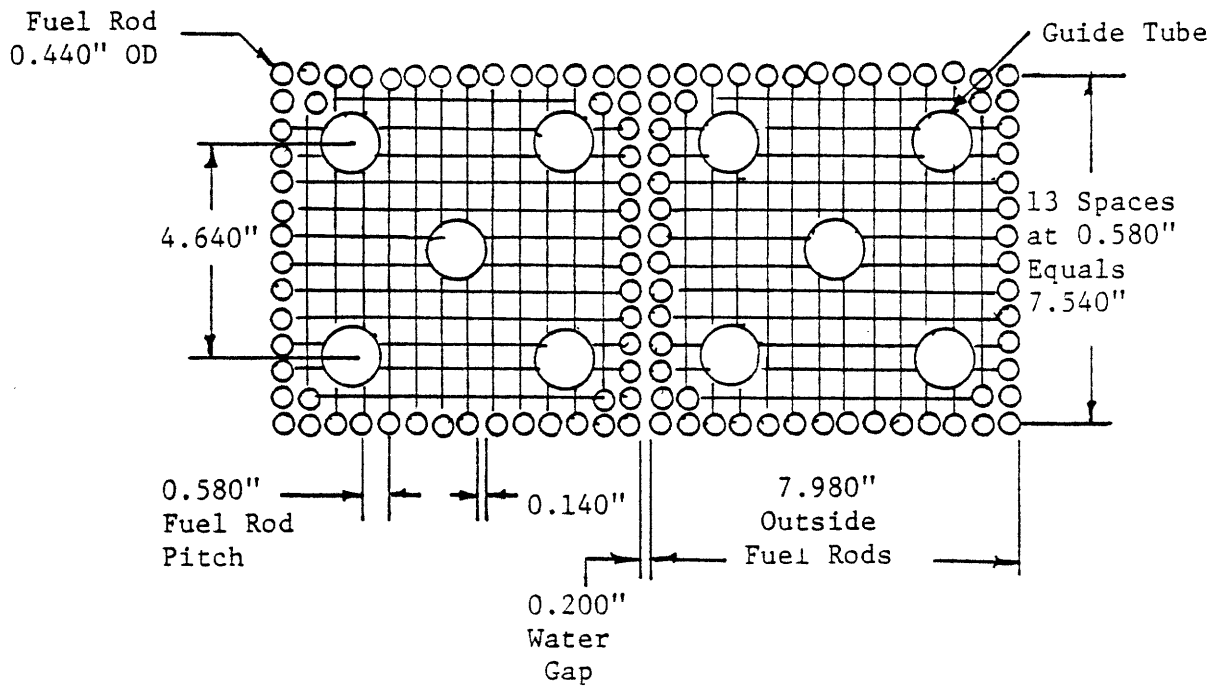
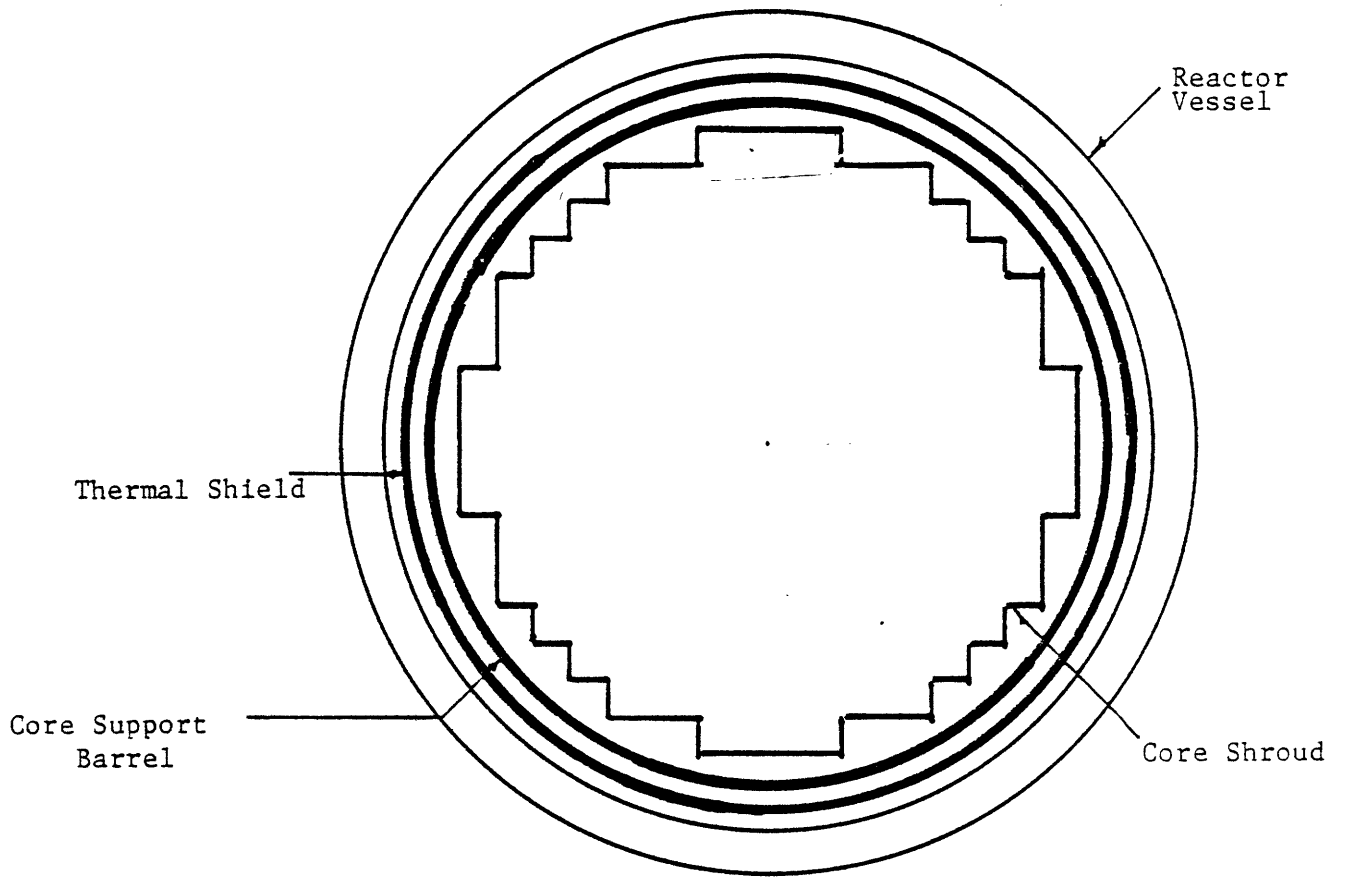


Figure 3.5 REACTOR CORE CROSS-SECTION

TABLE 3.2

MECHANICAL DESIGN FEATURES

Fuel Assembly:

Overall Length, in.	156.718
Spacer Grid Size (in)	8.115
No. Zircaloy Grids	8
No. Inconel Grids	1
Fuel rod growth clearance, in.	1.021

Fuel Rod:

Active Fuel Length, in.	136.7
Plenum Length, in.	8.575
Clad OD, in.	0.440
Clad ID, in.	0.384
Clad Wall Thickness, in.	0.028
Pellet OD, in.	0.3765
Pellet Length, in.	0.450
Dish Depth, in.	0.023
Clad Material	Zr-4
Pellet Density	95%

TABLE 3.2 (CONT'D)

THERMAL-HYDRAULIC PARAMETERS AT FULL POWER

<u>Characteristics</u>		
	MWT	2,440
Total Heat Output	10 ⁶ Btu/hr	8,328
Fraction of Heat Generated in Fuel Rod		0.975
Nominal Pressure	psig	2,085
Design Inlet Temperature (Steady State)	°F	546
Total Reactor Coolant Flow (Design)	10 ⁶ lb/hr	136.0
Coolant Flow Through Core (Design)	10 ⁶ lb/hr	132.1
Hydraulic Diameter (Nominal Channel)	ft	0.044
Average Mass Velocity	10 ⁶ lb/hr-ft ²	2.47
Pressure Drop Across Core (Design Flow)	psi	9.9
Total Pressure Drop Across Vessel (Based on Nominal Dimensions and Design Flow)	psi	33.1
Core Average Heat Flux	Btu/hr-ft ²	165,830
Total Heat Transfer Area	ft ²	48,978
Film Coefficient at Average Conditions	Btu/hr-ft ² -°F	5,660
Maximum Clad Surface Temperature	°F	646
Average Film Temperature Difference	°F	29.3
Average Linear Heat Rate of Rod	kw/ft	5.60
Average Core Enthalpy Rise	Btu/lb	63.1

actual commercial operation.

The PDQ-7 model used for assembly calculations represented each fuel cell explicitly, with a mesh point in each cell. The PDQ-7 model used for core calculations employed a one-dimensional coarse mesh representation of the reactor. A DB^2 correction to the absorption cross section accounted for radial leakage.

3.4.2 Seed-Blanket Cores

The slab configuration shown in Figure 3.6 was used as the design basis for this study. The blanket region contained depleted UO_2 (0.2 w/o U^{235}) and the seed region contained slightly enriched UO_2 fuel. As shown in Figure 3.6, the seed-blanket geometry is obtained by segregating the seed and blanket material in a fuel pin; alternate layers of enriched fuel and blanket pellets were stacked in the fuel pin. We analyzed three cases; for each case the thickness of each region was varied. However, the thickness of the blanket, t_B , and the thickness of the seed, t_S , were kept equal to each other ($t_B = t_S$) for each case. The nuclear and mechanical properties for this seed-blanket configuration are shown in Table 3.2. In this study, we analyzed one segment of the fuel assembly, in other words an infinite medium calculation (region enclosed by the dashed lines as shown in Figure 3.6). The PDQ-7 model represented this "sectioned" region as a one-dimensional slab. Similarly, we analyzed one segment of a fuel assembly in which the enrichment was kept constant axially. A buckling value was used to account for leakage. The BOL fissile inventory for the seed/blanket core and reference core were the same.

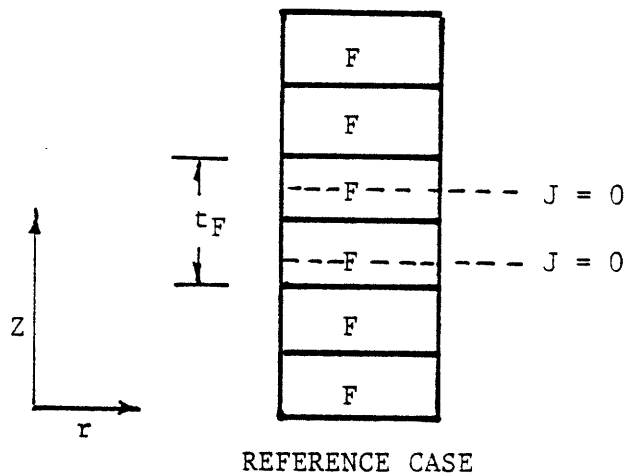
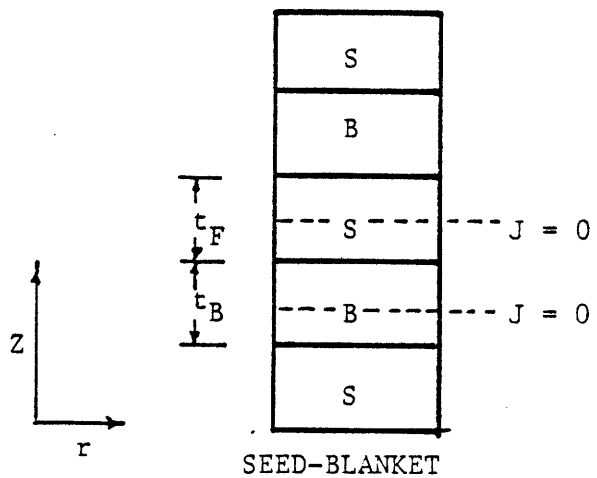


Figure 3.6 AXIAL SEED-BLANKET GEOMETRY

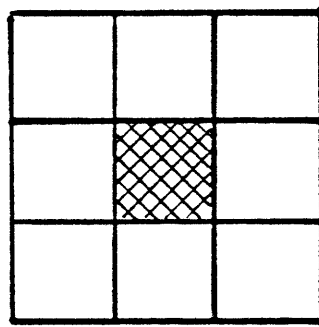
3.4.3 Movable Fuel Reactivity Control

A nine assembly module shown in Figure 3.7 was used as the design basis for this study. The geometric characteristics of these assemblies is shown in Table 3.2. Two different configurations were analyzed: Figure 3.7 and 3.8. As one can see, the blanket and fuel materials are stacked differently in each fuel assembly. In both cases, the central assembly is movable, while the eight outer assemblies are stationary. A coarse mesh, r-z geometry was employed in PDQ-7 to analyze these 9-assembly module configurations.

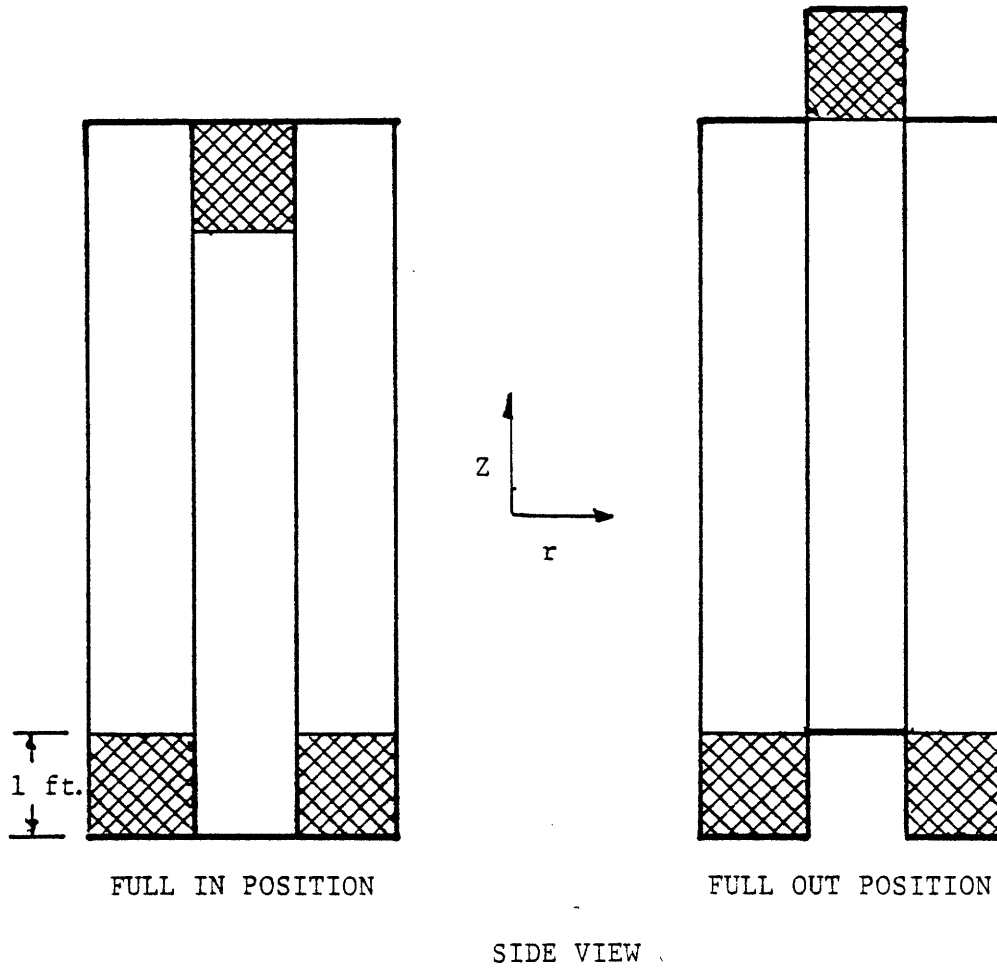
3.4.4 Enhanced Reflector Design

The C-E PWR system as described in Section 3.4.1 was used as the design basis for this study. Additional design characteristics used in this study are shown in Figure 3.9 and Table 3.3. The PDQ-7 model used for core depletion calculations employed a one-dimensional cylindrical coarse mesh representation of the reactor. A DB^2 correction to the absorption cross section accounted for axial leakage.

Three cases were analyzed, a standard 3 zone PWR with: (1) a borated H_2O reflector, (2) a pure BeO reflector, and (3) a depleted UO_2 (0.2%) reflector; the fissile loading of the core remained constant, only the reflector material was changed. For case (2), a pure BeO reflector was used, no attempt was made to include the structural material, which will clad the BeO or the borated water, which will cool the reflector. For case (3) it was assumed that the UO_2 (0.2 w/o) pellets were loaded into standard design fuel assemblies (Table 3.2).



TOP VIEW OF NINE ASSEMBLY MODULE



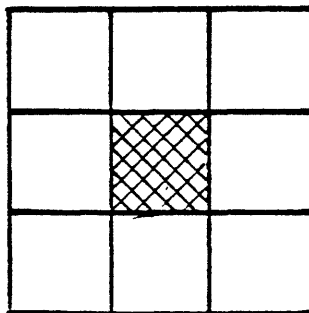
FULL IN POSITION

FULL OUT POSITION

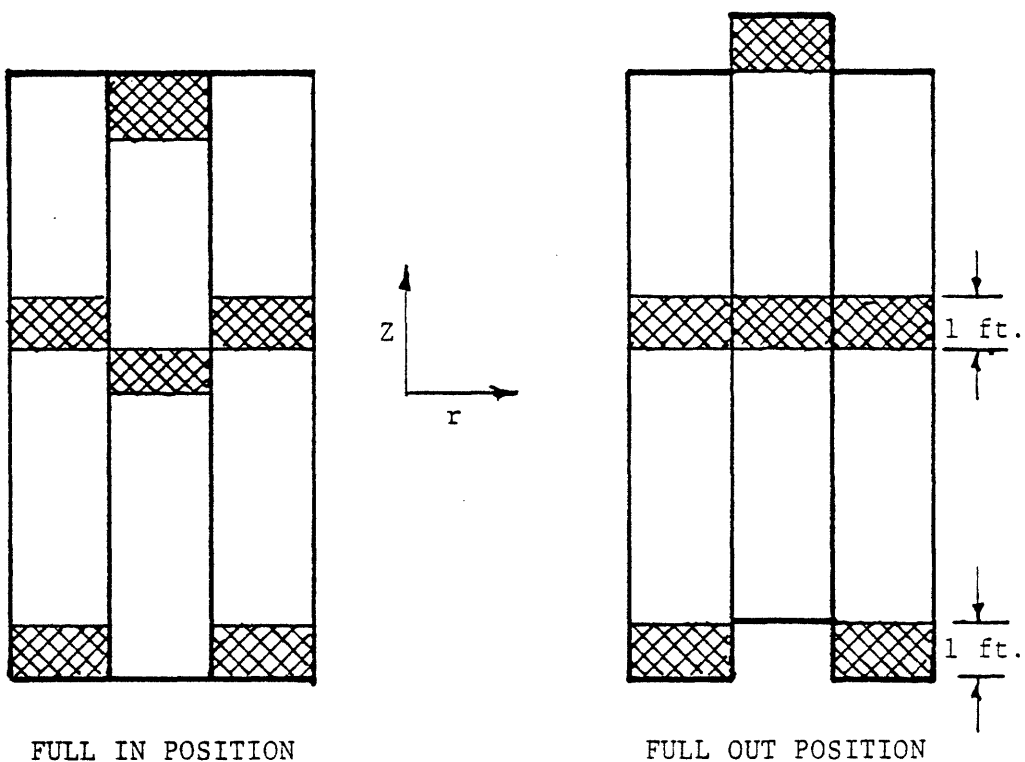
SIDE VIEW

(shaded areas are depleted Uranium blankets)

Figure 3.7 MOVABLE FUEL REACTIVITY CONTROL DESIGN #1



TOP VIEW OF NINE ASSEMBLY MODULE



FULL IN POSITION

FULL OUT POSITION

SIDE VIEW

(shaded areas are depleted Uranium blanket)

Figure 3.8 MOVABLE FUEL REACTIVITY CONTROL DESIGN #2

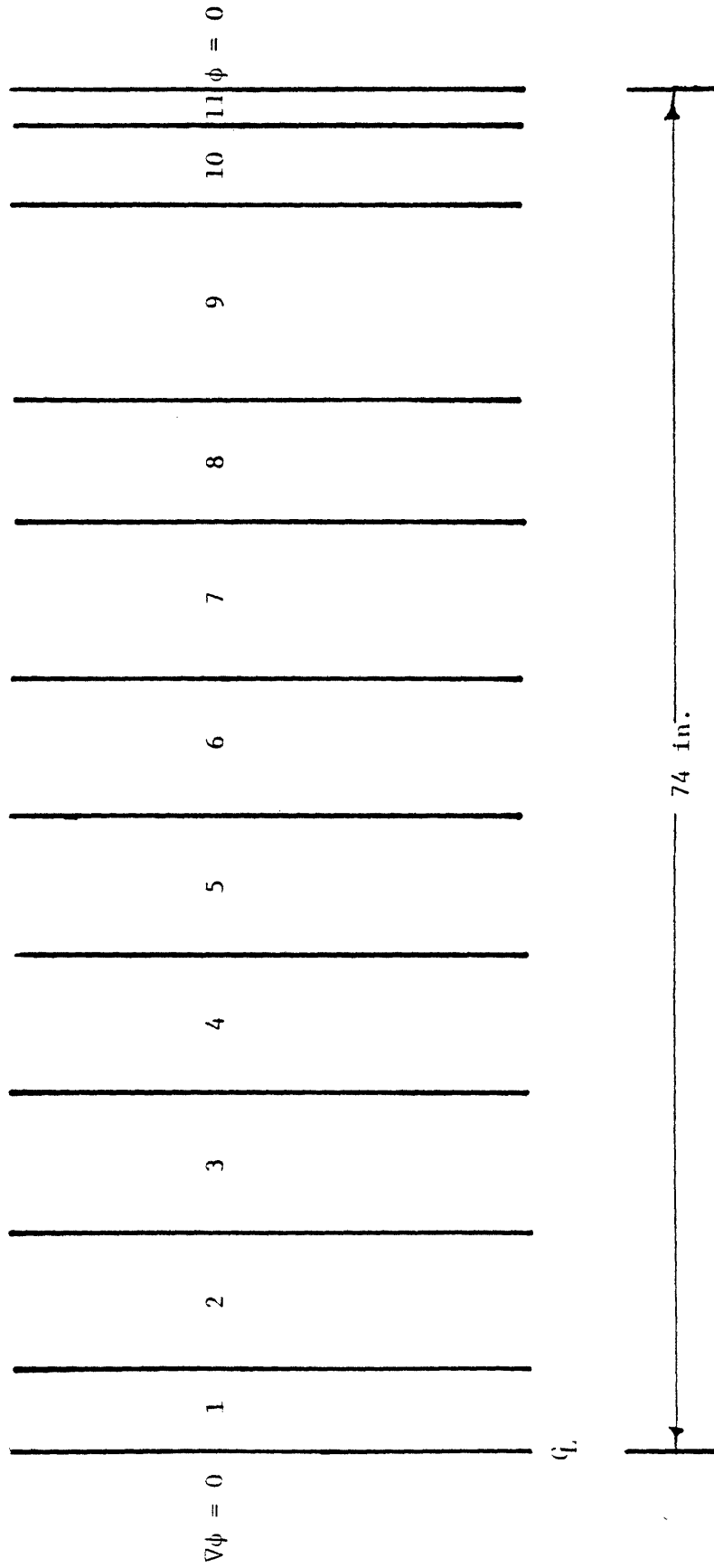


Figure 3.9 ENHANCED REFLECTOR STUDY, PDQ-7 GEOMETRICAL REPRESENTATION (CYLINDRICAL.)

TABLE 3.3

ENHANCED REFLECTOR STUDIES: DESIGN PARAMETERS

Three Batch Core

Equivalent Core Diameter, in. = 136

Equivalent Core Height, in. = 136.7

Power Level, Mw(th) = 2440

Pressure, Psi = 2100

Enrichments w/o

A Assembly* = 1.95

B Assembly* = 2.52

C Assembly* = 2.90

Zone Number	Assembly Type	Outer Radius (in.)
1	A	4.62
2	B	12.01
3	A	19.70
4	B	26.79
5	A	34.18
6	B	71.57
7	A	49.96
8	B	56.35
9	C	68
10	Reflector	72
11	Baffle	74

Reflector Materials: Borated H₂O, BeO, Depleted U (.2 w/o)

Baffle Material: S.S. 316 + H₂O

*Mechanical Data for assembly given in Table 3.2

3.5 RESULTS

3.5.1 Zone Loading

In this section, the results of employing enrichment gradation in the axial direction to improve the power distribution will be reported. The following points will be discussed: (1) the effect of zone loading on ore usage (2) representative cases of zone loading, in which the use of two axial enrichments has been employed to reduce the central power peak in BOL cores, (3) the possible safety consequences associated with zone loading.

3.5.1.1 Ore Usage Model

The ore usage model developed in section 2.3.2 will be used to analyze the benefits (ore savings) accrued when power flattening improvements are made. The relative annual ore usage by a system of reactors of a given design $[F'_{s_2}]$ STU₃O₈/GWe-yr, compared to a reference system $[F'_{s_1}]$ was found to be:

$$\frac{F'_{s_2}}{F'_{s_1}} = \left[\frac{1 + \frac{r}{100} N_2 T_2}{1 + \frac{r}{100} N_1 T_1} \right] \left[\left(\frac{X_1 - X_0}{X_1 - X_w} \right) \left[\frac{n_1}{n_2} \right] \left[\frac{n_2 + 1}{n_1 + 1} \right] + \left[\frac{X_0 - X_w}{X_1 - X_w} \right] \left[\frac{n_1 T_1 E_1}{n_2 T_2 E_2} \right] \right] \quad (2.2)$$

(The parameters have been defined in section 2.3.2) For an individual reactor in the steady state mode, $r \equiv 0\%$.

The above equation can be used to study the effect of power shape improvements (i.e. holding peak conditions fixed and increasing the average and total core thermal power rating), since the discharge burnup, B, is

$$B = \frac{8,766}{24} \frac{ET}{P} \text{ MWD/MTHM} \quad (3.2)$$

or

$$\frac{B_1}{B_2} = \frac{E_2 T_2 P_1}{E_1 T_1 P_2} \quad (3.3)$$

where

E = capacity-factor-weighted power level, MW(th)

T = period between refuelings, yrs

P = batch heavy metal loading, MTHM

Equation 3.2 shows that in order to increase the burnup for a given heavy metal loading either the irradiation time or the total core thermal power output (over the same time period) must be increased. However, if the burnup is increased the feed enrichment must also be increased to compensate for the increased ^{235}U depletion and fission product poisoning.

It will be shown in subsequent sections that increasing the burnup of spent fuel is the most promising option for achieving appreciable ore savings. Zone loaded cores must be operated in such a way as to maximize the discharge burnup in order to reduce specific ore usage (ST $\text{U}_3\text{O}_8/\text{GWe-yr}$) that is, for a given reactor operating on a fixed refueling schedule the improvement in the power shape (lower power peaking) must ultimately lead to an increased thermal power output to achieve a higher burnup (as shown in Equation 3.3). Power shape improvements which lead only to a higher specific power (with constant total thermal power output) in PWRs; in particular, cores with a lower heavy metal loading will not reduce the ore consumption. As shown in Section 2.3.2 a high power density core (having

a constant total power output will log the burnup in a shorter calendar time than a low power density core, thus more reloads per year are required; but the fissile mass flows are identical on a calendar time basis (when yearly energy output is held constant). On the other hand, if the thermal power level is increased (instead of decreasing the heavy metal inventory) and the irradiation time is held constant then Equation 3.2 shows that the discharge burnup of the spent fuel increases; as previously mentioned, increasing the burnup ultimately leads to improved ore usage.

There are problems associated with changing the thermal performance: in most cases the plant would have to be relicensed; and while the nuclear steam supply system may not be able to handle arbitrarily large thermal power increases, there are often modest margins built-in for moderate changes [S- 4].

Using a representative set of parameters for current PWRs, Table 3.4, in Equation 2.2 and Equation 3.2 it is found that (case 3) power shaping improvements (here translated into increased total thermal power) lead to modest ore savings over the life of the reactor. Case 3 has a total thermal power increase of 33%; also shown is the increased reload enrichment requirement, since increasing the thermal power by 33% increases the discharge burnup by 33% so that additional fissile mass is needed to offset the additional fission product poisoning and U^{235} depletion associated with the higher burnups. It should be obvious that case 1 and case 2 do not result in ore savings; in case 2 the reactor operated at the same power level as for the reference reactor, therefore, both attained the same discharge burnup. In case 1 the reactor operated at a power level 33% below that for the reference reactor, therefore, the discharge burnup was 33% below that for the reference reactor.

TABLE 3.4

ORE SAVINGS DUE TO POWER SHAPE IMPROVEMENT (THERMAL POWER UPGRATING)

$n_1 = n_2 = 3$, batches in core

$X_o = 1.0$ w/o ^{235}U , enrichment at which $k = 1$ with saturated Xe and Sm

$X_w = 0.2$ w/o ^{235}U , enrichment plant tails

$X_1 = 3.2$ w/o ^{235}U , reload enrichment for reference core

$N_1 = N_2 = 2.25$, equivalent number of reload batches in startup core

$B_1 = 33,000$ MWD/MTU, discharge burnup of reference case

Case	E_2/E_1^*	Reload Enrichment Zone Loaded Case	Discharge Burnup Zone Loaded Case (MWD/MTU)	Relative Ore Usage F'_2 / F'_1 @ $r = 0\%$
1	0.666	2.71 w/o	21,478	1.13
2 (Ref)	1.000	3.20 w/o	33,000	1.0
3	1.333	3.93 w/o	43,989	0.93

*Changing the thermal power level (at constant irradiation time) is equivalent to changing the irradiation time (at constant thermal power level); if peak power limits core performance then this column also represents the factor by which the peak-to-average power ratio is decreased.

3.5.1.2 One Group Model

In order to clarify some key effects of axial power flattening on LWR core neutronics, a simple one group model in slab geometry will be examined, in which the fissile concentration is varied continuously to achieve uniform power density. The governing equation in diffusion theory is

$$D \cdot \nabla^2 \phi(x) + [\nu \Sigma_f(x) - \Sigma_a(x) - DBr^2] \phi(x) = 0 \quad (3.4)$$

(The small variation of D is neglected.) Rearranging and solving Equation 3.4 in several steps, described in Appendix B, one finally obtains the ratio of the average enrichment for an axially power-flattened core to the enrichment for the uniformly loaded core to be (at BOL)

$$\frac{\bar{\epsilon}}{\epsilon(\text{uniform})} = K \left[1 - \frac{L}{H} (1 - e^{-d/t}) \right] \quad (3.5)$$

where

$$K = \frac{\Sigma_a^{28} + \Sigma_a^p + DBr^2}{DB^2 + \Sigma_a^{28} + \Sigma_a^p} \quad (3.6)$$

$$L = \frac{D}{\Sigma_a^{28} + \Sigma_a^p + DBr^2} \quad (3.7)$$

H = the half-height of the core

d = linear extrapolation distance

Using typical one-group parameters for a PWR, Table 3.5 and Equation 3.5, the ratio of the critical enrichment for an axially power-flattened core to uniformly-loaded cores having the same core volume is approximately

$$\frac{\bar{\epsilon}}{\epsilon(\text{uniform})} = 1.06$$

This ratio shows that a 6% critical mass penalty is incurred when reactors are zone loaded to achieve a flat power distribution. The reader should note that the above example is the extreme case; obviously reactor cores will not be loaded such that the power distribution is completely flat, therefore this mass penalty is not fully incurred. Also the reactor normally burns toward a power flattened condition, therefore the largest mass penalty will occur at the BOL of cycle 1; in subsequent cycles, two-thirds of the core have already been power-flattened so that the reload mass penalty is extremely small. Hence mass penalty effects will not appreciably offset ore savings obtained by zone loading.

3.5.1.3 Representative Zone Loaded Cores

Three different zone loaded core configurations have been compared to a reference core to study the changes in the core power shape and burnup limits. These zone loaded cores used only two axial enrichment zones to reduce the central power peak in the fresh fuel, while the reference core was uniformly loaded. For these three cases, the volume of the enrichment zones and the enrichments within each zone were varied, as summarized in Figures 3.10 and Table 3.6. As one can see, the central peaking is reduced, as much as 20% (case 2). The reader should not infer that the 20% reduction in peaking is necessarily the most one can achieve when

TABLE 3.5

MASS PENALTY DUE TO POWER FLATTENING

Equivalent Core Diameter, in.	136
Active Core Height, in.	136.7
$\Sigma_a^{28}, \text{ cm}^{-1}$	0.00751
$\Sigma_a^p, \text{ cm}^{-1}$	0.00608
D, cm	1.24461
d, cm	2.65103
$\epsilon, \text{ w/o } ^{235}\text{U}$	3.03

$$\frac{\bar{\epsilon}}{\epsilon(\text{uniform})} = 1.06$$

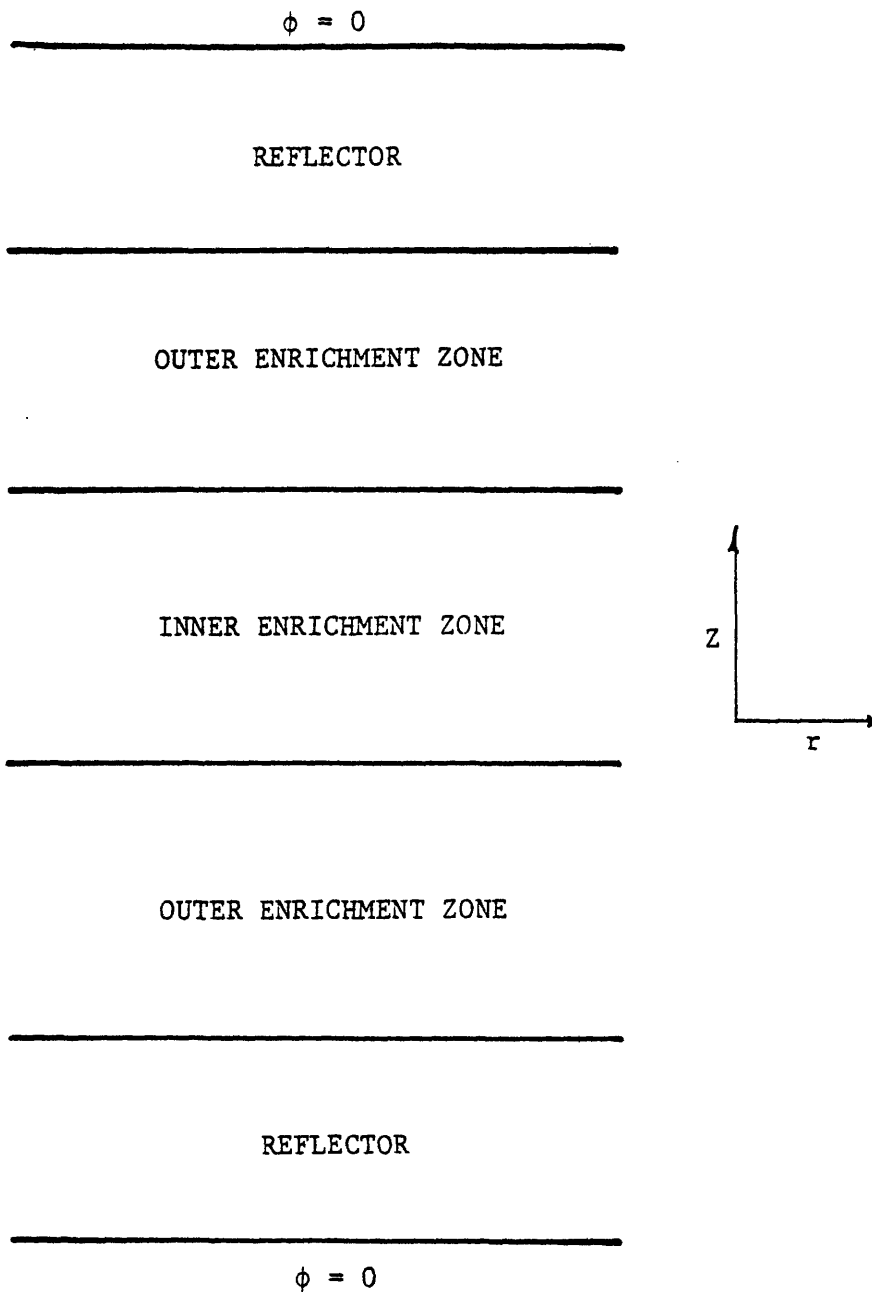


Figure 3.10 ZONE LOADED CORE LAYOUT

TABLE 3.6

ZONE LOADED CORE CHARACTERISTICS

Case	$q''' p/\bar{q}'''$ (BOL)	Fraction of core	Enrichment w/o	Fraction of core	Enrichment w/o	Relative Fissile Loading	Relative* Cycle Length
REF.	1.505	1.0	3.03	0.0	0.0	1.0	1.0
1	1.426	0.5256	3.03	0.4744	3.1	1.011	1.010
2	1.368	0.6571	2.9	0.3429	3.1	0.980	0.977
3	1.200	0.5913	2.9	0.4087	3.2	0.998	0.991

*Calculated using PDQ-7 at a constant thermal power level of 2440 MW

reactor cores are zone loaded since more zones could be used, and the dimensions and enrichments of the various zones can be fine-tuned to an extent greater than achieved here.

In developing the ore usage model in Section 2.3.1, we assumed that for large PWR cores, the reactivity-limited burnup of discharged fuel at steady state can be correlated as a linear function of reload enrichment. Table 3.6 shows that this assumption is quite valid; as one can see the agreement between the relative fissile loading and relative cycle length is good. (Enrichment is proportional to Burnup.) The reasons that the correspondence is not exact are: (1) the small mass penalty incurred when cores are made more heterogeneous (section 3.5.1.2) and (2) increased leakage of zone loaded cores (a consequence of higher enrichment at the periphery of the core). These calculations show that to the first order, the assumptions used in deriving the ore usage model are valid and that zone loaded cores do not offer an appreciable fissile mass penalty.

3.5.1.4 The Fuel Cycle Cost of Zone Loaded Cores

In this section, the fuel cycle cost of representative zone loaded cores will be presented. For each of the zone loaded cores described in the previous section, the levelized nuclear fuel cycle cost was calculated for the reactor operating at: (1) constant capacity factor and a 0.125 yr refueling shutdown and (2) constant availability-based capacity factor and a 0.125 yr refueling shutdown (see Figure 3.11). In addition to the above constraints, four different operational scenarios were defined for zone loaded cores. They are:

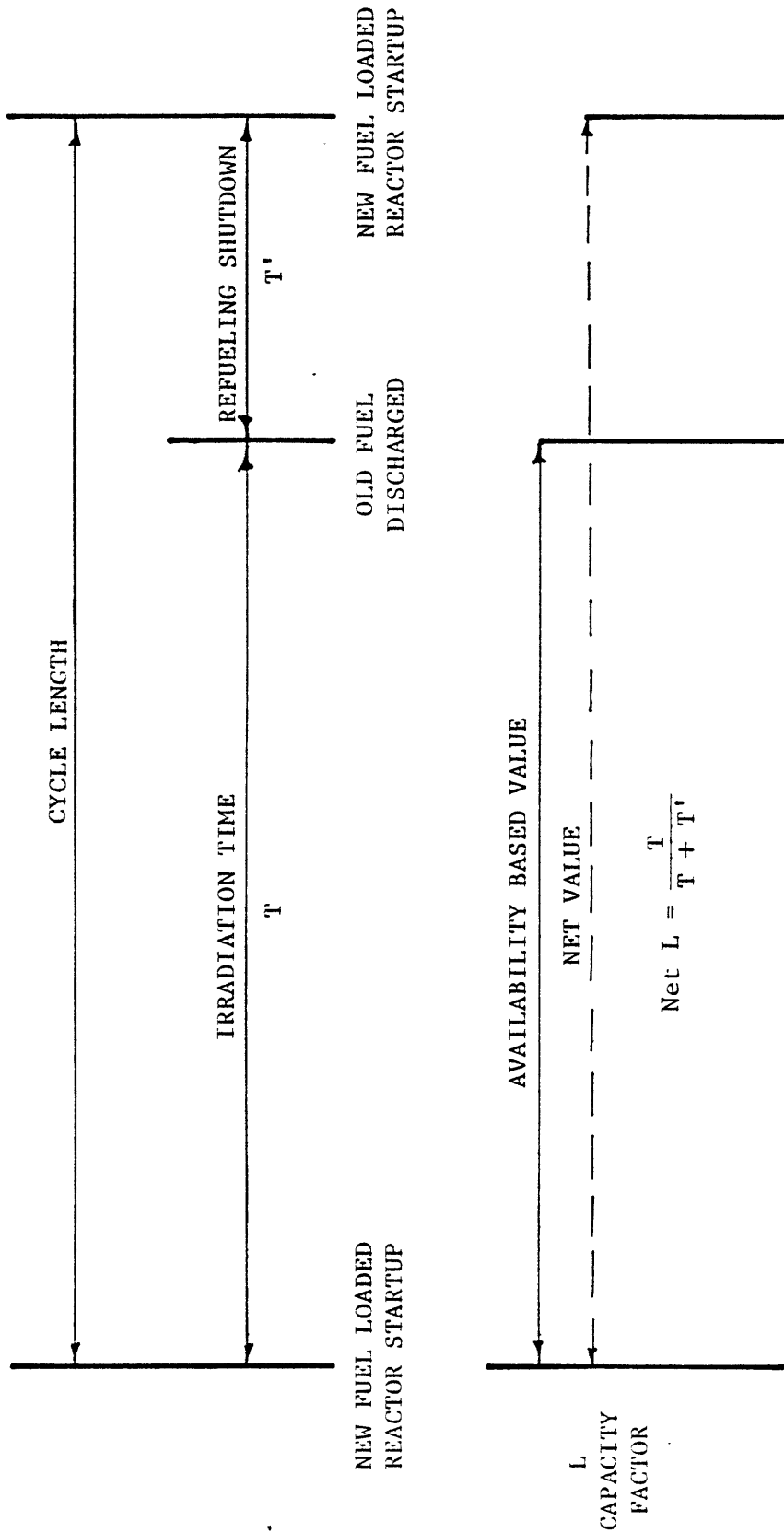


Figure 3.11 DEFINITION OF CAPACITY FACTOR

1. The power level of the reactor was maintained equal to that for the reference reactor. The core was depleted until reactivity-limited burnup was reached.
2. The thermal output of the reactor was increased but the irradiation period was decreased such that the electrical energy generated per cycle (and burnup) remained constant.
3. The reactor power level was maintained at the reference reactor's rated power level, but the heavy metal loading was decreased (increased specific power). The irradiation period was decreased so that the electrical energy generated per cycle (and burnup) remained constant.
4. The power level of the reactor was increased while the irradiation time was maintained equal to that for the reference reactor. The reload enrichment was increased to attain the higher burnups.

From the discussion in the previous section, the reader should realize that ore savings can only be attained by extending the burnup life of the fuel. Scenario (4) is the only way (from the four defined here) zone loaded cores can achieve an ore savings (defined as tons of U_3O_8 per MWe yr of energy delivered). In the second and third scenarios the reactor operates at a higher specific power than the reference reactor (since the discharge burnup was held fixed, operating the zone loaded reactor by scenarios (2) and (3) will not improve ore utilization).

In the first scenario the reactor was operated at the same power-level as the reference reactor; and this scenario is the least attractive way to operate zone loaded reactors. The first three scenarios are presented to show that zone loaded cores operating at higher specific power will not obtain ore savings but they may result in economic benefits (e.g. lower fuel cycle cost or lower capital cost).

For the scenarios which required increased thermal power output, it was assumed that an improvement in the power shape (reduction in the power peak) directly leads to an increased thermal power rating. For example, if zone loading the core reduced the peak-to-average power by 10% then a 10% increase in the total thermal power rating of the core was assumed. This assumption is highly optimistic, but Boyd's [B- 6] study showed that, up to a point, increasing the thermal rating can be done in such a way as to preserve current thermal hydraulic margins set for PWRs.

The levelized nuclear fuel cycle cost was calculated by the ECON code for each of the zone loaded cores described in the previous section. Table 3.7 summarizes the mass flows for each scenario and Table 2.2 summarizes the nuclear cost data used in the present study. As previously mentioned (Section 3.4.1.3) the irradiation times for the three zone loaded cores and the reference core were not equal; this is due to the fact that the four cores did not have the same fissile loading. This should not affect the final conclusions since the figure of merit is the levelized fuel cycle cost, a quantity which is the sum of all (present worth weighted) direct costs of the fuel divided by the (present worth of the value of) electricity generated.

TABLE 3.7

MASS FLOWS FOR ZONE LOADED CORES

Case*	U ₃ O ₈		Separative Work Requirements (MTSWU)	Heavy Metal Loading (MTHM)	Relative Thermal Power	Relative Irradiation Time	Relative Burnup
	Requirements	STU ₃₈					
Ref.	210.90	128.07	29	1.0	1.0	1.0	1.0
Scenario (1) (Constant P)							
1	213.37	130.21	29	1.0	1.010	1.010	1.010
2	205.00	124.15	29	1.0	0.977	0.977	0.977
3	209.16	124.49	29	1.0	0.991	0.991	0.991
Scenario (2) (Constant Burnup, increased P, and decreased T)							
1	213.37	130.21	29	1.055	0.957	1.010	1.010
2	205.00	124.15	29	1.100	0.888	0.977	0.977
3	209.16	124.99	29	1.254	0.790	0.991	0.991
Scenario (3) (Constant power, decreased T, and decreased HM)							
1	202.17	123.37	27.5	1.0	0.957	1.010	1.010
2	186.34	112.85	26.4	1.0	0.888	0.977	0.977
3	166.77	99.66	23.1	1.0	0.790	0.991	0.991
Scenario (4) (Constant T, increased P, increased B, and increased enrichment)							
1	222.47	138.09	29	1.055	1.010	1.066	1.066
2	223.40	138.91	29	1.100	0.977	1.075	1.075
3	251.60	163.63	29	1.257	0.991	1.254	1.254

*Geometry of each case described in Table 3.6

As previously mentioned, the levelized fuel cycle cost was calculated for (1) constant capacity factor and (2) constant availability based capacity factor; both maintained a refueling shutdown interval of 0.125 years. These calculations are summarized in Tables 3.8 through 3.10. As shown, the levelized fuel cycle cost for the zone loaded cores compares favorably with the reference case for all four scenarios. It is interesting to note that in cases where the fissile loading is the same but the irradiation period is shortened (e.g. scenario (1) vs. scenario (2)) the fuel cycle cost is reduced. This is due to the fact the same energy is produced by both reactors but one generates it in a shorter time interval so that revenue from the sale of electricity is received sooner, and therefore has a higher present worth (see Appendix E). For this reason there is a slight economic incentive for PWR cores to operate at higher specific powers even though the reactor is not operating in an ore saving mode (e.g. scenario 4).

Scenario (4) (or similar extended burnup schemes) is the most attractive way to operate a zone loaded PWR. These zone-loaded cores do not suffer an economic penalty for operating in this mode, but the zone loaded cores improve the ore utilization modestly, as shown in Table 3.11 and 3.12. As one can see, the ore savings increase as the burnup and (as defined by scenario (4)) thermal power output are increased, but these ore savings are small. Zone loading the core and increasing the power rating is one way to save ore by extending the burnup; in the next chapter other and potentially better ways to extend the burnup will be examined.

TABLE 3.8

LEVELIZED FUEL CYCLE COST AT A
CONSTANT CAPACITY FACTOR OF 75%

Case*/Scenario**	Fuel Cycle Cost (mills/kwhr)			
	(1)	(2)	(3)	(4)
1	8.766	8.506	8.507	8.676
2	8.561	8.139	8.140	8.495
3	8.641	7.701	7.701	8.385

Ref. Core = 8.707 mills/kwhr

* Representative zone loaded cores as described in Table 3.6

** Heavy metal loading, relative thermal power, and irradiation time given in Table 3.7

Key

Case 1 Slightly Flattened
Case 2 Moderately Flattened
Case 3 Heavily Flattened

Scenario 1 Constant P
2 Constant Burnup, increased P and decreased T
3 Constant P, decreased T, and decreased HM
4 Constant T, increased P, increased B and increased enrichment

TABLE 3.9

LEVELIZED FUEL CYCLE COST AT A CONSTANT AVAILABILITY

BASED CAPACITY FACTOR OF 90%

Case*/Scenario**	Fuel Cycle Cost (mills/kwhr)			
	(1)	(2)	(3)	(4)
1	8.387	8.176	8.137	8.343
2	8.199	7.860	7.783	8.216
3	8.265	7.500	7.325	8.213

* Representative zone loaded cores as described in Table 3.6

** Heavy metal loading, relative thermal power, and irradiation time given in Table 3.7

Key

- Case 1 Slightly Flattened
- Case 2 Moderately Flattened
- Case 3 Heavily Flattened

- Scenario 1 Constant P
- 2 Constant Burnup, increased P and decreased T
- 3 Constant P, decreased T and decreased HM
- 4 Constant T, increased P, increased B and increased enrichment

TABLE 3.10

LEVELIZED FUEL CYCLE COST AT A CONSTANT AVAILABILITY
BASED CAPACITY FACTOR OF 80%

Case*/Scenario**	Fuel Cycle Cost (mills/kwhr)			
	(1)	(2)	(3)	(4)
1	8.830	8.652	8.547	8.848
2	8.622	8.288	8.153	8.696
3	8.696	7.867	7.673	8.686

*Representative zone loaded cores as described in Table 3.6

**Heavy metal loading, relative thermal power, and irradiation time given in Table 3.7

Key

Case 1 Slightly Flattened
Case 2 Moderately Flattened
Case 3 Heavily Flattened

Scenario 1 Constant P
2 Constant Burnup, increased P and decreased T
3 Constant P, decreased T and decreased HM
4 Constant T, increased P, increased B and increased enrichment

TABLE 3.11

ORE USAGE (STU_3O_8 /GW(e)yr) FOR ZONE LOADED CORES:

SCENARIO (4)

<u>Case</u>	(1) <u>L = 75</u>	(2) <u>L' = 90</u>	(2) <u>L' = 80</u>	<u>Relative Thermal Power and Extended Burnup</u>
Ref.	186.5	202.5	181.9	1.0
1	184.0	200.6	180.2	1.055
2	183.8	199.2	179.0	1.100
3	179.0	194.2	174.5	1.254

(1) constant capacity factor

(2) constant availability based capacity factor

TABLE 3.12

RELATIVE* ORE USAGE AND FUEL CYCLE COST

<u>Case**</u>	<u>Relative Ore Usage</u>	<u>Relative Fuel Cycle Cost</u>
Ref.	1.000	1.000
1	0.987	0.996
2	0.986	0.976
3	0.960	0.963

* For a constant capacity factor of 75%

** Representative zone loaded core (Scenario 4) as described in Table 3.7

3.5.1.5 Xenon Oscillations

In large PWRs the coupling between distant parts of the reactor is weak, so that power peaking can occur in any one of several core regions. This makes the power distribution of large PWRs very sensitive to small local reactivity effects such as xenon-induced spatial oscillations. The instability of large cores can be explained mathematically; the eigenvalues associated with the various power peaks in large cores are almost identical. In addition, if the power distribution is relatively flat, the higher harmonic flux modes become quite important and the eigenvalues associated with these higher order modes may be as large as that for the fundamental mode. The excitation of these higher order modes (large eigenvalues) causes unstable oscillations.

The effect of power-flattening is crucial in our study since the probability of xenon oscillation is increased when the power distribution (BOL) is changed from a chopped cosine distribution to a flatter power distribution. For example, Randall and St. John[R-2] showed that with a flat axial flux, the core height for sustained Xe oscillations is a factor of $\sqrt{3}$ smaller than a core with a cosine flux distribution.

Xenon oscillations can only occur above a certain threshold flux level. This threshold flux level mainly depends upon the size of the reactor, the magnitude of the temperature coefficient, and the power shape within the reactor. Since it may be desirable to reduce the core size when power shaping improvements are applied (extracting the same energy from a lower heavy metal mass); we calculated the threshold flux level for xenon oscillations as a function of axial core height. The method developed by Randall and St. John[R-2] was used; these results are summarized in Table 3.13.

TABLE 3.13

AVERAGE ϕ 's FOR UNDAMPED XENON OSCILLATION

(ZERO TEMPERATURE COEFFICIENT)

Height of Core (ft.)	$\bar{\phi}$ (cosine)	$\bar{\phi}$ (flat)
6.90	∞	1.5×10^{13}
7.97	10^{14}	1.2×10^{13}
8.91	3×10^{13}	1.1×10^{13}
12.6	1.3×10^{13}	6×10^{13}

FOR STABILITY

$$H (\text{FLAT}) = \frac{H (\text{Cosine})}{\sqrt{3}}$$

As shown, the stability increases as core height decreases for both the cosine and flat distributions. This stability gained by decreasing the core height will be offset somewhat by the increase in the flux level when the power density is increased. It should be stated that these calculations are for the limiting case; that is, the flux distribution is flat (not the power distribution) and the calculations did not include the effect of the temperature coefficient. As shown in Figure 3.12 a flat power core still has an appreciably buckled flux. In addition the stability increases significantly when temperature coefficients are included.

Until further evidence is available to the contrary one should assume that xenon oscillations can occur in zone loaded cores. However, this does not affect the basic feasibility of this design, since reactors have previously been operated successfully in the presence of xenon oscillations. Furthermore, current large PWR reactors are susceptible to xenon oscillations at EOL; their technical specifications[Y-1] do not require PWRs to be stable with regard to Xe oscillations.

3.5.2 Seed/Blanket Cores

Three similar axial seed and blanket cores were analyzed as described in Section 3.5.2. The seed region contained slightly enriched UO_2 and the blanket region contained depleted UO_2 (0.2 w/o U^{235}). Infinite medium calculations were performed for three different thicknesses of the blanket and seed region; however, the fissile loading for the three cases and the reference core was kept constant. The results are summarized in Figure 3.13 and Table 3.14. As shown, the seed/blanket cores have slightly, but not significantly, longer irradiation times (burnup) than

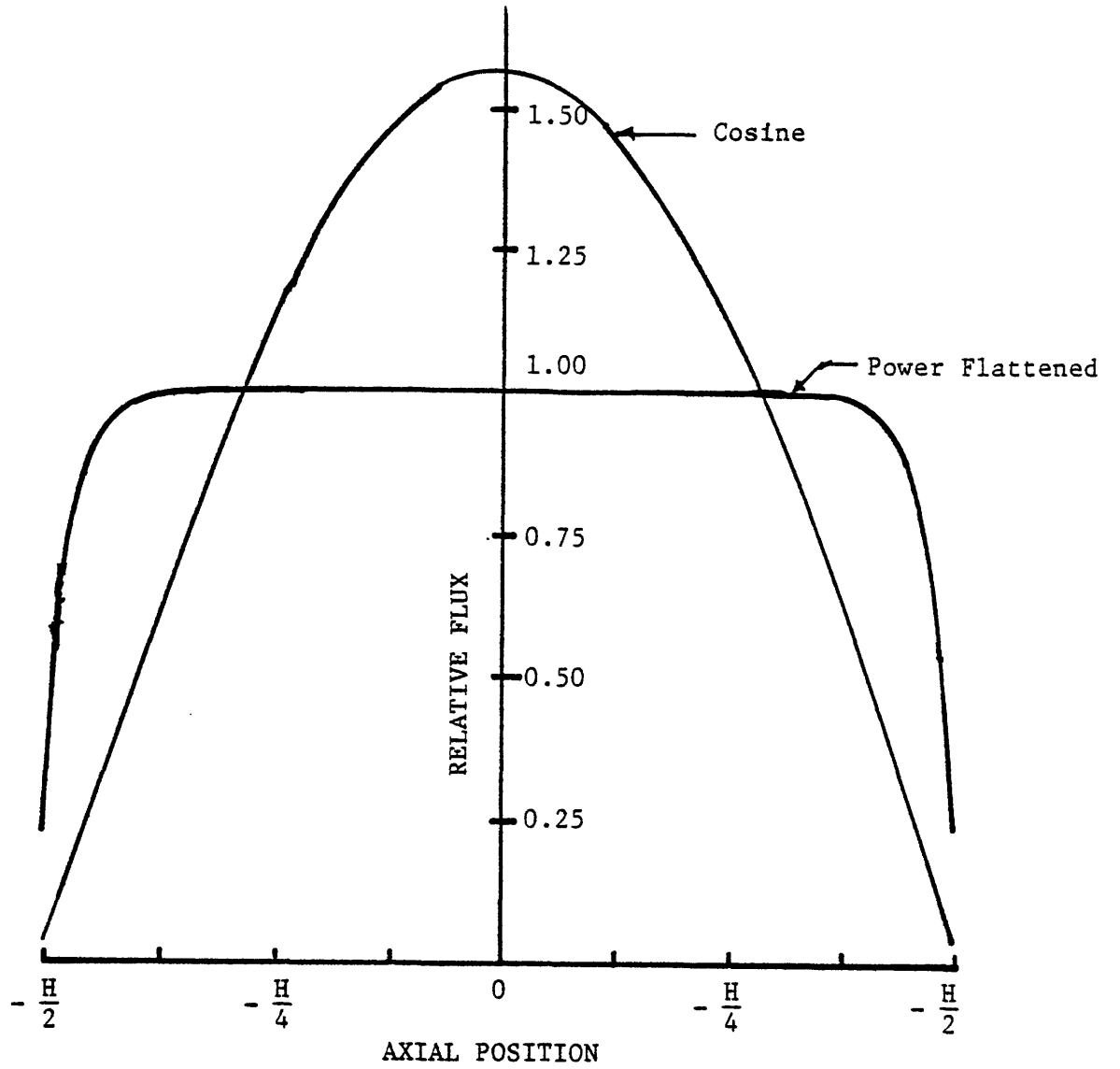


Figure 3.12 COSINE FLUX DISTRIBUTION vs POWER-FLATTENED FLUX DISTRIBUTION

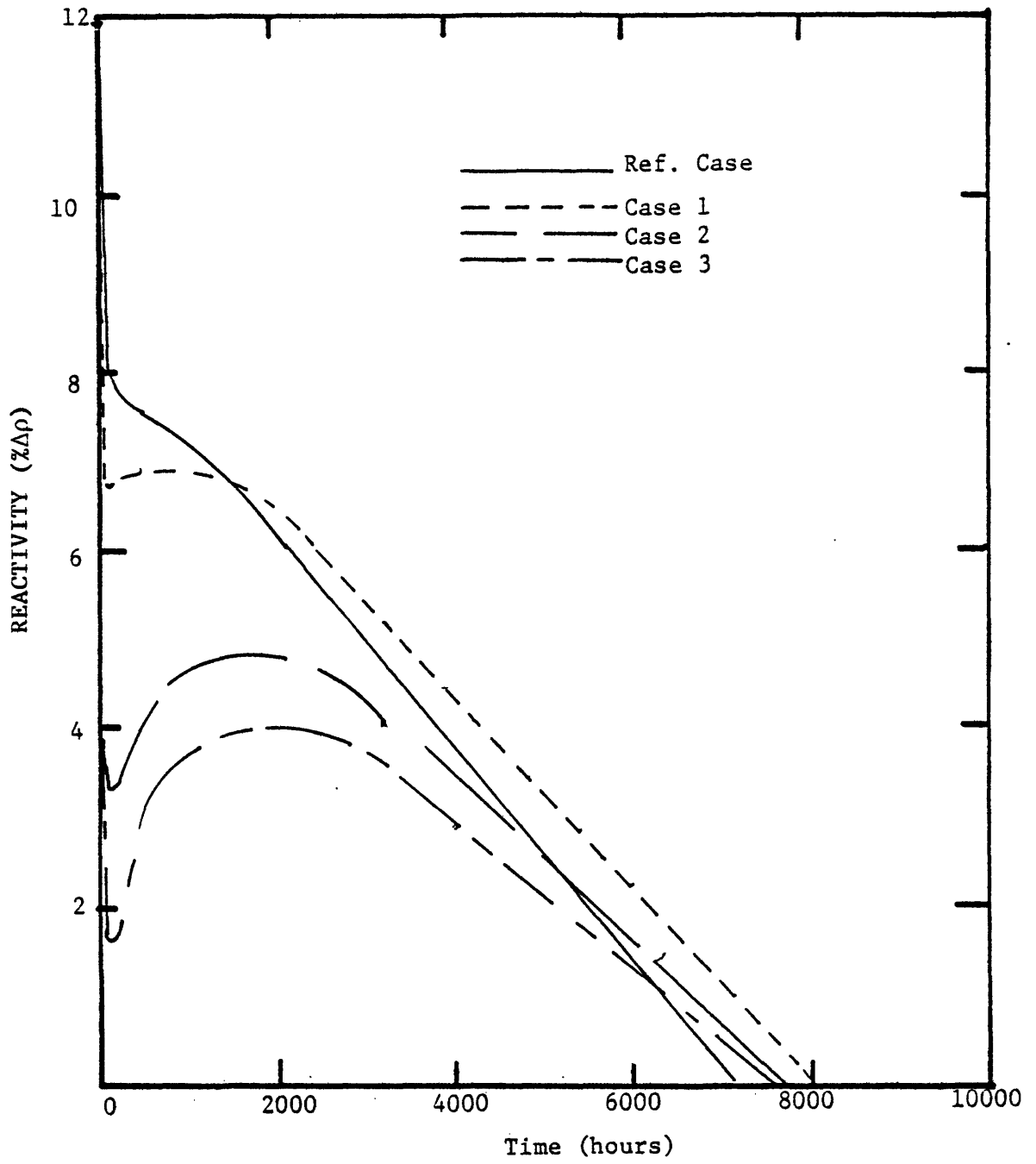


Figure 3.13 REACTIVITY vs BURNUP FOR SEED/BLANKET CORES

TABLE 3.14

SEED-BLANKET CORES EXAMINED IN THE PRESENT WORK

	<u>Thickness of Seed and Blanket Regions (cm)</u>	<u>Reactivity-Limited Irradiation Lifetime (hrs.)</u>	<u>U₃O₈ Requirements* STU₃O₈/GW(e) yr.</u>
1	4.0	7943	172.34
2	8.0	7677	177.13
3	12.0	7388	183.94
Ref. Case	-	7132	184.71

*at a constant capacity factor of 75%

the reference case. A larger reactivity contribution from fissile material production in the blanket was hoped for to offset some of the reactivity loss due to burnup and fission product poisoning, but our results do not show this.

The calculations show that modest ore savings can be attained when PWR cores are loaded in a seed/blanket configuration. Since the simple seed/blanket cores did not yield significant reductions in enrichment requirements further analysis of this concept was dropped, and effort was focused on the more attractive prospects. It is quite possible, however, that other seed/blanket designs, in particular the radial seed/blanket configuration of the Shippingport PWR, might prove to have some attractive benefits for the once-through fuel cycle. Additional work in this area may be of some interest.

3.5.3 Movable Fuel Reactivity Control

As previously mentioned, the use of fertile material as control elements was tested. Two simple different nine-assembly-module configurations, as described in section 3.4.3 were analyzed. In both cases the central assembly is movable, while the eight outer assemblies are stationary. We have calculated the change in reactivity when the central assembly is withdrawn from the fully inserted position to the fully withdrawn position. A static eigenvalue problem was performed for each configuration and each control position (full in or full out); the results are summarized in Table 3.15. As shown, the reactivity change is quite small for both cases (case 2 is slightly better). It is concluded that fertile materials can not replace control materials in the simple manner studied since the worth of relatively small axial movement of fertile material is small;

TABLE 3.15

REACTIVITY CALCULATION FOR MOVABLE FUEL-REACTIVITY CONTROL

	K_{eff}		$\Delta\rho\%$
	Assembly-in	Assembly-out	
Configuration #1	1.252189	1.252477	2.3×10^{-2}
Configuration #2	1.236386	1.238392	0.162

$$\Delta \rho = \frac{K' - K}{K'}$$

more sophisticated designs would have to be implemented (LWBR) if control poisons are to be replaced by fertile materials

3.5.4 Enhanced Reflector Designs

As previously mentioned, two enhanced reflector designs were studied; the borated water reflector used in current PWRs was replaced by BeO and depleted UO_2 (0.2 w/o) reflectors. The design basis for this study is described in Section 3.4.4.

The PDQ-7 code was used to calculate the reactivity-limited burnup for the reference reactor (H_2O reflector) and the two improved reflectors. As shown in Figure 3.14 the BOC reactivity for the reactor with BeO reflectors is greater than the reference case. In addition the burnup slopes (k/T) for all three cases are approximately equal. The difference in reactivity between the BeO reflector case and the reference case can be attributed to reduced parasitic absorptions in the reflector, and to spatial effects. In current PWRs the core is reflected by light water (containing soluble control poison) closely backed by a core shroud and barrel. These materials have high absorption cross sections which lead to large parasitic captures in the reflector, thus degrading the neutron economy. Table 3.16 summarizes the thermal absorption properties of these reflector materials; as shown the macroscopic absorption cross section of water and boron is significantly greater than BeO. Thus with the BeO reflector the neutron economy is improved modestly (the improvement is small since leakage effects are small, approximately 4% of the fission neutrons are lost to leakage).

As previously mentioned, spatial effects may contribute modestly to the increase in reactivity when borated- H_2O is replaced by BeO. It was found that the power peaks occurred closer to the reflector when BeO was used,

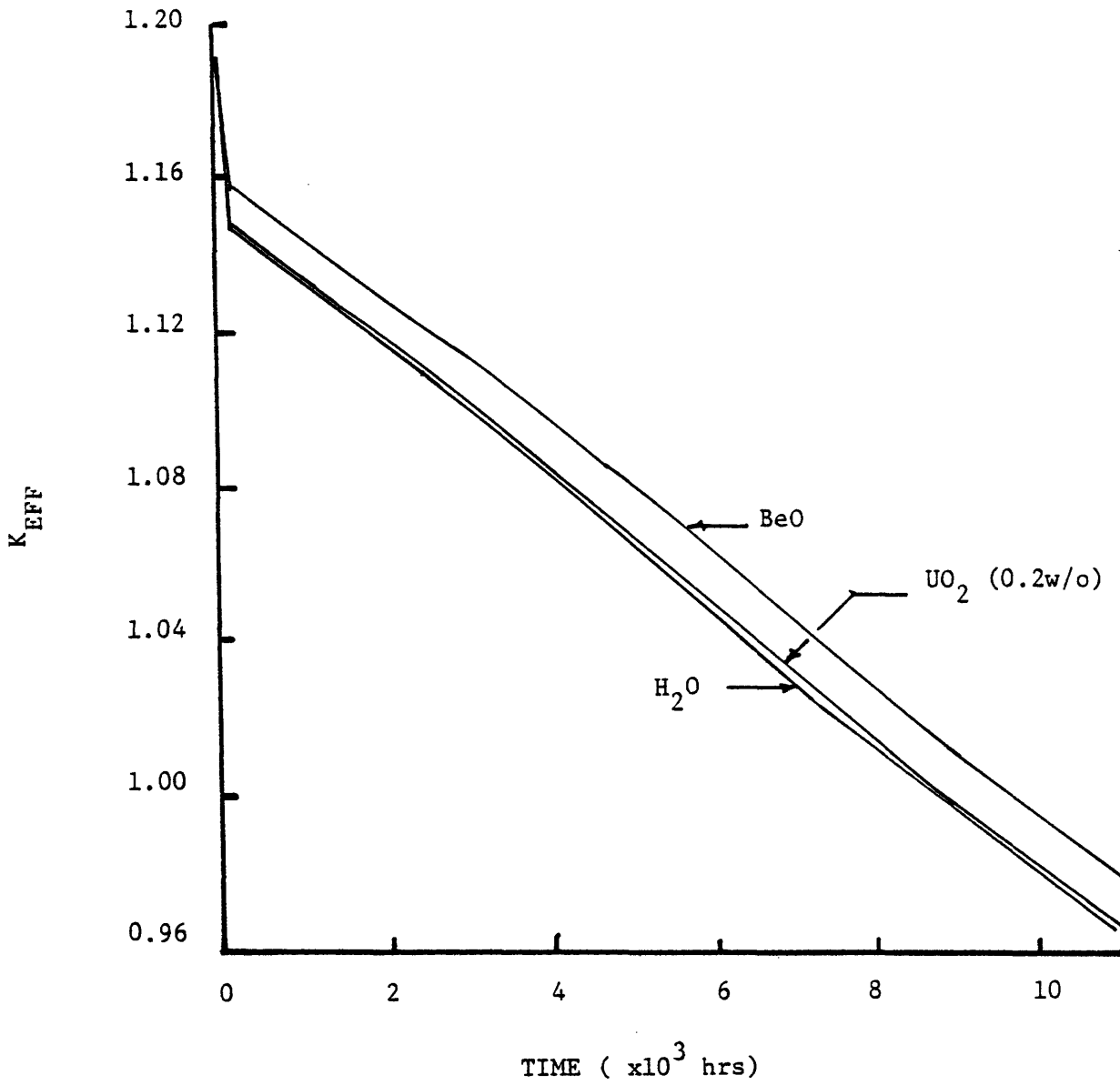


FIGURE 3.14 ENHANCED REFLECTOR STUDIES: K_{EFF} VS. TIME

TABLE 3.16

THERMAL ABSORPTION PROPERTIES* OF BeO, H₂O and Boron

	σ_a	Σ_a
	Microscopic Absorption Cross Section (barns)	Macroscopic Absorption Cross Section (cm ⁻¹)
BeO	0.007	0.00045
H ₂ O (pure)	0.184	0.00889
Boron**	2131.378	0.00679

* Typical value at the middle of burnup cycle (16,000 MWD/MTU)

** Mid-cycle value of 400 ppm in H₂O.

thus increasing the importance for neutrons near the reflector and giving a slight increase in the reactivity.

Also shown in Figure 3.14 is the case when the water reflector is replaced by depleted UO_2 fuel assemblies. As shown, this case is almost indistinguishable from the reference case.

The ore savings was found for both cases (BeO reflector and depleted UO_2 reflector) by reducing the reload enrichment such that the multiplication factor, K_{eff} , of the two changed cases was equal to that of the reference case at BOC. Since the burnup slope was approximately the same for all three cases the cycle lengths are also equal. These results are summarized in Table 3.17. As shown the ore requirements for the BeO reflected reactor is reduced by 5.0% (relative to the H_2O + Boron reflected reactor). The ore requirements for the depleted UO_2 reflected reactor is not significantly lowered.

The 5% savings in ore (BeO case) should be interpreted as an upper bound since no attempt was made to include in the analysis the structural material, which will clad the BeO or the borated water which will cool the reflector. In addition, the BeO reflected reactor may have severe power peaking problems near the reflector-core interface such that the fuel management strategy (fuel loading) may have to be changed. Aside from these problems, the ore utilization of PWRs may be modestly improved if BeO is used for the reflector.

TABLE 3.17

ORE SAVINGS: ENHANCED REFLECTOR STUDIES

CYCLE BURNUP, MWD/MTU	11,000
TOTAL CORE HEAVY METAL LOADING, MTHM	87
REFERENCE CORE RELOAD ENRICHMENT, w/o	3.0
AVERAGE BORON CONCENTRATION, ppm in H ₂ O	400.0

Reflector Material	Relative* Annual Ore Usage	Reload Enrichment (w/o)
BeO	0.952	2.87
UO ₂	0.990	2.97

*Relative to Reference Reactor (H₂O Reflected)

3.6 Conclusions

In this chapter several types of heterogeneous core designs have been considered, namely (1) enrichment gradation in the axial direction (zone loaded core), (2) seed/blanket cores, (3) movable fuel-reactivity control, and (4) enhanced reflector designs. The main emphasis of this present study was to focus attention on core designs that reduce uranium ore consumption in current PWRs and still maintain current thermal-hydraulic margins.

Three different zone loaded core configurations have been compared to a reference core to study the changes in the core power shape and burnup limits. From these studies the following was concluded:

- (1) Two different axial enrichment zones can reduce the central power peak in the fresh fuel; in some cases as much as 20%. This 20% reduction in peaking is not necessarily the most one can achieve when reactor cores are zone loaded since more zones could be used, and the dimensions and enrichments of the various zones can be fine-tuned to an extent greater than achieved here.
- (2) In order to clarify some key effects of axial power-flattening on LWR core neutronics, a simple one-group model was developed. It was found that a 6% critical mass penalty is incurred when reactors are zone loaded to achieve a flat distribution. This was found to be the extreme case; the reactor will not be

loaded such that the power distribution is completely flat and the reactor normally burns toward a power flattened condition; therefore the largest mass penalty will occur at the BOL of cycle 1.

- (3) Zone loaded cores must be operated in such a way as to maximize the discharge burnup in order to reduce ore usage, that is, the improvement in the power shape (lower power peaking) can ultimately lead to an improved total thermal power rating and/or a higher burnup. Power shape improvements which lead to a higher specific power (with the same system thermal output but a lower heavy metal loading) will not reduce ore consumption.
- (4) An ore usage model was developed to analyze the benefits (ore savings) accrued when power flattening improvements are made. The simple ore usage model predicted only modest ore savings.
- (5) The state-of-the-art PDQ-7 calculations verified the results of the simple ore usage model, namely that power shape improvements in PWRs can only achieve modest ore savings. These calculations show that to the first order, the assumptions used in deriving the ore usage model are valid (the reactivity-limited burnup of discharged fuel at steady state can be correlated as a linear function of reload enrichment).

- (6) The fuel cycle cost was calculated for the three representative zone loaded cores and reference core. The calculations show that the fuel cycle costs of zone loaded cores do not differ significantly from the reference case. These calculations also showed that the use of cores having higher specific powers reduce the fuel cycle cost slightly.

- (7) It is recognized that more exact thermal-hydraulic analyses must be performed. In addition, calculations must be performed to check the operational characteristics of the zone loaded PWRs (e.g. xenon stability, LOCA analysis).

- (8) The reader should be careful when totaling up the ore savings when power shape improvements are used. The amount of ore savings depends upon the amount of extended burnup and one should be careful not to double-count the advantages of several schemes to improve burnup. Power flattening may be an advantageous adjunct to other methods if peak local burnup limits useful assembly life (i.e. a materials limited design) as opposed to ones which are average burnup limited (reactivity limited designs).

Three similar axial seed/blanket cores were analyzed to see if a large reactivity contribution from fissile material production in the blanket can be achieved to offset some of the reactivity loss due to

burnup and fission product poisoning, but our results did not show this. It is recommended that other designs be investigated, in particular the radial seed/blanket configuration of the Shippingport PWR which might prove to have some attractive benefits for the once-through fuel cycle. Substitution of thorium for uranium in the blanket zones might be advantageous even if recycle is not contemplated.

The use of fertile material as control elements was tested. From the results it was concluded that fertile materials can not replace control materials in the manner shown; more sophisticated designs would have to be implemented (LWBR) if control poisons are to be replaced by fertile materials.

The use of different reflector materials in current PWRs was tested. From the results it was concluded that PWRs reflected by BeO may improve the ore utilization by 5%; the results for the depleted UO₂ reflected reactor were less promising. Thus BeO appears to be a better reflector than H₂O in terms of ore utilization. However, the BeO reflected reactors may have severe power peaking problems near the core-reflector interface such that the fuel management strategy may have to be changed.

Summarizing, in this chapter several types of heterogeneous core designs were considered, namely (1) enrichment gradation in the axial direction (zone loaded core), (2) seed/blanket cores, (3) movable fuel-reactivity control, and (4) enhanced reflector designs. Modest ore savings was predicted to be possible. In order to implement these ore savings a significant Research and Development program would need to be carried out to make the fuel and core design changes in PWRs.

CHAPTER 4

SIX-BATCH HIGH BURNUP CORE

4.1. Introduction

The optimum cycle length and batch size are determined by considering fuel cycle economics, the availability of the plant, unit maintenance requirements, and the cyclic nature of the electric demand on the utility. Most LWRs are currently refueled annually, although 6 and 18 month schedules have also been proposed [A-6]. The refueling interval has been established in part by the need to schedule the refueling outage during periods of low electrical demand. Although annual refueling may be the best strategy for currently operating plants, this should be re-examined with respect to ore utilization since the commercial attractiveness and useful lifetime of the LWR will depend upon the amount and price of available uranium resources.

It has been long recognized that ore utilization can be improved by extending the burnup of the fuel. But to exploit this advantage, the number of batches in the core must be increased (to increase reactivity lifetime) and/or the irradiation interval must be extended (by increasing reload enrichment). In subsequent sections, it will be shown that with a six-month equilibrium fuel cycle and with a constant discharge burnup, the reload enrichment is reduced by approximately 0.3 %. The reduction in feed enrichment results in an ore savings of about 10%. But to exploit the benefits from increasing the number of batches, the time require to execute refueling operations must be reduced. Otherwise, the savings could be offset by increased downtime. Westinghouse has proposed a quick refueling

scheme [A-6] which reduces the refueling outage from 6 weeks to 3 weeks, such that the six-batch core semi-annual-refueling fuel management scheme will not be severely penalized by refueling outages. But a significant number of utilities have not purchased this fuel management scheme, and its prospects do not appear to be promising. If anything, utilities may be more interested in an 18 month cycle. As previously mentioned, the burnup of the fuel can be extended by increasing the length of the irradiation cycle. Higher reload enrichment is required to extend the burnup, but one obtains an ore savings nevertheless, since one extracts the same energy from a smaller heavy metal mass. It will be shown that extending the burnup of the fuel by a factor of two will result in an ore savings of 10%.

In this chapter, a six-batch core with a semi-annual fuel management scheme will be examined to see if there is a large potential for ore savings. Next, the refueling interval of the six-batch core will be extended to one year. Thus dual ore savings are expected; namely, through a (relative) reduction of reload enrichment requirements (due to the increased number of batches); and through higher discharge burnups (the same energy output from a smaller heavy metal mass). The analyses of these individual and combined cases will be developed in subsequent sections.

4.2. Motivation

4.2.1. Ore Usage Model

The motivation for analyzing a six batch core fuel management scheme can best be explained by the ore usage model introduced previously. As shown in Appendix A, the relative annual ore usage by a system of reactors of a given design $[F_{s_2}']$ compared to a reference system $[F_{s_1}']$ was found to be:

$$\frac{F'_{s2}}{F'_{s1}} = \left[\frac{1 + \frac{r}{100} N_2 T_2}{1 + \frac{r}{100} N_1 T_1} \right] \left[\frac{x_1 - x_0}{x_1 - x_w} \right] \left[\frac{n_1}{n_2} \right] \left[\frac{n_2 + 1}{n_1 + 1} \right] + \left[\frac{x_o - x_w}{x_1 - x_w} \right] \left[\frac{n_1 T_1 E_1}{n_2 T_2 E_2} \right] \quad [4.1]$$

where the parameters have been defined in Appendix A.

Using a typical set of parameters (Table 4.1) in Equation [4.1], relative ore usage plots can be obtained for the following two cases: (1) fix the number of batches in the core and vary the burnup (refueling interval) and (2) fix the discharge burnup and vary the number of batches in the core. As shown in Figure 4.1, changing the discharge burnup can effect a modest improvement in ore usage; in fact, a savings of 10% may be obtained if the discharge burnup is doubled (relative to the reference case). Also shown in Figure 4.1 is the case for fixed discharge burnup (i.e., $n_1=3$, n_2 varied). As can be seen, one can achieve ore savings of on the order of 10% by going to semi-annual refueling (i.e., a 6-batch core in place of a 3-batch core). By combining the two improvements, a six-batch core with annual refueling should achieve an ore savings on the order of 20% or more.

4.2.2. DOE Extended Burnup Studies

The key technical question associated with high discharge burnup is fuel performance reliability. As shown in the previous section, significant ore savings are obtained when the discharge burnup of the fuel is doubled (relative to current PWR practice). Extending burnup by so large an increment would require a substantial research and development effort. Nevertheless, extending the burnup lifetime of the fuel is the most promising way of obtaining ore savings.

Currently, DOE has embarked on a research and development program to extend the PWR fuel burnup design limit. Their primary emphasis is to

TABLE 4.1

DATA BASE FOR COMPUTING RELATIVE ORE USAGE FOR 6-BATCH CORES

$n_1 = 3$, number of batches in the reference core

$P_1 = P_2$, core heavy metal loading

$X_0 = 1.0\%$ ^{235}U , enrichment at which $k = 1$ with saturated Xe and Sm

$X_w = 0.2\%$ ^{235}U , enrichment plant tails

$X_1 = 3.2\%$ ^{235}U , reload enrichment for reference case

$N_1 = N_2 = 2.25$, equivalent number of reload batches in startup core

$T_1 = 1$ yr., refueling interval

$r = 0\%$, reactor system growth rate (i.e., results here apply to a single reactor).

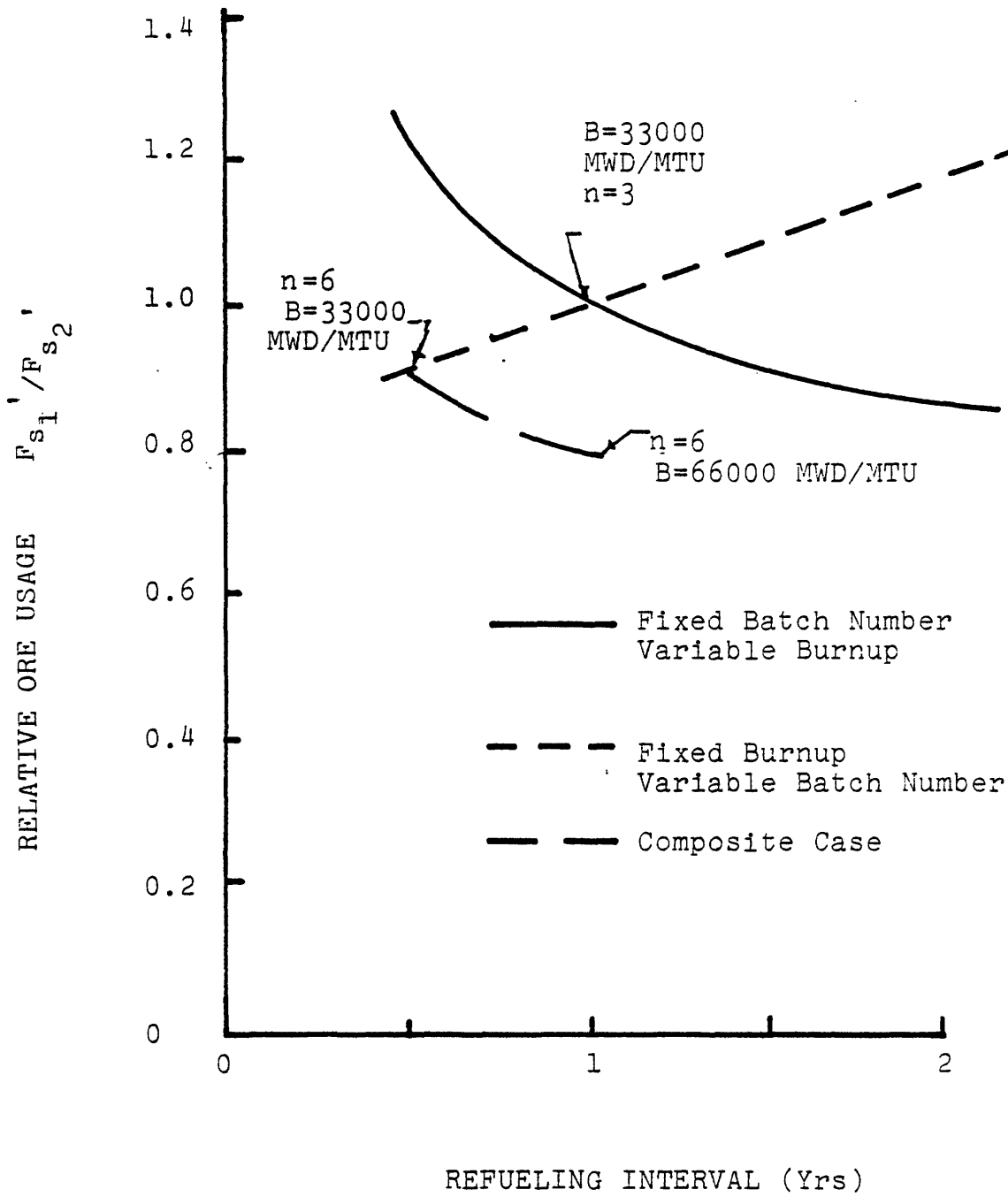


FIGURE 4.1
RELATIVE ORE USAGE AS A FUNCTION OF BATCH NUMBER AND BURNUP

extend the burnup life of the fuel such that the demand for U_3O_8 in current PWRs is reduced. Aspects of interest are development and demonstration of high burnup fuel designs for PWRs; in particular, the targeted discharge burnup of 70 assemblies in OCONEE (880 MWe PWR) is 38000 MWD/MTU and is 45000 MWD/MTU in ANO 1 (880 MWe PWR). Figure 4.2 summarizes the above programs and the expected reduction in U_3O_8 demand in current PWRs.

The points to be made here are that the utility of high burnup fuel is recognized, and improvements are in prospect. Our decision to examine fuel having an average burnup of 66,000 MWD/MTU does not imply, however, that this is an assured accomplishment. While low by FBR standards, it is not clear that solutions will be found to Zircaloy PCI interaction problems, internal chemical attack by fission products or corrosion induced hydriding. Furthermore, reversion to stainless steel clad on LWR fuel incurs an enrichment penalty which offsets at least part of the burnup gain. Correa [C-4] has shown that reversion to stainless steel clad incurs a 20% penalty in enrichment, that is, the enrichment must be increased by 20% relative to current PWRs.

4.3.3. Use of Isotopically Separated Improved Clad

The use of Laser Isotope Separation (LIS) processes to separate out the more highly absorbing isotopes in Zircaloy and stainless steel cladding can improve the ore utilization by a small amount. In addition, stainless steel cladding prepared by this process might conceivably be used in high burnup core applications since the mechanical integrity of S.S. clad fuel rods is better than for Zircaloy clad fuel rods. This option is a long range option and commercial prospects are quite uncertain at this time. Reductions in U_3O_8 requirements resulting from this option are expected to be

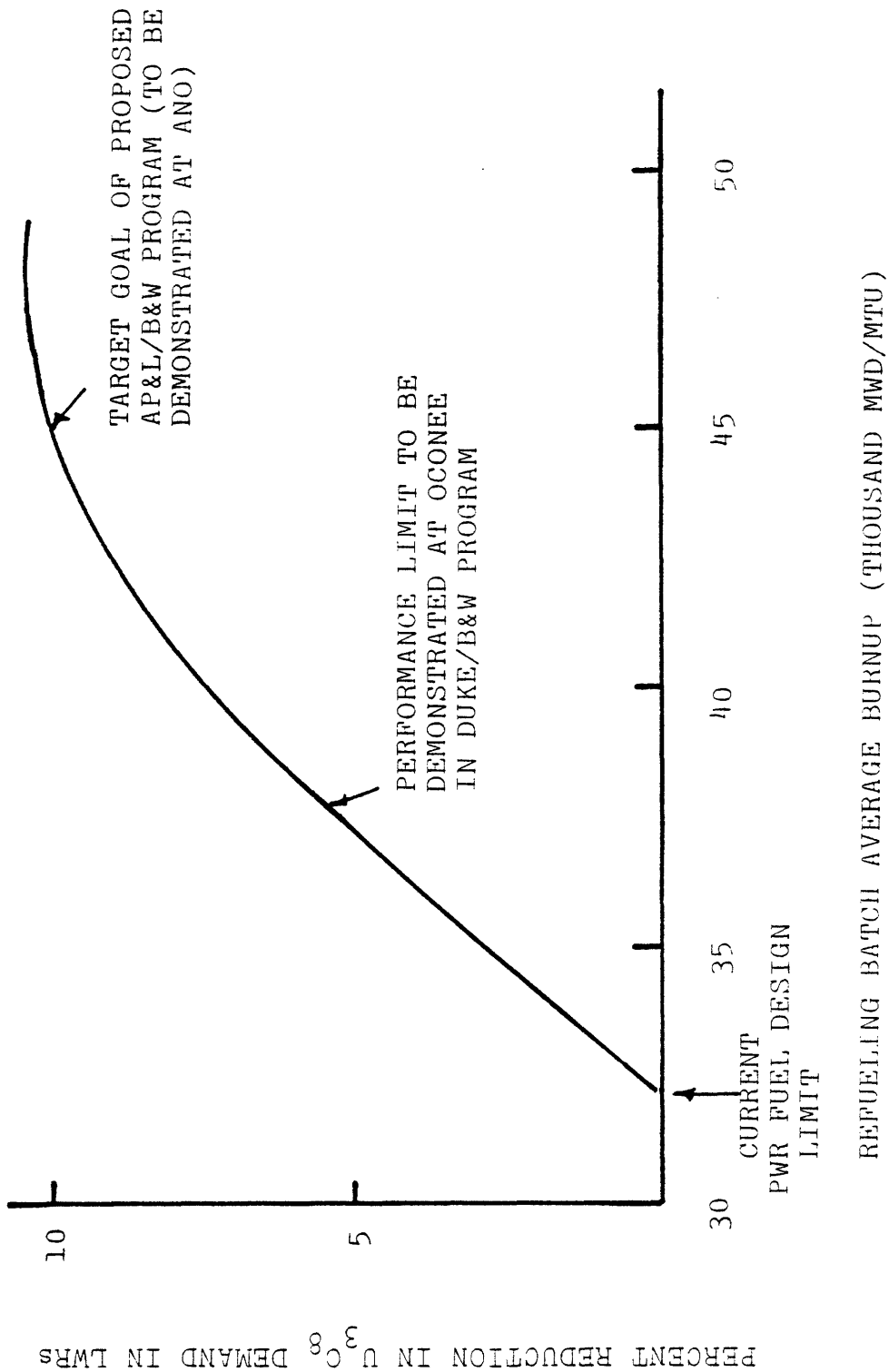


FIGURE 4.2

LWR FUEL UTILIZATION BENEFITS BASED ON DEFERRAL OF PROCESSING [U-1]

5% or less. This 5% value was calculated by using LEOPARD assuming a 100% reduction in σ_a , while reductions of 50% are probably all that would be achieved in practice. Some pertinent details are as follows: (1) The LEOPARD code was used to calculate the reactivity-limited burnup for the reference reactor (see Table 3.2) and the changed case (zero σ_a cross section). (2) The ore saving was found by reducing the reload enrichment (changed case) such that the discharge burnup of both cases were equal.

4.3. Depletion Model

In order to investigate the six-batch core a consistent method for evaluation of the fuel depletion process in a reactor was needed. In the subsequent sections the spatial diffusion-depletion model used for this purpose will be described.

4.3.1. Cross Section Generation and BOC Power Distributions

The same method developed in Section 3.3.1., which relies primarily upon the LEOPARD code, was used to calculate the appropriate diffusion theory parameters needed for this study. In addition LEOPARD point depletion calculations were performed to determine the fitted constants required for the FLARE-G code (e.g., k_∞ vs. burnup).

The PDQ-7 code was used to calculate a power distribution for the reactor core, in particular, two dimensional X-Y and r-z power distributions were calculated at the beginning of each cycle. Since the fuel loading patterns for a 6 zone core were not established prior to this work, a trial and error process was used to determine the BOC power distribution in which the power-peaking factors were acceptable. Different patterns were tried until the maximum peak-assembly-to-average power ratio was less than 1.40. An exhaustive search was not performed to find the optimum power distribu-

tion (lowest power peaking factors) since the time and computational costs are prohibitive. In addition, pin power peaking factors were not determined since our primary goal was to determine ore saving benefits, but it is recognized that this is important in assuring the safe operation of the reactor and hence further work is recommended in this area.

4.3.2. Nodal Depletion

The FLARE-G code described in Section 2.2.4. was used to calculate the burnup history for the reactor core for each cycle. Initially the FLARE-G code is used to calculate a three dimensional BOC power distribution. The horizontal and vertical albedos are varied so that the three dimensional power distribution calculated by the FLARE-G code matches the power distribution calculated by PDQ-7 (X-Y and R-Z power distribution). Once the BOC power distribution is normalized, the FLARE-G code is used to calculate the burnup distribution for the reactor. The reactor is depleted until reactivity limited burnup is reached.

4.3.3. Reload Analysis

The diffusion-depletion model is summarized below.

(1) The cross section generation method developed in Section 3.3.1. was used to calculate the diffusion theory constants needed for this study.

(2) The PDQ-7 code was used to calculate the X-Y power distributions for various fuel loading patterns. This procedure was continued until the maximum assembly peak-to-average power ratio was less than 1.40.

(3) The PDQ-7 code was used to calculate an R-Z power distribution for the reactor (for the X-Y loading pattern which has acceptable peaking).

(4) The FLARE-G code was used to calculate a three-dimensional BOC

power distribution. The albedo boundary conditions were varied such that the power distribution calculated by FLARE-G is in good agreement with the power distributions calculated in steps 2 and 3.

(5) LEOPARD supercell depletion calculations were performed to obtain diffusion theory constants as a function of burnup. These constants were input to FLARE-G for the nodal depletion calculations.

(6) The FLARE-G code was used to calculate the burnup history of the reactor. These depletion calculations were performed until reactivity-limited-burnup was reached.

(7) The isotopic concentration for each heavy isotope was determined by interpolating and extrapolating the results of the point depletion calculation (step 5). Thus the EOC compositions for each assembly are determined.

(8) Steps 1 through 8 were repeated for each cycle for the lifetime of the reactor.

4.4. Reactor Investigated

The Westinghouse PWR system shown in Figure 4.3. was used as the design basis for this study. The fuel assembly is 8.5 inches square and 12 ft. in height. The assembly consists of a 15 x 15 array of fuel cells; 204 of these positions contain the fuel rods of enriched uranium while twenty of these positions contain control rod guide tubes and one position contains an instrumentation tube. The major design characteristics for the reactor are shown in Table 4.2. This system was chosen to be the design basis since it is typical of a large PWR in actual commercial operation (Z10N), and a substantial amount of supplementary information, which expedited the present study was available from prior work at MIT on the

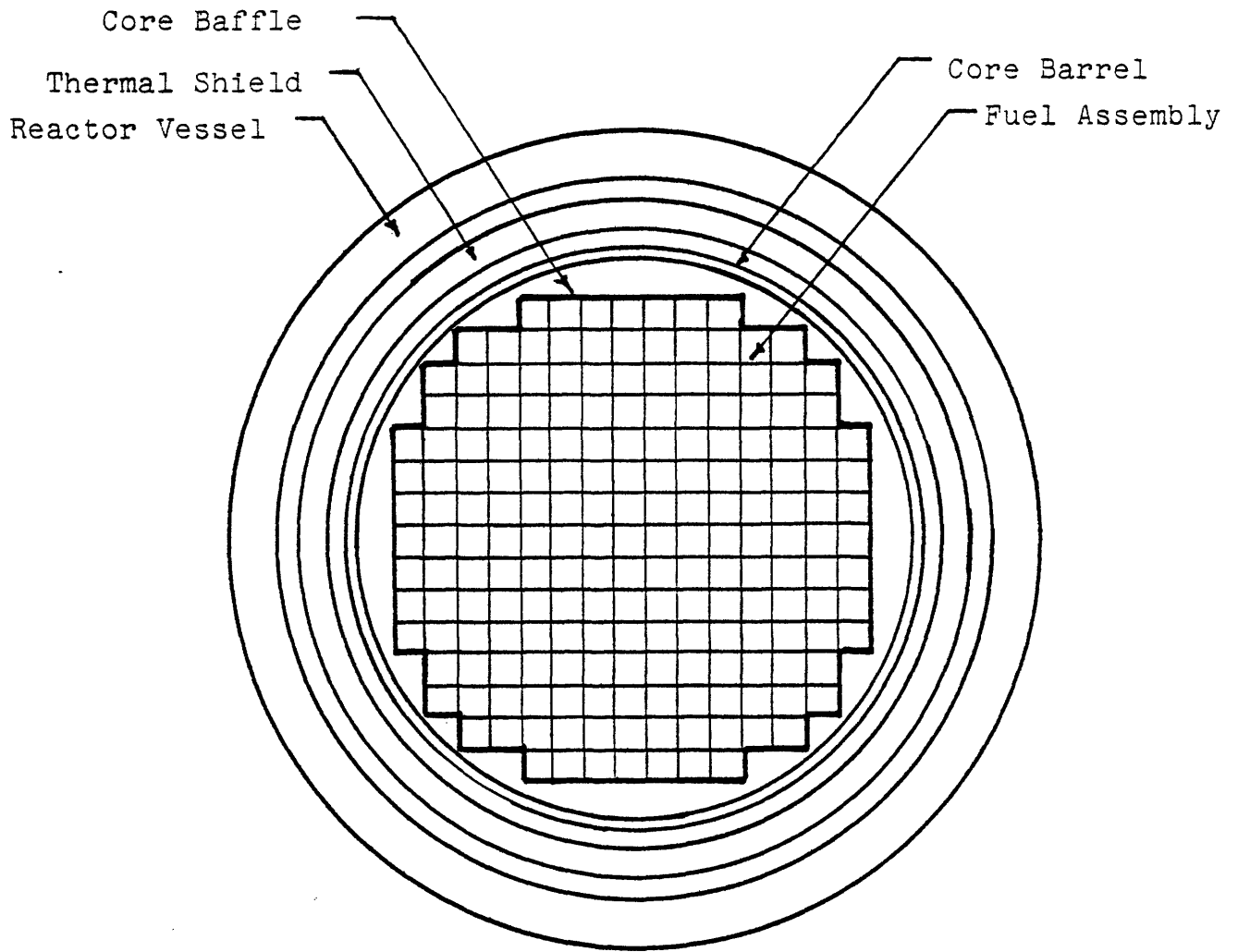


Figure 4.3

REACTOR CORE CROSS SECTION

TABLE 4.2

ZION REACTOR CORE DESIGN DATA

Fuel Rod Characteristics

Fuel Rod Diameter, Cold (in.)	0.422
Clad Material	Zircaloy-4
Diametral Gap, cold (in.)	0.0085
UO ₂ Pellet Diameter, Cold (in.)	0.3649
Active Fuel Length, Cold (in.)	142.3

Fuel Assembly Characteristics

Lattice Configuration	15x15
Lattice Pitch, Cold (in.)	0.563
Number of Fuel Rods/Assembly	204
Coolant Temperatures, °F	
Design Inlet, Hot Full Power	527.2
Initial Inlet, Hot Full Power	524.9
Design Core Average, Hot Full Power	559.4
Initial Core Average, Hot Full Power	557.1
Operating Pressure, psia	2250
Heat Output, MWth	3250
Average Linear Heat Generation Rate, kw/ft	6.70
Power Density, kw/liter	99.5

reference core for this reactor [R-3].

In the analysis of this reactor the PDQ-7 model for core calculations employed a coarse mesh 2 dimensional representation of the reactor. Each fuel assembly was explicitly represented by 25 mesh points (5x5). In addition, the core baffle and reflector were represented by a coarse mesh (approximately 2 cm.). The Flare-G model for core calculations employed a 3 dimensional coarse mesh representation of the reactor. Each fuel assembly contained one radial node with 12 planar regions. The reflector and baffle were represented by albedo boundary conditions.

4.5. Results

4.5.1. Ore Savings

As previously mentioned, two six batch core fuel management schemes were analyzed; namely, (1) a six-batch core with semi-annual refueling and (2) a six-batch core with annual refueling. These two cases were compared to a typical 3-batch core refueled annually, in particular, the Westinghouse designed ZION PWR [R-3]. In all of the above cases, a 90% availability based capacity factor and a refueling shutdown of 0.125 yrs. were assumed.

The depletion model described in Section 4.3 was used to analyze the 6-batch cases. As previously mentioned the fuel loading patterns for a 6 zone core were not established prior to this work; a trial and error procedure was used to determine the BOC power distribution in which the power peaking factors were acceptable. Different patterns were tried until the maximum peak-assembly-to-average power ratio was less than 1.40 (this was the same maximum allowable peaking factor used by Rieck [R-3] for his 3-batch studies in the burnup range ≤ 33000 MWD/MT on the same reactor).

The initial fuel loading for the first core and subsequent cores is

summarized in Table 4.3. As shown, the 3-batch core fuel loading is slightly smaller than the equilibrium fuel loading; this is done to reduce the relative density of UO_2 and cross section of fertile U-238 which in turn, results in lower fissile loadings to support criticality. This refinement was not incorporated for the 6-batch core since our primary interest is the ore savings when the reactor has reached equilibrium conditions, but the results of this present work could later be refined for the initial transient cycles.

The burnup and electric energy generation history is summarized in Tables [4.4] thru [4.6]. The results for the 3 batch core were generated by Rieck [R-3] and the results for the 6-batch core were calculated using the depletion model developed in Section 4.3. A condensed version of the above three tables is shown in Table [4.7]. As shown, the 6-batch core with semi-annual refueling uses a lower equilibrium reload enrichment than the 3-batch core; hence an ore savings of approximately 10% is obtained. For the 6 batch case with annual refueling the equilibrium reload enrichment is significantly higher than the 3 batch core. This is due to the fact that a higher enrichment is needed to compensate for the additional burnup (nearly doubled) but an ore savings is obtained since greater energy is extracted from the fuel (6 batch core) from the same heavy metal mass (relative to 3 batch core). Thus an ore savings of approximately 20% is obtained when the current fuel management scheme (3 batch core) is changed to a fuel management scheme involving a 6 batch core refueled annually.

Some comments are in order on the above comparisons. The diffusion depletion models and their cross section base library used by Rieck [R-3], LEOPARD/CITATION/SIMULATE, were similar but not identical to those used in the present work: LEOPARD/PDQ/FLARE. This should not have any appreciable

TABLE 4.3

INITIAL FUEL LOADING FOR 3-BATCH AND 6-BATCH CORES

Fuel lots	Mass of Uranium Per Assembly (kg)			Enrichment (w/o)		
	3-Batch Core*	6-Batch Core 1/2 yr**	6-Batch Core 1 yr***	3-Batch Core*	6-Batch Core 1/2 yr**	6-Batch Core 1 yr***
1	455.8	460.9	460.9	2.25	1.30	2.25
2	447.2	460.9	460.9	2.80	1.60	2.80
3	436.5	460.9	460.9	3.30	1.90	3.20
4	460.9	460.9	460.9	3.20	2.20	3.60
5	460.9	460.9	460.9	3.20	2.50	4.20
6	460.9	460.9	460.9	3.20	3.00	5.00
7	460.9	460.9	460.9	3.20	3.00	5.20
.
.
.
.

* From Ref. [R-3]

** 6-Batch Core with Semi-annual Refueling

*** 6-Batch Core with Annual Refueling

TABLE 4.4 BURNUP AND ELECTRIC ENERGY GENERATION HISTORY: 3-BATCH CORE ANNUAL REFUELING

LOT	JOB	PER- JOB	START TIME YR	BURNUP TIME YR	BURNUP KWD/TONNE HR	ELECTRICITY KWH	CAPAC FACTORY	LOT	SUB JOB	PER- JOB	START TIME YR	BURNUP TIME YR	BURNUP KWD/TONNE HR	ELECTRICITY KWH	CAPAC FACTORY
1	1	1	0.0	1.2553	1.694100E+09	3.66770E+09	0.933	1	2	1	0.0	1.2553	1.595301E+09	5.68770E+07	0.900
1	1	2	1.3803	0.7818	0.0	0.0	0.900	1	2	2	1.3803	0.7818	0.0	0.0	0.900
1	1	3	2.2871	0.8111	0.0	0.0	0.900	1	2	3	2.2871	0.8111	0.0	0.0	0.900
1	1	4	3.2232	0.8572	0.0	0.0	0.900	1	2	4	3.2232	0.8572	0.0	0.0	0.900
2	1	1	0.0	1.2553	1.644000E+09	1.626516E+09	0.900	2	2	1	0.0	1.2553	1.493400E+09	5.226846E+07	0.900
2	1	2	1.3803	0.7818	0.700350E+09	1.518203E+09	0.900	2	2	2	1.3803	0.7818	0.721003E+09	1.052317E+07	0.900
2	1	3	2.2871	0.8111	0.0	0.0	0.900	2	2	3	2.2871	0.8111	0.000000E+03	2.813971E+07	0.900
2	1	4	3.2232	0.8572	0.0	0.0	0.900	2	2	4	3.2232	0.8572	0.0	0.0	0.900
3	1	1	0.0	1.2553	1.328000E+09	2.054147E+09	0.900	3	2	1	0.0	1.2553	1.039400E+09	3.492496E+07	0.900
3	1	2	1.3803	0.7818	1.631200E+09	2.180630E+09	0.900	3	2	2	1.3803	0.7818	0.553000E+03	2.921894E+07	0.900
3	1	3	2.2871	0.8111	0.671500E+09	1.866190E+09	0.900	3	2	3	2.2871	0.8111	0.601700E+03	2.938293E+07	0.900
3	1	4	3.2232	0.8572	0.0	0.0	0.900	3	2	4	3.2232	0.8572	0.547000E+03	2.919845E+07	0.900
4	1	1	0.0	0.7818	1.024200E+09	2.127714E+09	0.900	4	2	1	1.3803	0.7818	0.828090E+03	2.462966E+07	0.900
4	1	2	1.3803	0.8111	1.074300E+09	2.441570E+09	0.900	4	2	2	2.2871	0.8111	1.105100E+04	3.906301E+07	0.900
4	1	3	2.2871	0.8572	0.0	0.0	0.900	4	2	3	3.2232	0.8572	0.291000E+03	3.352157E+07	0.900
4	1	4	3.2232	0.8939	0.0	0.0	0.900	4	2	4	4.2054	0.8939	0.296000E+03	2.919845E+07	0.900
5	1	1	0.0	0.8111	1.031100E+09	2.149197E+09	0.900	5	2	1	2.2871	0.8111	7.051300E+03	2.812000E+07	0.900
5	1	2	1.3803	0.8572	1.102900E+09	2.504512E+09	0.933	5	2	2	3.2232	0.8572	1.127300E+04	4.006379E+07	0.900
5	1	3	2.2871	0.8939	0.0	0.0	0.900	5	2	3	4.2054	0.8939	0.791000E+03	3.171077E+07	0.900
5	1	4	3.2232	0.9397	0.0	0.0	0.900	5	2	4	5.1663	0.9397	0.149000E+03	2.939496E+07	0.900
6	1	1	0.0	0.8572	1.066000E+09	2.422715E+09	0.900	6	2	1	3.2232	0.8572	0.059000E+03	2.906664E+07	0.900
6	1	2	1.3803	0.8939	1.065100E+09	2.421124E+09	0.900	6	2	2	4.2054	0.8939	1.086900E+04	3.920650E+07	0.900
6	1	3	2.2871	0.9397	0.0	0.0	0.900	6	2	3	5.1663	0.9397	0.881000E+03	3.205066E+07	0.900
6	1	4	3.2232	0.9794	0.0	0.0	0.900	6	2	4	6.1310	0.9794	0.162000E+03	2.944106E+07	0.900
7	1	1	0.0	0.8939	1.056200E+09	2.460448E+09	0.900	7	2	1	4.2054	0.8939	0.010000E+03	2.891157E+07	0.900
7	1	2	1.3803	0.9397	1.073100E+09	2.439406E+09	0.900	7	2	2	5.1663	0.9397	1.095400E+04	3.951312E+07	0.900
7	1	3	2.2871	0.9794	0.0	0.0	0.900	7	2	3	6.1310	0.9794	0.872000E+03	3.200294E+07	0.900
7	1	4	3.2232	1.0191	0.0	0.0	0.900	7	2	4	7.0954	1.0191	0.162000E+03	2.944106E+07	0.900
8	1	1	0.0	0.9397	1.057100E+09	2.402447E+09	0.900	8	2	1	5.1663	0.9397	0.015000E+03	2.891157E+07	0.900
8	1	2	1.3803	0.9794	1.072500E+09	2.437467E+09	0.900	8	2	2	6.1310	0.9794	1.095400E+04	3.951312E+07	0.900
8	1	3	2.2871	1.0191	0.0	0.0	0.900	8	2	3	7.0954	1.0191	0.872000E+03	3.200294E+07	0.900
8	1	4	3.2232	1.0588	0.0	0.0	0.900	8	2	4	8.0598	1.0588	0.156000E+03	2.944106E+07	0.900
9	1	1	0.0	0.8939	1.057100E+09	2.402447E+09	0.900	9	2	1	6.1310	0.8939	0.015000E+03	2.891157E+07	0.900
9	1	2	1.3803	0.9397	1.072500E+09	2.437467E+09	0.900	9	2	2	7.0954	0.9397	1.095400E+04	3.951312E+07	0.900
9	1	3	2.2871	0.9794	0.0	0.0	0.900	9	2	3	8.0598	0.9794	0.872000E+03	3.200294E+07	0.900
9	1	4	3.2232	1.0191	0.0	0.0	0.900	9	2	4	9.0243	1.0191	0.156000E+03	2.944106E+07	0.900
10	1	1	0.0	0.9794	1.057100E+09	2.402447E+09	0.900	10	2	1	7.0954	0.9794	0.015000E+03	2.891157E+07	0.900
10	1	2	1.3803	1.0191	1.072500E+09	2.437467E+09	0.900	10	2	2	8.0598	1.0191	1.095400E+04	3.951312E+07	0.900
10	1	3	2.2871	1.0588	0.0	0.0	0.900	10	2	3	9.0243	1.0588	0.872000E+03	3.200294E+07	0.900
10	1	4	3.2232	1.0985	0.0	0.0	0.900	10	2	4	10.9532	1.0985	0.156000E+03	2.944106E+07	0.900
11	1	1	0.0	0.9397	1.057100E+09	2.402447E+09	0.900	11	2	1	8.0598	0.9397	0.015000E+03	2.891157E+07	0.900
11	1	2	1.3803	0.9794	1.072500E+09	2.437467E+09	0.900	11	2	2	9.0243	0.9794	1.095400E+04	3.951312E+07	0.900
11	1	3	2.2871	1.0191	0.0	0.0	0.900	11	2	3	9.9887	1.0191	0.872000E+03	3.200294E+07	0.900
11	1	4	3.2232	1.0588	0.0	0.0	0.900	11	2	4	10.9532	1.0588	0.156000E+03	2.944106E+07	0.900
12	1	1	0.0	0.9794	1.057100E+09	2.402447E+09	0.900	12	2	1	9.0243	0.9794	0.015000E+03	2.891157E+07	0.900
12	1	2	1.3803	1.0191	1.072500E+09	2.437467E+09	0.900	12	2	2	9.9887	1.0191	1.095400E+04	3.951312E+07	0.900

25	1	4	24.4553	0.8394	0.0	0.0	0.900	25	2	4	24.4553	0.8394	0.156000E+03	2.942021E+07	0.900
26	1	1	22.5264	0.8394	1.057100E+04	2.402487E+09	0.900	26	2	1	22.5264	0.8394	0.015000E+03	2.891157E+07	0.900
26	1	2	23.4908	0.8394	1.072500E+04	2.437487E+09	0.900	26	2	2	23.4908	0.8394	1.095400E+04	3.951312E+07	0.900
26	1	3	24.4553	0.8394	9.016000E+03	2.049080E+09	0.900	26	2	3	24.4553	0.8394	0.072000E+03	3.200294E+07	0.900
26	1	4	25.4197	0.8394	0.0	0.0	0.900	26	2	4	25.4197	0.8394	0.156000E+03	2.942021E+07	0.900
27	1	1	23.4908	0.8394	1.057100E+04	2.402487E+09	0.900	27	2	1	23.4908	0.8394	0.015000E+03	2.891157E+07	0.900
27	1	2	24.4553	0.8394	1.072500E+04	2.437487E+09	0.900	27	2	2	24.4553	0.8394	1.095400E+04	3.951312E+07	0.900
27	1	3	25.4197	0.8394	9.016000E+03	2.049080E+09	0.900	27	2	3	25.4197	0.8394	0.072000E+03	3.200294E+07	0.900
27	1	4	26.3841	0.8394	0.0	0.0	0.900	27	2	4	26.3841	0.8394	0.156000E+03	2.942021E+07	0.900
28	1	1	24.4553	0.8394	1.057100E+04	2.402487E+09	0.900	28	2	1	24.4553	0.8394	0.015000E+03	2.891157E+07	0.900
28	1	2	25.4197	0.8394	1.072500E+04	2.437487E+09	0.900	28	2	2	25.4197	0.8394	1.095400E+04	3.951312E+07	0.900
28	1	3	26.3841	0.8394	9.016000E+03	2.049080E+09	0.900	28	2	3	26.3841	0.8394	0.072000E+03	3.200294E+07	0.900
28	1	4	27.3486	0.8394	0.0	0.0	0.900	28	2	4	27.3486	0.8394	0.156000E+03	2.942021E+07	0.900
29	1	1	25.4197	0.8394	1.057100E+04	2.402487E+09	0.900	29	2	1	25.4197	0.8394	0.015000E+03	2.891157E+07	0.900
29	1	2	26.3841	0.8394	1.072500E+04	2.437487E+09	0.900	29	2	2	26.3841	0.8394	1.095400E+04	3.951312E+07	0.900
29	1	3	27.3486	0.8394	9.016000E+03	2.049080E+09	0.900	29	2	3	27.3486	0.8394	0.072000E+03	3.200294E+07	0.900
29	1	4	28.3130	0.8394	0.0	0.0	0.900	29	2	4	28.3130	0.8394	0.156000E+03	2.942021E+07	0.900
30	1	1	26.3841	0.8394	1.057100E+04	2.402487E+09	0.900	30	2	1	26.3841	0.8394	0.015000E+03	2.891157E+07	0.900
30	1	2	27.3486	0.8394	1.072500E+04	2.437487E+09	0.900	30	2	2	27.3486	0.8394	1.095400E+04	3.951312E+07	0.900
30	1	3	28.3130	0.8394	9.016000E+03	2.049080E+09	0.900	30	2	3	28.3130	0.8394	0.072000E+03	3.200294E+07	0.900
30	1	4	29.2774	0.8394	0.0	0.0	0.900	30	2	4	29.2774	0.8394	0.156000E+03	2.942021E+07	0.900
31	1	1	27.3486	0.8394	1.057100E+04	2.402487E+09	0.900	31	2	1	27.3486	0.8394	0.015000E+03	2.891157E+07	0.900
31	1	2	28.3130	0.8394	1.072500E+04	2.437487E+09	0.900	31	2	2	28.3130	0.8394	1.095400E+04	3.951312E+07	0.900
31	1	3	29.2774	0.8394	9.016000E+03	2.049080E+09	0.900	31	2	3	29.2774	0.8394	0.072000E+03	3.200294E+07	0.900
31	1	4	0.0	0.0	0.0	0.0	0.0	31	2	4	0.0	0.0	0.0	0.0	0.900
32	1	1	28.3130	0.8394	1.057100E+04	2.402487E+09	0.900	32	2	1	28.3130	0.8394	0.015000E+03	2.891157E+07	0.900
32	1	2	29.2774	0.8394	1.072500E+04	2.437487E+09	0.900	32	2	2	29.2774	0.8394	1.095400E+04	3.951312E+07	0.900
32	1	3	0.0	0.0	0.0	0.0	0.900	32	2	3	0.0	0.0	0.0	0.0	0.900
32	1	4	0.0	0.0	0.0	0.0	0.0	32	2	4	0.0	0.0	0.0	0.0	0.900
33	1	1	29.2774	0.8394	1.057100E+04	2.402487E+09	0.900	33	2	1	29.2774	0.8394	0.015000E+03	2.891157E+07	0.900
33	1	2	0.0	0.0	0.0	0.0	0.900	33	2	2	0.0	0.0	0.0	0.0	0.900
33	1	3	0.0	0.0	0.0	0.0	0.900	33	2	3	0.0	0.0	0.0	0.0	0.900
33	1	4	0.0	0.0	0.0	0.0	0.0	33	2	4	0.0	0.0	0.0	0.0	0.900

TABLE 4.5 BURNUP AND ELECTRIC ENERGY GENERATION HISTORY: 6-BATCH CORE, SEMI-ANNUAL REFUELING

LOT	SUB LOT	PER-IOD	START TIME YR	IRR TIME YR	BURNUP MW/TONNE HM	ELECTRICITY FACTOR KWHE	LOT	SUB LOT	PER-IOD	START TIME YR	IRR TIME YR	BURNUP MW/TONNE HM	ELECTRICITY FACTOR KWHE	
1	1	1	0.0	0.7818	9.946000E+03	1.140160E+09	0.900	1	2	1	0.0	0.0	0.0	
1	1	2	0.9068	0.3121	0.0	0.0	0.900	1	2	2	0.9068	0.0	0.0	
1	1	3	1.3439	0.3162	0.0	0.0	0.900	1	2	3	1.3439	0.0	0.0	
1	1	4	1.7851	0.3719	0.0	0.0	0.900	1	2	4	1.7851	0.0	0.0	
1	1	5	2.2820	0.4331	0.0	0.0	0.900	1	2	5	2.2820	0.0	0.0	
1	1	6	2.8401	0.4711	0.0	0.0	0.900	1	2	6	2.8401	0.0	0.0	
1	1	7	3.4362	0.5155	0.0	0.0	0.900	1	2	7	3.4362	0.0	0.0	
2	1	1	0.0	0.7818	9.646000E+03	1.113528E+09	0.900	2	2	1	0.0	0.7818	7.546000E+03	2.721981E+07
2	1	2	0.9068	0.3121	3.343000E+03	3.855675E+08	0.900	2	2	2	0.9068	0.3121	3.324000E+03	1.199029E+07
2	1	3	1.3439	0.3162	0.0	0.0	0.900	2	2	3	1.3439	0.3162	4.036000E+03	1.455860E+07
2	1	4	1.7851	0.3719	0.0	0.0	0.900	2	2	4	1.7851	0.3719	0.0	0.500
2	1	5	2.2820	0.4331	0.0	0.0	0.900	2	2	5	2.2820	0.4331	0.0	0.500
2	1	6	2.8401	0.4711	0.0	0.0	0.900	2	2	6	2.8401	0.4711	0.0	0.900
2	1	7	3.4362	0.5155	0.0	0.0	0.900	2	2	7	3.4362	0.5155	0.0	0.900
3	1	1	0.0	0.7818	1.065800E+04	1.191900E+09	0.900	3	2	1	0.0	0.7818	9.330000E+03	3.368390E+07
3	1	2	0.9068	0.3121	3.778000E+03	4.225016E+08	0.900	3	2	2	0.9068	0.3121	3.832000E+03	1.30274E+07
3	1	3	1.3439	0.3162	3.720000E+03	4.160156E+08	0.900	3	2	3	1.3439	0.3162	3.433000E+03	1.238347E+07
3	1	4	1.7851	0.3719	0.0	0.0	0.900	3	2	4	1.7851	0.3719	4.354000E+03	1.570569E+07
3	1	5	2.2820	0.4331	0.0	0.0	0.900	3	2	5	2.2820	0.4331	0.0	0.900
3	1	6	2.8401	0.4711	0.0	0.0	0.900	3	2	6	2.8401	0.4711	0.0	0.900
3	1	7	3.4362	0.5155	0.0	0.0	0.900	3	2	7	3.4362	0.5155	0.0	0.900
4	1	1	0.0	0.7818	1.281000E+04	1.434806E+09	0.900	4	2	1	0.0	0.7818	1.065600E+04	3.844538E+07
4	1	2	0.9068	0.3121	3.802000E+03	4.251850E+08	0.900	4	2	2	0.9068	0.3121	3.892000E+03	1.40317E+07
4	1	3	1.3439	0.3162	3.662000E+03	4.095293E+08	0.900	4	2	3	1.3439	0.3162	4.954000E+03	1.787000E+07
4	1	4	1.7851	0.3719	4.126000E+03	4.614193E+08	0.900	4	2	4	1.7851	0.3719	4.023000E+03	1.451717E+07
4	1	5	2.2820	0.4331	0.0	0.0	0.900	4	2	5	2.2820	0.4331	5.282000E+03	1.905315E+07
4	1	6	2.8401	0.4711	0.0	0.0	0.900	4	2	6	2.8401	0.4711	0.0	0.500
4	1	7	3.4362	0.5155	0.0	0.0	0.900	4	2	7	3.4362	0.5155	0.0	0.500
5	1	1	0.0	0.7818	7.351000E+03	8.223022E+08	0.900	5	2	1	0.0	0.7818	4.247000E+03	1.531972E+07
5	1	2	0.9068	0.3121	4.216000E+03	4.714848E+08	0.900	5	2	2	0.9068	0.3121	4.304000E+03	1.509247E+07
5	1	3	1.3439	0.3162	4.012000E+03	4.406705E+08	0.900	5	2	3	1.3439	0.3162	4.593000E+03	1.651005E+07
5	1	4	1.7851	0.3719	4.492000E+03	5.023449E+08	0.900	5	2	4	1.7851	0.3719	4.611000E+03	1.670488E+07
5	1	5	2.2820	0.4331	4.862000E+03	5.417279E+08	0.900	5	2	5	2.2820	0.4331	5.226000E+03	1.805837E+07
5	1	6	2.8401	0.4711	0.0	0.0	0.900	5	2	6	2.8401	0.4711	5.684000E+03	2.050325E+07
5	1	7	3.4362	0.5155	0.0	0.0	0.900	5	2	7	3.4362	0.5155	0.0	0.500
6	1	1	0.0	0.7818	6.228000E+03	6.964900E+08	0.900	6	2	1	0.0	0.7818	4.235000E+03	1.529086E+07
6	1	2	0.9068	0.3121	3.722000E+03	4.162394E+08	0.900	6	2	2	0.9068	0.3121	2.668000E+03	9.623977E+06
6	1	3	1.3439	0.3162	4.594000E+03	5.137569E+08	0.900	6	2	3	1.3439	0.3162	4.577000E+03	1.651005E+07
6	1	4	1.7851	0.3719	5.126000E+03	5.732516E+08	0.900	6	2	4	1.7851	0.3719	4.941000E+03	1.782310E+07
6	1	5	2.2820	0.4331	5.201000E+03	5.816389E+08	0.900	6	2	5	2.2820	0.4331	5.197000E+03	2.235373E+07
6	1	6	2.8401	0.4711	5.177000E+03	5.709553E+08	0.900	6	2	6	2.8401	0.4711	5.481000E+03	2.457709E+07
6	1	7	3.4362	0.5155	0.0	0.0	0.900	6	2	7	3.4362	0.5155	0.0	0.900
7	1	1	0.9068	0.3121	3.703000E+03	4.138908E+08	0.900	7	2	1	0.9068	0.3121	2.811000E+03	1.013900E+07
7	1	2	1.3439	0.3162	3.636000E+03	4.066217E+08	0.900	7	2	2	1.3439	0.3162	2.369000E+03	8.545417E+06
7	1	3	1.7851	0.3719	5.000000E+03	5.591600E+08	0.900	7	2	3	1.7851	0.3719	4.911000E+03	1.771488E+07
7	1	4	2.2820	0.4331	6.361000E+03	7.113646E+08	0.900	7	2	4	2.2820	0.4331	6.172000E+03	2.226355E+07
7	1	5	2.8401	0.4711	5.980000E+03	6.697628E+08	0.900	7	2	5	2.8401	0.4711	6.301000E+03	2.301746E+07
7	1	6	3.4362	0.5155	6.045000E+03	6.760253E+08	0.900	7	2	6	3.4362	0.5155	6.201000E+03	2.236816E+07
7	1	7	4.0767	0.4479	0.0	0.0	0.900	7	2	7	4.0767	0.4479	5.440000E+03	1.962309E+07
8	1	1	1.3439	0.3162	3.173000E+03	3.548434E+08	0.900	8	2	1	1.3439	0.3162	2.114000E+03	7.625592E+06

8	1	2	1-7851	0.3719	4.329000E+03	4.841211E+03	0.500	4	2	2	1-7851	0.3719	2.737000E+03	9.872469E+06	0.900
8	1	3	2-2820	0.4331	6.211000E+03	7.084004E+04	0.900	8	3	3	2-2820	0.4331	6.211000E+03	2.251770E+07	0.900
8	1	4	2-8401	0.4711	6.311000E+03	7.085546E+04	0.900	8	2	4	2-8401	0.4711	6.311000E+03	2.294114E+07	0.500
8	1	5	3-8362	0.5155	6.110000E+03	7.056609E+04	0.900	8	2	5	3-8362	0.5155	6.110000E+03	2.319816E+07	0.900
8	1	6	4-8767	0.4879	5.120000E+03	5.725409E+04	0.900	8	2	6	4-8767	0.4879	5.120000E+03	1.922246E+07	0.900
8	1	7	4-6496	0.4202	0.0	0.0	0.900	8	2	7	4-6496	0.4202	4.650000E+03	1.785111E+07	0.900
9	1	1	1-7851	0.3719	3.404000E+03	4.258568E+04	0.900	9	2	1	1-7851	0.3719	3.064000E+03	1.113995E+07	0.900
9	1	2	2-2820	0.4331	4.339000E+03	4.652194E+04	0.900	9	2	2	2-2820	0.4331	3.153000E+03	1.133853E+07	0.900
9	1	3	2-8401	0.4711	6.444000E+03	7.410111E+04	0.900	9	2	3	2-8401	0.4711	6.426000E+03	2.310699E+07	0.900
9	1	4	3-8362	0.5155	6.550000E+03	7.325007E+04	0.900	9	2	4	3-8362	0.5155	6.752000E+03	2.435371E+07	0.900
9	1	5	4-8767	0.4879	5.540000E+03	6.195507E+04	0.900	9	2	5	4-8767	0.4879	5.736000E+03	2.045502E+07	0.900
9	1	6	4-6496	0.4202	4.450000E+03	5.206304E+04	0.900	9	2	6	4-6496	0.4202	4.130000E+03	1.742997E+07	0.900
9	1	7	5-1949	0.4314	0.0	0.0	0.900	9	2	7	5-1949	0.4314	5.150000E+03	1.480398E+07	0.900
10	1	1	2-2820	0.4331	4.135000E+03	4.628291E+04	0.900	10	2	1	2-2820	0.4331	3.552000E+03	1.129119E+07	0.900
10	1	2	2-8401	0.4711	5.104000E+03	5.707914E+04	0.900	10	2	2	2-8401	0.4711	3.702000E+03	1.164230E+07	0.900
10	1	3	3-8362	0.5155	6.211000E+03	7.505971E+04	0.900	10	2	3	3-8362	0.5155	6.015000E+03	2.458290E+07	0.900
10	1	4	4-8767	0.4879	5.499000E+03	6.566702E+04	0.900	10	2	4	4-8767	0.4879	6.015000E+03	2.467362E+07	0.900
10	1	5	4-6496	0.4202	5.106000E+03	5.710189E+04	0.900	10	2	5	4-6496	0.4202	5.810000E+03	1.915414E+07	0.900
10	1	6	5-1949	0.4319	4.913000E+03	5.494113E+04	0.900	10	2	6	5-1949	0.4319	5.150000E+03	1.800580E+07	0.900
10	1	7	5-7518	0.4377	0.0	0.0	0.900	10	2	7	5-7518	0.4377	4.137000E+03	1.812292E+07	0.900
11	1	1	2-8401	0.4711	4.071000E+03	5.447342E+04	0.900	11	2	1	2-8401	0.4711	4.226000E+03	1.524396E+07	0.900
11	1	2	3-8362	0.5155	6.042000E+03	6.754092E+04	0.900	11	2	2	3-8362	0.5155	6.740000E+03	1.709805E+07	0.900
11	1	3	4-8767	0.4879	5.945000E+03	6.693153E+04	0.900	11	2	3	4-8767	0.4879	5.996000E+03	2.162868E+07	0.900
11	1	4	4-6496	0.4202	5.475000E+03	6.064895E+04	0.900	11	2	4	4-6496	0.4202	5.588000E+03	2.015694E+07	0.900
11	1	5	5-1949	0.4319	5.512000E+03	6.104191E+04	0.900	11	2	5	5-1949	0.4319	5.778000E+03	2.084231E+07	0.900
11	1	6	5-7518	0.4377	4.801000E+03	5.349060E+04	0.900	11	2	6	5-7518	0.4377	4.852000E+03	1.750206E+07	0.900
11	1	7	6-3145	0.4394	0.0	0.0	0.900	11	2	7	6-3145	0.4394	4.257000E+03	1.535570E+07	0.900
12	1	1	3-8362	0.5155	5.478000E+03	6.565021E+04	0.900	12	2	1	3-8362	0.5155	5.102000E+03	1.840386E+07	0.900
12	1	2	4-8767	0.4879	5.077000E+03	5.679954E+04	0.900	12	2	2	4-8767	0.4879	5.030000E+03	1.741551E+07	0.900
12	1	3	4-6496	0.4202	4.231000E+03	4.968264E+04	0.900	12	2	3	4-6496	0.4202	5.540000E+03	2.01453E+07	0.900
12	1	4	5-1949	0.4319	5.119000E+03	5.930246E+04	0.900	12	2	4	5-1949	0.4319	5.703000E+03	2.237518E+07	0.900
12	1	5	5-7518	0.4377	5.106000E+03	5.710347E+04	0.900	12	2	5	5-7518	0.4377	5.175000E+03	1.846716E+07	0.900
12	1	6	6-3145	0.4394	4.644000E+03	5.197957E+04	0.900	12	2	6	6-3145	0.4394	4.666000E+03	1.643112E+07	0.900
12	1	7	6-8789	0.4274	0.0	0.0	0.900	12	2	7	6-8789	0.4274	4.315000E+03	1.556591E+07	0.900
13	1	1	4-8767	0.4879	4.802000E+03	5.459845E+04	0.900	13	2	1	4-8767	0.4879	4.226000E+03	1.524396E+07	0.900
13	1	2	4-6496	0.4202	4.604000E+03	5.198751E+04	0.900	13	2	2	4-6496	0.4202	3.200000E+03	1.157805E+07	0.900
13	1	3	5-1949	0.4319	4.186000E+03	6.917931E+04	0.900	13	2	3	5-1949	0.4319	6.185000E+03	2.231043E+07	0.900
13	1	4	5-7518	0.4377	5.376000E+03	6.012099E+04	0.900	13	2	4	5-7518	0.4377	5.495000E+03	1.978541E+07	0.900
13	1	5	6-3145	0.4394	4.906000E+03	5.579511E+04	0.900	13	2	5	6-3145	0.4394	5.079000E+03	1.832040E+07	0.900
13	1	6	6-8789	0.4274	4.651000E+03	5.201311E+04	0.900	13	2	6	6-8789	0.4274	4.725000E+03	1.724395E+07	0.900
13	1	7	7-4313	0.4365	0.0	0.0	0.900	13	2	7	7-4313	0.4365	4.280000E+03	1.546604E+07	0.900
14	1	1	4-6496	0.4202	4.510000E+03	5.043624E+04	0.900	14	2	1	4-6496	0.4202	3.667000E+03	1.222755E+07	0.900
14	1	2	5-1949	0.4319	4.851000E+03	5.424974E+04	0.900	14	2	2	5-1949	0.4319	2.935000E+03	1.040152E+07	0.900
14	1	3	5-7518	0.4377	5.552000E+03	6.214513E+04	0.900	14	2	3	5-7518	0.4377	5.540000E+03	2.017494E+07	0.900
14	1	4	6-3145	0.4394	4.205000E+03	6.490301E+04	0.900	14	2	4	6-3145	0.4394	5.106000E+03	1.813714E+07	0.900
14	1	5	6-8789	0.4274	4.251000E+03	5.580251E+04	0.900	14	2	5	6-8789	0.4274	5.130000E+03	1.852850E+07	0.900
14	1	6	7-4313	0.4365	4.449000E+03	5.422740E+04	0.900	14	2	6	7-4313	0.4365	4.649000E+03	1.693933E+07	0.900
14	1	7	7-9928	0.4365	0.0	0.0	0.900	14	2	7	7-9928	0.4365	4.263000E+03	1.546604E+07	0.900
15	1	1	5-1949	0.4319	4.581000E+03	5.123031E+04	0.900	15	2	1	5-1949	0.4319	3.516000E+03	1.269008E+07	0.900
15	1	2	6-3145	0.4394	5.350000E+03	5.962466E+04	0.900	15	2	2	6-3145	0.4394	5.470000E+03	1.938674E+07	0.900
15	1	3	6-8789	0.4274	5.126000E+03	5.956180E+04	0.900	15	2	3	6-8789	0.4274	5.470000E+03	1.901587E+07	0.900
15	1	4	7-4313	0.4365	5.189000E+03	5.602772E+04	0.900	15	2	4	7-4313	0.4365	5.203000E+03	1.704954E+07	0.900
15	1	5	7-9928	0.4365	5.250000E+03	6.066895E+04	0.900	15	2	5	7-9928	0.4365	5.106000E+03	1.842550E+07	0.900
15	1	6	8-5543	0.4365	4.849000E+03	5.422740E+04	0.900	15	2	6	8-5543	0.4365	4.649000E+03	1.693933E+07	0.900
15	1	7	8-5543	0.4365	0.0	0.0	0.900	15	2	7	8-5543	0.4365	4.280000E+03	1.546604E+07	0.900
16	1	1	5-7518	0.4377	5.331000E+03	6.299505E+04	0.900	16	2	1	5-7518	0.4377	4.920000E+03	1.597262E+07	0.900
16	1	2	6-3145	0.4394	5.192000E+03	6.806326E+04	0.900	16	2	2	6-3145	0.4394	3.900000E+03	1.407845E+07	0.900
16	1	3	6-8789	0.4274	5.350000E+03	5.986376E+04	0.900	16	2	3	6-8789	0.4274	5.444000E+03	1.963752E+07	0.900

16	1	7.9313	0.4165	5.485000E+03	6.049236E+08	0.900	16	4	7.9313	0.4165	5.294000E+03	1.901643E+07	0.900
16	1	7.9928	0.4165	5.425000E+03	6.066975E+08	0.900	16	2	7.9928	0.4165	5.400000E+03	1.882553E+07	0.900
16	1	8.5543	0.4165	4.804500E+03	5.422740E+08	0.900	16	2	8.5543	0.4165	4.870000E+03	1.623913E+07	0.900
16	1	9.1158	0.4165	0.0	0.0	0.900	16	2	9.1158	0.4165	4.286300E+03	1.546040E+07	0.900
17	1	6.3145	0.4194	5.555000E+03	6.122270E+08	0.900	17	2	6.3145	0.4194	4.741000E+03	1.710168E+07	0.900
17	1	6.8749	0.4274	5.290000E+03	5.817644E+08	0.900	17	2	6.8749	0.4274	4.872000E+03	1.799271E+07	0.900
17	1	7.4313	0.4165	5.766000E+03	6.494244E+08	0.900	17	2	7.4313	0.4165	5.441000E+03	1.792465E+07	0.900
17	1	7.9928	0.4165	5.465000E+03	6.019216E+08	0.900	17	2	7.9928	0.4165	5.294000E+03	1.949681E+07	0.900
17	1	8.5543	0.4165	5.425000E+03	6.066975E+08	0.900	17	2	8.5543	0.4165	5.100000E+03	1.842553E+07	0.900
17	1	9.1158	0.4165	4.804500E+03	5.422740E+08	0.900	17	2	9.1158	0.4165	4.656000E+03	1.657933E+07	0.900
17	1	9.6773	0.4165	0.0	0.0	0.900	17	2	9.6773	0.4165	4.266000E+03	1.546040E+07	0.900
18	1	6.8749	0.4274	5.468000E+03	6.114970E+08	0.900	18	2	6.8749	0.4274	4.672000E+03	1.685277E+07	0.900
18	1	7.4313	0.4165	5.924000E+03	6.506616E+08	0.900	18	2	7.4313	0.4165	5.491000E+03	1.801556E+07	0.900
18	1	7.9928	0.4165	5.716000E+03	6.494244E+08	0.900	18	2	7.9928	0.4165	5.491000E+03	1.802462E+07	0.900
18	1	8.5543	0.4165	5.465000E+03	6.035260E+08	0.900	18	2	8.5543	0.4165	5.294000E+03	1.929481E+07	0.900
18	1	9.1158	0.4165	5.425000E+03	6.066975E+08	0.900	18	2	9.1158	0.4165	5.100000E+03	1.842553E+07	0.900
18	1	9.6773	0.4165	4.804500E+03	5.422740E+08	0.900	18	2	9.6773	0.4165	4.656000E+03	1.657933E+07	0.900
18	1	10.2308	0.4165	0.0	0.0	0.900	18	2	10.2308	0.4165	4.286300E+03	1.546040E+07	0.900
19	1	7.4313	0.4165	5.189700E+03	5.750236E+08	0.900	19	2	7.4313	0.4165	4.737000E+03	1.637901E+07	0.900
19	1	7.9928	0.4165	5.924000E+03	6.506616E+08	0.900	19	2	7.9928	0.4165	5.491000E+03	1.801556E+07	0.900
19	1	8.5543	0.4165	5.716000E+03	6.494244E+08	0.900	19	2	8.5543	0.4165	5.491000E+03	1.802462E+07	0.900
19	1	9.1158	0.4165	5.465000E+03	6.035260E+08	0.900	19	2	9.1158	0.4165	5.294000E+03	1.929481E+07	0.900
19	1	9.6773	0.4165	5.425000E+03	6.066975E+08	0.900	19	2	9.6773	0.4165	5.100000E+03	1.842553E+07	0.900
19	1	10.2308	0.4165	4.804500E+03	5.422740E+08	0.900	19	2	10.2308	0.4165	4.656000E+03	1.657933E+07	0.900
19	1	10.8003	0.4165	0.0	0.0	0.900	19	2	10.8003	0.4165	4.286300E+03	1.546040E+07	0.900
20	1	7.9928	0.4165	5.189000E+03	5.750236E+08	0.900	20	2	7.9928	0.4165	4.707000E+03	1.637901E+07	0.900
20	1	8.5543	0.4165	5.924000E+03	6.506616E+08	0.900	20	2	8.5543	0.4165	5.491000E+03	1.801556E+07	0.900
20	1	9.1158	0.4165	5.716000E+03	6.494244E+08	0.900	20	2	9.1158	0.4165	5.491000E+03	1.802462E+07	0.900
20	1	9.6773	0.4165	5.465000E+03	6.035260E+08	0.900	20	2	9.6773	0.4165	5.294000E+03	1.929481E+07	0.900
20	1	10.2308	0.4165	5.425000E+03	6.066975E+08	0.900	20	2	10.2308	0.4165	5.100000E+03	1.842553E+07	0.900
20	1	10.8003	0.4165	4.804500E+03	5.422740E+08	0.900	20	2	10.8003	0.4165	4.656000E+03	1.657933E+07	0.900
20	1	11.3618	0.4165	0.0	0.0	0.900	20	2	11.3618	0.4165	4.286300E+03	1.546040E+07	0.900
21	1	8.5543	0.4165	5.189000E+03	5.750236E+08	0.900	21	2	8.5543	0.4165	4.707000E+03	1.637901E+07	0.900
21	1	9.1158	0.4165	5.924000E+03	6.506616E+08	0.900	21	2	9.1158	0.4165	5.491000E+03	1.801556E+07	0.900
21	1	9.6773	0.4165	5.716000E+03	6.494244E+08	0.900	21	2	9.6773	0.4165	5.491000E+03	1.802462E+07	0.900
21	1	10.2308	0.4165	5.465000E+03	6.035260E+08	0.900	21	2	10.2308	0.4165	5.294000E+03	1.929481E+07	0.900
21	1	10.8003	0.4165	5.425000E+03	6.066975E+08	0.900	21	2	10.8003	0.4165	5.100000E+03	1.842553E+07	0.900
21	1	11.3618	0.4165	4.804500E+03	5.422740E+08	0.900	21	2	11.3618	0.4165	4.656000E+03	1.657933E+07	0.900
21	1	11.9213	0.4165	0.0	0.0	0.900	21	2	11.9213	0.4165	4.286300E+03	1.546040E+07	0.900
22	1	9.1158	0.4165	5.189000E+03	5.750236E+08	0.900	22	2	9.1158	0.4165	4.707000E+03	1.637901E+07	0.900
22	1	9.6773	0.4165	5.924000E+03	6.506616E+08	0.900	22	2	9.6773	0.4165	5.491000E+03	1.801556E+07	0.900
22	1	10.2308	0.4165	5.716000E+03	6.494244E+08	0.900	22	2	10.2308	0.4165	5.491000E+03	1.802462E+07	0.900
22	1	10.8003	0.4165	5.465000E+03	6.035260E+08	0.900	22	2	10.8003	0.4165	5.294000E+03	1.929481E+07	0.900
22	1	11.3618	0.4165	5.425000E+03	6.066975E+08	0.900	22	2	11.3618	0.4165	5.100000E+03	1.842553E+07	0.900
22	1	11.9213	0.4165	4.804500E+03	5.422740E+08	0.900	22	2	11.9213	0.4165	4.656000E+03	1.657933E+07	0.900
22	1	12.4848	0.4165	0.0	0.0	0.900	22	2	12.4848	0.4165	4.286300E+03	1.546040E+07	0.900
23	1	9.6773	0.4165	5.189000E+03	5.750236E+08	0.900	23	2	9.6773	0.4165	4.707000E+03	1.637901E+07	0.900
23	1	10.2308	0.4165	5.924000E+03	6.506616E+08	0.900	23	2	10.2308	0.4165	5.491000E+03	1.801556E+07	0.900
23	1	10.8003	0.4165	5.716000E+03	6.494244E+08	0.900	23	2	10.8003	0.4165	5.491000E+03	1.802462E+07	0.900
23	1	11.3618	0.4165	5.465000E+03	6.035260E+08	0.900	23	2	11.3618	0.4165	5.294000E+03	1.929481E+07	0.900
23	1	11.9213	0.4165	5.425000E+03	6.066975E+08	0.900	23	2	11.9213	0.4165	5.100000E+03	1.842553E+07	0.900
23	1	12.4848	0.4165	4.804500E+03	5.422740E+08	0.900	23	2	12.4848	0.4165	4.656000E+03	1.657933E+07	0.900
23	1	13.0463	0.4165	0.0	0.0	0.900	23	2	13.0463	0.4165	4.286300E+03	1.546040E+07	0.900
24	1	10.2308	0.4165	5.189000E+03	5.750236E+08	0.900	24	2	10.2308	0.4165	4.707000E+03	1.637901E+07	0.900
24	1	10.8003	0.4165	5.924000E+03	6.506616E+08	0.900	24	2	10.8003	0.4165	5.491000E+03	1.801556E+07	0.900
24	1	11.3618	0.4165	5.716000E+03	6.494244E+08	0.900	24	2	11.3618	0.4165	5.491000E+03	1.802462E+07	0.900
24	1	11.9213	0.4165	5.465000E+03	6.035260E+08	0.900	24	2	11.9213	0.4165	5.294000E+03	1.929481E+07	0.900
24	1	12.4848	0.4165	5.425000E+03	6.066975E+08	0.900	24	2	12.4848	0.4165	5.100000E+03	1.842553E+07	0.900
24	1	13.0463	0.4165	4.804500E+03	5.422740E+08	0.900	24	2	13.0463	0.4165	4.656000E+03	1.657933E+07	0.900

24	1	6	13.0463	0.4365	4.849000E+03	5.422740E+08	0.900	29	2	6	13.0463	0.4365	4.849000E+03	1.693933E+07	0.900
24	1	7	13.6078	0.4365	0.0	0.0	0.900	29	2	7	13.6078	0.4365	4.246000E+03	1.546400E+07	0.900
25	1	1	10.0003	0.4365	5.149000E+03	5.750216E+08	0.900	25	2	1	10.0003	0.4365	4.707000E+03	1.697901E+07	0.900
25	1	2	11.1618	0.4365	4.924000E+03	5.506616E+08	0.900	25	2	2	11.1618	0.4365	3.491200E+03	1.493556E+07	0.900
25	1	3	11.9213	0.4365	5.766000E+03	6.440241E+08	0.900	25	2	3	11.9213	0.4365	5.441300E+03	1.962669E+07	0.900
25	1	4	12.4848	0.4365	5.465000E+03	6.089260E+08	0.900	25	2	4	12.4848	0.4365	5.294000E+03	1.909643E+07	0.900
25	1	5	13.0463	0.4365	5.475000E+03	6.066495E+08	0.900	25	2	5	13.0463	0.4365	5.294000E+03	1.909643E+07	0.900
25	1	6	13.6078	0.4365	4.849000E+03	5.422740E+08	0.900	25	2	6	13.6078	0.4365	4.849000E+03	1.693933E+07	0.900
25	1	7	14.1693	0.4365	0.0	0.0	0.900	25	2	7	14.1693	0.4365	4.246000E+03	1.546400E+07	0.900
26	1	1	11.1618	0.4365	5.149000E+03	5.750216E+08	0.900	26	2	1	11.1618	0.4365	4.707000E+03	1.697901E+07	0.900
26	1	2	11.9213	0.4365	4.924000E+03	5.506616E+08	0.900	26	2	2	11.9213	0.4365	3.491200E+03	1.493556E+07	0.900
26	1	3	12.4848	0.4365	5.766000E+03	6.440241E+08	0.900	26	2	3	12.4848	0.4365	5.441300E+03	1.962669E+07	0.900
26	1	4	13.0463	0.4365	5.465000E+03	6.089260E+08	0.900	26	2	4	13.0463	0.4365	5.294000E+03	1.909643E+07	0.900
26	1	5	13.6078	0.4365	5.475000E+03	6.066495E+08	0.900	26	2	5	13.6078	0.4365	5.294000E+03	1.909643E+07	0.900
26	1	6	14.1693	0.4365	4.849000E+03	5.422740E+08	0.900	26	2	6	14.1693	0.4365	4.849000E+03	1.693933E+07	0.900
26	1	7	14.7308	0.4365	0.0	0.0	0.900	26	2	7	14.7308	0.4365	4.246000E+03	1.546400E+07	0.900
27	1	1	11.9213	0.4365	5.149000E+03	5.750216E+08	0.900	27	2	1	11.9213	0.4365	4.707000E+03	1.697901E+07	0.900
27	1	2	12.4848	0.4365	4.924000E+03	5.506616E+08	0.900	27	2	2	12.4848	0.4365	3.491200E+03	1.493556E+07	0.900
27	1	3	13.0463	0.4365	5.766000E+03	6.440241E+08	0.900	27	2	3	13.0463	0.4365	5.441300E+03	1.962669E+07	0.900
27	1	4	13.6078	0.4365	5.465000E+03	6.089260E+08	0.900	27	2	4	13.6078	0.4365	5.294000E+03	1.909643E+07	0.900
27	1	5	14.1693	0.4365	5.475000E+03	6.066495E+08	0.900	27	2	5	14.1693	0.4365	5.294000E+03	1.909643E+07	0.900
27	1	6	14.7308	0.4365	4.849000E+03	5.422740E+08	0.900	27	2	6	14.7308	0.4365	4.849000E+03	1.693933E+07	0.900
27	1	7	15.2923	0.4365	0.0	0.0	0.900	27	2	7	15.2923	0.4365	4.246000E+03	1.546400E+07	0.900
28	1	1	12.4848	0.4365	5.149000E+03	5.750216E+08	0.900	28	2	1	12.4848	0.4365	4.707000E+03	1.697901E+07	0.900
28	1	2	13.0463	0.4365	4.924000E+03	5.506616E+08	0.900	28	2	2	13.0463	0.4365	3.491200E+03	1.493556E+07	0.900
28	1	3	13.6078	0.4365	5.766000E+03	6.440241E+08	0.900	28	2	3	13.6078	0.4365	5.441300E+03	1.962669E+07	0.900
28	1	4	14.1693	0.4365	5.465000E+03	6.089260E+08	0.900	28	2	4	14.1693	0.4365	5.294000E+03	1.909643E+07	0.900
28	1	5	14.7308	0.4365	5.475000E+03	6.066495E+08	0.900	28	2	5	14.7308	0.4365	5.294000E+03	1.909643E+07	0.900
28	1	6	15.2923	0.4365	4.849000E+03	5.422740E+08	0.900	28	2	6	15.2923	0.4365	4.849000E+03	1.693933E+07	0.900
28	1	7	15.8538	0.4365	0.0	0.0	0.900	28	2	7	15.8538	0.4365	4.246000E+03	1.546400E+07	0.900
29	1	1	13.0463	0.4365	5.149000E+03	5.750216E+08	0.900	29	2	1	13.0463	0.4365	4.707000E+03	1.697901E+07	0.900
29	1	2	13.6078	0.4365	4.924000E+03	5.506616E+08	0.900	29	2	2	13.6078	0.4365	3.491200E+03	1.493556E+07	0.900
29	1	3	14.1693	0.4365	5.766000E+03	6.440241E+08	0.900	29	2	3	14.1693	0.4365	5.441300E+03	1.962669E+07	0.900
29	1	4	14.7308	0.4365	5.465000E+03	6.089260E+08	0.900	29	2	4	14.7308	0.4365	5.294000E+03	1.909643E+07	0.900
29	1	5	15.2923	0.4365	5.475000E+03	6.066495E+08	0.900	29	2	5	15.2923	0.4365	5.294000E+03	1.909643E+07	0.900
29	1	6	15.8538	0.4365	4.849000E+03	5.422740E+08	0.900	29	2	6	15.8538	0.4365	4.849000E+03	1.693933E+07	0.900
29	1	7	16.4153	0.4365	0.0	0.0	0.900	29	2	7	16.4153	0.4365	4.246000E+03	1.546400E+07	0.900
30	1	1	13.6078	0.4365	5.149000E+03	5.750216E+08	0.900	30	2	1	13.6078	0.4365	4.707000E+03	1.697901E+07	0.900
30	1	2	14.1693	0.4365	4.924000E+03	5.506616E+08	0.900	30	2	2	14.1693	0.4365	3.491200E+03	1.493556E+07	0.900
30	1	3	14.7308	0.4365	5.766000E+03	6.440241E+08	0.900	30	2	3	14.7308	0.4365	5.441300E+03	1.962669E+07	0.900
30	1	4	15.2923	0.4365	5.465000E+03	6.089260E+08	0.900	30	2	4	15.2923	0.4365	5.294000E+03	1.909643E+07	0.900
30	1	5	15.8538	0.4365	5.475000E+03	6.066495E+08	0.900	30	2	5	15.8538	0.4365	5.294000E+03	1.909643E+07	0.900
30	1	6	16.4153	0.4365	4.849000E+03	5.422740E+08	0.900	30	2	6	16.4153	0.4365	4.849000E+03	1.693933E+07	0.900
30	1	7	16.9768	0.4365	0.0	0.0	0.900	30	2	7	16.9768	0.4365	4.246000E+03	1.546400E+07	0.900
31	1	1	14.1693	0.4365	5.149000E+03	5.750216E+08	0.900	31	2	1	14.1693	0.4365	4.707000E+03	1.697901E+07	0.900
31	1	2	14.7308	0.4365	4.924000E+03	5.506616E+08	0.900	31	2	2	14.7308	0.4365	3.491200E+03	1.493556E+07	0.900
31	1	3	15.2923	0.4365	5.766000E+03	6.440241E+08	0.900	31	2	3	15.2923	0.4365	5.441300E+03	1.962669E+07	0.900
31	1	4	15.8538	0.4365	5.465000E+03	6.089260E+08	0.900	31	2	4	15.8538	0.4365	5.294000E+03	1.909643E+07	0.900
31	1	5	16.4153	0.4365	5.475000E+03	6.066495E+08	0.900	31	2	5	16.4153	0.4365	5.294000E+03	1.909643E+07	0.900
31	1	6	16.9768	0.4365	4.849000E+03	5.422740E+08	0.900	31	2	6	16.9768	0.4365	4.849000E+03	1.693933E+07	0.900
31	1	7	17.5383	0.4365	0.0	0.0	0.900	31	2	7	17.5383	0.4365	4.246000E+03	1.546400E+07	0.900
32	1	1	14.7308	0.4365	5.149000E+03	5.750216E+08	0.900	32	2	1	14.7308	0.4365	4.707000E+03	1.697901E+07	0.900
32	1	2	15.2923	0.4365	4.924000E+03	5.506616E+08	0.900	32	2	2	15.2923	0.4365	3.491200E+03	1.493556E+07	0.900
32	1	3	15.8538	0.4365	5.766000E+03	6.440241E+08	0.900	32	2	3	15.8538	0.4365	5.441300E+03	1.962669E+07	0.900
32	1	4	16.4153	0.4365	5.465000E+03	6.089260E+08	0.900	32	2	4	16.4153	0.4365	5.294000E+03	1.909643E+07	0.900
32	1	5	16.9768	0.4365	5.475000E+03	6.066495E+08	0.900	32	2	5	16.9768	0.4365	5.294000E+03	1.909643E+07	0.900
32	1	6	17.5383	0.4365	4.849000E+03	5.422740E+08	0.900	32	2	6	17.5383	0.4365	4.849000E+03	1.693933E+07	0.900
32	1	7	18.0998	0.4365	0.0	0.0	0.900	32	2	7	18.0998	0.4365	4.246000E+03	1.546400E+07	0.900

57	1	6	31-5756	0.4365	4.489000E+03	5.422740E+08	0.900	57	2	6	31-5756	0.4365	4.489000E+03	1.691931E+07	0.900
57	1	7	32-1371	0.4365	0.0	0.0	0.900	57	2	7	32-1371	0.4365	4.286000E+03	1.546606E+07	0.900
58	1	1	29-3297	0.4365	5.149000E+03	5.758236E+08	0.900	58	2	1	29-3297	0.4365	4.707000E+03	1.697901E+07	0.900
58	1	2	30-4527	0.4365	4.924000E+03	5.506616E+08	0.900	58	2	2	30-4527	0.4365	3.891000E+03	1.403556E+07	0.900
58	1	3	31-0181	0.4365	5.766000E+03	6.448241E+08	0.900	58	2	3	31-0181	0.4365	5.441000E+03	1.962684E+07	0.900
58	1	4	31-5756	0.4365	5.445000E+03	6.049280E+08	0.900	58	2	4	31-5756	0.4365	5.294000E+03	1.909684E+07	0.900
58	1	5	32-1371	0.4365	5.425000E+03	6.066095E+08	0.900	58	2	5	32-1371	0.4365	5.100000E+03	1.842502E+07	0.900
58	1	6	32-6986	0.4365	4.489000E+03	5.422740E+08	0.900	58	2	6	32-6986	0.4365	4.489000E+03	1.691931E+07	0.900
58	1	7	33-8216	0.4365	0.0	0.0	0.900	58	2	7	33-8216	0.4365	4.286000E+03	1.546606E+07	0.900
59	1	1	29-0912	0.4365	5.149000E+03	5.758236E+08	0.900	59	2	1	29-0912	0.4365	4.707000E+03	1.697901E+07	0.900
59	1	2	30-4527	0.4365	4.924000E+03	5.506616E+08	0.900	59	2	2	30-4527	0.4365	3.891000E+03	1.403556E+07	0.900
59	1	3	31-0181	0.4365	5.766000E+03	6.448241E+08	0.900	59	2	3	31-0181	0.4365	5.441000E+03	1.962684E+07	0.900
59	1	4	31-5756	0.4365	5.445000E+03	6.049280E+08	0.900	59	2	4	31-5756	0.4365	5.294000E+03	1.909684E+07	0.900
59	1	5	32-1371	0.4365	5.425000E+03	6.066095E+08	0.900	59	2	5	32-1371	0.4365	5.100000E+03	1.842502E+07	0.900
59	1	6	32-6986	0.4365	4.489000E+03	5.422740E+08	0.900	59	2	6	32-6986	0.4365	4.489000E+03	1.691931E+07	0.900
59	1	7	33-8216	0.4365	0.0	0.0	0.900	59	2	7	33-8216	0.4365	4.286000E+03	1.546606E+07	0.900
60	1	1	30-4527	0.4365	5.149000E+03	5.758236E+08	0.900	60	2	1	30-4527	0.4365	4.707000E+03	1.697901E+07	0.900
60	1	2	31-0181	0.4365	4.924000E+03	5.506616E+08	0.900	60	2	2	31-0181	0.4365	3.891000E+03	1.403556E+07	0.900
60	1	3	31-5756	0.4365	5.766000E+03	6.448241E+08	0.900	60	2	3	31-5756	0.4365	5.441000E+03	1.962684E+07	0.900
60	1	4	32-1371	0.4365	5.445000E+03	6.049280E+08	0.900	60	2	4	32-1371	0.4365	5.294000E+03	1.909684E+07	0.900
60	1	5	32-6986	0.4365	5.425000E+03	6.066095E+08	0.900	60	2	5	32-6986	0.4365	5.100000E+03	1.842502E+07	0.900
60	1	6	33-2601	0.4365	4.489000E+03	5.422740E+08	0.900	60	2	6	33-2601	0.4365	4.489000E+03	1.691931E+07	0.900
60	1	7	33-8216	0.4365	0.0	0.0	0.900	60	2	7	33-8216	0.4365	4.286000E+03	1.546606E+07	0.900
61	1	1	31-0181	0.4365	5.149000E+03	5.758236E+08	0.900	61	2	1	31-0181	0.4365	4.707000E+03	1.697901E+07	0.900
61	1	2	31-5756	0.4365	4.924000E+03	5.506616E+08	0.900	61	2	2	31-5756	0.4365	3.891000E+03	1.403556E+07	0.900
61	1	3	32-1371	0.4365	5.766000E+03	6.448241E+08	0.900	61	2	3	32-1371	0.4365	5.441000E+03	1.962684E+07	0.900
61	1	4	32-6986	0.4365	5.445000E+03	6.049280E+08	0.900	61	2	4	32-6986	0.4365	5.294000E+03	1.909684E+07	0.900
61	1	5	33-2601	0.4365	5.425000E+03	6.066095E+08	0.900	61	2	5	33-2601	0.4365	5.100000E+03	1.842502E+07	0.900
61	1	6	33-8216	0.4365	4.489000E+03	5.422740E+08	0.900	61	2	6	33-8216	0.4365	4.489000E+03	1.691931E+07	0.900
61	1	7	0.0	0.0	0.0	0.0	0.900	61	2	7	0.0	0.0	0.0	0.900	
62	1	1	31-5756	0.4365	5.149000E+03	5.758236E+08	0.900	62	2	1	31-5756	0.4365	4.707000E+03	1.697901E+07	0.900
62	1	2	32-1371	0.4365	4.924000E+03	5.506616E+08	0.900	62	2	2	32-1371	0.4365	3.891000E+03	1.403556E+07	0.900
62	1	3	32-6986	0.4365	5.766000E+03	6.448241E+08	0.900	62	2	3	32-6986	0.4365	5.441000E+03	1.962684E+07	0.900
62	1	4	33-2601	0.4365	5.445000E+03	6.049280E+08	0.900	62	2	4	33-2601	0.4365	5.294000E+03	1.909684E+07	0.900
62	1	5	33-8216	0.4365	5.425000E+03	6.066095E+08	0.900	62	2	5	33-8216	0.4365	5.100000E+03	1.842502E+07	0.900
62	1	6	0.0	0.0	0.0	0.0	0.900	62	2	6	0.0	0.0	0.0	0.900	
62	1	7	0.0	0.0	0.0	0.0	0.900	62	2	7	0.0	0.0	0.0	0.900	
63	1	1	32-1371	0.4365	5.149000E+03	5.758236E+08	0.900	63	2	1	32-1371	0.4365	4.707000E+03	1.697901E+07	0.900
63	1	2	32-6986	0.4365	4.924000E+03	5.506616E+08	0.900	63	2	2	32-6986	0.4365	3.891000E+03	1.403556E+07	0.900
63	1	3	33-2601	0.4365	5.766000E+03	6.448241E+08	0.900	63	2	3	33-2601	0.4365	5.441000E+03	1.962684E+07	0.900
63	1	4	33-8216	0.4365	5.445000E+03	6.049280E+08	0.900	63	2	4	33-8216	0.4365	5.294000E+03	1.909684E+07	0.900
63	1	5	0.0	0.0	0.0	0.900	63	2	5	0.0	0.0	0.0	0.900		
63	1	6	0.0	0.0	0.0	0.900	63	2	6	0.0	0.0	0.0	0.900		
63	1	7	0.0	0.0	0.0	0.900	63	2	7	0.0	0.0	0.0	0.900		
64	1	1	32-6986	0.4365	5.149000E+03	5.758236E+08	0.900	64	2	1	32-6986	0.4365	4.707000E+03	1.697901E+07	0.900
64	1	2	33-2601	0.4365	4.924000E+03	5.506616E+08	0.900	64	2	2	33-2601	0.4365	3.891000E+03	1.403556E+07	0.900
64	1	3	33-8216	0.4365	5.766000E+03	6.448241E+08	0.900	64	2	3	33-8216	0.4365	5.441000E+03	1.962684E+07	0.900
64	1	4	0.0	0.0	0.0	0.900	64	2	4	0.0	0.0	0.0	0.900		
64	1	5	0.0	0.0	0.0	0.900	64	2	5	0.0	0.0	0.0	0.900		
64	1	6	0.0	0.0	0.0	0.900	64	2	6	0.0	0.0	0.0	0.900		
64	1	7	0.0	0.0	0.0	0.900	64	2	7	0.0	0.0	0.0	0.900		
65	1	1	33-2601	0.4365	5.149000E+03	5.758236E+08	0.900	65	2	1	33-2601	0.4365	4.707000E+03	1.697901E+07	0.900
65	1	2	33-8216	0.4365	4.924000E+03	5.506616E+08	0.900	65	2	2	33-8216	0.4365	3.891000E+03	1.403556E+07	0.900
65	1	3	0.0	0.0	0.0	0.900	65	2	3	0.0	0.0	0.0	0.900		
65	1	4	0.0	0.0	0.0	0.900	65	2	4	0.0	0.0	0.0	0.900		
65	1	5	0.0	0.0	0.0	0.900	65	2	5	0.0	0.0	0.0	0.900		
65	1	6	0.0	0.0	0.0	0.900	65	2	6	0.0	0.0	0.0	0.900		
65	1	7	0.0	0.0	0.0	0.900	65	2	7	0.0	0.0	0.0	0.900		

66	1	1	33.8216	0.4365	5.149000E+03	5.758236E+08	0.900	66	2	1	33.8216	0.4365	4.707000E+03	1.697901E+07	0.900
66	1	2	0.0	0.0	0.0	0.0	0.900	66	2	2	0.0	0.0	0.0	0.0	0.900
66	1	3	0.0	0.0	0.0	0.0	0.900	66	2	3	0.0	0.0	0.0	0.0	0.900
66	1	4	0.0	0.0	0.0	0.0	0.900	66	2	4	0.0	0.0	0.0	0.0	0.900
66	1	5	0.0	0.0	0.0	0.0	0.900	66	2	5	0.0	0.0	0.0	0.0	0.900
66	1	6	0.0	0.0	0.0	0.0	0.900	66	2	6	0.0	0.0	0.0	0.0	0.900
66	1	7	0.0	0.0	0.0	0.0	0.0	66	2	7	0.0	0.0	0.0	0.0	0.900

TABLE 4.6 BURNUP AND ELECTRIC ENERGY GENERATION HISTORY: 6-BATCH CORE, ANNUAL REFUELING

LOT	SUB LOT	PER-IOD	START TIME YR	IRR TIME YR	BURNUP MWD/TORNE HM	ELECTRICITY CAPAC FACTOR	LOF	SUB LOT	PER-IOD	START TIME YR	IRR TIME YR	BURNUP MWD/TORNE HM	ELECTRICITY CAPAC FACTOR	
1	1	1	0.0	1.7460	1.047700E+04	2.132971E+09	0.900	1	1	0.0	1.7460	1.797800E+04	6.484998E+07	
1	1	2	1.8710	0.8266	0.161300E+04	9.421355E+08	0.900	2	2	1.8710	0.8266	7.421000E+03	2.676893E+07	
1	1	3	2.8226	0.6958	0.0	0.0	0.900	3	3	2.8226	0.6958	6.700600E+03	3.130251E+07	
1	1	4	3.6434	0.8764	0.0	0.0	0.900	4	4	3.6434	0.8764	0.0	0.0	
1	1	5	4.6448	1.0413	0.0	0.0	0.900	5	5	4.6448	1.0413	0.0	0.0	
1	1	6	5.8111	1.0086	0.0	0.0	0.900	6	6	5.8111	1.0086	0.0	0.0	
1	1	7	6.9447	0.9345	0.0	0.0	0.900	7	7	6.9447	0.9345	0.0	0.0	
2	1	1	0.0	1.7460	2.062000E+04	2.345724E+09	0.900	2	1	0.0	1.7460	1.797800E+04	6.484998E+07	
2	1	2	1.8710	0.8266	0.161300E+04	9.421355E+08	0.900	2	2	1.8710	0.8266	7.421000E+03	2.676893E+07	
2	1	3	2.8226	0.6958	0.0	0.0	0.900	3	3	2.8226	0.6958	6.700600E+03	3.130251E+07	
2	1	4	3.6434	0.8764	0.0	0.0	0.900	4	4	3.6434	0.8764	0.0	0.0	
2	1	5	4.6448	1.0413	0.0	0.0	0.900	5	5	4.6448	1.0413	0.0	0.0	
2	1	6	5.8111	1.0086	0.0	0.0	0.900	6	6	5.8111	1.0086	0.0	0.0	
2	1	7	6.9447	0.9345	0.0	0.0	0.900	7	7	6.9447	0.9345	0.0	0.0	
3	1	1	0.0	1.7460	2.119600E+04	2.373377E+09	0.900	3	1	0.0	1.7460	2.086600E+04	7.526755E+07	
3	1	2	1.8710	0.8266	0.161300E+04	9.421355E+08	0.900	3	2	1.8710	0.8266	8.206000E+03	2.960056E+07	
3	1	3	2.8226	0.6958	0.0	0.0	0.900	3	3	2.8226	0.6958	7.166000E+03	2.534907E+07	
3	1	4	3.6434	0.8764	0.0	0.0	0.900	4	4	3.6434	0.8764	0.0	0.0	
3	1	5	4.6448	1.0413	0.0	0.0	0.900	5	5	4.6448	1.0413	0.0	0.0	
3	1	6	5.8111	1.0086	0.0	0.0	0.900	6	6	5.8111	1.0086	0.0	0.0	
3	1	7	6.9447	0.9345	0.0	0.0	0.900	7	7	6.9447	0.9345	0.0	0.0	
4	1	1	0.0	1.7460	2.160400E+04	2.435893E+09	0.900	4	1	0.0	1.7460	2.140730E+04	7.721901E+07	
4	1	2	1.8710	0.8266	0.161300E+04	9.421355E+08	0.900	4	2	1.8710	0.8266	8.762000E+03	3.160014E+07	
4	1	3	2.8226	0.6958	0.0	0.0	0.900	4	3	2.8226	0.6958	5.538000E+03	2.001266E+07	
4	1	4	3.6434	0.8764	0.0	0.0	0.900	4	4	3.6434	0.8764	0.0	0.0	
4	1	5	4.6448	1.0413	0.0	0.0	0.900	4	5	4.6448	1.0413	1.050000E+04	3.801974E+07	
4	1	6	5.8111	1.0086	0.0	0.0	0.900	4	6	5.8111	1.0086	0.0	0.0	
4	1	7	6.9447	0.9345	0.0	0.0	0.900	4	7	6.9447	0.9345	0.0	0.0	
5	1	1	0.0	1.7460	1.944300E+04	2.174337E+09	0.900	5	1	0.0	1.7460	1.846400E+04	6.663306E+08	
5	1	2	1.8710	0.8266	0.161300E+04	9.421355E+08	0.900	5	2	1.8710	0.8266	9.607600E+03	3.465423E+08	
5	1	3	2.8226	0.6958	0.0	0.0	0.900	5	3	2.8226	0.6958	6.890000E+03	2.445352E+08	
5	1	4	3.6434	0.8764	0.0	0.0	0.900	5	4	3.6434	0.8764	0.0	0.0	
5	1	5	4.6448	1.0413	0.0	0.0	0.900	5	5	4.6448	1.0413	1.057000E+04	3.812795E+08	
5	1	6	5.8111	1.0086	0.0	0.0	0.900	5	6	5.8111	1.0086	0.0	0.0	
5	1	7	6.9447	0.9345	0.0	0.0	0.900	5	7	6.9447	0.9345	0.0	0.0	
6	1	1	0.0	1.7460	1.971900E+04	2.265263E+09	0.900	6	1	0.0	1.7460	1.974900E+04	7.123030E+07	
6	1	2	1.8710	0.8266	0.161300E+04	9.421355E+08	0.900	6	2	1.8710	0.8266	8.316000E+03	3.006950E+07	
6	1	3	2.8226	0.6958	0.0	0.0	0.900	6	3	2.8226	0.6958	4.949000E+03	1.785195E+07	
6	1	4	3.6434	0.8764	0.0	0.0	0.900	6	4	3.6434	0.8764	7.534000E+03	2.716541E+07	
6	1	5	4.6448	1.0413	0.0	0.0	0.900	6	5	4.6448	1.0413	9.235000E+03	3.691954E+07	
6	1	6	5.8111	1.0086	0.0	0.0	0.900	6	6	5.8111	1.0086	0.0	0.0	
6	1	7	6.9447	0.9345	0.0	0.0	0.900	6	7	6.9447	0.9345	0.0	0.0	
7	1	1	0.0	1.7460	1.986600E+04	2.215160E+09	0.900	7	1	0.0	1.7460	1.087500E+04	3.922814E+07	
7	1	2	1.8710	0.8266	0.161300E+04	9.421355E+08	0.900	7	2	1.8710	0.8266	9.933000E+03	3.583018E+07	
7	1	3	2.8226	0.6958	0.0	0.0	0.900	7	3	2.8226	0.6958	6.266000E+03	3.472277E+07	
7	1	4	3.6434	0.8764	0.0	0.0	0.900	7	4	3.6434	0.8764	9.384000E+03	4.992706E+07	
7	1	5	4.6448	1.0413	0.0	0.0	0.900	7	5	4.6448	1.0413	1.0086	9.646000E+03	3.479491E+07
7	1	6	5.8111	1.0086	0.0	0.0	0.900	7	6	5.8111	1.0086	0.0	0.0	
7	1	7	6.9447	0.9345	0.0	0.0	0.900	7	7	6.9447	0.9345	0.0	0.0	
8	1	1	0.0	1.7460	1.975900E+04	2.091363E+09	0.900	8	1	0.0	1.7460	1.047000E+04	2.549198E+07	
8	1	2	1.8710	0.8266	0.161300E+04	9.421355E+08	0.900	8	2	1.8710	0.8266	0.0	0.0	

0	1	2	3	4	5	6	7	8	9	10	11	12	13	14	15	16	17	18	19	20	21	22	23	24	25	26	27	28	29	30	31	32	33	34	35	36	37	38	39	40	41	42	43	44	45	46	47	48	49	50	51	52	53	54	55	56	57	58	59	60	61	62	63	64	65	66	67	68	69	70	71	72	73	74	75	76	77	78	79	80	81	82	83	84	85	86	87	88	89	90	91	92	93	94	95	96	97	98	99	00																																				
0.4764	0.4765	0.4766	0.4767	0.4768	0.4769	0.4770	0.4771	0.4772	0.4773	0.4774	0.4775	0.4776	0.4777	0.4778	0.4779	0.4780	0.4781	0.4782	0.4783	0.4784	0.4785	0.4786	0.4787	0.4788	0.4789	0.4790	0.4791	0.4792	0.4793	0.4794	0.4795	0.4796	0.4797	0.4798	0.4799	0.4800	0.4801	0.4802	0.4803	0.4804	0.4805	0.4806	0.4807	0.4808	0.4809	0.4810	0.4811	0.4812	0.4813	0.4814	0.4815	0.4816	0.4817	0.4818	0.4819	0.4820	0.4821	0.4822	0.4823	0.4824	0.4825	0.4826	0.4827	0.4828	0.4829	0.4830	0.4831	0.4832	0.4833	0.4834	0.4835	0.4836	0.4837	0.4838	0.4839	0.4840	0.4841	0.4842	0.4843	0.4844	0.4845	0.4846	0.4847	0.4848	0.4849	0.4850	0.4851	0.4852	0.4853	0.4854	0.4855	0.4856	0.4857	0.4858	0.4859	0.4860	0.4861	0.4862	0.4863	0.4864	0.4865	0.4866	0.4867	0.4868	0.4869	0.4870	0.4871	0.4872	0.4873	0.4874	0.4875	0.4876	0.4877	0.4878	0.4879	0.4880	0.4881	0.4882	0.4883	0.4884	0.4885	0.4886	0.4887	0.4888	0.4889	0.4890	0.4891	0.4892	0.4893	0.4894	0.4895	0.4896	0.4897	0.4898	0.4899	0.4900

24	1	6	24-3779	0.8999	7.821000E+03	8.746325E+08	0.930	24	2	7	24-3779	0.8999	4.000000E+03	3.246467E+07	0.900
24	1	7	25-4028	0.8999	0.0	0.0	0.900	24	2	7	25-4028	0.8999	8.251000E+03	2.977010E+07	0.900
25	1	1	20-2782	0.8999	1.237700E+04	1.308137E+09	0.933	25	2	1	23-2782	0.8999	1.020300E+04	3.709269E+07	0.900
25	1	2	21-3031	0.8999	1.186100E+04	1.326425E+09	0.930	25	2	2	21-3031	0.8999	7.551000E+03	2.464434E+07	0.900
25	1	3	22-3280	0.8999	1.195100E+04	1.316497E+09	0.930	25	2	3	22-3280	0.8999	1.196500E+04	8.315637E+07	0.900
25	1	4	23-3530	0.8999	1.133035E+04	1.221494E+09	0.933	25	2	4	23-3530	0.8999	1.196500E+04	8.315637E+07	0.900
25	1	5	24-3779	0.8999	1.133035E+04	1.221494E+09	0.933	25	2	5	24-3779	0.8999	1.196500E+04	8.315637E+07	0.900
25	1	6	25-4028	0.8999	7.999999E+03	1.111205E+09	0.930	25	2	6	25-4028	0.8999	1.196500E+04	8.315637E+07	0.900
25	1	7	26-4278	0.8999	7.999999E+03	1.111205E+09	0.930	25	2	7	26-4278	0.8999	1.196500E+04	8.315637E+07	0.900
26	1	1	21-3031	0.8999	1.237700E+04	1.308137E+09	0.930	26	2	1	21-3031	0.8999	1.237700E+04	3.709269E+07	0.900
26	1	2	22-3280	0.8999	1.186100E+04	1.326425E+09	0.930	26	2	2	22-3280	0.8999	7.551000E+03	2.464434E+07	0.900
26	1	3	23-3530	0.8999	1.195100E+04	1.316497E+09	0.930	26	2	3	23-3530	0.8999	1.196500E+04	8.315637E+07	0.900
26	1	4	24-3779	0.8999	1.133035E+04	1.221494E+09	0.933	26	2	4	24-3779	0.8999	1.196500E+04	8.315637E+07	0.900
26	1	5	25-4028	0.8999	7.999999E+03	1.111205E+09	0.930	26	2	5	25-4028	0.8999	1.196500E+04	8.315637E+07	0.900
26	1	6	26-4278	0.8999	7.999999E+03	1.111205E+09	0.930	26	2	6	26-4278	0.8999	1.196500E+04	8.315637E+07	0.900
26	1	7	27-4527	0.8999	0.0	0.0	0.900	26	2	7	27-4527	0.8999	0.251000E+03	2.977010E+07	0.900
27	1	1	22-3280	0.8999	1.237700E+04	1.308137E+09	0.930	27	2	1	22-3280	0.8999	1.020300E+04	3.709269E+07	0.900
27	1	2	23-3530	0.8999	1.186100E+04	1.326425E+09	0.930	27	2	2	23-3530	0.8999	7.551000E+03	2.464434E+07	0.900
27	1	3	24-3779	0.8999	1.195100E+04	1.316497E+09	0.930	27	2	3	24-3779	0.8999	1.196500E+04	8.315637E+07	0.900
27	1	4	25-4028	0.8999	1.133035E+04	1.221494E+09	0.933	27	2	4	25-4028	0.8999	1.196500E+04	8.315637E+07	0.900
27	1	5	26-4278	0.8999	7.999999E+03	1.111205E+09	0.930	27	2	5	26-4278	0.8999	1.196500E+04	8.315637E+07	0.900
27	1	6	27-4527	0.8999	7.999999E+03	1.111205E+09	0.930	27	2	6	27-4527	0.8999	1.196500E+04	8.315637E+07	0.900
27	1	7	28-4776	0.8999	0.0	0.0	0.900	27	2	7	28-4776	0.8999	0.251000E+03	2.977010E+07	0.900
28	1	1	24-3779	0.8999	1.237700E+04	1.308137E+09	0.930	28	2	1	24-3779	0.8999	1.020300E+04	3.709269E+07	0.900
28	1	2	25-4028	0.8999	1.186100E+04	1.326425E+09	0.930	28	2	2	25-4028	0.8999	7.551000E+03	2.464434E+07	0.900
28	1	3	26-4278	0.8999	1.195100E+04	1.316497E+09	0.930	28	2	3	26-4278	0.8999	1.196500E+04	8.315637E+07	0.900
28	1	4	27-4527	0.8999	1.133035E+04	1.221494E+09	0.933	28	2	4	27-4527	0.8999	1.196500E+04	8.315637E+07	0.900
28	1	5	28-4776	0.8999	7.999999E+03	1.111205E+09	0.930	28	2	5	28-4776	0.8999	1.196500E+04	8.315637E+07	0.900
28	1	6	29-5026	0.8999	7.999999E+03	1.111205E+09	0.930	28	2	6	29-5026	0.8999	1.196500E+04	8.315637E+07	0.900
28	1	7	29-5026	0.8999	0.0	0.0	0.900	28	2	7	29-5026	0.8999	0.251000E+03	2.977010E+07	0.900
29	1	1	24-3779	0.8999	1.237700E+04	1.308137E+09	0.930	29	2	1	24-3779	0.8999	1.020300E+04	3.709269E+07	0.900
29	1	2	25-4028	0.8999	1.186100E+04	1.326425E+09	0.930	29	2	2	25-4028	0.8999	7.551000E+03	2.464434E+07	0.900
29	1	3	26-4278	0.8999	1.195100E+04	1.316497E+09	0.930	29	2	3	26-4278	0.8999	1.196500E+04	8.315637E+07	0.900
29	1	4	27-4527	0.8999	1.133035E+04	1.221494E+09	0.933	29	2	4	27-4527	0.8999	1.196500E+04	8.315637E+07	0.900
29	1	5	28-4776	0.8999	7.999999E+03	1.111205E+09	0.930	29	2	5	28-4776	0.8999	1.196500E+04	8.315637E+07	0.900
29	1	6	29-5026	0.8999	7.999999E+03	1.111205E+09	0.930	29	2	6	29-5026	0.8999	1.196500E+04	8.315637E+07	0.900
29	1	7	30-5275	0.8999	0.0	0.0	0.900	29	2	7	30-5275	0.8999	0.251000E+03	2.977010E+07	0.900
30	1	1	25-4028	0.8999	1.237700E+04	1.308137E+09	0.930	30	2	1	25-4028	0.8999	1.020300E+04	3.709269E+07	0.900
30	1	2	26-4278	0.8999	1.186100E+04	1.326425E+09	0.930	30	2	2	26-4278	0.8999	7.551000E+03	2.464434E+07	0.900
30	1	3	27-4527	0.8999	1.195100E+04	1.316497E+09	0.930	30	2	3	27-4527	0.8999	1.196500E+04	8.315637E+07	0.900
30	1	4	28-4776	0.8999	1.133035E+04	1.221494E+09	0.933	30	2	4	28-4776	0.8999	1.196500E+04	8.315637E+07	0.900
30	1	5	29-5026	0.8999	7.999999E+03	1.111205E+09	0.930	30	2	5	29-5026	0.8999	1.196500E+04	8.315637E+07	0.900
30	1	6	30-5275	0.8999	7.999999E+03	1.111205E+09	0.930	30	2	6	30-5275	0.8999	1.196500E+04	8.315637E+07	0.900
30	1	7	31-5524	0.8999	0.0	0.0	0.900	30	2	7	31-5524	0.8999	0.251000E+03	2.977010E+07	0.900
31	1	1	26-4278	0.8999	1.237700E+04	1.308137E+09	0.930	31	2	1	26-4278	0.8999	1.020300E+04	3.709269E+07	0.900
31	1	2	27-4527	0.8999	1.186100E+04	1.326425E+09	0.930	31	2	2	27-4527	0.8999	7.551000E+03	2.464434E+07	0.900
31	1	3	28-4776	0.8999	1.195100E+04	1.316497E+09	0.930	31	2	3	28-4776	0.8999	1.196500E+04	8.315637E+07	0.900
31	1	4	29-5026	0.8999	1.133035E+04	1.221494E+09	0.933	31	2	4	29-5026	0.8999	1.196500E+04	8.315637E+07	0.900
31	1	5	30-5275	0.8999	7.999999E+03	1.111205E+09	0.930	31	2	5	30-5275	0.8999	1.196500E+04	8.315637E+07	0.900
31	1	6	31-5524	0.8999	7.999999E+03	1.111205E+09	0.930	31	2	6	31-5524	0.8999	1.196500E+04	8.315637E+07	0.900
31	1	7	0.0	0.0	0.0	0.0	0.0	31	2	7	0.0	0.0	0.0	0.0	0.900
32	1	1	27-4527	0.8999	1.237700E+04	1.308137E+09	0.930	32	2	1	27-4527	0.8999	1.020300E+04	3.709269E+07	0.900
32	1	2	28-4776	0.8999	1.186100E+04	1.326425E+09	0.930	32	2	2	28-4776	0.8999	7.551000E+03	2.464434E+07	0.900
32	1	3	29-5026	0.8999	1.195100E+04	1.316497E+09	0.930	32	2	3	29-5026	0.8999	1.196500E+04	8.315637E+07	0.900
32	1	4	30-5275	0.8999	1.133035E+04	1.221494E+09	0.933	32	2	4	30-5275	0.8999	1.196500E+04	8.315637E+07	0.900
32	1	5	31-5524	0.8999	7.999999E+03	1.111205E+09	0.930	32	2	5	31-5524	0.8999	1.196500E+04	8.315637E+07	0.900
32	1	6	0.0	0.0	0.0	0.0	0.0	32	2	6	0.0	0.0	0.0	0.0	0.900
32	1	7	0.0	0.0	0.0	0.0	0.0	32	2	7	0.0	0.0	0.0	0.0	0.900

33	1	1	24.4776	0.8999	1.237700E+04	1.384137E+09	0.900	33	2	1	24.4776	0.8999	1.028300E+04	3.709269E+07	0.900
33	1	2	29.5026	0.8999	1.166300E+04	1.326432E+09	0.900	33	2	2	29.5026	0.8999	7.453000E+03	2.608434E+07	0.900
33	1	3	30.5275	0.8999	1.195100E+04	1.364970E+09	0.900	33	2	3	30.5275	0.8999	1.196400E+04	4.315637E+07	0.900
33	1	4	31.5524	0.8999	1.103400E+04	1.233347E+09	0.900	33	2	4	31.5524	0.8999	1.190600E+04	4.114355E+07	0.900
33	1	5	0.0	0.0	0.0	0.0	0.900	33	2	5	0.0	0.0	0.0	0.0	0.900
33	1	6	0.0	0.0	0.0	0.0	0.900	33	2	6	0.0	0.0	0.0	0.0	0.900
33	1	7	0.0	0.0	0.0	0.0	0.900	33	2	7	0.0	0.0	0.0	0.0	0.900
34	1	1	27.5026	0.8999	1.237700E+04	1.394137E+09	0.900	34	2	1	27.5026	0.8999	1.028300E+04	3.709269E+07	0.900
34	1	2	30.5275	0.8999	1.166300E+04	1.326432E+09	0.900	34	2	2	30.5275	0.8999	7.453000E+03	2.608434E+07	0.900
34	1	3	31.5524	0.8999	1.195100E+04	1.364970E+09	0.900	34	2	3	31.5524	0.8999	1.196400E+04	4.315637E+07	0.900
34	1	4	0.0	0.0	0.0	0.0	0.900	34	2	4	0.0	0.0	0.0	0.0	0.900
34	1	5	0.0	0.0	0.0	0.0	0.900	34	2	5	0.0	0.0	0.0	0.0	0.900
34	1	6	0.0	0.0	0.0	0.0	0.900	34	2	6	0.0	0.0	0.0	0.0	0.900
34	1	7	0.0	0.0	0.0	0.0	0.900	34	2	7	0.0	0.0	0.0	0.0	0.900
35	1	1	30.5275	0.8999	1.237700E+04	1.394137E+09	0.900	35	2	1	30.5275	0.8999	1.028300E+04	3.709269E+07	0.900
35	1	2	31.5524	0.8999	1.166300E+04	1.326432E+09	0.900	35	2	2	31.5524	0.8999	7.453000E+03	2.608434E+07	0.900
35	1	3	0.0	0.0	0.0	0.0	0.900	35	2	3	0.0	0.0	0.0	0.0	0.900
35	1	4	0.0	0.0	0.0	0.0	0.900	35	2	4	0.0	0.0	0.0	0.0	0.900
35	1	5	0.0	0.0	0.0	0.0	0.900	35	2	5	0.0	0.0	0.0	0.0	0.900
35	1	6	0.0	0.0	0.0	0.0	0.900	35	2	6	0.0	0.0	0.0	0.0	0.900
35	1	7	0.0	0.0	0.0	0.0	0.900	35	2	7	0.0	0.0	0.0	0.0	0.900
36	1	1	31.5524	0.8999	1.237700E+04	1.394137E+09	0.900	36	2	1	31.5524	0.8999	1.028300E+04	3.709269E+07	0.900
36	1	2	0.0	0.0	0.0	0.0	0.900	36	2	2	0.0	0.0	0.0	0.0	0.900
36	1	3	0.0	0.0	0.0	0.0	0.900	36	2	3	0.0	0.0	0.0	0.0	0.900
36	1	4	0.0	0.0	0.0	0.0	0.900	36	2	4	0.0	0.0	0.0	0.0	0.900
36	1	5	0.0	0.0	0.0	0.0	0.900	36	2	5	0.0	0.0	0.0	0.0	0.900
36	1	6	0.0	0.0	0.0	0.0	0.900	36	2	6	0.0	0.0	0.0	0.0	0.900
36	1	7	0.0	0.0	0.0	0.0	0.900	36	2	7	0.0	0.0	0.0	0.0	0.900

TABLE 4.7
RELATIVE ORE SAVINGS FOR 3-BATCH AND 6-BATCH PWR CORES

	Equilibrium Reload Enrich- ment (w/o)	Equilibrium Cycle Average Burnup (MWD/ MTU) (And fuel discharge burnup)	Total Heavy Metal Loading (MT)	Relative* Ore Usage
3-Batch Core** Annual Refueling	3.2	10083 (30312)	89	1.00
6-Batch Core Semi-Annual Refueling	3.0	5250 (31588)	89	0.896
6-Batch Core Annual Refueling	5.2	10808 (65043)	89	0.790

*ST/GWe-yr (delivered) relative to 3-batch core, based on a 90% availability based capacity factor, 0.2% enrichment plant tails.

** From Ref. [R-3]

effect on the comparison, however, as the following argument shows. Garel [G-1] has found that a bias of approximately + 0.3% in the multiplication factor results from use of the version of LEOPARD employed in the present work (Rieck's results should be of comparable accuracy). This result was obtained by benchmarking LEOPARD against 63 uranium critical experiments. Overprediction of the effective multiplication factor results in an underprediction of the critical enrichment according to the approximate relation

$$\frac{\Delta X}{X} \sim -2 \frac{\Delta K}{K} \quad [4.2]$$

where X is the enrichment and K the multiplication factor. Using the above prescription, a + 0.3% bias in K leads to a -0.6% bias in fissile enrichment (i.e., 3.00 % U²³⁵ would be computed as 2.98% U²³⁵); this corresponds to a reduction in ore usage by a factor of 0.993. Discrepancies of this magnitude are well within the precision required of scoping studies of the present type.

4.5.2 Fuel Cycle Cost

The MITCOST-II code was used to calculate the levelized nuclear fuel cycle cost for each of the 3 cases. The use of this code and its simpler counterpart, ECON, for this and similar applications is being documented by Abbaspour [A-5]. The nuclear fuel cycle data are given in Table 2.2. The results are summarized in Tables [4.8] and [4.9]. As shown, the levelized fuel cost per period is approximately equal for all three cases throughout the lifetime of the core but the 6 batch cores are penalized at the end of life. This is due to the fact that the last few fuel batches are only partially burned; for example, the last fuel

TABLE 4.8

LEVELIZED NUCLEAR FUEL COST PER PERIOD FOR 3-BATCH AND 6-BATCH CORES,
ANNUAL REFUELING

PERIOD *	3-Batch Core		6-Batch Core	
	PERIOD	AGGREGATES	PERIOD	AGGREGATES
	LEV COST M/KWHE	REV REQ \$	LEV COST M/KWHE	REV REQ \$
1	6.8597	6.633707E+07	6.1926	8.134838E+07
2	6.9326	3.731320E+07	6.4442	3.482774E+07
3	7.4157	3.777486E+07	6.9128	2.881211E+07
4	8.0095	3.922267E+07	7.4512	3.575562E+07
5	8.6383	3.747509E+07	7.8429	4.012195E+07
6	9.3146	3.690720E+07	8.9589	3.774640E+07
7	10.0469	3.618336E+07	9.7319	3.569370E+07
8	10.8415	3.549643E+07	10.5378	3.294323E+07
9	11.7065	3.484707E+07	11.4231	3.282648E+07
10	12.6460	3.422262E+07	12.4222	3.241584E+07
11	13.6642	3.361914E+07	13.4505	3.167186E+07
12	14.7648	3.302586E+07	14.6030	3.114021E+07
13	15.9544	3.244306E+07	15.8592	3.058594E+07
14	17.2454	3.188341E+07	17.2225	3.002387E+07
15	18.6488	3.134448E+07	18.7097	2.947128E+07
16	20.1796	3.083662E+07	20.3330	2.894490E+07
17	21.8451	3.034904E+07	22.1053	2.843526E+07
18	23.6535	2.987653E+07	24.0379	2.793970E+07
19	25.6124	2.941072E+07	26.1489	2.747365E+07
20	27.7335	2.895174E+07	28.4524	2.701504E+07
21	30.0392	2.851067E+07	30.9692	2.656952E+07
22	32.5498	2.808576E+07	33.7251	2.615379E+07
23	35.2924	2.768635E+07	36.7372	2.574667E+07
24	38.2819	2.730230E+07	40.0341	2.535221E+07
25	41.5327	2.693024E+07	43.6436	2.498246E+07
26	45.0598	2.656205E+07	47.4239	2.453126E+07
27	48.8848	2.619766E+07	52.5285	2.455339E+07
28	53.0486	2.584710E+07	59.8486	2.527776E+07
29	57.6383	2.553104E+07	71.4448	2.727664E+07
30	70.4215	2.236019E+07	92.4623	3.190154E+07
31	113.6257	4.162272E+07	141.7975	4.420637E+07
	*****	*****	*****	*****
	OVERALL TOTALS		OVERALL TOTALS	
	14.7180	1.020151E+09	14.0257	9.917990E+08

* Each period corresponds to one interval between refuelings (here ~1 yr)

TABLE 4.9

LEVELIZED NUCLEAR FUEL COST PER PERIOD FOR 6-BATCH CORE SEMI-ANNUAL REFUELING

Period*	PERIOD AGGREGATES		Period*	PERIOD AGGREGATES	
	LEV COST M/KWHE	REV REQ \$		LEV COST M/KWHE	REV REQ \$
1	5.9459	3.664062E+07	31	22.1882	1.452025E+07
2	6.1421	1.413565E+07	32	23.2378	1.438537E+07
3	6.2682	1.399571E+07	33	24.3425	1.425479E+07
4	6.5669	1.646914E+07	34	25.5019	1.412820E+07
5	6.9648	1.930749E+07	35	26.7166	1.400502E+07
6	7.2231	2.057018E+07	36	27.9921	1.388066E+07
7	7.4762	2.192006E+07	37	29.3337	1.375985E+07
8	7.8074	1.873194E+07	38	30.7424	1.364385E+07
9	8.1749	1.741368E+07	39	32.2192	1.352912E+07
10	8.5968	1.782446E+07	40	33.7701	1.341405E+07
11	9.0236	1.793754E+07	41	35.4016	1.330216E+07
12	9.4269	1.779797E+07	42	37.1154	1.319588E+07
13	9.8812	1.717186E+07	43	38.9130	1.308886E+07
14	10.2564	1.722667E+07	44	40.8010	1.298228E+07
15	10.6846	1.697838E+07	45	42.7874	1.287857E+07
16	11.1304	1.673490E+07	46	44.8748	1.278121E+07
17	11.6669	1.659368E+07	47	47.0653	1.268121E+07
18	12.2479	1.647850E+07	48	49.3663	1.258241E+07
19	12.8324	1.633526E+07	49	51.7876	1.248616E+07
20	13.4230	1.616644E+07	50	54.3326	1.239650E+07
21	14.0441	1.600038E+07	51	57.0047	1.230336E+07
22	14.6957	1.583795E+07	52	59.8122	1.221167E+07
23	15.3771	1.568111E+07	53	62.7637	1.212269E+07
24	16.0916	1.552441E+07	54	65.8702	1.203874E+07
25	16.8430	1.537121E+07	55	69.1329	1.195226E+07
26	17.6318	1.522142E+07	56	72.3404	1.183090E+07
27	18.4566	1.507789E+07	57	77.6128	1.200906E+07
28	19.3221	1.493213E+07	58	86.2668	1.262955E+07
29	20.2325	1.479120E+07	59	101.3484	1.403572E+07
30	21.1878	1.465280E+07	60	131.0188	1.716418E+07
			61	199.5887	2.473982E+07
				*****	*****
				OVERALL TOTALS	
				14.9431	9.404434E+08

*Each period corresponds to one interval between refuelings (here ~6 months.)

batch is discharged with only one-sixth of normal discharge burnup. Thus further studies are needed to reduce this economic penalty, such as use of the last fuel lot in other similar reactors.

Table 4.10 summarizes the levelized nuclear fuel cycle cost as calculated by MITCOST-II. As shown, the 6 batch core with annual refueling is the most attractive fuel management scheme; in addition to its lower levelized nuclear fuel cycle cost, this scheme has the largest ore savings.

The 6 batch core with semi-annual refueling is heavily penalized when a 6 week refueling shutdown time is used. If the refueling interval is reduced by a factor of 2 then this fuel management scheme becomes more attractive (as shown in Table 4.10).

4.6. Conclusions

In this chapter we have looked at different fuel management strategies to extend the burnup life of the fuel. The following can be concluded:

- (1) One of the most straightforward ways of improving uranium ore utilization is to increase the discharge burnup of the fuel.
- (2) The discharge burnup of the fuel may be increased by increasing the reload enrichment of the fuel and the irradiation period and/or increasing the number of batches in the core.
- (3) Of the three cases we tested, the 6-batch core with annual refueling showed the best potential for ore savings. In addition the 6-batch core with annual refueling had a smaller fuel cycle cost than a typical 3-batch core with annual refueling.
- (4) The reload enrichments for batches near the end of life condition should be optimized since these batches are discharged far

TABLE 4.10

LEVELIZED NUCLEAR FUEL CYCLE COST FOR 3-BATCH AND 6-BATCH PWR CORES

	Fuel Cycle Cost (Mills/kwhr)
3-Batch Core Annual refueling	14.7185
6-Batch Core Semi-Annual refueling	14.9430 (14.4232)
6-Batch Core Annual Refueling	14.0257

Key Assumptions:

- (1) Same refueling shutdown each refueling all cases (6 weeks) note that this penalized semi-annual refueling: value in parenthesis assumed downtime per refueling is cut in half.
- (2) Same availability-based capacity factor (90%) when not shutdown for refueling.

NOTE: These costs higher than those in Chapter 3 because the price of electricity is not escalated here (this can be done in ECON but not MITCOST).

below their nominal discharge burnup and harsh economic penalties may be incurred. It may also be possible to use these fuel lots in new reactors (for initial startup cores).

(5) In this analysis, burnable poisons were not used to flatten the power distribution or to hold down the excess reactivity. The NRC General Design Criteria specify the moderator temperature to be non-positive through the cycle. Thus, further study is needed to determine the balance of soluble poison and burnable poison in the core such that: the temperature coefficient is non-positive throughout the cycle, the control worth is sufficient to hold down the excess reactivity during normal power operation, and power peaking factors are not excessive.

(6) Large research and development programs are needed in the area of fuel modeling behavior analysis. It is not clear that solutions will be found to Zircaloy PCI interaction problems, internal chemical attack by fission products, or corrosion induced hydriding problems. Furthermore, reversion to stainless steel clad or a thicker zircaloy clad may incur an enrichment penalty which offsets, at least in part, the burnup gain.

It should be noted, however, that a savings of 0.5 mills/kwhr in the fuel cycle cost will generate on the order of 4 billion dollars if applied to 100 reactors over a 10 year period; this should certainly more than outweigh the costs needed to develop and license high burnup fuel.

CHAPTER 5

COASTDOWN

5.1 Introduction

Current PWR's produce electric energy at their full rated power level until reactivity-limited burnup is reached (the point in time at which the reactor cannot be made critical at the full rated steady state power level); when this occurs the reactor can either be shut down for refueling, or the reactor can still produce power but at less than optimum conditions.

The reactor can still be made critical after full power end of life has been reached by utilizing the positive reactivity insertions from reduced fuel and coolant temperature (due to their negative temperature/power coefficients) and from the reduced xenon poisoning at lower power levels.

By reducing the fuel temperature, the parasitic absorptions in U-238 resonances are reduced and a positive reactivity insertion results. Similarly, a reduction in the moderator temperature results in a positive reactivity insertion since the water density increases as the temperature of the moderator decreases. If the reactor is operated at lower power levels the equilibrium xenon concentration is lower, since the steady state xenon concentration is a function of the flux level; hence the neutron economy is improved and a positive reactivity insertion results. The term coastdown or stretchout is used when the reactor utilizes any or all of the above reactivity mechanisms to maintain power operation after reactivity limited burnup at full power is reached.

From an operational standpoint, coastdown can be achieved by two different methods in a PWR: (1) The average core moderator temperature can

be reduced below its nominal value (usually by a reduction in the coolant inlet temperature). The thermal power is kept at its rated value by fully opening the governing valves to the high pressure turbine and allowing the steam pressure and electrical energy output to coast down. This procedure allows full thermal power to be maintained, but the electrical energy output is reduced since there is a reduction in plant efficiency when the steam supply system is operated in the above mode. (2) The average core moderator and fuel temperatures are reduced below their nominal values; that is, the thermal power of the reactor is gradually reduced which inserts positive reactivity.

The objective of planned coastdown is to minimize fuel cycle cost and uranium ore usage by stretching the reactivity lifetime of nuclear fuels. The coastdown duration is usually determined by economic and engineering considerations, along with the specific needs of each utility system. Coastdown will reduce plant capacity factor and requires re-scheduling the refueling shutdown, but modest ore savings can be attained along with a reduction in fuel cycle cost. Utilities must weigh the above alternatives (ore savings due to extended burnup versus replacement power cost) to fit their own needs, but most prior analyses have shown that coastdown is an economically desirable strategy.

5.2 Previous Work

Previous work in the area of present interest for the most part deals with the economic considerations of coastdown [W-2] and [K-1], with some concurrent attention to neutronic and engineering limits [B-7]. Until recently, interest has not been shown in using coastdown primarily as a means of reducing uranium consumption [S-5]. In this study, our primary

objective is to show that coastdown operation results in a modest ore savings.

Banister [B-7] studied the neutronics of extending the irradiation period of a PWR past the full power end of life by coastdown, and the effects on the subsequent core operations. He has found that the core power distribution at BOL following coastdown is affected; but his results indicate that radial power sharing limits will not be exceeded in the cycle following coastdown unless the average core burnup extension due to coastdown exceeds 3100 MWD/MTU. Also, with regard to the neutronics, Martin [M-1] showed that the reactivity effects of a coastdown equivalent to two full power months had damped out almost completely within three cycles following the coastdown, with the greatest effect coming during the cycle immediately following coastdown. These studies show that coastdown is a viable way of increasing the discharge burnup (increase ore savings) without severely compromising any neutronic or thermal-hydraulic constraints.

The economic advantage of coastdown in PWR's has been discussed frequently. Most of the studies have investigated the economic benefits for an isolated cycle of coastdown, without including the economic penalty in subsequent cycles (shorter cycle length) or the high replacement energy cost. Economic studies of repetitive coastdown at the end of each full power cycle have been performed by Kusner [K-1] and Watt [W-2]. They both showed that the average energy cost first decreases (relative to a core with the same loading and no coastdown) as the duration of coastdown increases, then reaches a broad minimum, and finally increases. This broad minimum affords the operator some flexibility as to when the coastdown is terminated, without adversely affecting the economics.

A study has recently been completed at MIT in which the additional burnup gain as a function of coastdown power level for the thorium and uranium fuel cycles in PWR's has been computed. It was found that a reduction in the average moderator temperature of 30°F coupled with a reduction in the power level to 40% below rated power results in a burnup gain of around 3000 MWD/MTU for uranium systems; larger burnup gains were found for the thorium systems (around 4500 MWD/MTU). In the present work, these results will be used as a data base for input to a simple model developed to analyze coastdown scenarios.

Advantages have been claimed regarding the use of coastdown in thorium-uranium-fueled HTGR's [D-4]. This coastdown capability comes from reduced xenon poisoning, the negative temperature/power coefficient and reduced Pa-233 poisoning. A typical coastdown scenario, comparing HTGR and PWR systems is shown in Table 5.1. As shown, the possible additional operation down to 50% power is greater for the HTGR system by 40 days. Also shown is that the reduced Pa-233 poisoning is the dominant positive reactivity addition mechanism in coastdown operation of HTGR's while in PWR's, operating on the uranium fuel cycle, the temperature/power coefficient effects dominate. In view of these findings a brief study has been conducted to see if PWR's operating in the thorium cycle can achieve substantial positive reactivity from reduced Pa-233 poisoning during coastdown operation.

5.3 Coastdown Model Development

The phenomenon of coastdown is relatively complex; not only are the neutronic (e.g., additional burnup) and economic (e.g., fuel cycle cost and replacement power cost) performance affected during the coastdown cycle, but the effects of coastdown are felt up to 3 cycles following coastdown, with the greatest effect coming during the cycle immediately following coastdown. As one can infer, coastdown is quite complex, and its analysis may require

TABLE 5.1

COMPARATIVE COASTDOWN CAPABILITY FOR HTGR's AND PWR's [D-4]

	Possible Additional Operation at 50% Power (days)	
	HTGR (Thorium Cycle)	PWR (Uranium Cycle)
From Reduced Xenon Poisoning	35	45
From Temperature Coefficient	30	90
From Reduced Pa-233 Poisoning	<u>110</u>	<u>----</u>
TOTAL	175	135

sophisticated techniques. The use of state-of-the-art methods generally requires significant computational time and money, and may set practical limits on the number of solutions which can be investigated. Thus, the need for "simple" analytical methods for scoping calculations is evident; such methods can be used to evaluate many different coastdown scenarios so that one can concentrate on the more promising solutions. This study will demonstrate that coastdown can be analyzed accurately by simple physics and economics models. In addition, the simplicity of these models facilitates updating of the results which is especially useful in today's rapidly changing economic environment.

5.3.1 Xenon Model

The most important fission product poison is Xe-135, whose thermal (0.025eV) absorption cross section is 2.7×10^6 barns. Xe-135 is formed from the decay of I-135 and is also produced directly in fission. It is part of the fission product chain shown in Figure 3.3; the appropriate decay constants, λ , and fission yield fractions have already been provided in Table 3.1. None of the other isotopes in this chain have appreciable absorption cross sections.

Because the half lives of I-135 and Xe-135 are so short and the absorption cross section of xenon is so large, the concentrations of these isotopes quickly rise to their equilibrium values. In a typical PWR, the xenon concentration attains its equilibrium value within 100 hours, so that a significant amount of poison is inserted into the core in a short period of time. In a current PWR the (full power) equilibrium xenon worth is approximately 3% $\Delta\rho$. This value stays fairly constant throughout the life of the core, rising slightly over the burnup cycle. Therefore, a significant amount of neutrons and reactivity are lost to this fission product poison.

During coastdown operation the power level (and flux) of the reactor are reduced, which results in a lower xenon concentration (since the Xe concentration

is dependent upon the flux level): hence, the neutron economy is improved and a positive reactivity insertion results. As shown in Appendix C, the fractional change in reactivity due to coastdown (reduction in power level) is

$$\frac{\Delta\rho}{\rho_{100\%}} = \frac{\lambda_{Xe}/\phi_{100\%}}{\lambda_{Xe} + \frac{\sigma_{Xe}P'}{P}} \frac{\Delta P}{P} \quad [5.1]$$

where

λ_{Xe} = decay constant of Xe, sec^{-1}

σ_{Xe} = spectrum-averaged microscopic absorption cross section for Xe-135, cm^2

P', P = reduced power level and rated power level, respectively, MW(th); $\Delta P = P - P'$

ϕ_{100} = flux level at rated power level, $\#/\text{cm}^2\text{-sec}$

$\rho_{100\%}$ = full power equilibrium Xe worth, % $\Delta\rho$

The above equation can be used to calculate the positive reactivity insertions, $\Delta\rho$ when the reactor is coasted down. In addition, the duration of coastdown permitted by reduced Xe levels may be inferred from $\Delta\rho$; hence, one can easily interpolate and extrapolate coastdown scenarios.

5.3.2 Protactinium Model

When neutrons are absorbed by fertile Th-232, an intermediate precursor is formed (Pa-233) before it is converted to fissile U-233. The half-life of Pa-233 is 27 days, and the thermal absorption cross section and the infinitely-dilute resonance integral are 41.46b and 857.0b, respectively. Hence, there is a non-negligible probability that a neutron will be absorbed by Pa-233 (parasitic capture) and thereby eliminate a potential fissile atom in addition to losing the neutron. While this U-233 loss may be significant, it is not totally deleterious since neutrons absorbed by Pa-233 form the fertile material U-234 which upon capture of another neutron produces fissile U-235.

The parasitic capture of Pa-233 may be reduced by operating the reactor in a well thermalized spectrum (low epithermal flux) or at a low flux level. The latter

strategy adds positive reactivity when the reactor is coasted down since there are fewer parasitic captures by Pa-233, and an increased production of U-233. This insertion rate is relatively slow since the half life is 27 days.

As shown in Appendix C, the positive reactivity insertion, $\Delta\rho$, due to reduced Pa burnout is

$$\Delta\rho = \frac{N_{13} \sigma_{13}}{N_f \sigma_{a_f}} \frac{\Delta P}{P_{100\%}} \quad [5.2]$$

where

N_{13}, N_f = atom density of Pa-233 and total core fissile material, respectively, $\#/cm^3$

σ_{13} = spectrum-averaged microscopic capture cross section of Pa-233, cm^2

σ_{a_f} = spectrum-averaged microscopic absorption cross section of core fissile material, cm^2

$P_{100\%}$ = rated thermal power level, MW(th)

ΔP = change in thermal power level, MW(th).

The above equation can be used to calculate the positive reactivity insertion (as a function of power level) due to reduced Pa burnout when ThO_2/UO_2 fueled reactors are coasted down at EOC. The inventory of Pa-233 in an operating core is quite high, typically 8 to 10% of the total fissile inventory, so the reactivity insertion can be as large as 1.5 to 4.0% $\Delta\rho$. In deriving the above equation it was assumed that the positive reactivity from reduced Pa²³³ burnout is inserted instantaneously. This is obviously not true since Pa²³³ has a 27 day half-life. Thus, ThO_2 reactors which are coasted must rely on reduced Xenon poisoning and reduced temperatures to keep the reactor critical in the initial stages of coastdown. Afterwards, positive reactivity from reduced Pa²³³ burnout can help keep the reactor critical.

5.3.3 Temperature/Power Coefficient Model

In order to evaluate the coastdown capability of a PWR, the temperature/power coefficients must be known, in particular, the amount of reactivity ($\% \Delta \rho$) available as a function of load. In this section a simple model is proposed which calculates the temperature/power coefficients and the amount of additional burnup days due to coastdown as a function of load.

In any study similar to the present where many options are available, the calculational methodology has to be based on a relatively simple reactor model in order to reduce the cost of, and time required for the analysis. In the present work, the LEOPARD code was used for evaluating coastdown scenarios. This code was chosen because it satisfied the requirement that the methodology be simple, quick, and accurate. It has been shown by Garel [G-1] and others that the LEOPARD code calculates average parameters (i.e., reload enrichment, discharge burnup, etc.) quite accurately (in good agreement with more sophisticated spatial diffusion-depletion models). Thus, calculation of reactivity coefficients and coastdown burnup histories should also be well within the precision required for scoping studies of the present type.

In general, when large PWR's are coasted down the power is reduced steadily, such that the reactor is continuously critical (typically a reactor may coast at a rate of 0.25% power/day). In calculating the various parameters of current interest (e.g., additional burnup), it was assumed that the power level is reduced in a stepwise fashion, in particular, the data base generated by Bamdad-Haghighi [B-8] for this study assumed a power reduction in increments of 20%. This assumption is valid if the neutron spectrum is not significantly changed when reducing the power level in a stepwise fashion since the nuclide concentrations would

be the same for the continuous coastdown and the stepwise-coasted case. It was found that the spectrum did change, and that calculated nuclide concentrations did depend upon the size of the power reduction, but the errors are small (see Section 2.3.2). The error can be reduced by reducing the size of the increment but as shown in Section 2.3.2, the change in the isotopics is less than 1% even when there is a reduction of 50% in power; thus the error is quite tolerable.

In calculating the additional burnup due to coastdown, the positive reactivity effects from reduced moderator temperature and fuel temperature should be evaluated separately. This is due to the fact that the average moderator temperature does not vary linearly with load during coastdown operation. (During normal operation, the average moderator temperature varies linearly from hot-zero-power, HZP, to hot-full-power, HFP.) The reactor is coasted at a constant rate, and the average moderator temperature is adjusted to keep the reactor critical. Thus fuel and moderator feedback effects should be determined separately.

The following procedure was used to determine the reactivity coefficients at EOC. LEOPARD runs were performed with different fuel temperatures and the moderator temperature held constant; this determined the fuel temperature coefficient. Likewise, the moderator temperature coefficient was found by fixing the fuel temperatures and varying the moderator temperature. To find the additional burnup due to coastdown, LEOPARD point depletion runs were made with the fuel temperature corresponding to reduced power levels and the moderator temperature held constant. Similarly, depletion runs were made with the fuel temperature held fixed and the moderator temperature changed.

5.3.4 Additional Burnup Gain Due To Coastdown

It is possible to show (see Appendix D) that if one starts with a steady-state fuel cycle and keeps the reload composition fixed, use of coastdown to extend burnup an increment, ΔB^c , (either for a single cycle, or forever thereafter) results in a net ultimate burnup gain of

$$\Delta B_{\text{net}} = \sum_{i=1}^N \frac{2}{n+1} \Delta B_i^c \quad [5.3]$$

where

n = number of fuel batches in the core

N = number of coastdown cycles.

The above relation shows that net burnup gain in a multi-batch core is not ΔB^c , but rather some fraction of ΔB^c . This is due to the fact that in the cycle following coastdown ($\frac{n-1}{n}$) of the fuel is more depleted than it would have been had refueling occurred when full power end-of-life was reached. Because of this the burnup histories of subsequent cycles are affected (shorted full-power cycle lengths are experienced, assuming of course that reload fuel enrichment and batch size are held constant.)

As shown in Appendix D, the linear reactivity model can predict the burnup behavior of cycles following the coastdown. For example, Equation [D.6] shows that for a two-batch core the burnup increment for the cycle following coastdown is

$$\Delta B_2 = 2/3 \bar{B} - 1/2 \Delta B^c \quad [5.4]$$

where

ΔB = burnup increment for the cycle, MWD/MTU

\bar{B} = reactivity limited discharge burnup of a one-batch core having the same reload enrichment as the multi-batch core.

Further application of this model shows that a convergent oscillatory behavior is observed between under and over-reactive subsequent cycles (for either a single coastdown or for coastdown after each cycle).

5.3.5 Coastdown Economics Model

The duration of coastdown not only depends upon neutronic and thermal-hydraulic considerations but also upon economic considerations. In the past, economic analysis of coastdown considered only direct and indirect nuclear fuel cycle costs. However, the cost of replacement power during coastdown is high, so that the total energy cost must include the cost of replacement energy.

It can be shown [S-5] that the total energy cost per unit energy, C_T , is

$$C_T = \frac{C_c E_c + C_R E_R}{E_c + E_R} \quad [5.5]$$

where

C_c = levelized nuclear fuel cycle cost, mills/kwhr(e)

C_R = levelized replacement energy cost, mills/kwhr(e)

E_c = total energy produced by nuclear fuel during a burnup cycle, kwhr(e)

E_R = total replacement energy during coastdown, kwhr(e)
(includes energy replacement for coastdown, refueling, and forced outages).

The above equation shows that the total fuel cycle cost can be found if the replacement energy cost, the duration of coastdown (energy generated by the coasted reactor), and the levelized nuclear fuel cycle cost are known. The duration of coastdown can be found from the reactivity models developed in the previous sections. The nuclear fuel cycle cost can be determined

using typical present-day cost assumptions [A-1] in the ECON code. The determination of replacement energy cost is system and time dependent and, therefore, subject to uncertainty. However, a replacement energy cost of 25 mills/kwhr appears to be typical of the numbers quoted today [W-2]. Therefore, Equation 5.5 can be used to calculate the total fuel cycle cost for different coastdown scenarios.

5.4 Reactor Investigated

The C-E PWR system described in Section 3.4.1 was used as the design basis for this study. The assembly consists of a 14 x 14 array of fuel cells and five large control rod channels. The design characteristics for the assembly and reactor are shown in Tables 3.2 and 3.3. This system was chosen to be the design basis since it is typical of a large PWR in actual commercial operation.

The same reactor and assembly design were used as the design basis for evaluating coastdown operation in PWR's operating on the thorium fuel cycle. Garel [G-1] has found equilibrium mass and burnup parameters for reactor types and fissile species (e.g. U-235, Pu-239, U-233); in particular, for a UO_2 (93% enriched U-235) reactor recycling uranium-233 (and small amounts of bred plutonium) to itself, and recycling bred U-233 to a $^{233}UO_2/ThO_2$ PWR reactor. Garel's results (mass flows) for the $^{233}UO_2/ThO_2$ PWR reactor (see Table 5.2) will be used as a data base (e.g., isotopic composition input into LEOPARD) in the current analysis of coastdown in $^{233}UO_2/ThO_2$ PWR reactors.

TABLE 5.2
CHARGE AND DISCHARGED MASSES FOR A $^{233}\text{UO}_2/\text{ThO}_2$ FUELED
PWR REACTOR* [G-1]

ISOTOPE	INITIAL INVENTORIES (kg/INITIAL MT HM)	DISCHARGED INVENTORIES (kg/INITIAL MT HM)
U-233	30.378	18.079
U-234	2.691	5.052
U-235	0.418	1.145
U-236	-----	0.205
Th-232	966.513	940.222
Pa-233	-----	1.086

* LATTICE parameters have been defined in Table 3.2.

5.5 Results

5.5.1 Reactor Efficiency

As previously mentioned, coastdown scenarios require that the reactor and the steam supply system operate at less than ideal conditions (e.g., lower thermal power, lower average coolant temperature, etc.), and operating at these conditions reduces the overall efficiency of the plant. The reduction in the average coolant temperature, T_{AVE} , is handled by the standard T-Average Reference Controller which provides a pre-programmed coastdown policy. During normal operation, the average moderator temperature is varied linearly from hot zero power to hot full power. The advantage of changing T_{AVE} linearly is that the turbine plant pressure change is minimized as load is changed. In some plants the T_{AVE} Reference Controller is programmed to keep the average coolant temperature constant as function of power level (as shown in Figure 5.1). Constant average coolant temperature results in a constant inventory of water in the reactor coolant system; thus a smaller pressurizer is needed for plants designed for constant T_{AVE} since the need to bleed or add water to maintain a constant pressurizer level with changing load is eliminated. In coastdown situations, it is more advantageous to operate with a reduced T_{AVE} , since there is a concurrent

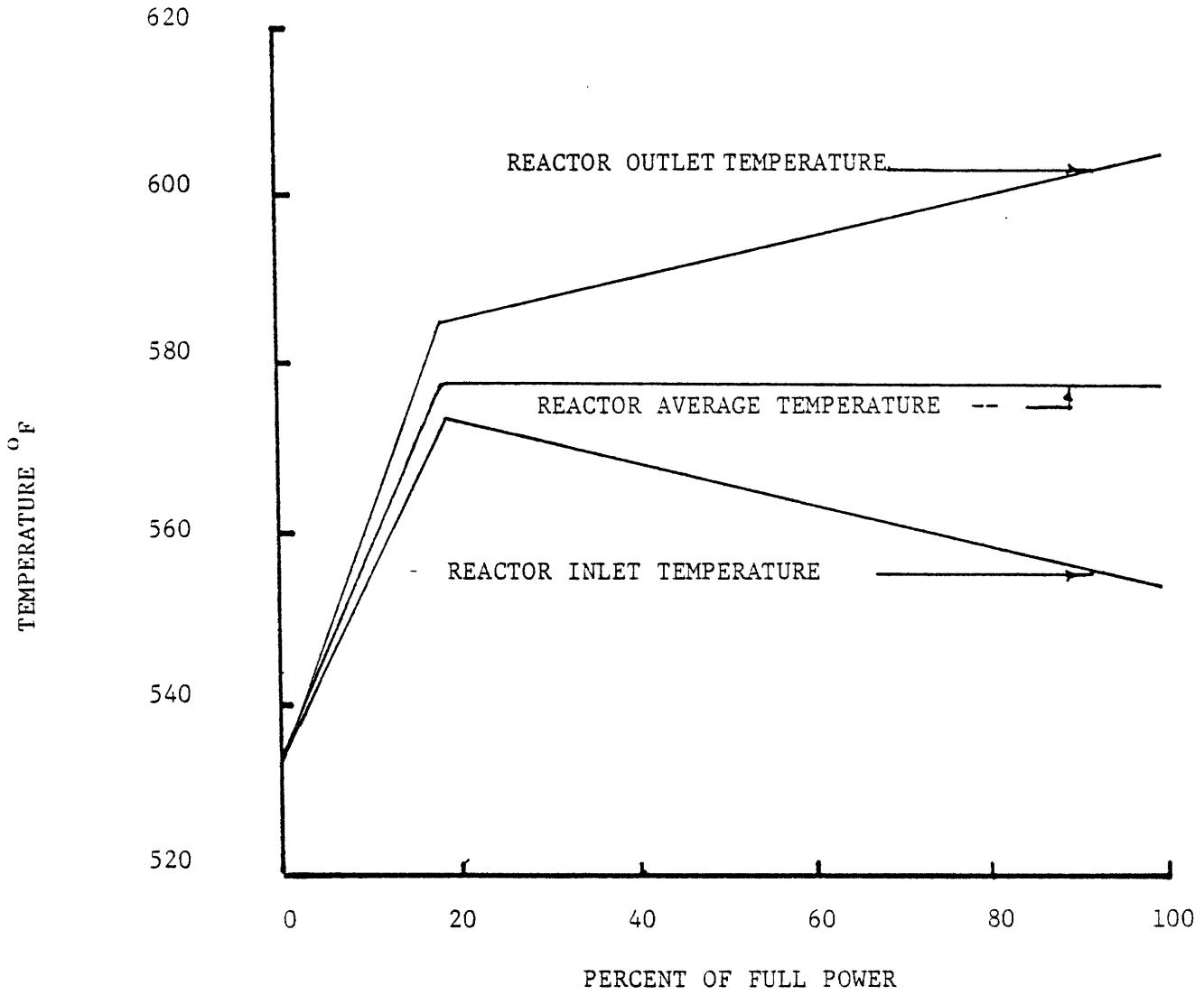


FIGURE 5.1 REACTOR COOLANT TEMPERATURES VS. REACTOR POWER (B-9) FOR A CONSTANT T_{AV} UNIT

positive reactivity insertion because of the coolant temperature change (negative moderator temperature coefficient).

The overall efficiency of the plant as a function of load was calculated using the BAHAR code [N- 1]. The design basis used in this study is the C-E PWR as described in Section 3.4.1. The plant layout of the nuclear steam supply system is shown in Figure 5.2 and the nomenclature is described in Table 5.3. Using the plant characteristics shown in Table 5.4, the BAHAR code was used to calculate the overall efficiency of the plant as a function of load (see Figure 5.3). As one can see, the efficiency decreases as the load decreases; however, the curve shows that the efficiency is not degraded significantly when the load is reduced. This is due to the fact that when the load is reduced, the average moderator temperature is reduced such that turbine plant pressure change is minimized and the temperature of the steam remains constant. This analysis shows that the efficiency of the plant is reduced when the reactor is operated in a coastdown mode but the drop in efficiency is quite small so that harsh economic penalties (replacement power costs) are not felt.

5.5.2 Reactivity Models

The accuracy of the coastdown reactivity models was tested by comparing the results of the simple models against more exact calculations, in particular, the results from the Maine Yankee Cycle 3 Design Report [S-6].

The accuracy of the Xenon reactivity model was first tested. As shown in Section 5.3.1, the fractional change in reactivity (due to reduced

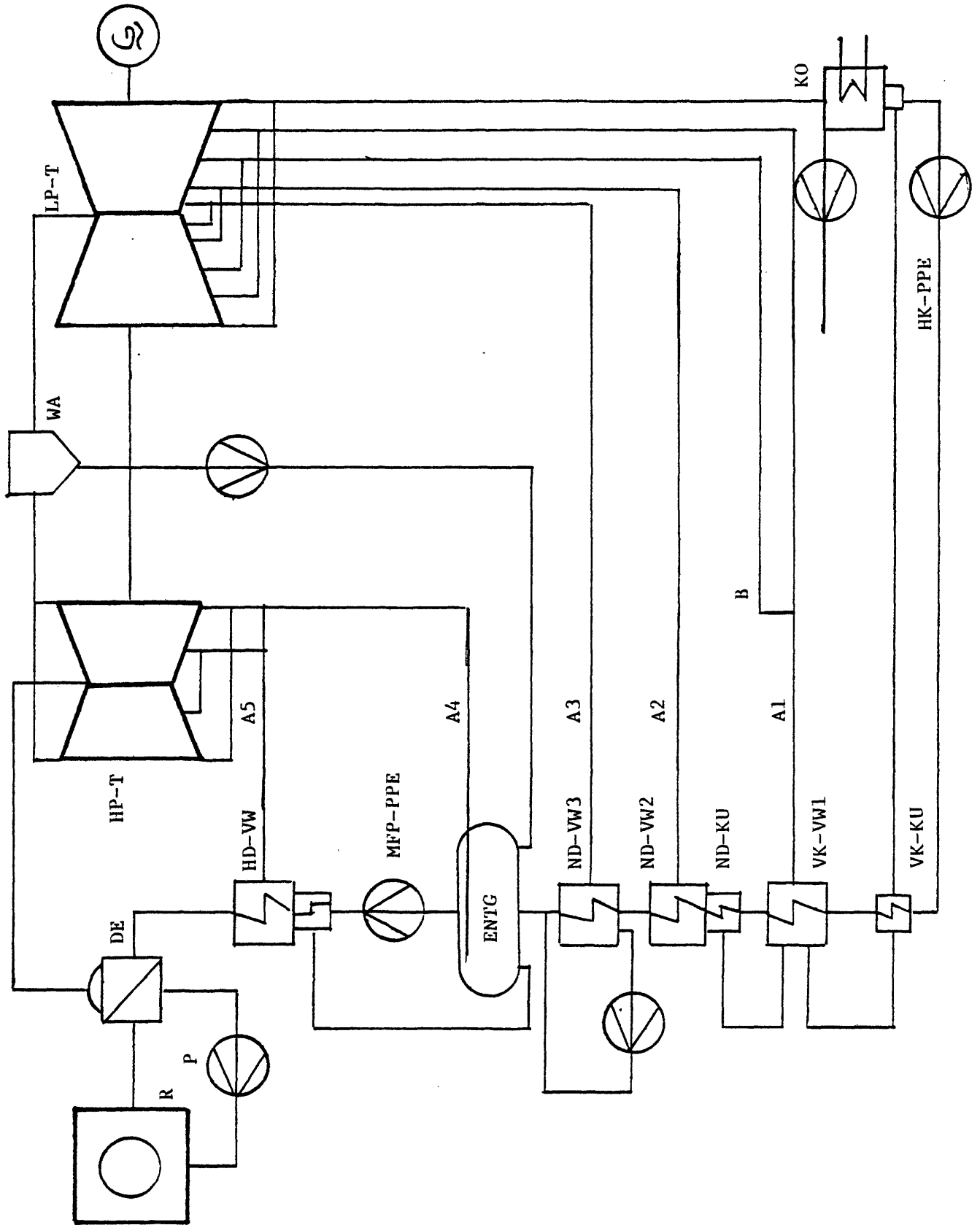


FIGURE 5.2 NUCLEAR STEAM SUPPLY SYSTEM LAYOUT

TABLE 5.3

NOMENCLATURE FOR NUCLEAR STEAM SUPPLY SYSTEM: FIGURE 5.2

R	:	Reactor
P	:	Pump in Primary Loop
G	:	Generator
HP-T	:	High Pressure Turbine
LP-T	:	Low Pressure Turbine
DE	:	Steam Generator
A1...A5	:	Bleeds
B	:	Dehydration
ENTG	:	Degasifier
HD-VW	:	High Pressure - Preheater
ND-VW1...3	:	Low Pressure - Preheater
VK-VW	:	Vacuum Cooler
ND-KU	:	Low Pressure - Cooler
VK-KU	:	Vacuum Cooler
MFP-PPE	:	Main Feedwater Pump
HK-PPE	:	Condensate Pump
KO	:	Condenser
WA	:	Water Separator
NK-PPE	:	By-Condensate Pump

TABLE 5.4
STEAM SUPPLY SYSTEM DATA

TOTAL HEAT OUTPUT	2440 MWE
REACTOR COOLANT FLOW	136.0 x 10 ⁶ lb/hr
PRESSURE DROP ACROSS CORE	9.9 psi
REACTOR PRESSURE	2100 psi
TOTAL PRESSURE DROP ACROSS VESSEL	33.1 psi
AVERAGE CORE ENTHALPY RISE	63.1 BTU/lb
STEAM GENERATOR STEAM PRESSURE	900 psi
PRESSURE DROP IN STEAM GENERATOR	51 psi
STEAM CONTENT	0.9975
INLET TEMPERATURE (STEAM GENERATOR)	432 ^o F
OUTLET TEMPERATURE (STEAM GENERATOR)	565 ^o F
NUMBER OF BLEEDS	5
COOLING WATER INLET TEMPERATURE	72 ^o F
COOLING WATER TEMPERATURE RISE	18 ^o F
MECHANICAL POWER LOSSES	1.0 MW
INTERNAL POWER CONSUMPTION	1.0 MW

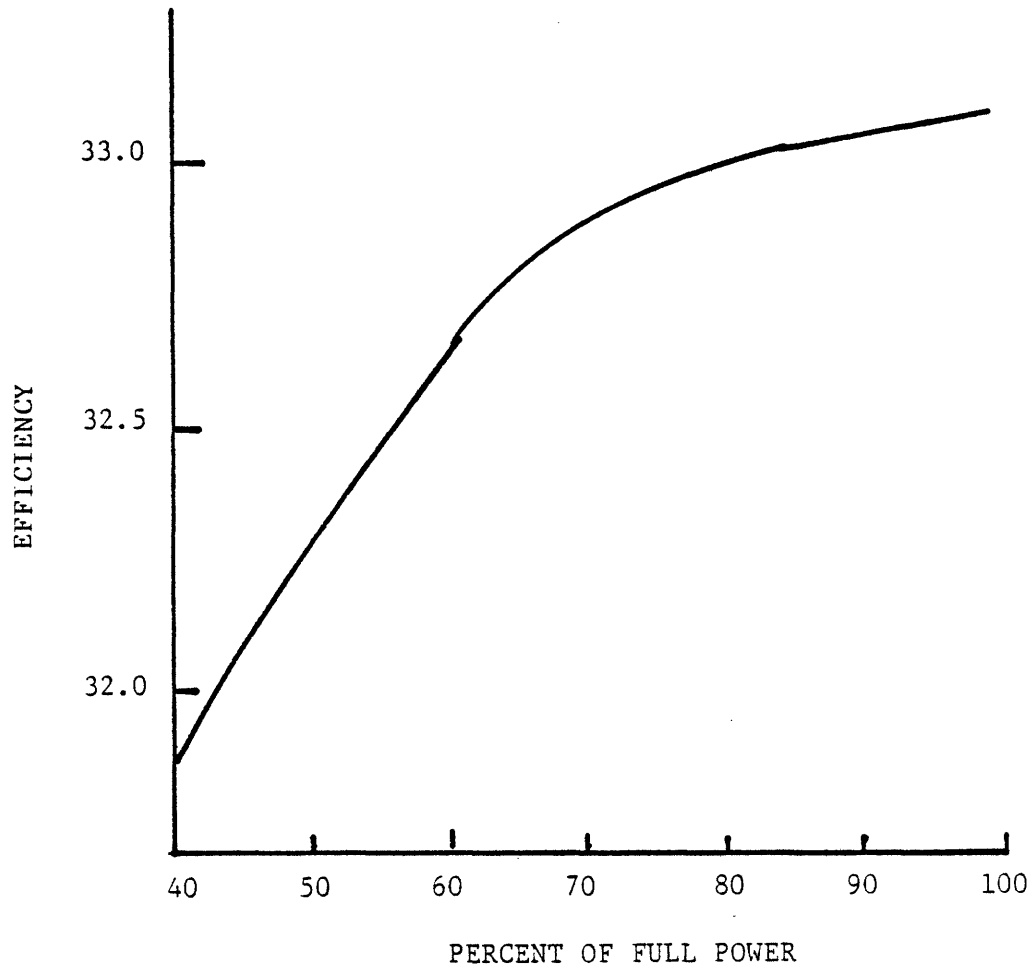


FIGURE 5.3 REPRESENTATIVE PLANT EFFICIENCY VS. LOAD FOR A TYPICAL PWR

Xe poisoning) is

$$\frac{\Delta\rho}{\rho_{100\%}} = \frac{\lambda_{xe}/\phi_{100\%}}{\frac{\lambda_{xe}}{\phi_{100\%}} + \frac{\sigma_{xe}P}{P}}, \quad \frac{\Delta P}{P} \quad [5.5]$$

(The parameters are defined in Section 5.3.1). Using the nuclear parameters calculated by the LEOPARD code (Table 5.5) in Equation [5.1] one finds the fractional change in Xe reactivity as a function of load (Figure 5.4). As shown, there is good agreement with the more exact calculations. Thus the simple Xe reactivity model can accurately predict the Xenon worth as a function of load during coastdown. Also shown in this figure is that most of the reactivity contribution from Xe occurs below 40% of full power; hence, one cannot take full advantage of the Xenon worth (since reactors are rarely coasted below 40% of full power). Moderator and fuel reactivity effects were calculated using the LEOPARD code, as discussed in Section 5.3.3. Using the design base discussed in Section 5.4, the moderator and fuel temperature coefficient were calculated for the hot full power EOC conditions (i.e., no soluble boron and a core average burnup of 22,000 MWD/MTU). The results are summarized in Table 5.6. As shown there is good agreement between the exact calculations and the LEOPARD results; thus the accuracy of this method is acceptable for the present study.

As previously mentioned, Bamdad-Haghighi [B- 8] generated a data base (additional burnup as a function of fuel and moderator temperature decrease) for this study. Using his results, the accuracy of the simple model was tested against Maine Yankee Cycle 3 values. The comparison is shown in Figures 5.5 and 5.6. As shown in Figure 5.5, there is good agreement between the LEOPARD calculations and the more exact calculation for predicting the additional burnup from load reduction. Figure 5.6 shows

TABLE 5.5

NUCLEAR PARAMETERS FOR XENON MODEL

$$\lambda_{xe}, \text{ DECAY CONSTANT OF Xe}^{135} = 2.09 \times 10^{-5} \text{ sec}^{-1}$$

$$\sigma_{xe}, \text{ MICROSCOPIC ABSORPTION CROSS SECTION OF Xe}^{135} = 1.724 \times 10^6 \text{ BARNS} *$$

$$\phi_{100\%}, \text{ FLUX LEVEL AT 100\% POWER} = 4.884 \times 10^{13} \frac{\text{neutrons}}{\text{cm}^2 \text{ sec}} *$$

* Thermal Flux and Thermal Absorption Cross Section

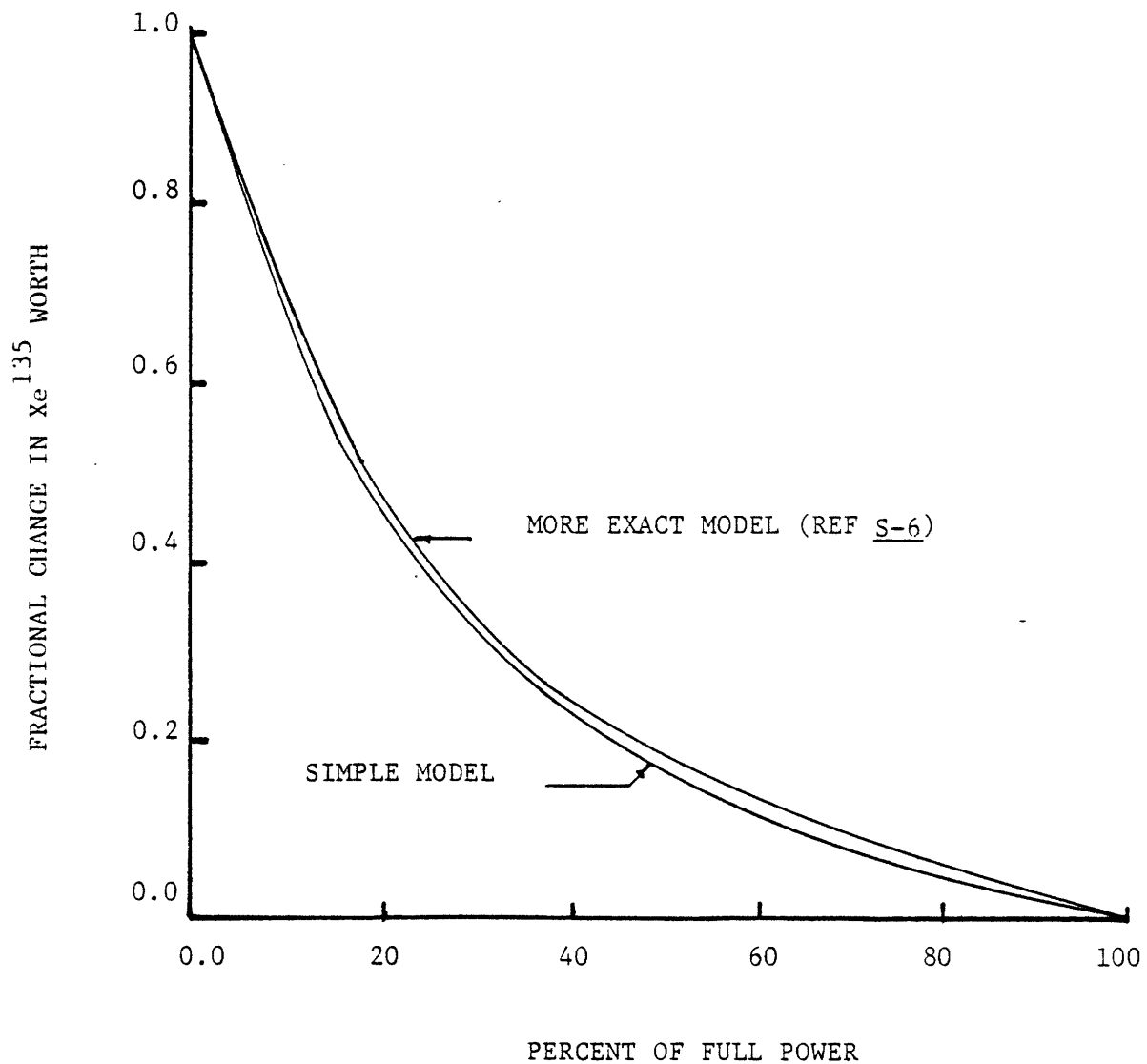


FIGURE 5.4 FRACTIONAL CHANGE IN Xe^{135} WORTH VERSUS LOAD

TABLE 5.6
COMPARISON OF LEOPARD AND MORE EXACT
TEMPERATURE COEFFICIENT VALUES

	Moderator* Temperature Coefficient ($10^{-4} \Delta\rho/^\circ\text{F}$)	Fuel* Temperature Coefficient ($10^{-5} \Delta\rho/^\circ\text{F}$)
LEOPARD	-2.18	-1.20
MORE EXACT**	-2.24	-1.33

* EOC, Hot Full Power, and Equilibrium Xe

** From Reference [S-6]

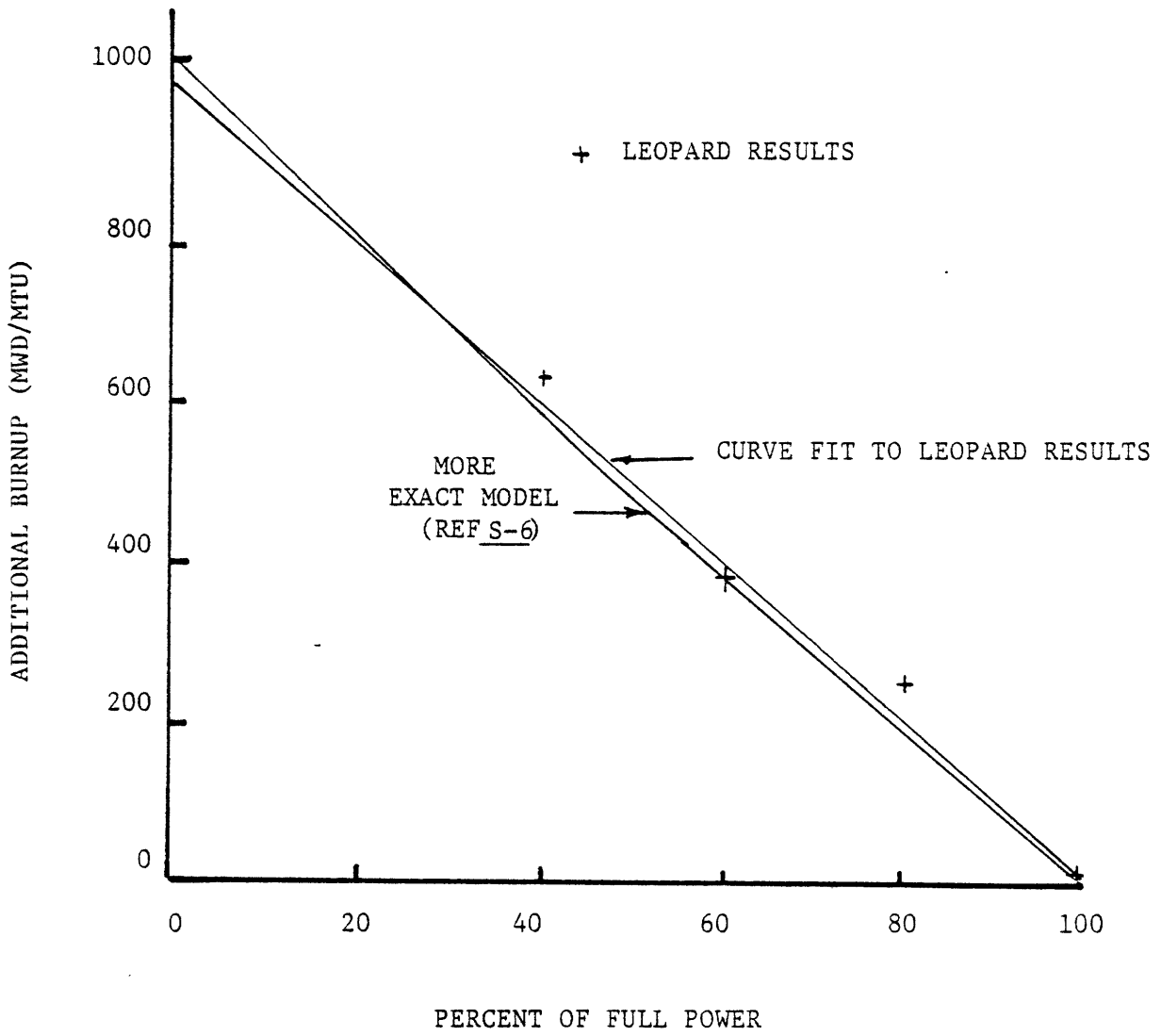


FIGURE 5.5 ADDITIONAL BURNUP FROM FUEL TEMPERATURE EFFECTS AS A FUNCTION OF LOAD

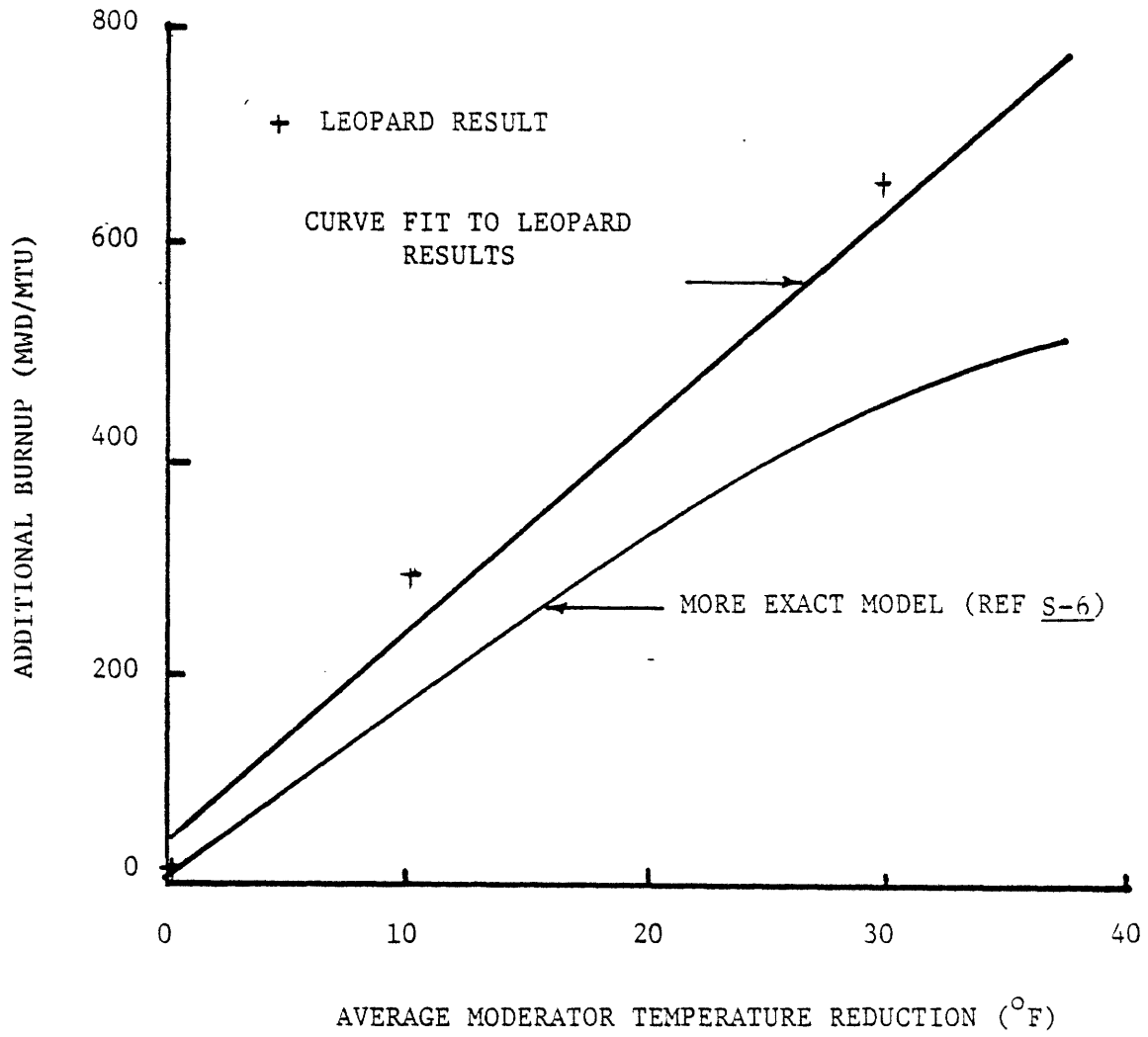


FIGURE 5.6 ADDITIONAL BURNUP FROM MODERATOR TEMPERATURE EFFECTS AS A FUNCTION OF AVERAGE MODERATOR TEMPERATURE REDUCTION

that LEOPARD over-predicts the additional burnup when the average moderator temperature is reduced, but the agreement is fairly good for small temperature reductions.

The above analysis has shown the LEOPARD code and supplementary simple models can be used to predict the additional burnup when the reactor is coasted; this is especially true for xenon and fuel temperature reactivity effects. For the case of the moderator temperature effects, the errors are tolerable. The overprediction of the additional burnup by the moderator temperature model will overpredict the total coastdown capability of the reactor. Since the reactor is coasted at a constant rate (the power is reduced X% per day) and the average moderator temperature is reduced such that the reactor is kept critical; the simple model will predict the correct coastdown rate, but the average moderator temperature will be slightly higher than in the real core. Thus, this model can analyze different coastdown scenarios, but it will slightly overpredict the total coastdown capability of the reactor.

5.5.3 Ore Savings and Fuel Cycle Cost

As previously shown, in Section 5.3.4, the net burnup gain, ΔB_{net} , due to coastdown is

$$\Delta B_{\text{net}} = \frac{2}{n+1} \Delta B^C \quad [5.6]$$

where

n = number of fuel batches in the core

ΔB^C = coastdown burnup increment, MWD/MTU.

It was shown that this relation is valid for a single coastdown or for coastdown forever thereafter. In addition, it was shown in Appendix D that if one starts with a steady-state fuel cycle and keeps the reload composition and coastdown burnup increment fixed, a convergent oscillatory

behavior is observed between under and over-reactive subsequent cycles, that is, a new equilibrium state is reached. As shown in Appendix D, the new equilibrium full power cycle burnup length, X, is

$$X = \left[\frac{2}{n+1}\right]\bar{B} - \left(\frac{n-1}{n+1}\right)\Delta B^c \quad [5.7]$$

where

\bar{B} = EOC single batch burnup.

The total cycle burnup length is just the sum of Equations [5.6] and [5.7].

The equations and the simple models developed in the previous section will be used to evaluate a typical coastdown scenario, in particular, the coastdown scenario used by the Maine Yankee Reactor will be investigated. In general, when the Maine Yankee Reactor has reached its full power end-of-cycle burnup the reactor is coasted at a rate of 0.604% power/day. Using this coastdown rate the ore savings was calculated as a function of coastdown burnup length (Table 5.7). As shown modest ore savings can be obtained as the coastdown burnup interval is increased, but as the coastdown interval is increased, the full power cycle burnup length and cycle-average capacity factor decrease.

The previous analysis showed that modest ore savings can be attained. However, the duration of coastdown is selected by a utility based primarily on overall economic considerations. In the past, economic analyses of coastdown considered only direct and indirect nuclear fuel cycle costs. However, the replacement cost of power is high in today's economic environment so that the total energy cost must include the cost of replacement energy.

As shown in Section 5.3.5, the total energy cost per unit energy, C_T , is

$$C_T = \frac{C_c E_c + C_R E_R}{E_c + E_R} \quad [5.8]$$

(The parameters have been defined in Section 5.3.5.)

TABLE 5.7

ORE SAVING FROM COASTDOWN OPERATION

COASTDOWN BURNUP LENGTH (MWD/MTU)	FULL-POWER ⁽¹⁾ CYCLE BURNUP LENGTH (MWD/MTU)	TOTAL CYCLE BURNUP (MWD/MTU)	COASTDOWN ⁽²⁾ DURATION (DAYS)	RELATIVE ⁽³⁾ ORE USAGE
0	11000	11000	0	1.000
250	10875	11125	8.68	0.989
500	10750	11250	18.02	0.978
750	10625	11375	27.88	0.967
1000	10500	11500	38.50	0.957
1250	10375	11675	50.04	0.946
1500	10250	11750	63.07	0.936

Rated Full-Power Level = 2440 MWt

Heavy Metal Loading = 83 MTHM

- (1) Found using Equation 5.7; this is burnup logged at rated power prior to start of coastdown. For repetitive burnup, the discharged batch's burnup is 3 times the cycle burnup.
- (2) Found by simple model Section 5.5.2.
- (3) Ore usage in ST U_3O_8 /GWe-yr relative to the non-coastdown case.

For the coastdown scenario defined in Table 5.7, the total nuclear fuel cycle cost was calculated using Equation [5.8]. The cost basis used is found in Table 2.2 and the mass flows and other pertinent data are found in Table 5.8. The results of these calculations are shown in Figure 5.7. As shown, the relative fuel cycle cost (relative to a core with the same loading and no coastdown) decreases, passes through a broad minimum and finally increases. From an economic standpoint the optimum coastdown duration is approximately 35 to 45 days, but it could be extended to 60 days without penalizing the customer.

In the above analysis, it was shown that the use of coastdown to extend the burnup life of the fuel will lead to modest ore savings (5%). In addition, the nuclear fuel cycle cost can be reduced, and is shown to have a broad minimum: thus the operator has some flexibility as to when the coastdown is terminated without adversely affecting the economics. Utilities must weigh all of the alternatives before selecting a planned coastdown scenario, since in addition to the advantages just cited, coastdown will reduce the plant capacity factor and will require rescheduling of the refueling shutdown if it is not made a part of routine operations.

The preceding analysis has been done in conformance with the methods ascribed to various utility planners [W-2], [K-1], and [S-5]. There are, however, some points requiring clarification with respect to the treatment of average plant capacity factor in the presence of coastdown; they do not have an important effect on the results, as discussed in Appendix F.

5.5.4 Reactivity Addition from Reduced Pa²³³ Burnout

As previously mentioned, a study has been performed which compared the coastdown capability in HTGR and PWR systems [D-4]. It was found that

TABLE 5.8

PARAMETERS FOR THE COASTDOWN SCENARIO

U_3O_8 *	3.98137×10^5 lb
Conversion to UF_6	3.37612×10^5 lb
Separative Work	1.20463×10^5 kg SWU
Fabrication	2.76667×10^4 kg
Throwaway*	2.76667×10^4 kg
Number of Batches	30
Power Level (100%)	2440 MWt
Replacement Energy Cost	25 mills/kwhr(e)
Availability Based Capacity Factor	0.90
Refueling Downtime	0.125 yrs.

* All masses shown are for one batch of fuel in a three-batch core.

** Includes spent fuel storage, transportation, and disposal for throwaway alternative.

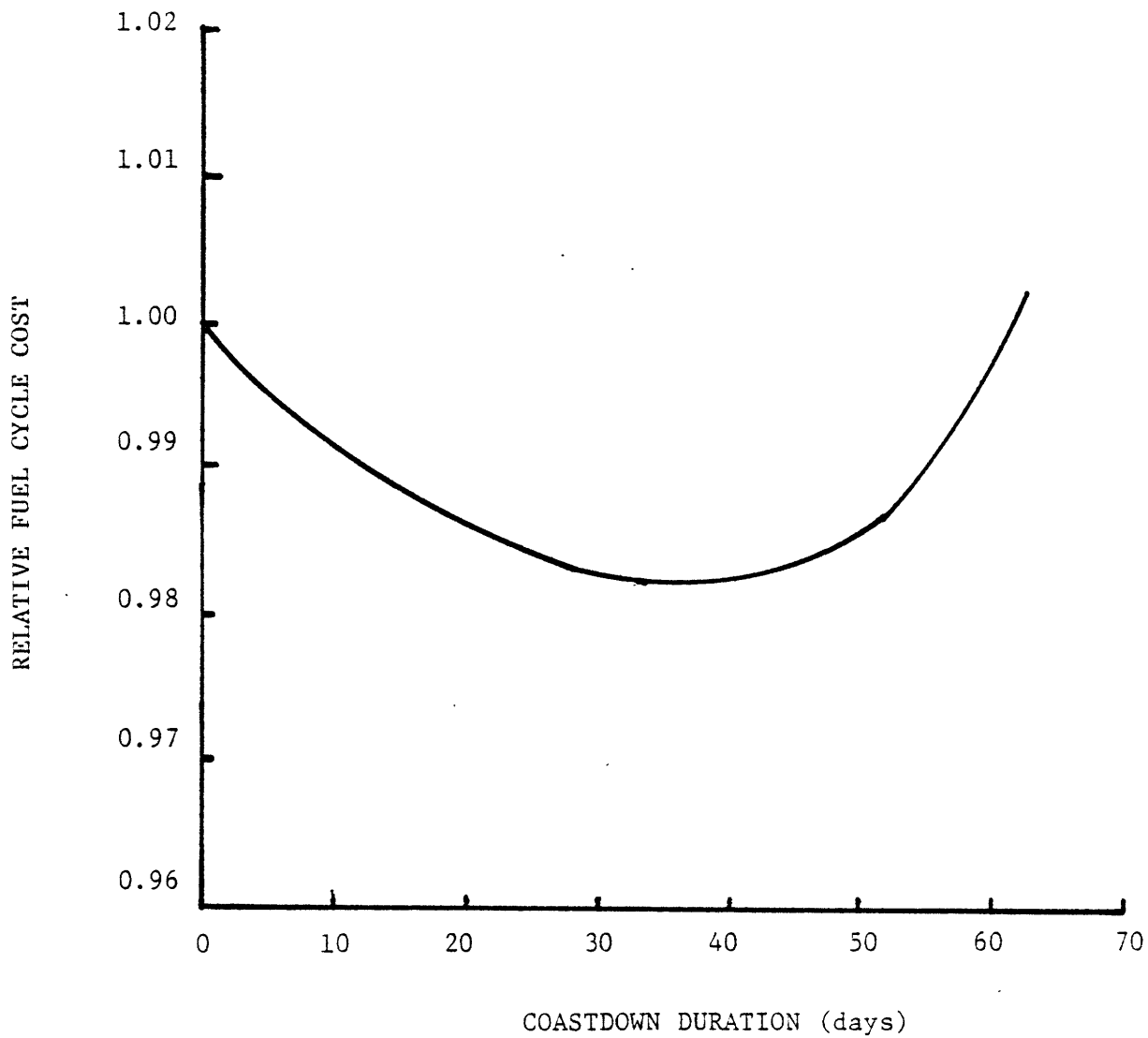


FIGURE 5.7 RELATIVE FUEL CYCLE COST VERSUS COASTDOWN DURATION

in $^{233}\text{UO}_2/\text{ThO}_2$ fueled HTGR systems a large positive reactivity insertion (due to reduced Pa-233 poisoning) occurs when the reactor is coasted down (see Table 5.1). In the present work coastdown in $^{233}\text{UO}_2/\text{ThO}_2$ fueled PWR systems was examined to see if there are comparable gains due to reduced Pa²³³ burnout. It was recognized that a once through system of this type would be impractical, but nevertheless the results should be a useful indicator as to whether this phenomenon would be worth exploiting in other modifications.

The simple model developed in Section 5.3.2 was used to calculate the positive reactivity from reduced Pa-233 burnout. As shown in Section 5.3.2, the positive reactivity, $\Delta\rho$, due to reduced Pa burnout is

$$\Delta\rho = \frac{N_{13} \sigma_{13}}{N_f \sigma_{af}} \frac{\Delta P}{P_{100\%}} \quad [5.8]$$

(The parameters have been defined in Section 5.3.2). The above equation shows that the reactivity is a function of the ratio of Pa-233 atoms to the total fissile atoms in a reactor core; and the ratio is a function of its previous operating history (i.e., fuel composition and power level). This ratio will be the highest in thorium cores with high neutron flux levels (as shown in Appendix C the equilibrium concentration of Pa-233 is directly proportional to the neutron flux level; however, as the flux level increases, so do the parasitic captures in Pa-233).

Using the results (mass balances) generated by Garel [G-1] (Table 5.2) and the spectrum-averaged cross sections generated using the LEOPARD code (Table 5.9) for a UO_2/ThO_2 PWR, in Equation 5.8, the maximum additional reactivity, $\Delta\rho$, (corresponding to a coastdown from full to zero power) was found to be 1.74% $\Delta\rho$. This corresponds to an additional burnup increment of approximately 2000 MWD/MTU. This reactivity insertion is not incurred instantaneously since Pa²²³ has a long half-life (27 days). Thus the

TABLE 5.9

SPECTRUM AVERAGED CROSS SECTIONS FOR A TYPICAL UO_2/ThO_2 -
FUELED PWR SYSTEM

<u>ISOTOPE</u>	GROUP 1 MICROSCOPIC ABSORPTION* CROSS-SECTION (BARNs)	GROUP 2 MICROSCOPIC ABSORPTION CROSS SECTION (BARNs)	SPECTRUM** AVERAGED (BARNs)
Pa	24.0 (capture only)	19.2 (capture only)	23.13
U-233	27.6	291.0	75.49
U-235	14.1	318.7	69.48

fast-to-thermal flux ratio,
 $\phi_1/\phi_2 = 4.50$ (thermal group ≤ 0.625 eV)

$$\Delta\rho = 1.74\%$$

* Calculated using the LEOPARD code for representative current
PWR lattice defined by Gare1 (see Table 5.2)

** One-group spectrum averaged constant given by $\bar{\sigma} = \frac{\sigma_1\phi_1 + \sigma_2\phi_2}{\phi_1 + \phi_2}$

ThO₂ reactors which are coasted must rely on reduced Xenon poisoning and reduced fuel and/or coolant temperatures to keep the reactor critical in the initial stages of coastdown. Afterwards, positive reactivity from reduced Pa²³³ burnout can help keep the reactor critical.

The additional burnup gain from reduced Pa²³³ is substantial but it is highly dependent on the ratio of Pa²³³ atoms to fissile atoms. A recent study completed by Combustion Engineering [S- 1] showed that in a typical PWR fueled with ThO₂ the Pa²³³ inventory can be as high as 8 to 10% of the total fissile inventory, in which case the reactivity insertion can be large (1.5 to 4.0% Δρ). Thus the above analysis shows that there is an additional reactivity mechanism (reduced Pa²³³) which can permit a significant amount of additional burnup when ²³³UO₂/ThO₂ reactors are coasted down. For example, a power coastdown to 50% power would permit 3500 MWD/MTU extra burnup in our example: about 1.2 times the power defect increment in a similarly coasted reactor fueled with ²³⁵U/²³⁸U.

5.6 Conclusions

In this chapter we have looked at the use of coastdown in current large PWR's to extend the burnup life of the fuel. The following can be concluded: 1) Simple models (analytical and computer) can be used to analyze the relatively complex phenomena of coastdown. These models were compared with more exact calculations and the agreement was found to be good. 2) It was found that if one starts with a steady-state fuel cycle and keeps the reload composition fixed, use of coastdown to extend burnup an increment, ΔB^C, (either for a single cycle, or forever thereafter) results in a net ultimate burnup gain of $(\frac{2}{n+1}) \Delta B^C$ for every coastdown, where n = number of fuel batches. Thus a three-batch PWR could gain 1/2 ΔB^C

for each cycle in which coastdown was applied. One cannot realize 100% of ΔB^C except for the batch reload case ($n=1$). 3) The net burnup gain relation shows that for cores with a large number of batches (n), the net burnup gain due to coastdown is small. Thus the stratagem of increasing core batch number, shown to be advantageous in Chapter 4 will negate much of the incentive for coastdown. For example, one should be careful not to ascribe the advantages of coastdown with a 3-batch core to the case of a 6-batch core; nor should the advantages of extended burnup be double counted. 4) If one coasts an amount ΔB^C for every cycle and keeps the reload enrichment the same, a convergent oscillatory behavior is observed between under and over-reactive subsequent cycles. This oscillatory behavior eventually damps out and leads to a new equilibrium state. 5) The simple reactivity models derived in this chapter were used to analyze a typical coastdown scenario. It was found that modest ore savings can be obtained (~5%). 6) An economic analysis of coastdown showed that a broad optimum coastdown duration exists. This relatively broad minimum implies that considerable operational flexibility exists (i.e., when to terminate the coastdown) without adversely affecting the economics. 7) The use of coastdown in PWR's is determined by the individual needs of the utility in question, and ore savings are only one input factor. 8) A simple model was developed to calculate the additional burnup from reduced Pa-233 burnout when UO_2/ThO_2 -fueled PWR's are coasted down. This model showed that reactivity depends on Pa²³³ inventory (relative to the total fissile inventory). In addition, the reactivity insertion was found to be a linear function of power reduction. 9) Using typical numbers for a UO_2/ThO_2 fueled PWR, it was found that an additional burnup of 3500 MWD/MTU can be

obtained (coasted to 50% power). 10) UO_2/ThO_2 -fueled reactors which are coasted must rely on reduced xenon poisoning and reduced fuel and moderator temperatures to keep the reactor critical in the initial stages of coastdown (since the half-life of Pa^{233} is long). Afterwards, positive reactivity from reduced Pa^{233} burnout can help keep the reactor critical.

CHAPTER 6

SUMMARY, CONCLUSIONS, AND RECOMMENDATIONS

6.1 Introduction

Until recently, it was envisioned that light water reactors (LWR) would serve an interim role, as precursors to Fast Breeder Reactors (FBR); a status testified to by the omission of "advanced LWR's" in long range system studies. The LWR's would remain the mainstay of commercial nuclear power development only until the breeder concept was shown to be commercially feasible and sufficient fissile reserves were bred to permit their widespread deployment. This transition has not taken place, and it is not in prospect, particularly in the United States, for several decades; hence, the role of LWR's in less transitory scenarios merits reassessment.

The present commercial attractiveness and useful lifetime of the LWR will depend upon the amount and price of available uranium resources. A breakeven yellowcake price of approximately \$150/lb U_3O_8 (compared to today's price of less than \$50/lb U_3O_8) is currently estimated for current LWR's competing with LMFBR or coal-fired units. The current restriction to a once through fuel cycle in the United States imposes an added burden. Therefore, a prime, long range concern of the industry today must be on better utilization of uranium by optimizing both reactor core design and fuel management strategy. Evaluation of these prospects was the central objective of the present investigation.

Generally speaking, there are two divergent approaches being pursued today to optimize LWR ore utilization: (1) development of fundamentally altered LWR concepts (e.g., the LWBR [E-1] and spectral shift reactors

[E-2]) and (2) use of conventional LWR designs, with a minimum of reactor and fuel cycle changes. The present work is of the latter genre; and, more importantly, only non-recycle concepts will be considered. These ground rules were established from the outset on quite pragmatic grounds: the United States nuclear industry is currently in a non-recycle mode of indefinite duration; and the less severe the changes proposed, the more rapidly they can be implemented and their benefits realized. However, it should be noted that some of the avenues to improvement would also benefit LWR cores operated in the recycle mode. Similarly, we will limit our analysis to PWR's, which represent approximately two-thirds of the current United States and World LWR reactor population in being, under construction or on order; but, BWR's could profit equally well from many of the same changes, as discussed in Reference [W-1].

6.2 Background and Research Objectives

Generally speaking, there are three distinct approaches being pursued today to optimize LWR ore utilization on the once-through fuel cycle: (1) increase the discharge burnup of the spent fuel, (2) reduce control poison requirements, and (3) reduce critical mass requirements at beginning of cycle (BOC). These general approaches can be embodied, singly or in combination, in various specific designs and/or operating procedures. Although some attention has been given to establishing ultimate theoretical limits, the present work concentrated primarily on specifics. For example, the following methods were investigated to increase the discharge burnup: (1) axial power flattening, (2) operating the reactor in coastdown scenarios at end-of-cycle (EOC), (3) increasing the number of batches in the core, and (4) increasing the refueling interval.

Ore utilization can also be improved by reducing the control poison requirements, since control poisons degrade the neutron economy by wasting neutrons on parasitic captures. There are two divergent approaches to reduce control poison requirements: (1) use control materials that will reap a benefit from parasitic captures (e.g., fertile materials) and (2) reduce the BOC reactivity to reduce the reload enrichment; but in this case a shorter irradiation period results. One possible way to avoid shorter cycle lengths would be to increase the conversion ratio of the reactor. This would reduce equilibrium enrichments and annual ore requirements by increasing fissile production during the cycle. Unfortunately, the improved conversion ratio is coupled to a penalty in the initial startup requirements.

In view of the above, the following compromise scenarios have been investigated: (1) axial seed/blanket cores, (2) movable-fertile-fuel reactivity control, and (3) enhanced reflector designs.

The initial objective was to assemble the analytic and numerical models needed to analyze the reactor core and fuel cycle design changes. Once this was completed, a cursory review of lattice design was performed to put the key independent design variables such as fuel pin diameter and pin-to-pin spacing into perspective. Finally, a neutronic and economic analysis was performed of each of the options outlined above to evaluate the resulting improvement in ore usage.

6.3 Ore Usage Model

Many design and operating changes have been proposed to better utilize uranium ore in current PWR's. Such changes must be evaluated in a consistent manner, considering both the ore investment needed to place a reactor system

into operation and the ore needed to operate it for a certain period of years. Different reactor systems should be compared after some years of post-startup operation. After this transient period, the annual demand for ore has settled down since the reactor has reached equilibrium conditions. When equilibrium occurs, the annual system uranium ore demand per GWe-yr, $F's$ can be rather accurately approximated by a simple linear combination of average annual ore usage and startup requirements:

$$F's = \dot{F} + rF \quad [6.1]$$

where

\dot{F} = annual makeup ore usage requirement, $STU_3O_8/GWe\text{-yr}$

F = initial startup requirement, STU_3O_8/GWe

r = growth rate of the nuclear electric system, $r\%$ per yr/100
($r=0$ when a single reactor is to be examined over its lifetime)

If we are to evaluate different reactor strategies, the parameters F and \dot{F} should be related to the appropriate characteristics (lattice pitch, batch size, reload enrichment, etc.) of each system. For neutronically similar large PWR cores, the ratio of the annual ore usage by a system of reactors of a given design [$F's_2$] to the annual ore usage of a reference case [$F's_1$] can be shown to be:

$$\frac{F's_2}{F's_1} = \left[\frac{1 + \frac{F}{100} \frac{N_2 T_2}{N_1 T_1}}{1 + \frac{r}{100}} \right] \left[\left(\frac{X_1 - X_o}{X_1 - X_w} \right) \left(\frac{n_1}{n_2} \right) \left(\frac{n_2 + 1}{n_1 + 1} \right) + \left(\frac{X_o - X_w}{X_1 - X_w} \right) \left(\frac{n_1}{n_2} \right) \left(\frac{T_1 E_1}{T_2 E_2} \right) \right] \quad [6.2]$$

where

T = refueling interval, years

N = equivalent number of reload batches in the initial startup core in terms of ore usage, shown to be roughly 2.25 for a three-batch core by Garel, who devised a general scheme for estimating this parameter [G-1]

X = BOC enrichment of a reload batch at steady state

X_o = BOC enrichment at which K=1 with saturated Xe and Sm; actually a parameter extracted by curve-fitting reactivity versus burnup calculations, typically ~1% for representative PWR cores

X_w = enrichment plant tails composition, taken to be 0.2% in the present work

n̄ = number of fuel batches in the core, 3 for our reference case

E = capacity-factor-weighted electric power rating, MWe.

This equation provides the capability of computing ore savings as a function of changes in core design and fuel management strategy. For example, the effects of changing the average burnup of a discharged batch, B, the refueling interval, T, or batch heavy metal loading, P, can be studied using Equation 6.2 since:

$$\frac{B_2}{B_1} = \frac{T_2 n_2}{T_1 n_1} = \frac{T_2 P_1}{T_1 P_2} \quad [6.3]$$

Equation 6.2 is simple to evaluate, but still quite versatile.

6.4 Reference Reactor Design Basis

The CE PWR system was used as the design basis for this study; in particular, the Maine Yankee PWR [Y-1] was used for most comparisons. The reference M.Y. assembly consists of a 14 x 14 array of fuel cells and five large control rod channels. This system was chosen as the design basis since it is typical of a large PWR in actual commercial operation, because the Yankee Organization provided useful support for our effort, and because CE was also an active participant in NASAP/INFCE related studies in parallel with the present effort. In this regard it should be noted that the newer CE System 80 assemblies differ in several aspects: (1) the fuel rod array is 16 x 16, (2) the average power density is 95 kw/liter (compared to M.Y. value of 75 kw/liter), (3) the active fuel length is 150 in. (versus M.Y. value of 136 in.), and (4) the assembly fuel-to-moderator ratio is 0.490

(versus M.Y. value of 0.482).

6.5 Results

In this section the fuel utilization characteristics for the various fuel cycle and design changes previously mentioned will be quantified. Table 6.1 summarizes the major options investigated and the primary results obtained, using state-of-the-art LWR calculational methods (LEOPARD and PDQ-7). Additional information is discussed on a case-by-case basis in the subsections which follow.

6.5.1 Use of Alternative Fuel Types

Advantages have often been claimed regarding the use of metal fuels [Z-1] (thorium in particular) and diluent containing oxide fuel [S-1] in LWR's. These contentions have been examined, with an emphasis on core neutronics and it was concluded that the use of alternative fuel types in current design LWR's offers no evident fuel cycle advantages over continued reliance upon oxide fuels.

Metal-fueled lattices or diluent containing oxide fueled lattices are not neutronically superior to oxide fueled lattices for the following reason. One can always vary fuel pin diameter and lattice pitch to find an oxide fueled lattice which is neutronically equivalent to a metal or diluent containing fueled lattice. That is, the two lattices would have essentially identical isotopic compositions over a given burnup history. A simple thought experiment supports the above contention: first, change the fuel pin diameter to match resonance integrals, then vary the pitch-to-diameter ratio (fuel-to-moderator ratio) to match the ratio of epithermal to thermal reaction rates. We have verified this assertion using the LEOPARD code for thorium and uranium metal fuels and diluent containing oxide fuels. Given neutronic equivalence, the charge and discharge fuel

TABLE 6.1
Ore Savings for the Once-Through PWR Fuel Cycle

Changes in Design/Operating Procedures	Ore Savings, %*	Comments
(1) Use metallic fuel, low density, oxide, or oxide containing a diluent	0	One can always define a neutronically equivalent UO_2 core
(2) Re-optimize fuel pin diameter and lattice pitch	-2	Base case for comparison should be kept in mind; e.g., pre or post LOCA/ECCS induced assembly re-designs
(3) Axial power shaping by enrichment gradation in fresh fuel	<7	Effective only in as much as it permits extended burnup
(4) Use 6-batch core, semi-annual refueling	10	Has been contemplated in past by commercial reactor vendors
(5) Use 6-batch core, annual refueling, extended burnup (~ double)	10 more than case (4) 20 total	May require use of clad other than zircaloy, or an improved alloy, or re-design of fuel pin internals
(6) Use radial reflector assemblies (a) depleted uranium or (b) BeO	(a) ~1 (b) <5	More work on thermally and mechanically practical assemblies needed
(7) Use internally heterogeneous core (simple seed/blanket)	-2	This option has not been fully explored, i.e., use of low enriched seed optimized for once-through fueling
(8) Use power/temperature coastdown at end of life, to extend burnup by an increment ΔB , here 1000 MWD/MTHM per cycle	5	Net burnup gain = $(2/n+1)\Delta B$ where n = batches in core; hence gain decreases as n increases
(9) Use isotopically separated, low σ_a cladding material, hence lower reload enrichment	<5	A very long range option; commercial prospects uncertain at present but under consideration
(10) Use of thorium in uniform lattices	negative	Some advantage perhaps in seed/blanket arrangements or in reflectors, not studied here
POTENTIAL COMPOSITE SAVINGS	25-35%	i.e., about what one could achieve by Pu + U recycle in standard lattices

*Relative to base case: 3-batch core, annual refueling, Maine Yankee PWR

composition was found to be essentially the same for the same burnup, as shown in Table 6.2. Hence, in the absence of convincing arguments to the contrary, diluent-containing fuels or metal fuels do not appear attractive for use in conventional LWR's unless the use of these alternative fuel types would somehow permit operation in a superior neutronic regime denied to current oxide fuel designs or permit operation at a higher power density and a lower heavy metal inventory such that the capital cost of a redesigned plant would be smaller.

6.5.2 Re-optimize Fuel Pin Diameter and Lattice Pitch

It has been found that current PWR lattices (for a once-through fuel cycle) were already very nearly optimum for ore and separative work requirements and nuclear fuel cycle cost. In this study, we re-analyzed the results of Garel [G-1] to verify the above assumptions; namely, his study on: (1) the effect of fuel pin diameter on the ore and separative work requirements of PWR systems and (2) the effect of fuel-to-coolant volume ratio on the ore and separative work requirements of PWR systems. In addition, we performed a fuel cycle economics study for the lattices studied by Garel. It was found that the optimum V_f/V_m with respect to ore and separative work requirements and fuel cycle cost occurs near $V_f/V_m = 0.469$, which is close to the fuel-to-coolant volume ratio used in current PWR lattices (compare to our reference value of 0.482); and ore savings are less than 2%. For the reasons given above, we have eliminated lattice (pitch, diameter) optimization studies as major avenues for improving ore and separative work requirements in PWR's operating on the once-through fuel cycle. It should be noted, however, that small improvements are possible, and one should keep in mind the base case for comparisons of this sort: assemblies

TABLE 6.2

EQUIVALENT U-235/U-238 OXIDE AND METAL FUELED LATTICES

	<u>Ref. Oxide Lattice</u>	<u>Metal Lattice</u>	<u>Oxide Lattice Diluent in Fuel</u>
BOL U-235 enrichment, w/o	3.0	3.0	3.0
Fuel pellet diameter, in.	0.370	0.14	0.460
Power density, kw/liter	80.9	80.9	80.9
Moderator to fuel ratio	1.66	3.85	1.41
Fuel density, g/cc	10.04	19.1	8.76
BOL k_{∞}	1.27328	1.27567	1.26195
EOL k_{∞} (35,000 MWD/MT)	0.88354	0.80166	0.87935
BOL resonance integral, U-238, barns	22.1906	22.1439	22.2875
Fast/thermal flux ratio	5.00125	4.99947	5.03070
Diluent			ZrO ₂ *
Net U-235 consumption (KG/TONNE)	24.3818	24.4476	24.3119
Net Pu-239 production (KG/TONNE)	4.8689	4.7667	4.97812

*20% by volume of the fuel region

NOTE: Similar results obtained for U-233/Th-232 Fuel Cycle

were redesigned after the ECCS controversy of the recent past, and pre- and post-design lattices have slightly different V_f/V_m ratios. In addition, when quoting a V_f/V_m , the distinction between the fueled unit cell value and the assembly-averaged value should be kept in mind. In the present work we have cited the latter value. These qualifications are probably responsible for the range of results quoted by different workers in the field for the effects of optimizing pin diameter and spacing.

6.5.3 Zone Loaded Cores

A substantial reduction of the peak-to-average power ratio can be attained by charging fuel of different enrichments to different zones in the reactor, or by using different concentrations of poison in different parts of the reactor. This is generally associated with radial power shaping. However, the same techniques can be used to change the axial power distribution from the usual cosine distribution (associated with uniform loading) to a power distribution in which more of the reactor operates at the maximum permissible power density. The rearrangement of materials to improve the axial power shape will be called "zone loading" here.

It will be shown in subsequent sections that increasing the burnup of spent fuel is the most promising option for achieving appreciable ore savings. Zone loading is beneficial primarily as it may facilitate maximizing the discharge burnup (insofar as to reducing specific ore usage ($\text{STU}_{38}\text{O}_8/\text{GWe-yr}$) is concerned); that is, for a given reactor operating on a fixed refueling schedule, the improvement in the power shape (lower power peaking) must ultimately lead to an increased total reactor thermal power output, and hence a higher burnup if it is to be worthwhile. Power shape improvements which lead only to a higher specific power (with constant

total thermal power output), in particular cores with a lower heavy metal loading will not reduce the ore consumption. A high power density core (having a constant total power output) will log the burnup in a shorter calendar time than a low power density core, thus more reloads per year are required; but the fissile mass flows are identical on a calendar time basis (when yearly energy output is held constant). On the other hand, if the thermal power level is increased (instead of decreasing the heavy metal inventory) and the irradiation time is held constant then the discharge burnup of the spent fuel increases; as previously mentioned, increasing the burnup ultimately leads to improved ore usage.

There are problems associated with changing the thermal performance: in most cases the plant would have to be relicensed; and the nuclear steam supply system may not be able to handle arbitrarily large thermal increases, but there are often modest margins built-in for moderate changes (stretch capability). It may also be that certain cores are peak-limited on engineering constraints rather than average exposure limited.

Three different zone loaded core configurations have been compared to a reference core to study the changes achievable in the core power shape and burnup limits. For these zone loaded cores only two axial enrichment zones were used to reduce the central power peak in the fresh fuel. For these three cases, the volume of the enrichment zones and the enrichment within each zone were varied. A coarse mesh PDQ-7 diffusion-depletion model was used to calculate the power distribution and nuclide depletion for the reactor. It was found that the central power peaking was reduced as much as 20%. The reader should not infer that the 20% reduction in peaking is necessarily the most one can achieve when reactor cores are zone loaded since more zones could be used, and the dimensions and enrichments of the various zones can be fine-tuned to an extent greater than achieved here.

The ore usage model was used to calculate the ore savings for the zone-loaded cores (relative to the reference case). The results show that the power level increases achieved in this manner which lead to extended burnup life of the fuel, accrue small ore savings. For example, if the thermal power level of the reactor is increased by 10%, such that the discharge burnup is increased by 10%, then an ore savings of approximately 2% will result.

6.5.4 6-Batch High Burnup Core

The motivation for analyzing a six-batch core fuel management scheme can best be explained with the ore usage model introduced previously. Using a typical set of parameters in Equation [6.2], relative ore usage plots can be obtained for the following two cases: (1) fix the number of batches in the core and vary the burnup and (2) fix the discharge burnup and vary the number of batches in the core. As shown in Figure 6.1, changing the discharge burnup can effect modest improvement in ore usage; in fact, a savings of 10% may be obtained if the discharge burnup is doubled (relative to the reference case). Also shown in Figure 6.1 is the case for fixed discharge burnup (i.e., $n_1=3$, n_2 varied). As can be seen, one can achieve ore savings of on the order of 10% by going to semi-annual refueling (i.e., a 6-batch core in place of a 3-batch core). By combining the two improvements, a six-batch core with annual refueling should achieve an ore savings on the order of 20%.

Using state-of-the-art techniques (LEOPARD, PDQ-7, and FLARE-G) six-batch cores with semi-annual and annual fuel management schemes were examined to see if there is a large potential for ore savings. The calculations showed that an ore savings on the order of 20% is obtained for the 6-batch core (annual refueling). The results of the more exact calculations were

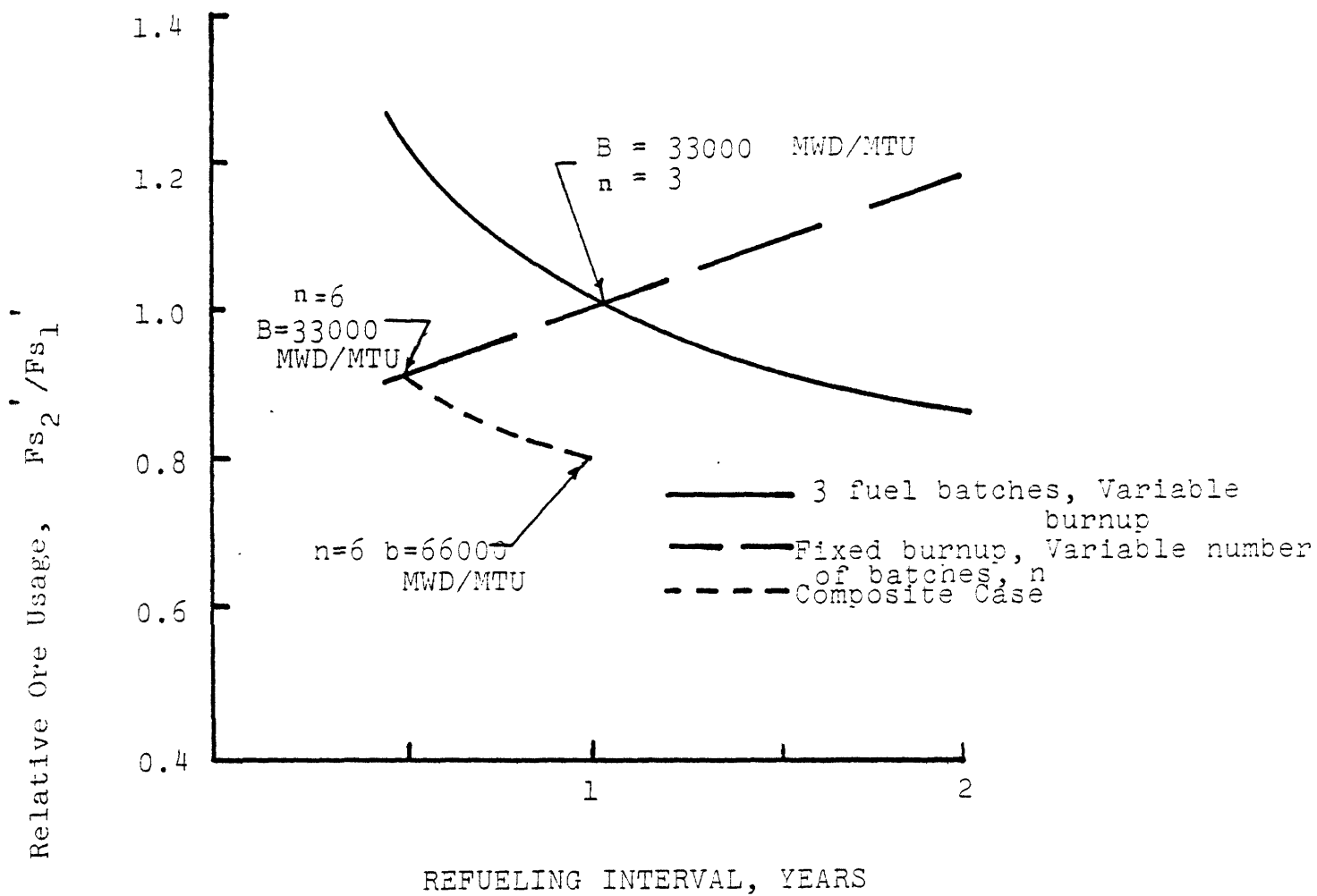


FIGURE 6.1

RELATIVE ORE USAGE AS A FUNCTION OF THE NUMBER OF CORE BATCHES AND BURNUP

found to be in good agreement with the results of the simple ore usage model. Thus extending the burnup lifetime of the fuel is the most straightforward way of obtaining rather sizeable ore savings (~20%); other design changes yield only modest savings. The utility of high burnup fuel is recognized and improvements are in prospect. Our decision to examine fuel having an average burnup of 66000 MWD/MTU does not imply, however, that this is an assured accomplishment. While low by FBR standards, it is not clear that solutions will be found to Zircaloy PCI interaction problems, internal chemical attack by fission products, or corrosion induced hydriding. Furthermore, reversion to stainless steel should this be employed, incurs an enrichment penalty which offsets the burnup gain.

6.5.5 Enhanced Reflector Design

In current PWR's the core is reflected by light water (containing soluble control poison) closely backed by a core shroud and barrel. These materials have high absorption cross sections which lead to large parasitic captures in the reflector, thus degrading the neutron economy. Replacing borated water by other materials (e.g., BeO) which have a lower absorption cross section could improve the neutron economy modestly, thus improving the ore utilization.

Three cases were analyzed, a standard 3 zone PWR with: (1) a borated H₂O reflector, (2) a pure BeO reflector, and (3) a depleted UO₂ (0.2w/o U-235) reflector. In case (2), a pure BeO reflector was used; no attempt was made to include the structural material, which will clad the BeO, or the borated water, which will cool the reflector. For case (3) it was assumed that the UO₂ (0.2w/o U-235) pellets were loaded into standard design fuel assemblies.

The ore savings was found for both cases (BeO reflector and depleted

UO₂ reflector) by reducing the reload enrichment such that the multiplication factor, K_{eff} , of the two changed cases were equal to that of the reference case at BOC. Depletion calculations were performed and it was found that the reactivity versus burnup slope was approximately the same for all three cases and the cycle lengths were also equal. The ore requirement for the BeO reflected reactor is reduced by 5.5% (relative to the borated H₂O reflected reactor). The ore requirement for the depleted UO₂ reflected reactor is not significantly lowered.

The 5% savings in ore (BeO) should be interpreted as an upper bound since no attempt was made to include in the analysis the structural material that will house the BeO. In addition, the BeO reflected reactor may have severe power peaking problems near the reflector-core interface such that the fuel management strategy may have to be changed. Aside from these problems, the ore utilization of PWR's may be modestly improved if BeO is used for the reflector.

6.5.6 Internally Heterogeneous Core (Simple Seed/Blanket)

Three similar axial seed and blanket cores were analyzed. The seed/blanket arrangement was obtained by segregating the seed and blanket material in a fuel pin; alternate layers of enriched fuel and blanket pellets were stacked in the fuel pin. The seed region contained slightly enriched UO₂ and the blanket region contained depleted UO₂ (0.2 w/o U²³⁵). Infinite medium calculations were performed for three different thicknesses of the blanket and seed region; however, the fissile loading for the three cases and the reference core was kept constant. It was found that the seed/blanket cores have slightly, but not significantly, longer reactivity-limited irradiation times (burnup) than the reference case. A larger reactivity contribution from fissile material production in the blanket was hoped for

to offset some of the reactivity loss due to burnup and fission product poisoning, but our results did not show this.

The calculations show that small ore savings result when PWR cores are loaded in a seed/blanket configuration. Since the simple seed/blanket cores did not yield significant reductions in enrichment requirements further analysis of this concept was dropped, and effort was focused on the more attractive prospects. It is quite possible, however, that other seed/blanket designs, in particular the radial seed/blanket configuration of the Shippingport PWR, might prove to have some attractive benefits for the once through fuel cycle. Additional work in this area may be of some interest.

6.5.7 Coastdown

We have looked at the use of coastdown in current large PWR's to extend the burnup life of the fuel. Simple models (analytical and numerical) were developed to analyze the relatively complex phenomena of coastdown. These models were compared with more exact calculations and the agreement was found to be good.

It was found that if one starts with a steady-state fuel cycle and keeps the reload composition fixed, use of coastdown to extend burnup an increment, ΔB^C , (either for a single cycle, or forever thereafter) results in a net ultimate burnup gain of $(\frac{2}{n+1})\Delta B^C$ for every coastdown, where n = number of fuel batches. Thus a three-batch PWR could gain $1/2 \Delta B^C$ for each cycle in which coastdown was applied. One cannot realize 100% of ΔB^C except for the batch reload case ($n=1$). The net burnup gain relation also shows that for cores with a large number of batches, the net burnup gain due to coastdown is small. Thus the stratagem of increasing core batch number,

shown to be advantageous in Section 6.5.4, will negate much of the incentive for coastdown. One should be careful not to ascribe the advantages of coastdown with a 3-batch core to the case of a 6-batch core, nor should the advantages of extended burnup be double counted.

The simple reactivity models developed in this work were used to analyze a typical coastdown scenario, in particular, the Maine Yankee PWR coasting at a rate of 0.604% of full power per day. It was found that modest ore savings can be obtained: for example if the reactor is coasted for 1000 MWD/MTU an ore savings of approximately 5% can be obtained, and further use of coastdown will increase the ore savings.

An economic analysis of coastdown showed that a broad optimum coastdown duration exists. This relatively broad minimum implies that considerable operational flexibility exists (i.e., when to terminate the coastdown) without adversely affecting the economics. The use of coastdown in PWR's is determined by the individual needs of the utility in question, and ore savings is only one input factor. It is interesting to note, however, that the duration of the economic optimum coastdown (at minimum cycle energy cost) can be roughly doubled without increasing the energy cost over that for the no-coastdown case. A government tax or regulatory policy might, therefore, be formulated to favor this extension to promote ore savings.

6.5.8 Use of Isotopically Separated Low σ_a Clad

The use of Laser Isotope Separation (LIS) processes to separate out the more highly absorbing isotopes in zircaloy and stainless steel cladding can improve the ore utilization by a small amount. In addition, stainless steel cladding prepared by this process might conceivably be used in high burnup core applications since the mechanical integrity of S.S. clad fuel

rods is better than for zircaloy clad fuel rods. This option is a long range option and commercial prospects are quite uncertain at this time. Reductions in U_3O_8 requirements resulting from this option are expected to be 5% or less: we calculated the 5% figure using LEOPARD assuming 100% reduction in σ_a , while reductions of 50% are probably all that could be achieved in practice.

6.5.9 Thorium in Uniform Lattices

A brief investigation was made of the use of Thorium in LWR's operating in the once-through fuel cycle. It was found by us and others [S-1], [C-5], and [W-1] that the use of ThO_2 in current LWR's required more U_3O_8 than current LWR's fueled with UO_2 . Furthermore, in uniform lattices the ore requirement increases monotonically as the Th-232/U-238 ratio increases. For this reason, it was concluded that ThO_2 should not be used in PWR's operating on the once-through fuel cycle. This study did not pursue this area (mixed oxide fuels) any further. We have also not examined the use of Thorium in seed/blanket configurations or in reflectors.

6.6 Conclusions

The major conclusion of this study is that reductions in ore usage of on the order of 30% (Table 6.1) are foreseeable relative to a current PWR operating on the once-through fuel cycle. Further points to be made are: (1) One of the most straightforward ways of improving uranium ore utilization is to increase the discharge burnup; ore savings on the order of 20% can be realized if this is combined with an increase in the number of batches in the core. (2) It is important to conduct all comparisons on an equivalent basis. For example, use of metal alloy fuel could appear to yield (false) advantages if it was not compared to a neutronically equivalent UO_2 lattice.

(3) It is important not to double count the advantages in summing individual improvements; for example, several schemes (power flattening, coastdown) are predicated on increasing burnup; if the ultimate limit is on time-integrated rather than local effects, then it may be immaterial as to how increased burnup is achieved, the net advantage depending only on total burnup. (4) Focusing on ore savings rather than near term fuel cycle economics may imply contradictory objectives between the individual utility fuel manager and national policy planners. Our analyses show a rough correspondence between minimizing ore usage and minimizing fuel cycle cost (as would be expected since ore usage over life is approaching 50% of projected lifetime fuel cycle costs), but it is important to keep in mind that individual changes would only be adopted when the economic incentive is generally perceived. (5) Some of the changes suggested for the once-through fuel cycle in Table 6.1 (but not increased burnup) would also save ore if applied to fuel recycle. (6) In order to implement many of these ore-saving design changes a significant research and development program would need to be carried out, particularly for high burnup fuel and isotopically separated cladding.

6.7 Recommendations

Although it is believed that the most promising approaches have now been scoped out, there is room for additional improvements: (1) Reduction of control poison requirements could lead to an additional ore savings of perhaps 15%. Simple fertile fuel reactivity control designs were investigated in this work but further analyses of this concept were dropped because the results were not promising. More exotic designs could be conceived and tested. (2) More advanced versions of a seed/blanket configuration might help ore usage, in particular, the radial seed/blanket

configuration of the Shippingport PWR, possibly using thorium in the seed, might prove to have some attractive benefits for the once-through fuel cycle.

(3) Analyses of each option in Table 6.1 with more attention to all pertinent details is in order. For example, attention must be paid to safety issues for these design changes such as xenon stability, LOCA, void and temperature coefficients of reactivity, and thermal-hydraulic margins.

(4) Analysis of a composite case incorporating all of the near term options in Table 6.1 is recommended. This analysis will determine the sensitivity of one design change to another, and demonstrate the extent to which the individual improvements are additive. (5) Considerable research and development work is needed in the area of the 6-batch high burnup cores; in particular, fuel behavior modeling is needed. (6) Fuel cycle economics studies are needed to define the circumstances under which utilities would find it attractive to adopt the various ore-saving steps studied here, and to show that the benefits justify the costs of the development programs in each area.

In brief, our basic conclusion is that through a combination of changes in operating procedures and design, the ore usage by PWR's (and inferentially for BWR's) operating on a once-through fuel cycle, could be reduced to a level roughly comparable with that for unmodified designs/practices with uranium and plutonium recycle. For policy planning purposes it may be important to know to what extent once-through optimization is a replacement for or a supplement to fuel recycle. This leads to our final recommendation, namely that the analysis reported here be repeated using fuel recycle to determine to what extent the ore savings of these two quite diverse approaches are additive.

APPENDIX A

ORE USAGE MODEL

In this appendix, relations useful for estimating the ore usage per MWe by a system of reactors growing at an annual rate of $r\%$ per year will be derived. An expression relating the system annual ore usage for a given design to the system annual ore usage for a reference case is developed below.

For large PWR cores with similar neutronic characteristics (same homogenized composition), the reactivity-limited burnup of discharged fuel at steady state can be correlated as a linear function of reload enrichment and the number of fuel batches in the core:

$$B = A(X - X_0) \left[\frac{2n}{n+1} \right] \quad (A.1)$$

where

B = average burnup, MWD/MTU

X_0 = Empirically determined (e.g. curve fit to LEOPARD output), approximately equal to BOL enrichment at which $k = 1$ with saturated Xe, Sm

X = BOL enrichment of a reload batch in steady state

n = number of fuel batches in the core.

As was shown in Section 3.5.3, Equation A.1 is a good approximation for very large PWR cores since the reactivity is a function of average fissile and poison concentration, and is insensitive to the moderate differences in spatial distribution encountered in situations of practical interest.

Thus, comparing a given design (2) to a reference case (1)

$$\frac{B_2}{B_1} = \left[\frac{\bar{X}_2 - X_0}{X_1 - X_0} \right] \left(\frac{n_2}{n_1} \right) \left(\frac{n_1 + 1}{n_2 + 1} \right) \quad (\text{A.2})$$

or

$$X = X + (X_1 - X_2) \left(\frac{B_2}{B_1} \right) \left(\frac{n_1}{n_2} \right) \left(\frac{n_2 + 1}{n_1 + 1} \right) \quad (\text{A.3})$$

For the once-through fuel cycle, ore usage per MWe is related to heavy metal inventory in a reload batch by:

$$F = 1.3 \frac{P}{E} \left(\frac{X - X_w}{X_f - X_w} \right), \text{ ST U}_3\text{O}_8/\text{MWe per batch} \quad (\text{A.4})$$

or

$$\left[\frac{F_2}{F_1} \right] = \left(\frac{E_2 P_2}{E_1 P_1} \right) \left[\frac{\bar{X}_2 - X_w}{X_1 - X_w} \right] \quad (\text{A.5})$$

where

P = batch heavy metal loading, MTHM

E = Electric power rating, MWe (weighed by the unit capacity factor)

F = yellowcake mined to fuel reactor, ST U₃O₈/MWe

X_w = enrichment plant tails composition

X_f = enrichment plant feed composition

we also have

$$P = 365 \frac{ET}{B\eta} = \frac{P_0}{n} \quad (\text{A.6})$$

where

η = thermal efficiency

T = refueling interval, years

P_0 = core heavy metal loading, MT

Combining Equations A.3, A.5 and A.6 yields

$$\frac{F_2}{F_1} = \left[\left(\frac{n_1}{n_2} \right) \left(\frac{X_0 - X_w}{X_1 - X_w} \right) + \left(\frac{E_2 T_2}{E_1 T_1} \right) \left(\frac{n_1}{n_2} \right) \left(\frac{n_2 + 1}{n_1 + 1} \right) \left(\frac{X_1 - X_0}{X_1 - X_w} \right) \right]$$

Annual ore usage by the reactor is given by the product of ore per batch, F , and batches per year, $1/T$:

$$\dot{F} = F/T \quad (\text{A.7})$$

Annual ore usage per MWe by a system of reactors growing at an annual rate of $r\%$ per year is:

$$F'_s = \frac{r}{100} FN + \dot{F}, \text{ ST } U_3O_8/\text{MWe-yr} \quad (\text{A.8})$$

or

$$F'_s = \frac{F}{T} \left[1 + \frac{r}{100} NT \right] \quad (\text{A.9})$$

where

N = equivalent number of reload batches in the initial startup core, approximately 2.2 for a 3-batch PWR core. Thus, to compare annual ore usage for two different designs the relative values are given by:

$$\frac{\begin{bmatrix} F'_2 \\ s_2 \\ F'_1 \\ s_1 \end{bmatrix}}{\begin{bmatrix} F'_2 \\ s_2 \\ F'_1 \\ s_1 \end{bmatrix}} = \frac{\begin{bmatrix} 1 + \frac{r}{100} N_2 T_2 \\ 1 + \frac{r}{100} N_1 T_1 \end{bmatrix}}{\begin{bmatrix} 1 + \frac{r}{100} N_2 T_2 \\ 1 + \frac{r}{100} N_1 T_1 \end{bmatrix}} \left[\frac{(X_1 - X_0) \binom{n_1}{n_2} \binom{n_2 + 1}{n_1 + 1}}{(X_1 - X_w) \binom{n_1}{n_2} \binom{n_2 + 1}{n_1 + 1}} + \frac{(X_0 - X_w)}{(X_1 - X_w)} \binom{n_1}{n_2} \frac{E_1 T_1}{E_2 T_2} \right] \quad (A.10)$$

This equation provides the capability of computing ore savings as a function of changes in core design and fuel management strategy.

The parameter N can also be determined using the linear reactivity model. We repeat here without proof the relation derived by Garel [G-]:

$$N = \frac{\left[\left(\frac{n+1}{2} \right) X_p + \left(\frac{n-1}{2} \right) X_0 - nX_w \right]}{X_p - X_w} \quad (A.11)$$

where

n = number of fuel batches in the core

X_p = BOL enrichment of a reload batch at steady state

X₀ = BOL enrichment at which k = 1 with equilibrium Xe and Sm

X_w = enrichment plant tails composition

APPENDIX B

MASS PENALTY DUE TO POWER FLATTENING

In this appendix, relations useful for estimating the mass penalty incurred when the core is zone loaded to achieve spatially uniform power profiles will be derived. An expression relating the enrichment distribution, $\epsilon(x)$, to core neutronic properties is developed below.

The one group diffusion equation, for a homogeneous critical one-region slab core is

$$-D\nabla^2\phi + \Sigma_a\phi = \nu\Sigma_f\phi \tag{B.1}$$

where

D is the diffusion coefficient,

Σ_f is the macroscopic fission cross section,

Σ_a is the macroscopic absorption cross section, and

ν is the neutron yield per fission.

For an axially power-flattened core, one has:

$$\nu\Sigma_f\phi \equiv A = \text{constant} \tag{B.2}$$

Defining the fertile-to-fissile fission ratio, δ_{28} , as

$$\delta_{28} = \frac{\Sigma_f^{28}}{\Sigma_f^{25}} \tag{B.3}$$

which will be approximated as a spatially invariant constant here,

one has

$$A = v\Sigma_f^{25}(1 + \delta^{28})\epsilon(x)\phi \quad (B.4)$$

where $\epsilon(x)$ is the enrichment of U^{235} as a function of axial position.

Separating the absorption term, Σ_a , into fertile absorption, Σ_a^{28} , fissile absorption, Σ_a^{25} , and non-fuel absorption, Σ_a^p , and radial leakage, $D\text{Br}^2$, one has:

$$\Sigma_a = \Sigma_a^{28}(1 - \epsilon(x)) + \Sigma_a^p + \Sigma_a^{25}\epsilon(x) + D\text{Br}^2 \quad (B.5)$$

Substituting Equations B.4 and B.5 into Equation B.1 there results,

$$\frac{d^2\phi}{dx^2} - \frac{1}{L^2}\phi = -\frac{A}{D} - \frac{Q}{D} \quad (B.6)$$

where

$$L^2 = \frac{D}{\Sigma_a^{28} + \Sigma_a^p + D\text{Br}^2} \quad (B.7)$$

and

$$Q = \frac{(\Sigma_a^{28} - \Sigma_a^{25})A}{v\Sigma_f^{25}(1 + \delta^{28})} \quad (B.8)$$

The general solution for Equation B.6 is:

$$\phi(x) = C \cosh(x/L) + \frac{L^2 A}{D} + \frac{L^2 Q}{D} \quad (B.9)$$

where C is a constant to be determined from the boundary conditions.

Applying the boundary condition,

$$\phi(H + d) = 0 \quad (\text{B.10})$$

where d is the linear extrapolation distance, one finds the neutron flux as a function of axial position to be

$$\phi(x) = \frac{L^2}{D} (A + Q) \left[1 - \frac{\cosh(x/L)}{\cosh\left(\frac{H+d}{L}\right)} \right] \quad (\text{B.11})$$

Substituting Equation B.11 into Equation B.4; the enrichment distribution for an axially power-flattened core as

$$\epsilon(x) = \frac{A D}{\nu \Sigma_f^{25} (1 + \delta^{28}) L^2 (A + Q) \left[1 - \frac{\cosh(x/L)}{\cosh\left(\frac{H+d}{L}\right)} \right]} \quad (\text{B.12})$$

For the case of uniform fuel loading, Equation B.1 can be rearranged as:

$$\nabla^2 \phi + B^2 \phi = 0 \quad (\text{B.13})$$

where

$$B^2 = B_r^2 + B_z^2 = \frac{\nu \Sigma_f - \Sigma_a}{D} \quad (\text{B.14})$$

Substituting Equations B.3, B.4 and B.5 into Equation B.14 and solving for $\epsilon(\text{uniform})$, the U^{235} enrichment in the homogeneous core is

$$\epsilon(\text{uniform}) = \frac{DB^2 + \Sigma_a^{25} + \Sigma_a^P}{\nu\Sigma_a^{25}(1 + \delta^{28}) + (\Sigma_a^{25} - \Sigma_a^{28})} \quad (\text{B.15})$$

The ratio of the enrichment distribution for the zone loaded core to the enrichment for the uniform core is found by dividing Equation B.15 into Equation B.12.

$$\frac{\epsilon(x)}{\epsilon(\text{uniform})} = \frac{\Sigma_a^{28} + \Sigma_a^P + DBr^2}{DB^2 + \Sigma_a^{28} + \Sigma_a^P} \frac{1}{\left[1 - \frac{\cosh(x/L)}{\cosh\left(\frac{H+d}{L}\right)} \right]} \quad (\text{B.16})$$

The average enrichment of the zoned loaded core is found by integrating Equation B.16 over the volume, that is:

$$\frac{\bar{\epsilon}}{\epsilon(\text{uniform})} = K \frac{1}{H} \int_0^H \frac{dx}{1 - (\cosh(x/L)/\cosh\left(\frac{H+d}{L}\right))} \quad (\text{B.17})$$

where

$$K = \frac{\Sigma_a^{28} + \Sigma_a^P + DBr^2}{DB^2 + \Sigma_a^{28} + \Sigma_a^P} \quad (\text{B.18})$$

Integrating Equation B.17 one gets

$$\frac{\bar{\epsilon}}{\epsilon(\text{uniform})} = \frac{K}{H} \frac{2L}{\sqrt{1-C^2}} \text{arc coth} \frac{(1-C) \coth\left(\frac{1}{2} \frac{H}{L}\right)}{\sqrt{1-C^2}} \quad (\text{B.19})$$

where

$$C = \frac{1}{\cosh\left(\frac{H+d}{L}\right)} \quad (\text{B.20})$$

The right hand side (R.H.S.) of Equation B.19 is cumbersome as it stands. An approximation to Equation B.19 will be derived below. First, the function C, can be approximated by

$$C \approx 2 e^{-\frac{H+d}{L}} \quad (B.21)$$

since the argument of the cosh function is much greater than one. Next, a Taylor Series expansion is performed on the R.H.S. of Equation B.19;

$$f(x-h) \approx f(x) - hf'(x) + \frac{h^2}{2!} f''(x) - \frac{h^3}{3!} f'''(x) + \dots \quad (B.22)$$

where

$$f(x) = \text{arc coth}(x) \quad (B.23)$$

$$x = \text{coth}(1/2 H/L) \quad (B.24)$$

$$h = C \text{coth}(1/2 H/L) \quad (B.25)$$

Substituting Equation B.21 into Equation B.19, and evaluating Equation B.22 one finds

$$\frac{\bar{\epsilon}}{\epsilon(\text{uniform})} = K \left[1 + \frac{L}{H} [e^{-d/L} + 1/2 e^{-2d/L} + 1/3 e^{-3d/L} + \dots] \right] \quad (B.26)$$

Noting that,

$$\ln(1-x) = -x - \frac{x^2}{2} - \frac{x^3}{3} - \frac{x^4}{4} \dots, \quad (B.27)$$

Equation B.26 finally becomes:

$$\frac{\bar{\epsilon}}{\epsilon(\text{uniform})} = K \left[1 - \frac{L}{H} \ln(1 - e^{-d/L}) \right] \quad (\text{B.28})$$

The above relation is the equation needed to calculate the mass penalty incurred when the power distribution is changed from the less desirable chopped cosine shape to the more desirable axially flat power distribution.

Starting from Equation B.1, an equation similar to Equation B.28 can be derived for a spherical reactor having a radius, R. One finds,

$$\frac{\bar{\epsilon}}{\epsilon(\text{uniform})} = K \frac{1}{\frac{4}{3}\pi R^3} \int_0^R \frac{4\pi r^2 dr}{[1 - C \sinh(r/L)/r]} \quad (\text{B.29})$$

where

$$K = \frac{\Sigma_a^{28} + \Sigma_a^P}{DB^2 + \Sigma_a^{28} + \Sigma_a^P} \quad (\text{B.30})$$

$$C = \frac{R + \delta}{\sinh\left(\frac{R+d}{L}\right)} \quad (\text{B.31})$$

(The diffusion theory parameters in Equation B.30 and B.31 have been defined previously.) The solution for Equation B.29 must be evaluated numerically since the integral does not have a closed form solution like Equation B.17. An equation similar to Equation B.28 for a cylindrical reactor can be found in Reference [T-2].

APPENDIX C

Xe AND Pa MODELS TO CALCULATE REACTIVITY EFFECTS DURING COASTDOWN

In this Appendix, relations will be developed which are useful for estimating the positive reactivity gain from reduced xenon and protactinium concentrations when power coastdown is used. Expressions relating the reactivity changes for Xe and for Pa to the power level are developed below.

C.1 Xenon

For a reactor that has been operated at a constant flux level for a long time, the asymptotic (steady-state) concentration of Xe¹³⁵ is

$$X_{e}^{\infty} = \frac{\gamma \Sigma_f \phi}{\lambda_{Xe} + \sigma_{Xe} \phi} \quad [C.1]$$

γ = average fission yield of the 135 fission product chain

λ_{Xe} = decay constant of Xe, sec⁻¹

Σ_f = macroscopic core fission cross section, cm⁻¹

σ_{Xe} = microscopic absorption cross section for Xe-135, cm²

ϕ = flux level, neutrons/cm²-sec

The xenon poisoning, XP, of a reactor is defined as the ratio of the macroscopic Xe absorption cross section, Σ_{Xe} , to the fuel absorption cross section, Σ^f , thus

$$XP = \frac{\Sigma_{Xe}}{\Sigma^f} = \frac{X_{e} \sigma_{Xe}}{\Sigma^f} \gamma \quad [C.2]$$

Substituting Equation [C.1] into [C.2]

$$XP = \frac{\sigma_{Xe} \gamma \Sigma_f \phi}{(\lambda_{Xe} + \sigma_{Xe} \phi)} \quad [C.3]$$

The thermal utilization in a reactor without Xe, f , and a reactor with Xe, f' , is

$$f = \frac{\Sigma^f}{\Sigma^f + \Sigma_m} \quad \text{and} \quad f' = \frac{\Sigma^f}{\Sigma^f + \Sigma_m + \Sigma_{Xe}} \quad [C.4]$$

where

Σ_m = macroscopic absorption cross section for the moderator and structure, cm^{-1} .

Of the factors (e.g., leakage, etc.) which make up the multiplication factor, K_{eff} , the thermal utilization is essentially the only one changed by the buildup of Xe; the leakage of neutrons will change to a small extent, but in most large power reactors the thermal nonleakage probability is very close to unity. The reactivity due to Xe poisoning is

$$P = \frac{k' - k}{k^1} = \frac{f' - f}{f'} \quad [C.5]$$

Substituting Equations [C.4] and [C.2] into [C.3] one has

$$P = \frac{-XP}{1+y} \quad [C.6]$$

where

$$y = \frac{\Sigma_m}{\Sigma^f}$$

The fractional change in reactivity due to coastdown (reduction in power level) is defined as the difference between the Xe reactivity at 100% power and the Xe reactivity at reduced power divided by the Xe reactivity at full power, $P_{100\%}$, thus,

$$\frac{\Delta\rho}{\rho_{100\%}} = \frac{XP' - XP}{XP} \quad [C.7]$$

If the Xe reactivity at full power is known, Equations [C.7] and [C.3] can calculate the positive reactivity insertion when the reactor is coasted since XP is defined in terms of the flux, ϕ , and the flux is proportional to the power level. In addition, the duration of coastdown permitted by reduced

Xe levels may be inferred from $\Delta\rho$ since Equation [C.7] is a simple function of power decrease, hence one can easily interpolate and extrapolate case histories.

Substituting Equation [C.3] into [C.7] and noting that the power, P, is proportional to the flux level, ϕ , one finds

$$\frac{\Delta\rho}{\rho_{100\%}} = \frac{\lambda_{Xe}/\phi_{100}}{\frac{\lambda_{Xe}}{\phi_{100\%}} + \sigma_{Xe} \frac{P'}{P}} \left(\frac{\Delta P}{P}\right) \quad [C.8]$$

where the prime indicates a reduced power level.

If the Xe reactivity at full power is known, Equation [C.8] can calculate the positive reactivity insertion when the reactor is coasted since $\Delta\rho$ is a simple function of power decrease. In addition, the duration of coastdown permitted by reduced Xe levels may be inferred from $\Delta\rho$, hence one can easily interpolate and extrapolate coastdown scenarios.

C.2 Protactinium

A positive reactivity insertion occurs when ThO_2/UO_2 fueled reactors that have been operated at full power are coasted down. This is due to the fact that at low power levels there are less parasitic captures in Pa and more fissile U^{233} can be produced. A relationship is developed below to estimate the positive reactivity insertion as a function of power level.

If a ThO_2/UO_2 reactor has been operated for a long time, typically one year or longer, it can be shown that the rate of production of U^{233} is equal to the rate of destruction of U^{233} ; thus,

$$\lambda_{13} N_{13} = N_{23} \sigma_a^{23} \phi \quad [C.9]$$

where

- λ_j = decay constant for the j^{th} isotope, sec^{-1}
 N_j = atom density for the j^{th} isotope, atoms/cm^3
 σ_a^j = microscopic absorption cross section for the j^{th} isotope, cm^2
 ϕ = neutron flux, $\text{neutrons/cm}^2\text{-sec}$.

Similarly, in the asymptotic limit, the rate of production of Pa^{13} is equal to the rate of destruction of Pa^{13} ; thus,

$$\frac{N_{13}}{N_{02}} = \frac{\sigma_{02}\phi}{\lambda_{13} + \sigma_{13}\phi} \approx \frac{\sigma_{02}\phi}{\lambda} \quad [\text{C.10}]$$

Substituting Equation [C.9] into [C.10] and rearranging

$$\frac{N_{23}}{N_{02}} = \frac{\lambda_{13} \sigma_{02}}{(\lambda_{13} + \sigma_{13}\phi)} \frac{1}{\sigma_a^{23}} \quad [\text{C.11}]$$

or

$$\frac{N_{23}}{N_{02}} \approx \left(\frac{\sigma_{02}}{\sigma_a^{23}} \right) \left(\frac{1 - \sigma_{13}\phi}{\lambda_{13}} \right)$$

If the change in N_{23} concentration is proportional to the flux level (power level) of the reactor then

$$\frac{\Delta N_{23}}{N_{02}} \approx \frac{\sigma_{13}\phi}{\lambda_{13}} \left(\frac{\Delta\phi}{\phi} \right) \left(\frac{\sigma_{02}}{\sigma_a^{23}} \right) \quad [\text{C.12}]$$

$$\frac{\Delta N_{23}}{N_{02}} \approx \frac{\sigma_{13}\phi}{\lambda_{13}} \left(\frac{\Delta P}{P} \right) \left(\frac{\sigma_{02}}{\sigma_a^{23}} \right) \quad [\text{C.12}]$$

The reactivity, ρ_u , associated with the change in U^{23} concentration can be calculated by

$$\rho_u = \frac{\Delta(v\Sigma_f - \Sigma_a)}{v\Sigma_f} = \frac{(v\sigma_f - \sigma_a)\Delta N_{23}}{v\Sigma_f} \quad [\text{C.13}]$$

Substituting Equation [C.12] into Equation [C.13]

$$\rho_u = \frac{(\eta-1)}{\nu\Sigma_f} N_{02} \left(\frac{\sigma_{13}^{\phi}}{\lambda_{13}} \right) \frac{\Delta P}{P} \sigma_{02} \quad [C.14]$$

The reactivity, ρ_p , associated with the change in Pa¹³ concentration can be calculated by

$$\rho_p = \frac{\Delta N_{13} \sigma_{13}}{\nu\Sigma_f} \quad [C.15]$$

or

$$\rho_p \approx \frac{\sigma_{02} N_{02}}{\lambda_{13}} \frac{\Delta\phi}{\nu\Sigma_f} \sigma_{13}$$

Taking the ratio of Equation [C.15] to [C.14] one gets

$$\frac{\rho_u}{\rho_p} = (\eta^{23} - 1) \quad [C.16]$$

Since the value of η is approximately 2, Equation [C.16] shows that the reactivity gains due to extra bred U²³ and fewer Pa captures are roughly equal.

Noting that

$$\nu\Sigma_f = \eta\Sigma_a \quad [C.17]$$

and

$$\frac{\Delta\phi}{\phi} = \frac{\Delta P}{P}, \quad [C.18]$$

Equation [C.15] becomes

$$\rho_p = \frac{1}{\eta} \frac{N_{13} \sigma_{13}}{N_f \sigma_{af}} \frac{\Delta P}{P} \quad [C.19]$$

where the subscript "f" refers to the fissile isotopes. The total reactivity change is just the sum of ρ_p and ρ_u ; thus

$$\rho = \rho_p(\eta-1) + \rho_p = \eta \rho_p \quad [C.20]$$

Substituting Equation [C.19] into [C.20] one gets

$$\rho = \left(\frac{N_{13} \sigma_{13}}{N_f \sigma_{af}} \right) \frac{\Delta P}{P} = \rho_{100} \frac{\Delta P}{P} \quad [C.21]$$

where

$$\rho_{100} = \frac{N_{13}\sigma_{13}}{N_f\sigma_{af}}$$

The above equation can be used to calculate the positive reactivity insertion (as a function of power level) due to reduced Pa burnout when ThO₂/UO₂ fueled reactors are coasted at E.O.C., since the extra available reactivity is a linear function of power decrease; hence one can easily interpolate and extrapolate case histories.

APPENDIX D

ADDITIONAL BURNUP GAIN DUE TO COASTDOWN

In this Appendix relations useful for estimating the net incremental burnup gain during coastdown for each successive cycle will be developed. For example, in a one-batch core, the nuclear fuel is burned an amount, ΔB MWD/MTU, and then is coasted for an amount, B^C MWD/MTU; the net burnup gain is B^C . However, in a multi-batch core the net burnup gain is not B^C but rather some fraction of B^C ; this is due to the fact that in the cycle following coastdown ($\frac{n-1}{n}$) of the fuel is more depleted than it would have been had refueling occurred when full power end-of-life was reached. Because of this the burnup histories of subsequent cycles are adversely affected (shorter full-power cycle lengths are experienced - assuming of course that reload fuel enrichment and batch size are held constant). An expression relating the net burnup gain as a function of batch size and the incremental burnup due to coastdown in each cycle is developed below.

Using the linear reactivity model [G-1], the discharge burnup (steady-state), B_{Dis} , is shown to be

$$B_{Dis} = \left(\frac{2^n}{n+1}\right) \bar{B} \quad [D.1]$$

where

n = number of fuel batches in the core

\bar{B} = reactivity limited discharge burnup of a one-batch core having the same reload enrichment as the multi-batch core.

Assuming that the power sharing among batches is constant (flat power distribution) then the burnup for each batch at EOC is found to be

$$B_1 = \left(\frac{2n}{n+1}\right) \bar{B} \quad [D.2]$$

$$B_2 = \left(\frac{2n}{n+1}\right) \left(\frac{n-1}{n}\right) \bar{B}$$

$$B_{m+1} = \left(\frac{2n}{n+1}\right) \left(\frac{n-m}{n}\right) \bar{B} \quad m=1,2,\dots,(n-1)$$

$$B_n = \left(\frac{2n}{n+1}\right) \left(\frac{1}{n}\right) \bar{B}$$

In order to simplify the discussion, let us consider a 2-batch core; the burnup for each batch at EOC is then

$$B_1 = \left(\frac{2n}{n+1}\right) \bar{B} = \frac{4}{3} \bar{B} \quad [D.3]$$

$$B_2 = \left(\frac{2n}{n+1}\right) \left(\frac{n-1}{n}\right) \bar{B} = \frac{4}{3} \cdot \frac{1}{2} \bar{B}$$

At EOC the reactor is coasted an amount ΔB^C (for this one cycle only), therefore, the batch burnup after the coastdown is

$$B_1 = \left(\frac{2n}{n+1}\right) \bar{B} + \Delta B^C \quad [D.4]$$

$$B_2 = \left(\frac{2n}{n+1}\right) \left(\frac{n-1}{n}\right) \bar{B} + \Delta B^C$$

Fuel lot number 1 is removed and fresh fuel is loaded into the reactor.

The BOC burnup of each batch is

$$B_2 = \left(\frac{2n}{n+1}\right) \left(\frac{n-1}{n}\right) B + \Delta B^C$$

$$B_3 = 0 \quad [D.5]$$

and the batch average BOC burnup, $\bar{B}_2(\text{BOC})$, is

$$\bar{B}_2(\text{BOC}) = \left(\frac{n-1}{n+1}\right) B + \frac{\Delta B^C}{n}$$

Assuming that the batch average EOC burnup, \bar{B} , is a constant (see Appendix A)

then

$$\bar{B} = \left(\frac{n-1}{n+1}\right) \bar{B} + \frac{\Delta B^c}{n} + \Delta B_2 \quad [D.6]$$

or

$$\Delta B_2 = \left(\frac{2}{n+1}\right) \bar{B} - \frac{\Delta B^c}{n}$$

where

ΔB = burnup increment for the cycle.

The EOL batch burnup is just the BOL batch burnup plus ΔB

$$\begin{aligned} B_2 &= \left(\frac{2n}{n+1}\right) \bar{B} + \left(\frac{n-1}{n}\right) \Delta B^c \\ B_3 &= \left(\frac{2n}{n+1}\right) \left(\frac{n-1}{n}\right) B - \frac{\Delta B^c}{n} \end{aligned} \quad [D.7]$$

Again the reactor is refueled and the batch average BOL burnup is found to be

$$\bar{B}_3(\text{BOL}) = \left(\frac{n-1}{n+1}\right) B - \frac{\Delta B^c}{2} \quad [D.8]$$

The burnup increment for this cycle is found to be

$$\Delta B_3 = \left(\frac{2}{n+1}\right) B + \frac{\Delta B^c}{2} \quad [D.9]$$

If the above procedure is repeated many times, one finds that the net burnup gain from coastdown (the sum of all B^c terms from Equations [D.4], [D.6], D.9], etc.) is

$$\Delta B_{\text{net}} = \Delta B^c \left(1 - \frac{1}{n} + \frac{1}{n^2} - \frac{1}{n^3} + \dots\right) \quad [D.10]$$

Noting that

$$\sum_{n=0}^{\infty} \left(\frac{-1}{k}\right)^n = \frac{k}{k+1} \quad [D.11]$$

Equation [D.10] now becomes

$$\Delta B_{\text{net}} = \left(\frac{n}{n+1}\right) \Delta B^c \quad [D.12]$$

or since $n=2$ for this case, $\Delta B_{net} = \frac{2}{3} \Delta B^C$. If one assumes that the reactor is coasted after each cycle, by using the above assumptions and procedures, a net ultimate burnup gain of

$$\Delta B_{net} = \frac{2}{3} \Delta B_1^C + \frac{2}{3} \Delta B_2^C + \frac{2}{3} \Delta B_3^C + \dots \quad [D.13]$$

can be achieved.

The above procedures can be extended to cores having more batches but a simple solution similar to Equation [D.11] has not been found. Table [D.1] summarizes the burnup gain as a function of the number of batches in the core. When each of the series is evaluated, one can empirically find the relationship between the net burnup gain, the batch size, n , and the incremental coastdown burnup, ΔB^C , to be

$$\Delta B_{net} = \frac{2}{n+1} \Delta B^C \quad [D.14]$$

If the reactor is coasted after each cycle, then

$$\Delta B_{net} = \sum_j \frac{2}{n+1} \Delta B_j^C \quad [D.15]$$

Equation [D.15] shows that if one starts with a steady-state fuel cycle and keeps the reload composition fixed, use of coastdown to extend burnup by an increment ΔB^C (either for a single cycle, or forever thereafter) results in a net ultimate burnup gain of $(\frac{2}{n+1}) \Delta B^C$ for every coastdown. Thus a three-batch PWR could gain $1/2 \Delta B^C$ for each cycle in which coastdown was applied. One cannot realize 100% of ΔB^C (except for the batch reload case, $n=1$); and as $n \rightarrow \infty$ no net gain results (e.g., online refueling negates coastdown - as in CANDU reactors for example).

Equation [D.13] could also have been derived in a more straightforward manner if one assumed that the coastdown burnup for each cycle is kept fixed. The simplified derivation is given below. Assume that the power sharing

TABLE D.1

NET BURNUP GAIN DUE TO COASTDOWN

CYCLES FOLLOWING COASTDOWN

BATCHES/CORE	(1)	(2)	(3)	(4)	(5)	(6)	(7)
n=1 ΔB^C (1)							
n=2 ΔB^C (1 -	$\frac{1}{n}$	$+\frac{1}{n^2}$	$-\frac{1}{n^3}$	$+\frac{1}{n^4}$	$-\frac{1}{n^5}$	$+\frac{1}{n^6}$	$-\frac{1}{n^7}$
n=3 ΔB^C (1 -	$(\frac{n-1}{n})$	$+\frac{1}{n^2}$	$+\frac{(n+1)}{n^3}$	$-(\frac{3n+2}{n^4})$	$+\frac{(n^2-5n-4)}{n^5}$	$+\frac{(5n^2-8n-8)}{n^6}$	$-(\frac{n^3-15n^2+12n+16}{n^7})$
n=4 ΔB^C (1 -	$(\frac{n-1}{n})$	$+\frac{1}{n^2}$	$+\frac{(n+1)}{n^3}$	$+\frac{(n+1)^2}{n^4}$	$-(\frac{6n^2+8n+3}{n^5})$	$-(\frac{3n^3-13n^2-22n-9}{n^6})$	$-(\frac{n^4-19n^3+24n^2+60n+27}{n^7})$
n=5 ΔB^C (1 -	$(\frac{n-1}{n})$	$+\frac{1}{n^2}$	$+\frac{(n+1)}{n^3}$	$+\frac{(n+1)^2}{n^4}$	$+\frac{(n+1)^3}{n^5}$	$-(\frac{10n^3+20n^2+15n+4}{n^6})$	$-(\frac{6n^4-26n^3-69n^2-57n-16}{n^7})$
n=6 ΔB^C (1 -	$(\frac{n-1}{n})$	$+\frac{1}{n}$	$+\frac{(n+1)}{n}$	$+\frac{(n+1)^2}{n^4}$	$+\frac{(n+1)^3}{n^5}$	$+\frac{(n+1)^4}{n^5}$	$-(\frac{15n^4+42n^3+73n^2+26n+5}{n^7})$

among batches is equal and the reactor is coasted an amount ΔB^C after each cycle (constant coastdown burnup). Let

X = new equilibrium full power cycle burnup length

\bar{B} = equilibrium full power batch burnup without coastdown.

The burnups by batch (n batch core) are found to be

$$B_1 = X \quad [D.15]$$

$$B_2 = 2X + \Delta B^C$$

$$B_3 = 3X + 2\Delta B^C$$

$$B_n = nX + (n-1) \Delta B^C$$

Noting that

$$\sum_{n=1}^k n = \frac{(k+1)k}{2}, \quad [D.16]$$

the batch average burnup, \bar{B}_a , is

$$\bar{B}_a = \frac{1}{n} \left[X \frac{(1+n)n}{2} + \Delta B^C \frac{(1+n-1)(n-1)}{2} \right] \quad [D.17]$$

But this must be equal to \bar{B} , the equilibrium full power batch burnup without coastdown.

$$\bar{B} = \bar{B}_a. \quad [D.18]$$

Using Equations [D.17] and [D.18] and rearranging one finds

$$X = \left[\frac{2}{n+1} \right] \bar{B} - \left(\frac{n-1}{n+1} \right) \Delta B^C \quad [D.19]$$

The total cycle length, B_T , is

$$B_T = X + \Delta B^C \quad [D.20]$$

or

$$B_T = \left(\frac{2}{n+1} \right) \bar{B} + \left(\frac{2}{n+1} \right) \Delta B^C \quad [D.21]$$

From Equation [D.21] one finds that the net burnup gain due to coastdown is

$$\Delta B \text{ net} = \left(\frac{2}{n+1}\right) \Delta B^c, \quad [\text{D.22}]$$

which is the same as Equation [D.14]. Note that ΔB is the gain per cycle; the added burnup in a discharged fuel batch is just n times ΔB .

APPENDIX E

THE EFFECT OF CORE POWER DENSITY ON FUEL CYCLE ECONOMICS

As discussed in the main body of the text, for a once-through fuel cycle, ore utilization is unaffected by core power density so long as discharge burnup is held constant. There is, however, a slight economic incentive to log the burnup in the shortest interval possible. The following simple example illustrates this point.

Consider two cores, one having twice the mean power density, the same total thermal rating, the same discharge burnup, and half the heavy metal loading of the other. Let all revenues for a given batch of fuel be credited at the midpoint of the irradiation period; and front end and back end transactions will each be represented by a single composite transaction. A present worth balance can be performed treating the fuel as an expensed rather than a depreciated entity. None of these simplifications will compromise the effect to be illustrated.

Figure E.1 shows the cash flow diagrams for representative batches in the two cores for the specific example of a 4 year irradiation period. Thus we have for the fuel cycle costs (e.g. mills/kwhr)

low power density

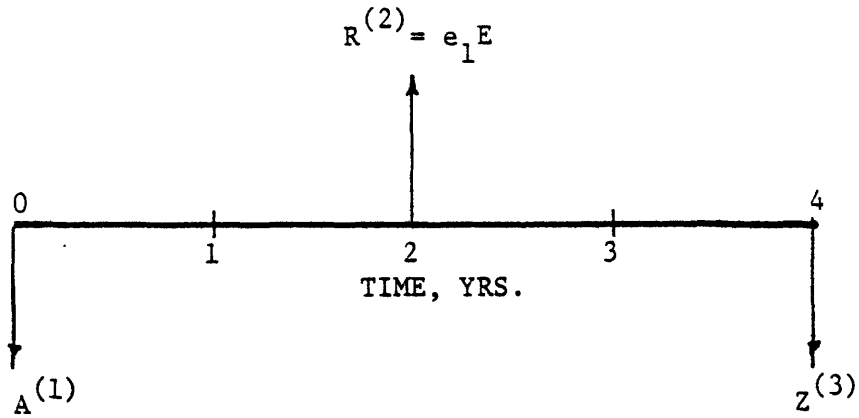
$$e_1 = \frac{A + Z (P/F, X, 4)}{E(P/F, X, 2)} \quad (E.1)$$

high power density

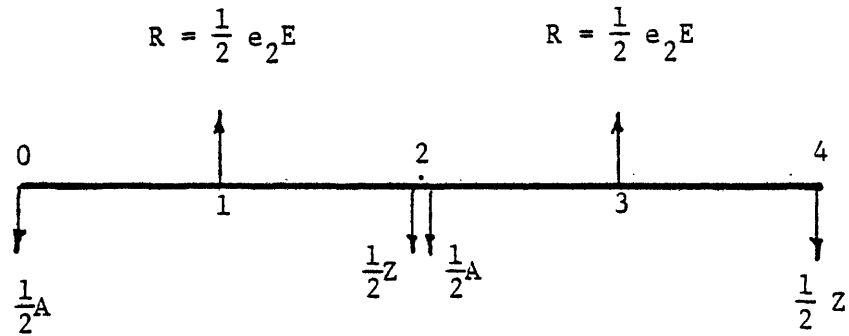
$$e_2 = \frac{A[1 + (P/F, X, 2)] + Z[(P/F, X, 2) + (P/F, X, 4)]}{E[(P/F, X, 1) + (P/F, X, 3)]} \quad (E.2)$$

where

LOW POWER DENSITY: ONE FUEL BATCH



HIGH POWER DENSITY: TWO FUEL BATCHES



- (1) Head end transaction
- (2) Revenue from sale of electrical energy, E(kwhr), at a levelized cost of e (mills/hr)
- (3) Tail end transaction

FIGURE E.1 CASH FLOW DIAGRAMS: FOR REPRESENTATIVE EXAMPLE

(P/F,X,N) = present worth factor

X = discount rate, %/yr

N = number of interest periods, yrs

Substituting the representative discount rate, X = 10% yr, and evaluating the present worth factors, gives

$$e_1 = 1.20999 \frac{A}{E} + 0.82645 \frac{Z}{E} \quad (E.3)$$

$$e_2 = 1.10000 \frac{A}{E} + 0.90909 \frac{Z}{E} \quad (E.4)$$

Since the head end transactions, A, (ore purchase, enrichment, fabrication) are larger in magnitude than back end transaction, Z, case 2, the high power density core, will have the lowest fuel cycle cost.

In general the advantage of high burnup rate (at constant total burnup) will be small. Even in the extreme examples above in which the burnup rate was doubled, a maximum advantage of around 10% is achieved. In practice, when one is likely to be dealing with burnup rate differences on the order of 10%, and when back end costs are not negligible (particularly true for the once-through fuel cycle which involves whole-assembly disposal and no offsetting credits), differences in fuel cycle costs are likely to be much less than 1%. Indeed, since increasing the burnup rate at constant total batch burnup requires more refueling shutdowns in the same calendar interval, the high power density case may actually turn out to be more expensive in the long run.

For the above reasons we have not assigned any particular merit to achieving high power densities in the present work except as it may

facilitate extending total burnup. Conversely, lower power densities, as might be characteristic, for example, of seed/blanket cores, would not be a serious economic penalty if total thermal output could be maintained, and could prove advantageous if their reactivity lifetime were inherently longer than homogeneous cores.

APPENDIX F

ALTERNATE ECONOMICS MODEL FOR COASTDOWN

The total cost of electric energy may be expressed as a linear combination of two terms each weighted by their appropriate fractional energy contribution: corresponding to energy generated by the nuclear reactor, and replacement energy purchased from another source. Thus the total cost, e_T , is

$$e_T = \frac{e_n E_n}{E_T} + \frac{E_R e_R}{E_T} \quad [F.1]$$

where

e_n = cost of energy generated by the reactor, mills/kwhr(e)

e_R = replacement energy cost, mills/kwhr(e)

E_R = replacement energy (includes replacement for coastdown, refueling, and forced outages), kwhr(e)

E_n = energy generated by the reactor in one cycle, kwhr(e)

E_T = total energy produced by the "utility" (sum of E_n and E_R), kwhr(e)

The nuclear-electric cost, e_n , can be further broken down into three cost components,

$$e_n = \frac{1000}{8766L} \left[\left(\frac{\phi I}{K} \right) + \left(\frac{O}{K} \right) \right] + e_f \quad [F.2]$$

where

L = capacity factor

K = electric rating of the reactor, kw(e)

ϕ = annual fixed charge rate, yr⁻¹

I = initial cost of the plant, \$

O = annual cost for operation, maintenance, and general expenses, \$/yr.

e_f = levelized nuclear fuel cycle cost, mills/kwhr(e).

The terms in the bracket in Equation F.2 can be considered to be a fixed cost (\$/kw(e)-yr); hence, Equation F.2 now becomes

$$e_n = \frac{C}{L} + e_f \quad [F.3]$$

where

$$C = \frac{1000}{8766} \left[\frac{\phi I}{K} + \frac{O}{K} \right] \quad [F.4]$$

As shown in Equation F.3 the nuclear-electric cost is a function of the fixed costs divided by the capacity factor plus the nuclear fuel cycle cost contribution. The first term is reduced when the capacity factor increases. Thus it is economically advantageous to operate at high capacity factor. If the duration of coastdown is sufficiently long, the overall capacity factor is reduced and the economics of coastdown will be adversely affected, particularly since the capital, operation, and maintenance cost term is approximately four times greater than the nuclear fuel cycle cost component.

In the previous analysis (Section 5.5.3), it was assumed that the replacement cost of energy accounts for the cost of purchasing energy from another utility and the cost of paying off the capital, operation and maintenance charges of the plant. In other words, the utility assumed that the capital and operational costs were paid for by the revenue generated by the sale of electricity produced from the reactor and the sale of replacement energy. This is a good assumption when the mean capacity factor does not change significantly when the reactor is coasted down. In most instances the utility will not coast the reactor below 70% of full power or for more than about 60 days, such that the cycle-averaged capacity factor will only change by on the order of 0.1%. Hence, their simplified economic analysis of coastdown is not necessarily invalid.

Before we examine this alternate method, let us define clearly what is meant by capacity factor. As shown in Figure 1, the capacity factor is the actual energy production during a given period divided by energy production during the same period if the reactor operated continuously at the rated power level. Thus the capacity factor is determined by the energy production in three time intervals; namely, the energy production during full power cycle life weighted by the availability based capacity factor (to account for forced outages caused by equipment breakdown), the energy production during coastdown, and energy production during refueling (which is zero). It is also assumed that when coastdown begins the reactor is able to coast down gradually from the full rated power level. If any prolonged forced outages occur, it is assumed that the reactor is shutdown for refueling.

Using this alternative economics model (Equations [F.1] and [F.2]), the relative cost of electricity was calculated as a function of coastdown duration for the coastdown scenario analyzed in Section 5.3.3. In this analysis it was assumed that the capital, operation, and maintenance cost term was 4 times greater than the nuclear fuel cost term for the reference case (no coastdown). As shown in Figure F.2, the new model predicts a smaller economic benefit when the reactor is coasted down. In addition, the optimum coastdown duration is shifted to the left (shortened). The new optimum is approximately 20 to 30 days instead of the 35 to 45 days predicted by the model in Section 5.5.3. However, benefits are still predicted, albeit small, and coastdown could still be extended to roughly 60 days without increasing costs to the consumer.

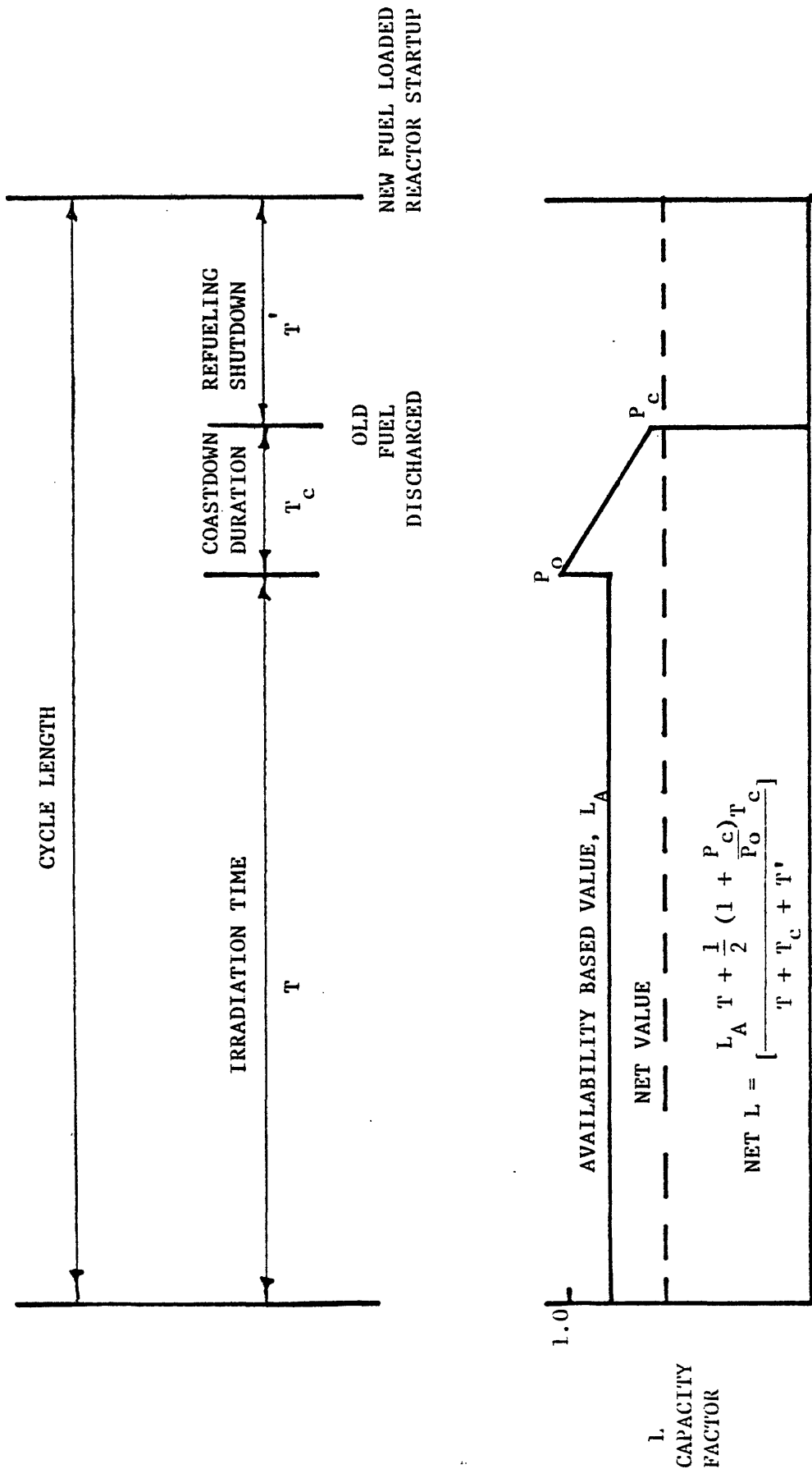


FIGURE F.1 DEFINITION OF CAPACITY FACTOR INCLUDING COASTDOWN OPERATION

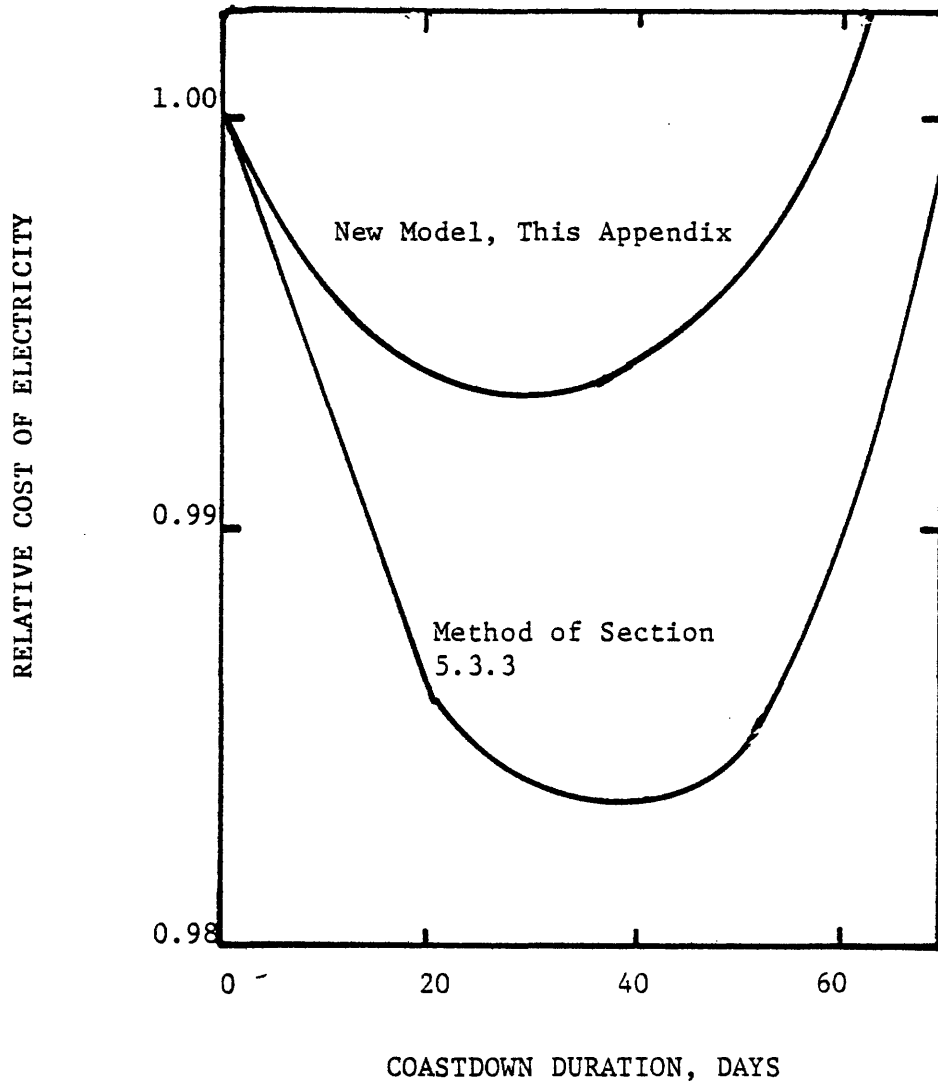


FIGURE F.2 RELATIVE COST OF ELECTRICITY VERSUS COASTDOWN DURATION

APPENDIX G

REFERENCES

- A-1. A.I.F., "Reprocessing-Recycle Economics," Atomic Industrial Forum, Washington, D.C., Nov., 1977.
- A-2. Adensam, E.G., et al., "Computer Methods for Utility-Reactor Physics Analysis," Reactor and Fuel-Processing Technology, Vol. 12, No. 2, Spring, 1969.
- A-3. Amster, H., Suarez, R., "The Calculation of Thermal Constants Averged over a Wigner-Wilkins Flux Spectrum: Description of the SOFOCATE Code," WAPD-TM-39 (1957).
- A-4. Amouyal, A., Benoist, P., Horowitz, J., "New Method of Determining the Thermal Utilization Factor in a Unit Cell," Journal of Nuclear Energy, 6, 79, (1957).
- A-5. Abbaspour, A.T., "Simple Modeling of the Fuel Cycle Economics of Light Water Reactors," S.M. Thesis, M.I.T., Dept. of Nuclear Engineering, Sept. 1978 (est.)
- A-6. Andrews, H.N., et al., "Optimizing the Refuel Cycle: Two Views," Nuclear News, September, 1973.
- B-1. Barry, R.F., "LEOPARD--A Spectrum Dependent, Non-Spatial Depletion Code for the IBM-7094," WCAP 3269-26, Westinghouse Electric Corporation (1973).
- B-2. Bohr, et al., "MUFT-4 Fast Neutron Spectrum Code for the IBM-704," WAPD-TM-72 (1957).
- B-3. Breen, R.J., "A One-Group Model for Thermal Activation Calculations," NSE 9, 91 (1961).
- B-4. Breen, R., Marlowe, O.J., Pfeifer, C.F., "HARMONY System for Nuclear Reactor Depletion Computation," Bettis Atomic Power Laboratory, WAPD-TM-478, 1965.
- B-5. Buslik, A.J., "The Description of the Thermal Neutron Spatially Dependent Spectrum by Means of Variational Principles," WAPD-BT-25 (May, 1962).
- B-6. Boyd, W.A., "Thermal-Hydraulic Analysis of Tight Lattice Light Water Reactors," S.M. Thesis, M.I.T. Dept. of Nuclear Engineering, May, 1977.
- B-7. Banister, R.M., "Considerations Pertaining to Power Reactor Core Stretchout in Pressurized Water Reactor," S.M. Thesis, M.I.T., Dept. of Nuclear Engineering, Feb., 1971.

- B-8. Bamdad-Haghighi, F., "Temperature and Power Coastdown in Thorium and Uranium Fueled Pressurized Water Reactors," Special Problem, M.I.T. Dept. of Nuclear Engineering, December, 1977.
- B-9. Babcock and Wilcox, "Steam--Its generation and use," Babcock and Wilcox Company, New York, 1972.
- C-1. Cacciapouti, R.J., Sarja, A.C., "CHIMP-II A Computer Program for Handling Input Manipulation and Preparation for PWR Reload Core Analysis," YAEC-1107, May, 1976.
- C-2. Cadwell, W.R., "PDQ-7 Reference Manual," Bettis Atomic Power Laboratory, WAPD-TM-678 (1967).
- C-3. Croft, A.G., "MITCOST-II--A computer Code for Nuclear Fuel Cycle Costs," N.E.Thesis, M.I.T. Nuclear Engineering Dept. (1974).
- C-4. Correa F., "Utilization of Thorium in Ultra-Tight-Pitch PWR Cores," Ph.D. Thesis, M.I.T. Dept. of Nuclear Eng. January, 1979 (est.)
- C-5. Correa, F., "Effect of the Th-232/U-238 Ratio on the Conversion Ratio of PWR's," Special Problem Report, M.I.T. Dept. of Nuclear Engineering, August, 1977.
- D-1. Dietrich, J.R., "Efficient Utilization of Nuclear Fuels," Power Reactor Technology, 6(4) 1-38 (1963).
- D-2. Delp et al., "FLARE, A Three-Dimensional Boiling Water Reactor Simulator," GEAP-4598 (July, 1964).
- D-3. Ducat, G.A., et al., "Evaluation of the Parfait Blanket Concept for Fast Breeder Reactors," COO-2250-5, MITNE-157, January, 1974.
- D-4. Dahlberg, R.C., "Benefits of HTGR Fuel Cycle Compilation and Summary," General Atomic, GA-A14398, March, 1977.
- E-1. Edlund, M.C., "Development in Spectral Shift Reactors," Proc. Third U.N. Conf. on Peaceful Uses of Atomic Energy, 6, 314 (1964).
- E-2 ERDA, Light Water Breeder Reactor, United States Energy Research and Development Administration, PSAR, 1975.
- F-1. Flatt, H.P., "The FOG One-Dimensional Neutron Diffusion Equation Code," NAA-SR-6104, December, 1960.
- G-1. Garel, K.C. and Driscoll, M.J., "Fuel Cycle Optimization of Thorium and Uranium Fueled PWR Systems," MIT-EL 77-018, MITNE-207, October, 1977.

- G-2. Gurinsky, D.H., and Dienes, G.J., Nuclear Fuels, D. Van Nostrand Company, Inc., New York, 1956.
- G-3. Gallagher, W.J. and McLeod, N.B., "Higher Power Densities in Water Reactors-Economic and Technical Bases," Reactor and Fuel-Processing Technology, Vol. 12, No. 1, Winter 1968-1969.
- H-1. Hageman, L.A., Pfeifer, C.J., "The Utilization of the Neutron Diffusion Program PDQ-5," WAPD-TM-395 (January, 1965).
- H-2. Hoppes, D.F., "Investigation of Axial Fuel Shuffling Schemes for a High-Temperature Gas-Cooled Reactor," M.S. Thesis, Georgia Institute of Technology, March, 1972.
- K-1. Kusner, D.E., et al., "Planned Cycle Stretchout in PWR's" Trans. Am. Nucl. Soc., 27, 467, (1977).
- L-1. Lamarsh, J.R., Introduction to Nuclear Reactor Theory," Addison-Wesley Publishing Company, Inc., Reading, Mass., 1966.
- M-1. Martin, D.F., "The Effect of Refueling Date Changes on Fuel Cycle Costs," S.M. Thesis, MIT, Dept. of Nuclear Engineering, Feb., 1971.
- N-1. Nobahar, A.N., "Computerized Thermal Analyses of PWR Power Plant Cycles," S.M. Thesis, M.I.T., Department of Nuclear Engineering, September, 1977.
- P-1. Pardue, W.M., "An Evaluation of Alternative Nuclear Strategies," Annuals of Nuclear Engineering, Vol. 2, Pergamon Press, 1975.
- P-2. Pasanen, A.A., Experience from Operating and Fuelling Nuclear Power Plants, IAEA, Vienna, 1974.
- P-3. Pilat, E. Private Communication, Energy Research Group, Westboro, Mass., March, 1978.
- R-1. Radkowsky, A., et al., "Seed and Blanket Reactors," Proc. Third U.N. Conf. on Peaceful Uses of Atomic Energy, 6, 304 (1964).
- R-2. Randall, D. and St. John, D.S., "Xenon Spatial Oscillations," Nucleonics 16, (3), pg. 82-86 (1958).
- R-3. Rieck, T.A., et al., "The Effect of Refueling Decisions and Engineering Constraints on the Fuel Management for a Pressurized Water Reactor," MITNE-158, January, 1974.

- S-1. Shapiro, N.L., J.R. Rec., and R.A. Matzie, "Assessment of Thorium Fuel Cycles in Pressurized Water Reactors," EPRI NP-359, Combustion Engineering Inc., February, 1977.
- S-2. Strawbridge, L.E., Barry, R.F., "Criticality Calculations for Uniform Water-Moderated Lattices," NSE: 23, 58-73 (1965).
- S-3. Shapiro, N.L., Private Communication, Combustion Engineering, Windsor, Conn., Feb., 1978.
- S-4. Solan, G.M., Private Communication, Yankee Atomic Electric Company, Westboro, Mass., Oct., 1977.
- S-5. Stevens, W., et al., "Reduced Enrichment Requirements Through Optimal Cycle Coastdown, San Onofre Unit 1," Trans.Am. Nucl. Soc., 24, 214 (1977).
- S-6. Solan, G.M., et al., "Maine Yankee Cycle 3 Design Report," Yankee Atomic Electric Company, YAEC-1134, August 1977.
- T-1. Till, C.E., and Y.I. Chang, "Once-Through Fuel Cycles," 18th Annual ASME Symposium on "Non-Proliferation, Albuquerque, New Mexico, March, 1978.
- T-2. Tagishi, A. and Driscoll, M.J., "The Effect of Reactor Size on the Breeding Economics of LMFBR Blankets," COO-2250-13, MITNE-168, February, 1975.
- U-1. Ujifusa, D., Private Communication, DOE, Division of Nuclear Power Development, April, 1978.
- V-1. Ver Planck, D.M., Ferguson, D.R., "SIMULATE, Reactor Simulator Code, User's Manual," Yankee Atomic Electric Company (1972).
- V-2. Varga, R.S., Matrix Iterative Analysis, Prentice-Hall (1962).
- W-1. Williamson, H.E., et al., "Assessment of Utilization of Thorium in BWR's," ORNL-Sub-4380-5, NEDG-24073, January, 1978.
- W-2. Watt, H.Y. and Pilat, E.E., "Optimal Coastdown Duration for Yankee Rowe," Trans. Am. Nucl. Soc. 22, 321 (1975).
- Y-1. Yankee Atomic Electric Company, "Preliminary Safety Analysis Report, Maine Yankee Atomic Power Station," September, 1967.
- Z-1. Zorzoli, G.B., "The Potential of Metallic Thorium for LWR's," Energia Nucleare, 20/2, Feb., 1973.